AN IMPROVED MODEL FOR PREDICTING METHANE EMISSIONS FROM LANDFILLS BASED ON RAINFALL, AMBIENT TEMPERATURE AND WASTE COMPOSITION

by

RICHA VIJAY KARANJEKAR

Presented to the Faculty of the Graduate School of

The University of Texas at Arlington in Partial Fulfillment

of the Requirements

for the Degree of

DOCTOR OF PHILOSOPHY

THE UNIVERSITY OF TEXAS AT ARLINGTON

August 2012

ACKNOWLEDGEMENTS

I would like to whole heartedly thank my advisor Dr. Melanie Sattler and Dr. Sahadat Hossain for guiding me throughout the research. This research would not have been possible without their continuous guidance, valuable suggestions and constant encouragement. Dr. Sattler has truly been a mentor, her patience and constructive suggestions helped me be a better researcher. I cannot express my gratitude to Dr. Hossain for providing excellent ideas and advice that propelled my research. I would especially like to like thank Dr. Chen for her invaluable inputs, guidance and support that took me through this research. I would also like to thank my committee members Drs. Hyeok Choi and Jorge Rodrigues for their guidance and support.

I also wish to thank the Environmental Research and Education Foundation for supporting me through their student scholarship. I also wish to express my gratitude to the Solid Waste Association of North America, and Air and Waste Management Association for their support via multiple scholarships.

I would like to take this opportunity to thank Dr. Syed Qasim for his valuable inputs and being constant motivator and a guardian to me. I also wish to thank Dr. John McEnery for giving me an opportunity to work with him and supporting me.

Special thanks to Arpita Gandhi, Said Altouqi, Pinki Bhandari, Shankar Vaidyanathan, Gunther Garcia, Meenakshi Ganguly, Juan Cruz, Madhu Rani, Shammi Rahman, Sonia Samir and Shahed Manzur; without them, I would still be in the lab.

I would like to thank my husband Neelesh, whose patience, understanding, and support allowed me to accomplish my mission. I would not have been able to finish this work without the love and encouragement from my parents, sister, and extended family.

June 20, 2012

ABSTRACT

AN IMPROVED MODEL FOR ESTIMATING METHANE EMISSIONS FROM LANDFILLS BASED ON RAINFALL, AMBIENT TEMPERATURE AND WASTE COMPOSITION

Richa Vijay Karanjekar, PhD

The University of Texas at Arlington, 2012

Supervising Professor: Melanie L. Sattler

Accurately estimating the emissions of methane (CH_4) and carbon dioxide (CO_2) in a landfill is important for quantifying its greenhouse gas (GHG) emissions and power generation potential. Previous studies have shown that variation in waste composition, rainfall and ambient temperature of a landfill significantly influences its methane generation potential. Current methane generation models, namely U.S. Environmental Protection Agency's (EPA) Landfill Gas Generation Model (LandGEM) and Intergovernmental Panel on Climate Change's (IPCC) methane generation model, are overly simplified and do not account for the variations in waste composition, rainfall and ambient temperature.

The goal of this research was to improve our ability to estimate methane generation rates from landfills worldwide, which can be used by any country/city, with any anticipated waste composition, or climatic conditions. The proposed Capturing Landfill Emissions for

Energy Needs (CLEEN) model allows methane generation to be estimated for any landfill, with basic information about waste composition, annual rainfall, and ambient temperature.

A statistical experimental design was used for determining the first order methane generation constants (*k* values) for laboratory scale landfills, with varying waste composition, temperature, and rainfall conditions. The experimental design was developed using incomplete block design, where the waste composition served as a blocking variable and combinations of temperature and rainfall were the primary predictor variables. 27 lab scale landfills reactors were simulated with varying waste compositions (ranging from 0 to 100 %); average rainfall rates of 2, 8, and 15 mm/day; and temperatures of 20, 30, and 37^{o}C. These rainfall rates encompass average precipitation rates for most locations worldwide, with the exception of deserts. Refuse components considered were the major biodegradable wastes, food, paper, yard/wood, and textile, as well as inert inorganic waste. Methane generation-from laboratory scale simulated landfills was monitored for a period of 180 to 400 days until the methane generation rates dropped to a low constant value. Based on the simulated landfill data, a comprehensive regression equation was developed for predicting the methane generation rate constant, (*k*) using waste composition, rainfall and temperature as predictor variables. Finally, the regression equation was incorporated into the CLEEN model and scale-up factors were evaluated for studying the applicability of the model for field scale studies.

It was observed from the simulated landfill data that the methane generation curves from reactors with high amounts of textile waste and food waste showed multiple peaks and did not follow a typical first-order decay curve. Methane generation curves from reactors with yard waste and paper waste followed a classic first order decay curve. Overall, the mixture of

waste components helped in supplying nutrients hence the combined waste followed a first order decay curve.

Multiple Linear Regression (MLR) analysis was used on the lab scale data to estimate the effect of waste composition, rainfall and ambient temperature on the first-order decay constant (*k*). The best model selected using the backward elimination method, best subsets method and stepwise regression method had an adjusted R^2 of 0.7538. From the MLR model it was observed that increasing the ambient temperature increased the rate of degradation. Likewise, increasing the amount of textile waste and yard waste increased the rate of degradation. It was observed that the rate of degradation was affected by the combined effect of food waste and rainfall. A change in the amount of paper waste affected the overall rate of degradation; however, that effect was not significant at 90% confidence level. The comprehensive regression equation was able to predict methane generation rates for rainfall from 2 mm/day to 12 mm/day, and ambient temperature between 20^{o}C to 37^{o}C, and was limited to 0 to 60% of food waste, 0 to 60% of textile waste, and 0-100% for paper and yard waste.

The Capturing Landfill Emissions for Energy Needs (CLEEN) model was developed by incorporating the comprehensive regression equation into first-order decay based model for estimating methane generation rates from landfills. Methane recovery and methane oxidation factors were also incorporated in the CLEEN model, to estimate the methane emissions from the landfill surfaces. A scale-up factor was computed to adapt the lab based regression equation to actual landfill scale methane generation using the City of Denton's landfill emissions data, which was found to be 0.012.

This study will possibly allow better estimation of the methane generation rate constant *k* based on waste composition, rainfall and ambient temperature. CLEEN model will also allow *k* values to be adjusted as recycling and composting increase, without developing new country-specific *k*s. Overall, this study will develop a model for better predictions of methane generation rates from any landfill worldwide.

TABLE OF CONTENTS

APPENDIX

LIST OF ILLUSTRATIONS

Figure Page

LIST OF TABLES

Table Page

CHAPTER 1

INTRODUCTION

1.1 Background

Landfills serve not only as waste repositories but also as significant sources of renewable energy. As microbes degrade the organic fraction of waste, methane (CH_4) is generated, along with carbon dioxide (CO_2), water, and other trace landfill gas (LFG) constituents. Methane, the primary constituent of natural gas, can be captured and used to generate electricity. Methane can also be used directly in industrial and manufacturing operations, or upgraded to pipeline–quality gas where the gas may be used directly or processed into an alternative vehicle fuel. Using LFG helps to reduce odors associated with LFG emissions, and can improve safety by reducing explosion hazards from gas accumulation in structures on or near the landfill.

Comprising 40-60% of landfill gas by volume, methane is not only potentially an energy source, but also a potent greenhouse gas: its global warming potential is 22 times that of CO_2 on a weight basis (over a 100 year time period) (Intergovernmental Panel for Climate Change (IPCC 2007). According to USEPA (2011), landfills are the fifth largest source of greenhouse gases (GHG) in the United States, accounting for about 117 MMT of CO_2 equivalents of emissions (USEPA 2011). Capturing and burning methane for energy is thus important as a measure for reducing the potency of greenhouse gas emissions. Converting a molecule of methane to CO_2 by burning it for energy reduces its ability to trap the Earth's outgoing radiation by a factor of 21/22, or 95% (IPCC 2007).

Accurate estimates of methane emissions from landfills are important for:

- Determining landfill's carbon footprint (quantify the greenhouse gases emitted by the landfill),
- Estimating power generation potential of the landfill,
- Designing the landfill's gas collection and purification system.

1.2 Problem Statement

Waste degradation in landfills is most commonly modeled using a first-order decay equation (Alexander et al. 2005; Eggleston et al. 2006; Kamalan et al. 2011). The two most critical factors in the model are the first-order decay constant (*k* value or half-life) and the ultimate methane generation potential (L_0). Amini et al. (2012) stated that the efficiency of current models to predict methane generation from landfills is most sensitive to the L_0 and *k* values used in the models (Amini et al. 2012). Figure 1.1 shows the effect of changing L_0 and *k* on the methane generation rate from a hypothetical landfill with an active life of 15 yrs. It can be seen that higher the *k* value, the faster is the methane generated in the landfill. Hence, if the *k* value is smaller, the methane generation from the landfill extends long after the landfill is closed, implying longer post-closure care duration, as well as longer carbon storage (Staley and Barlaz 2009).

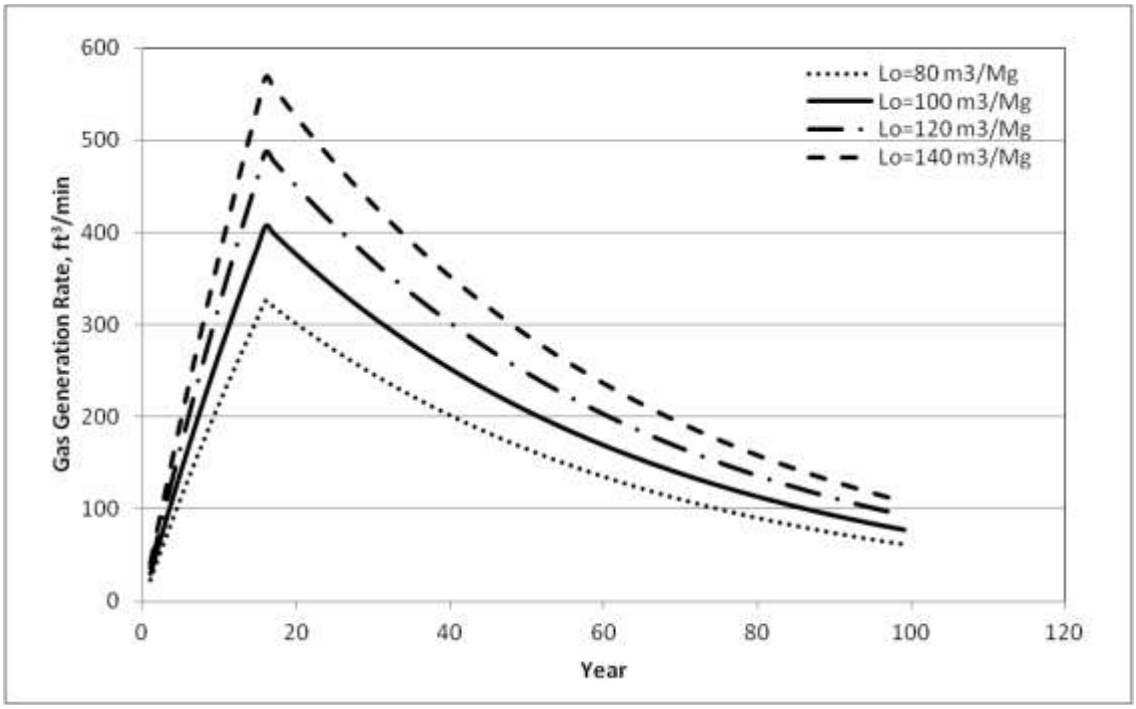

(a)

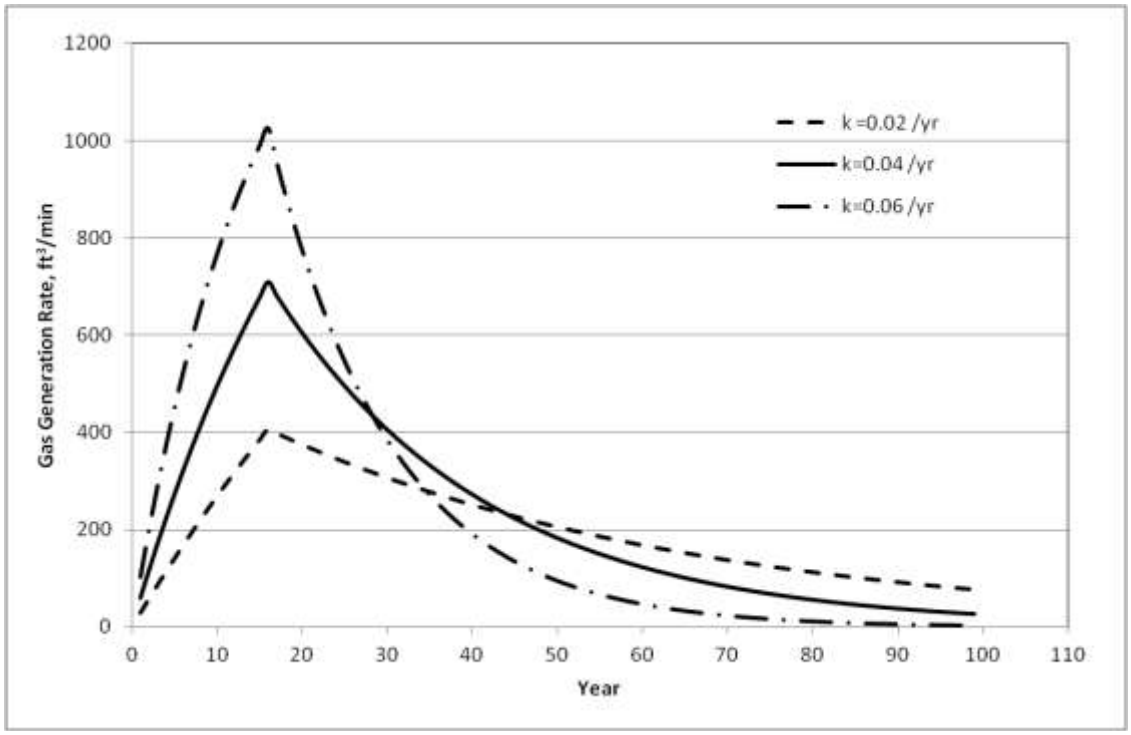

(b)

Figure 1.1: Effect of Changing Model Parameters on Methane Generation Rate, (a) L_0 and (b) k

According to IPCC (2006), the methane generation potential (L_0) of a landfill depends on waste composition and its degradable organic content. Since the waste composition in developing countries differs from that in developed countries, methane generation potential also differs. In general, waste from developing countries is composed of higher amount of food and putrescible matter (Guermoud et al. 2009). Because of the large amount of food in the waste streams of developing countries, the waste moisture content is also higher. Moreover, each type of waste degrades at a different rate. Thus, waste composition also affects the rate of degradation (*k* value) in landfills (Machado et al. 2009). Figure 1.2 shows a graphical representation of relative rate of degradation of waste components in a landfill.

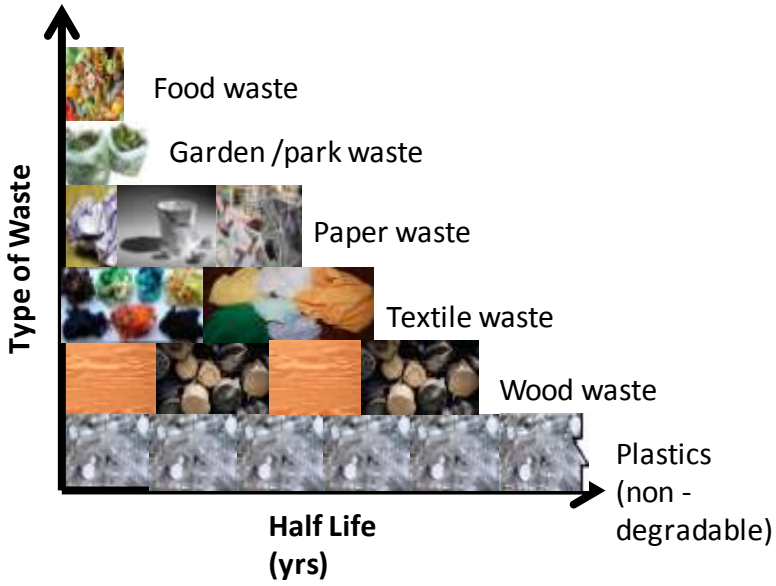

Figure 1.2: Graphical Representation of Rate of Degradation of Different Waste Components

Further, several researchers have pointed out that an increase in moisture content can increase the methane generation rate of landfills (Barlaz et al. 1990; Mehta et al. 2002; Wreford

et al. 2000). Moisture content within a landfill depends on the initial moisture content of waste, operational practice and the rainfall infiltrated into the landfill during its active life. Therefore, it is important to identify the effect of rainfall on the rate of degradation (*k*). Further, moisture absorption capacity of different types of waste is different, which primarily depends on the saturation limit of the wastes. Stone and Kahle (1972) observed that paper and textile waste can absorb about 4 times more moisture than yard waste (based on a dry weight basis). Hence, the impact of moisture content on the degradation of each waste component depends on its saturation limit (Stone and Kahle 1972). Furthermore, several researchers have observed that increase in temperature of the waste also enhances the microbial activity, thereby increasing the methane emissions from waste (Christensen and Kjeldsen 1989; Rees 1980; Bingemer and Crutzen 1987). Hence, it is important to incorporate the effect of waste composition, rainfall and temperature on *k* value while modeling gas generation from landfills.

Current landfill gas generation models, however, are typically overly simplified, not accounting for landfill-specific variations in waste composition, moisture content, and ambient temperature, which can significantly impact methane generation rates. The widely-used LandGEM, for example, contains default methane generation rate constant *k* values for a conventional landfills, arid areas, and bioreactors. These 3 default values account discretely for variations in moisture content due to rainfall and leachate recirculation, but do not account for variations in temperature or waste composition (USEPA 2005). Although the user can input site-specific parameter values, such information is often not available without laboratory test data. The IPCC Waste Model provides methane generation rate constant values for 2 temperature ranges (<20°C and >20°C) and 2 moisture contents (dry or wet). Rate constant values are provided for 4 categories of waste, but the method of combining the rate constant values to

arrive at an overall landfill *k* value is unclear, as stated by IPCC (IPCC 2006). Therefore, it can be summarized that existing models have limitations and cannot be used globally without developing site specific models.

1.3 Research Objective

The goal of this research was to develop a model for predicting methane generation rates from landfills, which can be used globally to estimate methane potential of the landfills, regardless of waste composition or climate. The proposed Capturing Landfill Emissions for Energy Needs (CLEEN) model allows methane generation to be estimated for any landfill with basic information about waste composition, annual rainfall, and ambient temperature. The proposed CLEEN model helps in predicting methane generation rate and methane emissions from the landfill surface by incorporating the methane recovery with gas collection and control system, and methane oxidation in landfill covers.

The specific objectives of this project were three-fold:

1. Developing laboratory scale simulated landfills to study the effect of rainfall, ambient temperature and waste composition on gas generation rates;
2. Developing a comprehensive regression equation for predicting methane generation rate constant (*k*) based on the laboratory scale data;
3. Incorporating the regression equation in CLEEN model for predicting methane generation rates from landfills, and developing scale-up factor for adapting the CLEEN model for landfill scale conditions.

1.4 Dissertation Outline

This dissertation is divided into six chapters as summarized below:

- Chapter 1 provides an introduction and presents the problem statement and objectives of the research.
- Chapter 2 presents a literature review of the stages of municipal solid waste (MSW) decomposition, current models used for predicting methane generation from landfills, methods for estimating the ultimate methane potential of landfills, factors affecting the rate of degradation and methods for determining the first-order decay constant.
- Chapter 3 describes the experimental procedures followed to collect MSW samples, to build laboratory scale landfill reactors and to measure the rate of decay of waste components as a function of waste composition, rainfall and ambient temperature.
- Chapter 4 presents the experimental results, discussion on the results, and comparison of the results with existing literature.
- Chapter 5 presents a statistical modeling procedure using multiple linear regression. The CLEEN model was developed using the scale-up factor calculated from landfill methane generation data.
- Chapter 6 summarizes the main conclusions from the current research and provides recommendations for future work.

CHAPTER 2

LITERATURE REVIEW

2.1 Background on Landfills Gas Generation

Municipal solid waste (MSW) disposed of in a landfill is comprised of several types of waste, such as food, paper, yard, plastic, textiles, and metal waste. The organic fraction of municipal solid waste in the landfill decomposes through a series of interacting microbial processes into methane (CH_4), carbon dioxide (CO_2) and water (H_2O). While water moves downward through the layers of waste in the landfill, forming "leachate", methane, carbon dioxide along with other gases migrate to the landfill cover, forming "Landfill Gas" (LFG).

Methane generation from landfills depends on several factors, such as the waste composition, compaction, unit weight, age, pH, particle size, and initial moisture content, as well as climatic factors such as the annual rainfall and temperature. Landfill gas primarily consists of methane (about 40-60%); therefore, it is potentially an energy source as well as a greenhouse gas. According to IPCC (2004), methane has 22 times more global warming potential than carbon dioxide (over a hundred year time period). Typical composition of landfill gas is shown in Table 2.1.

In addition, USEPA (2008) has identified above 100 trace constituents including non-methane organic compounds (NMOCs) and volatile organic compounds (VOCs) emitted from landfills. USEPA (2005) User's Guide for Landfill Gas Emissions model incorporates default emission factors for 46 trace components.

Table 2.1: Typical Composition of Landfill Gas (Source: Tchobanoglous et al. 1993)

Component	Percent (dry volume basis)
Methane	45-60
Carbon dioxide	40-60
Oxygen	2-5
Sulfides, disulfides, mercaptans, etc.	0.1-1.0
Ammonia	0.1-1.0
Hydrogen	0-0.2
Carbon monoxide	0-0.2
Trace constituents	0.01-0.6

2.1.1 Landfill Gas Production

The conversion of solid waste to methane and carbon dioxide is aided by microorganisms by a series of chemical conversions. The biochemistry of anaerobic degradation of waste can be divided in three stages. In first stage is the hydrolysis stage, where the solid waste and dissolved organic compounds are hydrolyzed and fermented to volatile fatty acids, alcohols, hydrogen and carbon dioxide. In the second stage, acetogenesis, the acetogenic groups of bacteria convert the products from first stage to acetic acid, hydrogen and carbon dioxide. In the final stage, methanogenesis phase, methane is produced by methanogenic bacteria (Barlaz et al. 1990; Christensen and Kjeldsen 1989).

The overall process of converting organic matter to methane and carbon-dioxide can be stoichiometrically expressed as shown in Eq. 2-1 (Cooper et al. 1992).

$$\mathrm{C}_a\mathrm{H}_\mathrm{b}\mathrm{O}_c\mathrm{N}_d\mathrm{S}_e + \left(\frac{4a-b-2c+3d-2e}{4}\right)\mathrm{H}_2\mathrm{O} \xrightarrow[bacteria]{} \left(\frac{4a+b-2c-3d-2e}{8}\right)\mathrm{CH}_4 + \left(\frac{4a-b+2c+3d+2e}{8}\right)\mathrm{CO}_2 + d\mathrm{NH}_3 + e\mathrm{H}_2\mathrm{S} \qquad (2\text{-}1)$$

2.1.2 Phases of Anaerobic Degradation

Gas generation from a landfill has been divided into 4 (or more) sequential phases. Typical phases in waste degradation are shown in Figure 2.1.

Phase I – Aerobic Phase - Aerobic decomposition occurs immediately after placement of the waste due to oxygen trapped within the landfill. Mainly carbon dioxide is produced during this phase, and the amount of carbon dioxide produced is approximately equivalent to the amount of oxygen consumed.

Phase II- Anaerobic Acid Phase - In this phase the acetogenic microorganisms are predominant. This leads to accumulation of carboxylic acids and the leachate pH decreases. There is very little methane generation in this phase, and the landfill gas predominantly consists of carbon-dioxide.

Phase III- Accelerated Methane Production Phase- The concentration of methane in landfill gas increases until it reaches a constant value (mostly between 40- 60%). The carboxylic acid concentration decreases. The pH stabilizes, and leachate strength decreases. Methanogenic and acid forming bacteria have a mutually beneficial, symbiotic relationship.

Phase IV- Decelerated Methane Production Phase- The methane and carbon dioxide concentrations are relatively constant in this phase. However, the methane generation rate decreases. In a landfill, this phase is expected to extend for 20-50 yrs. The pH is similar to phase III (Barlaz et al. 1990; Rees 1980; Tchobanoglous et al. 1993; Farquhar and Rovers 1973).

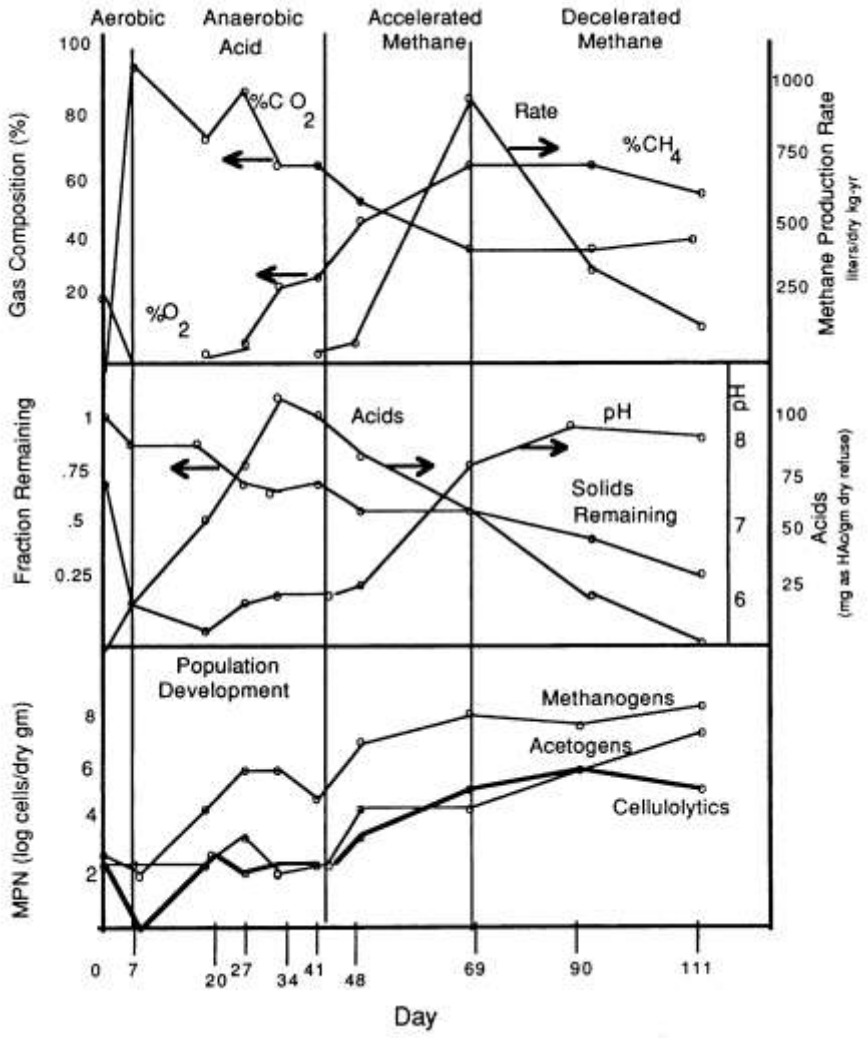

Figure 2.1: Phases in Anaerobic Degradation of Solid Waste (Source: Barlaz et al. 1990)

2.2 Models for Landfill Gas Generation

Various models have been developed to describe landfill waste degradation, including zero-order, first-order, second-order decay models, multiphase models, and combination models. A brief review of assumptions and equations used in some models is presented in Table 2.2

Table 2.2: Landfill Gas Generation Models (Oonk 2010; Faour et al. 2007; Solid Waste Association of North America, 1997)

Model	Equation
Zero-Order Decay Model Landfill gas generation in a certain amount of waste is assumed to be constant with time. Effect of waste age is not incorporated in the model.	$Q = \frac{ML_0}{(t_i - t_f)}$ for $t_i \le t \le t_f$ Where Q = Methane generation rate (m^3/yr); M = Mass of solid waste in place (yr); L_0 = Ultimate methane generation potential (m^3/yr); t = Time (yr); t_i = Lag time (time between waste placement and gas generation) (yr); t_f = Time to the end of gas generation (yr).
First-Order Decay (FOD) Model Landfill gas generation in a certain amount of waste is assumed to decrease exponentially. The first-order decay equation is used in US EPA's LandGEM.	$Q = ML_0 k e^{-k(t-t_i)}$ Where k = first-order decay rate constant (yr^{-1}).
Modified First-Order Model This model assumes that methane generation from a certain amount of waste may be initially low (due to the "lag phase"). The generation then rises to a peak before declining exponentially, like in the first-order decay model.	$Q = ML_0 \frac{k+s}{s} \left(1 - e^{-s(t-t_i)}\right)\left(k e^{-k(t-t_i)}\right)$ Where k = first-order decay rate constant (yr^{-1}); s= first-order rise phase rate constant (yr^{-1})
First-Order Multi-Phase Decay Model The first-order multi-phase decay model assumes that different fractions of the waste decay at different rates. The waste is divided into three (or more) fractions, depending on the rate of their decay. E.g., food waste and grass are assumed to degrade faster than paper or certain types of textile waste. However, each fraction is assumed to follow first-order decay.	$Q = \sum_{i=1}^{n} M_i L_0 \left[\begin{array}{l} F_r\left(k_r e^{-k_r(t-t_i)}\right) + F_m\left(k_m e^{-k_m(t-t_i)}\right) \\ + F_s\left(k_s e^{-k_s(t-t_i)}\right) \end{array} \right]$ Where F_r, F_m, F_s = fraction of rapidly, moderately or slowly decomposing wastes; k_r, k_m, k_s = first-order decay constants for rapidly, moderately, slowly degrading wastes (yr^{-1}); t_i = age of i^{th} increment (yr).
Second-Order Decay Model The second-order model is considered better when a large number of reactions, all of a first-order but with differing reaction rates, occur in the system.	$Q = Mk\left(\frac{L_0}{kL_0 t + 1}\right)^2$ Where k = second-order rate constant (m^3/kg /yr).

Oonk and Boom (1995) studied the prediction efficiency of zero-, first-, multiphase and second-order models using gas generation data from 9 Dutch landfills. The study concluded that the multiphase model best describes gas generation with a relative error of 18 percent, followed by the second- and first-order models each with a relative error of 22 percent, and the zero-order as the least reliable with a relative error of 44 percent. Oonk and Boom (1995) used the multiphase first-order equation by dividing the waste into 3 categories (rapidly, moderately and slowly degrading waste). However, the authors commented that further division of waste may help toward improving the performance of the model.

SWANA (1997) conducted a similar study to compare the model parameters and the prediction efficiency of zero-order, first-order, multiphase first-order and modified first-order models using methane recovery data from 18 U.S. landfills. SWANA observed that the regression coefficients (R^2) for all these models were in the range of 0.914 to 0.955. Although the regression coefficients were very close, the simple first-order decay had the maximum R^2 value of 0.955, suggesting that the simple first-order model is the most accurate for estimating methane emissions from landfills (Oonk and Boom 1995; Solid Waste Association of North America, 1997).

2.3 Current Landfill Gas Generation Models

Two of the most commonly used first-order and multi-phase first-order models are the U.S. Environmental Protection Agency's (EPA's) Landfill Gas Generation Model (LandGEM) and the Intergovernmental Panel on Climate Change (IPCC's) methane generation models, respectively (U.S. EPA 2005; IPCC 2006). This section includes a review of the assumptions, equations and constants used in these two models.

2.3.1 EPA's Landfill Gas Generation Model (LandGEM)

US EPA's LandGEM uses a simple first-order decay equation for predicting methane generation rate from landfills. First-order degradation can be expressed as a function of mass of waste (degradable waste) remaining, as shown in Eq. 2-2:

$$\frac{dM_r}{dt} = -kM_r \quad (2\text{-}2)$$

Integrating Eq. 2-2 yields the following equation.

$$M_r = M_0 e^{-kt} \quad (2\text{-}3)$$

Where,

M_r = remaining mass of waste at time t (Mg)

t = time elapsed (yr)

k = first-order degradation rate constant (yr^{-1})

M_0= initial mass of degradable waste (Mg)

Similarly, the total volume of methane that can be produced from a landfill depends on the ultimate methane generation potential of the waste and is represented as follows:

$$V = L_0 M(1 - e^{-kt}) \quad (2\text{-}4)$$

The rate of methane produced per year is obtained by differentiating Eq. 2-4 with respect to time.

$$Q = kL_0 M e^{-kt} \quad (2\text{-}5)$$

Where,

V= cumulative methane generated until time t (m^3)

L_0 = methane generation potential (m^3/Mg)

Q = methane production rate at time t (m^3/yr)

In a landfill the waste is continuously dumped for several years. Hence the amount of waste (*M*) keeps increasing. To incorporate this effect, Eq. 2.5 is modified by summing up the mass of waste added for each time increment. USEPA (2005) suggested the mass of waste added in a landfill to be included for 1/10th of a year, as shown in Eq. 2-6. This was done to improve the accuracy of the model.

$$Q_{CH_4} = \sum_{i=1}^{n} \sum_{j=0.1}^{1} kL_0 \frac{M_i}{10} e^{(-kt_{ij})} \quad (2\text{-}6)$$

where

Q_{CH_4} = methane emission rate at time *t* (m^3/yr)

k = first-order methane generation rate constant (yr^{-1})

L_0 = methane generation potential (m^3 CH_4/10^6 g refuse)

i = one year time increment

j = 0.1 year time increment

M_i = mass of waste in i^{th} section (annual increment) (Mg)

t_{ij} = age of j^{th} section of waste mass M_i accepted in i^{th} year (decimal years, e.g., 3.4 years)

Critical input parameters in this model are ultimate methane generation potential (L_0) and the methane generation rate constant (*k*). According to LandGEM User's Guide (USEPA 2005), methane generation potential (L_0) depends on the waste composition and the first-order rate constant (*k*) depends on moisture content, pH, temperature of waste mass and availability of nutrients. The default values for L_o and *k* for conventional landfill, arid area, and bioreactor landfills are shown in Table 2.3.

Table 2.3: Model Parameters for LandGEM (USEPA 2005)

Default Type	Landfill Type	L_0 (m^3/Mg)	k value (yr^{-1})
CAA[1]	Conventional (Rainfall > 25 in/yr)	170	0.05
CAA	Arid Area (Rainfall < 25 in/yr)	170	0.02
Inventory[2]	Conventional (Rainfall > 25 in/yr)	100	0.04
Inventory	Arid Area (Rainfall < 25 in/yr)	100	0.02
Inventory	Wet (Bioreactor)	96	0.7

NOTE: 1- CAA – Clean Air Act; 2- Inventory – AP 42 (1998)

Although it is simple to use, LandGEM has several shortcomings:

1. LandGEM assumes that the waste is a completely homogeneous; hence L_0 is assumed to be constant with space and time. However, L_0 is actually dependent on the degradable organic carbon present in the landfill and can change with waste composition.
2. The k value is assumed to be constant for the landfill. However, k actually depends on moisture content, temperature and waste composition (Barlaz et al. 1990). Flexibility of varying k values with changes in waste composition is not offered by LandGEM. In fact, LandGEM assumes that waste composition affects L_0 and not k.
3. The default values account discretely for variations in moisture content due to rainfall or leachate recirculation, but do not account for variations in temperature or waste composition. Although the user can input site-specific values, such information is often not available (USEPA 2005).

2.3.2 IPCC's Methane Generation Model

IPCC guidelines (2006) recommended the use of a "multiphase first-order decay model" for estimation of methane emissions from landfills (Eggleston et al. 2006). A simplified version of

the multiphase model is shown in Eq. 2-7. The landfilled waste is divided into categories: slowly-degrading waste, moderately-degrading waste, and rapidly-degrading waste.

$$Q_{CH_4} = M_i L_0 \left[F_r \left(k_r e^{-k_r (t-t_i)} \right) + F_m \left(k_m e^{-k_m (t-t_i)} \right) + F_s \left(k_s e^{-k_s (t-t_i)} \right) \right] \quad (2\text{-}7)$$

where

Q_{CH_4} = methane emission rate, m^3/yr

L_0 = methane generation potential, m^3 of CH_4/ Mg refuse

M_i = mass of waste in i^{th} section (annual increment), Mg

F_r, F_m, F_s = fraction of rapidly, moderately or slowly decomposing wastes

k_r, k_m, k_s= first-order decay constants for rapidly-, moderately- or slowly-decomposing waste

t_i = age of i^{th} increment in years

Variables k_r, k_m and k_s are assumed to be dependent on waste composition and other environmental factors such as moisture, ambient temperature, and the depth of the landfill, while L_0 is assumed to be dependent of the waste composition. Although a multiphase model is difficult to use, there are several advantages associated with it. Advantages of a multiphase model are that:

- It incorporates the degradability of waste components and waste composition while computing the methane generation rate.
- Multiphase models help in identifying the effect of recycling and changes in landfilling practices and its impact on landfill gas emissions over a period of time.

IPCC's methane generation model is based on the amount of degradable organic matter (DOC_m) in the waste disposed. The amount of degradable organic matter (DOC_m) in the waste is estimated from the information about the waste deposited in the landfill, and its components

such as paper, food waste, yard waste, and textile. The decomposable degradable organic matter (*DDOC*) is defined as the amount of DOC that can be degraded in a landfill under anaerobic conditions and can be calculated as shown in Eq. 2-8.

$$DDOC_m = W \cdot DOC \cdot DOC_f \cdot MCF \quad (2\text{-}8)$$

where

DDOCm = mass of decomposable DOC deposited (Mg)

W = mass of waste deposited (Mg)

DOC = degradable organic carbon in the year of deposition (Mg C/ Mg waste)

DOC_f = fraction of DOC that can decompose under anaerobic conditions;

MCF = methane correction factor for aerobic decomposition (before anaerobic decomposition starts) in the year of deposition.

The amount of DDOC accumulated in the landfill in a particular year is computed based on the first order decay rate equation, as follows:

$$DDOC_{ma_T} = DDOC_{md_T} + \left(DDOC_{ma_{T-1}} \cdot e^{-k}\right) \quad (2\text{-}9)$$

$$DDOC_{m\,decomp_T} = DDOC_{maT-1} \cdot \left(1 - e^{-k}\right) \quad (2\text{-}10)$$

Where,

T = inventory year

$DDOC_{ma_T}$ = DDOCm accumulated in the SWDS at the end of year *T* (Gg)

$DDOC_{maT-1}$ = DDOCm accumulated in the SWDS at the end of previous year *T*-1 (Gg)

$DDOC_{md_T}$ = DDOCm deposited into the SWDS in year *T* (Gg)

$DDOC_{m\,decomp_T}$ = DDOCm decomposed in the SWDS in year *T* (Gg)

k = first-order decay constant (yr^{-1})

The amount of methane generated from the decomposable organic matter present in the landfill in a particular year is found by using the relationship:

$$CH_{4\,generated_T} = DDOC_{m\,decomposed_T} \cdot F \cdot \frac{16}{12} \quad (2\text{-}11)$$

Where,

$CH_{4\,generated_T}$ = amount of methane generated from decomposable material in year 'T'.

16/12 = molecular weight ratio CH_4/C ratio

F = fraction of CH_4 by volume, in generated landfill gas (fraction)

$DDOC_{m\,decomposed_T}$ = mass of decomposable degradable organic matter (DDOCm) deposited in year T, Gg

The relationship between decomposable degradable organic carbon (DDOC) and L_0 is shown in Eq. 2-12.

$$L_0 = DDOC_m \times F \times 16/12 \quad (2\text{-}12)$$

IPCC's model incorporates the fact that waste is comprised of various components, and each component may degrade at a different rate. IPCC encourages use of site-specific values for DOC and *k* if available; else, the IPCC model allows use of default *k* values which are specific for a waste category and rainfall (See Tables 2.4 and 2.5).

IPCC provides default *k* values for only 2 ambient temperature ranges (< 20°C/ temperate and >20°C/tropical) and 2 moisture contents (dry, with Mean Annual Precipitation (MAP)/Potential Evapotranspiration (PET) < 1, or wet with MAP/PET >1). *k*s are provided for 4 categories of waste (and bulk waste), but the method of combining the rate constant values to

arrive at an overall landfill *k* value is unclear. IPCC (2006), states that there are two ways to select half-life (*k* value):

a. Compute a weighted average of half-lives (or *k* values) for rapidly-degrading waste, slowly-degrading waste, and moderately-degrading wastes to find an overall for half-life (*k* value) for a mixed municipal solid waste. This approach assumes that degradation of different types of waste is dependent or is influenced by each other.

b. Divide waste stream into categories according to rate of degradation and apply individual half-life (*k* values) to compute the total methane production. This approach assumes that degradation of different types of waste is completely independent of each other.

Table 2.4: Default Methane Generation Rate (*k*) Values Suggested by IPCC (2006)

Type of Waste		Climate Zone							
		Boreal Temperature (MAT/PET≤ 20°C)				Tropical (MAT> 20°C)			
		Dry (MAP/PET < 1)		Wet (MAP/PET>1)		Dry (MAP < 1000 mm)		Wet (MAP >1000 mm)	
		Default	Range	Default	Range	Default	Range	Default	Range
Slowly degrading waste	**Paper / Textiles**	0.04	0.03-0.05	0.06	0.05-0.07	0.045	0.04-0.06	0.07	0.0-0.085
	Wood/ straw	0.02	0.01-0.03	0.03	0.02-0.04	0.025	0.02-0.04	0.035	0.03-0.05
Moderately degrading waste	**Non-food organic / garden, park**	0.05	0.04-0.06	0.1	0.06-0.1	0.065	0.05-0.08	0.17	0.15-0.2
Rapidly degrading waste	**Food waste/ Sewage sludge**	0.06	0.05-0.08	0.185	0.1-0.2	0.085	0.07-0.1	0.4	0.17-0.7
Bulk Waste		0.05	0.04-0.06	0.09	0.08-0.1	0.065	0.05-0.08	0.17	0.15-0.2

Table 2.5: Default DOC Contents Suggested by IPCC (2006)

MSW component	Dry matter content % of wet weight	DOC content % of wet waste		DOC content % of dry waste	
	Default	Default	Range	Default	Range
Paper/cardboard	90	40	36-45	44	40-50
Textiles	80	24	20-40	30	25-50
Food waste	40	15	8-20	38	20-50
Wood	85	43	39-46	50	46-54
Garden and Park waste	40	20	18-22	49	45-55
Nappies	40	24	18-32	60	44-80
Rubber and Leather	84	39	39	47	47
Plastics	100	-	-	-	-
Metal	100	-	-	-	-
Glass	100	-	-	-	-
Other, inert waste	90	-	-	-	-

According to IPCC, "*the first approach assumes degradation of different types of waste to be completely dependent on each other. So the decay of wood is enhanced due to the presence of food waste, and the decay of food waste is slowed down due to the wood. The second approach assumes degradation of different types of waste is independent of each other. Wood degrades as wood, irrespective whether it is in an almost inert Solid Waste Disposal Site (SWDS) or in a SWDS that contains large amounts of more rapidly degrading wastes. In reality the truth will probably be somewhere in the middle. However there has been little research performed to identify the better one of both approaches* (Oonk and Boom 1995b; Scharff and Jacobs 2006) *and this research was not conclusive*." This is an area where further research needs to be done.

Further, IPCC (2006) mentions that the recommended *k* values are based mostly on waste characteristics of developed countries under temperate conditions. Few available results reflect the characteristics of developing countries and tropical conditions**.**

Besides the fact that LandGEM uses the first-order decay equation and IPCC uses the multiphase first order decay equation, there are several other dissimilarities between the models. For example, the lag time required for methane generation to begin after the waste is placed in the landfill is different for both models. LandGEM assumes about 0-1 year lag time, while IPCC considers it to be 0-6 months. Moreover, fugitive methane emissions due to the efficiency of the methane recovery system and methane oxidation are ignored by LandGEM. These factors induce considerable uncertainty in landfill gas modeling.

2.3.3 Other Landfill Gas Generation Models

Several models other have been developed and used for estimating methane emissions from landfills. A brief discussion of some of these models is provided here.

1. *Scholl Canyon Model:* This model is based on first-order kinetics. However, a lag period for initiation of methanogenesis is ignored in the Scholl Canyon Model (Oonk 2010; Reinhart et al. 2005; Thompson et al. 2009).
2. *Triangular Model:* This model assumes that the methane generation rate follows a linearly rising trend in the first phase. In the second phase, the methane generation drops at a linearly decreasing rate (Oonk 2010; Reinhart et al. 2005; Halkadavis, 1983).
3. *Palo Verdes Kinetic Model:* This is a two stage first-order model. In the first stage, gas production rate is assumed to increase exponentially with time, followed by the second stage where the gas production rate decreases exponentially with time. It is also assumed that the maximum gas production rate and transition from first stage to second occurs at the time when the half of ultimate gas production has been reached (Reinhart et al. 2005; USEPA 1998- background emissions).

4. *Sheldon Arleta Model:* Like the Palo Verdes Model, this model assumes a rising exponential curve in the first stage, followed by a decreasing exponential phase in the second, except that the maximum rate is assumed to occur at a time equal to 35% of the total generation period (Reinhart et al. 2005; USEPA 1998- background emissions).
5. *Landfill Gas Generation Model (LFGGEN):* This model assumes that a certain lag time (T_L) precedes anaerobic gas generation. The annual gas generation rate is assumed to increase linearly until it reaches a peak rate, which occurs at time (T_p), followed by an exponential decrease from peak rate to near zero at the end of the time (T_f). The factors T_L, T_P and T_F are dependent on type of waste and the moisture conditions (Cooper et al. 1992).
6. *California Landfill Methane Inventory Model (CALMIM Model):* This model relies on field validated modeling of methane emissions as "net" emissions rate than methane generation. Methane diffusion is calculated through the top layer, and methane oxidation in the top layer is used for estimating methane emissions. The methane emission depends on the top layer composition, and daily variations in climatic conditions. This model is currently being field validated (Spokas et al. 2009; Bogner et al. 2011).
7. *First-Order Kinetics Two Stage Reaction Model (FKSTR):* This model takes in to account the actual biochemistry for determining methane generation from landfills. FKSTR model first calculates the intermediate products (organic acid and carbon dioxide) based on acidification and methanation reactions. The gas generation rates are calculated in next step from the difference between the degraded waste and the generated intermediate products (Chen et al. 2009).

In addition, several researchers have attempted to model the methane generation from landfills using saturation kinetics (e.g. Monod's kinetics) under substrate-limiting or microbe-

limiting conditions (Alvarez and Martinez-Viturtia 1986; Meima et al. 2008; El-Fadel 1999). Meima et al. (2009) performed a sensitivity analysis and detailed literature review on the input parameters used in modeling methane emission using Monod's kinetics. They observed that the model is very sensitive to the input parameters, which are likely not available in actual landfill scale studies.

According to Oonk (2010), the Scholl Canyon Model, Triangular Model, and Zero order models were simplified models and predecessors of current models which are no longer used in practice since the current first order and multiphase first order models are more accurate as compared to its predecessors. Amini et al. (2012) performed a review of the studies that have compared the different landfill gas generation models (See Table 2.6).

From Table 2.6 it can be seen that most models tend to overestimate the methane generation from landfills. The errors are in some cases upto 1109% higher the measured data. The authors concluded that the model's performance usually depends on its input parameters (k and L_o), which are likely not available for a certain climatic condition. Further methane recovery and oxidation values are difficult to estimate, all these conditions contribute towards the errors in estimation (Oonk 2010, Amini et al. 2009, Thompson et al. 2009).

Table 2.6: Summary of Landfill Gas Generation Model Performance (Source: Amini et al. 2012)

Study	**Years of data**	**Models**	**Landfill characteristics**	***k*** yr^{-1}	L_0 $m^3\ g^{-1}$	**Error**	**References**
Validating LFG generation models based on 35 Canadian landfills	NA	Zero-order German EPER TNO Belgium Scholl Canyon LandGEM version 2.01	35 Canadian landfills	0.023–0.056	90–128	-81% to +589%	Thompson et al. 2009
The CDM landfill gas projects by the World Bank	1–3	IPCC First-order US EPA LandGEM Dutch Multiphase Scholl Canyon	Six landfills in South America and Europe	0.014–0.28	68–102	-3% to +1109%	Willumsen and Terraza 2007
Comparison of landfill methane emission models: A case study	NA	US EPA LandGEM French ADEME UK GasSim IPCC Tier 2	Four French landfills	0.04–0.50	44–170	−65% to +140%	Ogor and Guerbois 2005
Landfill gas energy recovery: economic and environmental evaluation for a case study	NA	Scholl Canyon	Casa Rota Landfill, Tuscan, Italy	0.07–0.36	13–30	5%	Corti et al. 2007

Most models use a first-order exponential decay equation for modeling methane generation from landfills, with a few modifications (Thompson et al. 2009). However, the model performance is dependent on the input parameters, which in case of first-order models are L_o and k values. Hence it is crucial to accurately estimate the model parameters for achieving higher accuracy in model predictions.

2.4 Ultimate Methane Generation Potential (L_0)

The ultimate methane generation potential of a landfill depends primarily on the waste composition. IPCC's model incorporates this effect by considering the degradable organic content of the waste. However, climatic factors such as rainfall also affect the amount of methane that can be generated from a landfill.

Ultimate methane generation potential of a landfill can be evaluated using the stoichiometric analysis and Cellulose-Hemicellulose-Lignin data, or using laboratory analysis such as Biochemical Methane Potential (BMP) and laboratory simulations.

2.4.1 Stoichiometric Analysis

Cooper et al (1992) illustrated that the methane potential of waste can be determined using stoichiometric analysis of the waste components, using a general equation (Eq. 2-1). The equations below were derived using Eq. 2-1 for determining the amount of methane and carbon dioxide that can be generated using the stoichiometric analysis of waste. The elemental composition for MSW components suggested by Cooper et al. (1992) is not included here due to inconsistent units.

The amount of methane that can be generation from any component can be calculated using Eqs. 2-13 and 2-14 (Cooper et al. 1992)

$$L_{0_{CH_4}} = \frac{(4a+b-2c-3d-2e)}{8} \times \frac{MW_{CH_4}}{\rho_{CH_4}} \times \frac{1}{MW_y} \times \left(1 - Ash_y\right) \times \left(1 - MC_y\right) \quad (2\text{-}13)$$

$$L_{0_{CO_2}} = \frac{(4a-b+2c+3d+2e)}{8} \times \frac{MW_{CO_2}}{\rho_{CO_2}} \times \frac{1}{MW_y} \times \left(1 - Ash_y\right) \times \left(1 - MC_y\right) \quad (2\text{-}14)$$

The elemental analysis of waste components was reported by several authors (Tchobanoglous et al. 1993; Cho et al. 1995; Jeon et al. 2007; Shanmugam and Horan 2009;

Chiemchaisri et al. 2007). A comparison of the stoichiometric analysis of waste components is shown is Table 2.7.

Table 2.7: Elemental Analysis of Waste Components Reported in the Literature

Source	Waste Component	C	H	O	N	S
Cho et al. (1995)	Boiled Rice	40.9	7.5	50.0	1.6	
	Cooked Meat	53.4	8.4	27.7	10.5	
	Fresh Cabbage	39.9	5.4	50.6	4.1	
	Mixed Korean Food Waste	51.2	7.8	37.8	3.2	
Jeon et al. (2007)	Food Wastes	38.1	2.5	23		
	Paper	38.7	5.5	43.9		
	Plastics	79.4	13.5	3.3		
	Wood	47.5	6.2	42.3		
	Textile	52.9	5.6	40.5		
	Rubber	68.1	7.8	5.3		
	Leather	52.2	6	28.6		
Tchobanoglous et al. (1993)	Food	48.0	6.4	37.6	2.6	0.4
	Paper	43.5	6	44	0.3	0.2
	Cardboard	44	5.9	44.6	0.3	0.2
	Plastics	60	7.2	22.8		
	Textiles	55	6.6	31.2	4.6	0.15
	Rubber	78	10		2	
	Leather	60	8	11.6	10	0.4
	Yard Wastes	47.8	6	38	3.4	0.3
	Wood	49.5	6	42.7	0.2	0.1
	Inorganic- Glass	0.5	0.1	0.4	<0.1	
	Inorganic- Metals	4.5	0.6	4.3	<0.1	
	Dirt, ash etc	26.3	3	2	0.5	0.2
Shanmugham and Horan (2008)	Bulk MSW	27.5	3.8	1.3	30.5	0.4
Cheimchaisri et al. (2007)	Bulk MSW	44.7	5.1	29.37	1.0	0.05

Jeon et al. (2007) determined the ultimate methane potential of waste components using stoichiometric analysis (See Table 2.7). The authors also attempted to find the ultimate

methane potential using Biochemical Methane Potential (BMP) analysis (explained in Section 2.4.3). The difference between the stoichiometric methane potential and the BMP values was used to determine the extent of degradation. However, the stoichiometric analysis done by Jeon et al. (2007) did not include nitrogen and sulfur content of solid waste; hence, some of the values are not consistent with those reported in the literature.

However, not all of the carbon present in the solid waste can be degraded under anaerobic conditions. Some carbon may be recalcitrant and will be stored in the landfill (Staley and Barlaz 2009). The amount of methane calculated from Eq. 2-13 needs to be corrected to the methane that can be generated under anaerobic conditions using a biodegradability factor (See Table 2.9).

2.4.2 Determination of Cellulose, Hemicellulose and Lignin (C, H, L)

Several researchers have attempted to find the ultimate methane potential of waste by finding the cellulose, hemicellulose and lignin content of the waste (Barlaz et al. 1990; Rees 1980; Eleazer et al. 1997; Komilis and Ham 2003; Rao et al. 2000; Brenda et al. 1998; Jones et al. 1983; Rhew and Barlaz 1995). Typical cellulose, hemicellulose and lignin content found in municipal solid waste components are shown below in Table 2.8.

While lignin is assumed to be poorly degradable and is unaffected during biological degradation, cellulose and hemicellulose are easily degraded under anaerobic conditions. Hence, the ratio of cellulose and hemicelluloses to lignin ((C+H)/L) is considered as an indicator of waste decomposition in landfills. It has been reported that the (C+H)/L ratio decreases as the waste age increases (Mehta et al. 2002; Barlaz 2006; Bookter and Ham 1982). The methane generated due to cellulose and hemicelluloses decomposition can be calculated using Eqs. 2-15 and 2-16 (Barlaz 2006):

$$(C_6H_{10}O_5)_n + nH_2O \rightarrow 3nCO_2 + 3nCH_4 \quad (2\text{-}15)$$

$$(C_5H_8O_4)_n + nH_2O \rightarrow 2.5nCO_2 + 2.5nCH_4 \quad (2\text{-}16)$$

Table 2.8: Cellulose, Hemicellulose, and Lignin Content of Waste Components Reported in the Literature

Waste	Reference	Cellulose	Hemi-cellulose	Lignin	Extent of decomposition
Grass	Eleazer et al. (1997)	26.5	10.2	28.4	94.3
	Komilis and Ham (2003)	39.67	16.89	17.63	
Leaves	Eleazer et al. (1997)	15.3	10.5	43.8	28.3
	Komilis and Ham (2003)	9.48	3.24	33.88	
Branches	Eleazer et al. (1997)	35.4	18.4	32.6	27.8
Food waste	Eleazer et al. 1997	55.4	7.2	11.4	84.1
	Komilis and Ham (2003)	46.09	0.0	12.03	
Coated paper	Eleazer et al. (1997)	42.3	9.4	15	39.2
Old newsprint	Eleazer et al. (1997)	48.5	9	23.9	31.1
Old corrugated containers	Eleazer et al. (1997)	57.3	9.9	20.8	54.4
Office paper	Eleazer et al. (1997)	87.4	8.4	2.3	54.6
Mixed paper	Komilis and Ham (2003)	69.66	7.79	15.90	
MSW	Eleazer et al. (1997)	28.8	9.0	23.1	58.4
	Barlaz (1990)	51.2	11.9	15.2	
	Rao et al. 2002)	15.5	19.5	8.5	
	Bookter and Ham (1982)	42.4		10.9	
	Brenda et. al (1998)	48.2	10.6	14.5	
	Rhew & Barlaz (1995)	38.5	8.7	28.0	
	Jones et al. (1983)	25.6	6.6	7.2	

Similar to the stoichiometric analysis, the methane calculated from C, H, L analysis also needs to be corrected using biodegradability factors (See Table 2.9).

2.4.3 Biochemical Methane Potential (BMP)

The third and the most commonly used method for finding ultimate methane potential (L_0) is the Biochemical Methane Potential test. The BMP test relies on methane production from

an anaerobically degrading sample in a defined nutrient media as a measure of decomposition. The measured amount of ground solid waste sample, preferably passing through a 2 mm sieve, is allowed to degrade with a measured amount of inoculum (seed) and nutrient medium in an air-tight bottle for 30-60 days. Gas that accumulates in the headspace of the bottle is measured using gas chromatography. A detailed procedure for conducting BMP test and for preparing nutrient medium has been described in Shelton and Tiedje (1984). Bogner (1990) and Wang et al. (1994) suggested further modifications to the BMP procedure. Chynoweth et al. (1993) found that the BMP test results are sensitive to the particle size of solid waste, inoculum-to-feed ratio, and the nutrient medium used for the test. Hansen et al. (2007) and Angelidaki et al. (2009) have suggested standard protocols for BMP tests to avoid such variability.

Owens and Chynoweth (1992) determined methane potential for waste components using the BMP method. The rate of degradation of waste components (*k* value) was also determined in this study. However conditions in a BMP assay are different compared to an actual landfill. Hence, the *k* values obtained from BMP tests cannot be used for landfill decay. The BMP assay has been used by several researchers for finding the ultimate methane potential of solid waste components. Gunaseelan (2004) found ultimate methane potential of 54 fruits and vegetables for using the BMP test. Chynoweth et al. (1993) attempted to find the ultimate methane potential of mixed MSW and MSW components such as yard waste, vegetable waste, grass, seaweeds, wood etc. Jeon et al. (2007) used the BMP test for finding ultimate methane potential of Korean waste and food waste components. Isci and Demirer (2007) found the methane potential of cotton stocks, cotton seed hull and cotton oil cake to be 65, 86 and 78 mL CH_4/g of waste, respectively. The ultimate methane potentials reported by these researchers are compiled in Figure 2.2 and 2.3.

In addition, the BMP is also used as an indicator of biodegradation. Francois et al. (2006) found that the BMP of old waste is less than the BMP of fresh waste. Wang et al. (1994) also observed that the BMP reduces as the waste age increases, suggesting that the BMP test can be used as an measure of remaining methane potential of old waste. Bigilli et al. (2009) used the BMP test to determine the initial and remaining methane potentials of solid waste during the operation of two pilot scale lab reactors which were operated with leachate recirculation and without leachate recirculation. The initial methane potential of solid waste was 0.347 L of CH_4/g of dry waste, and the final methane potentials of degraded solid waste samples obtained from leachate recirculated and non-recirculated reactors were 0.117 and 0.154 L of CH_4/g of dry waste, respectively.

2.4.4 Laboratory Scale Landfill Simulations

Eleazer et al. (1997) demonstrated that simulated landfill bioreactors can be used for finding the ultimate methane potential of waste components in a landfill. Eleazer et al. (1997) studied the biodegradability of waste components including grass, leaves, branches, food waste, coated paper, old newsprint paper, old corrugated containers, office paper and mixed MSW in 2-litre simulated landfill bioreactors. These reactors were operated under conditions suitable for biodegradation (test temperature = 40^{o}C, leachate was neutralized and recirculated and the waste was shredded) until the methane generation dropped to a low constant value. Although the ultimate methane potential values reported by Eleazer et al. (1997) gave a realistic estimate of the extent of degradation of waste components in a bioreactor landfill, the duration for this kind of test was very long. Moreover, this study did not consider the effect of temperature and moisture on the L_0. The ultimate methane potential values reported by Eleazer et al. (1997) are combined with BMP results and are shown in Figure 2.2 and 2.3.

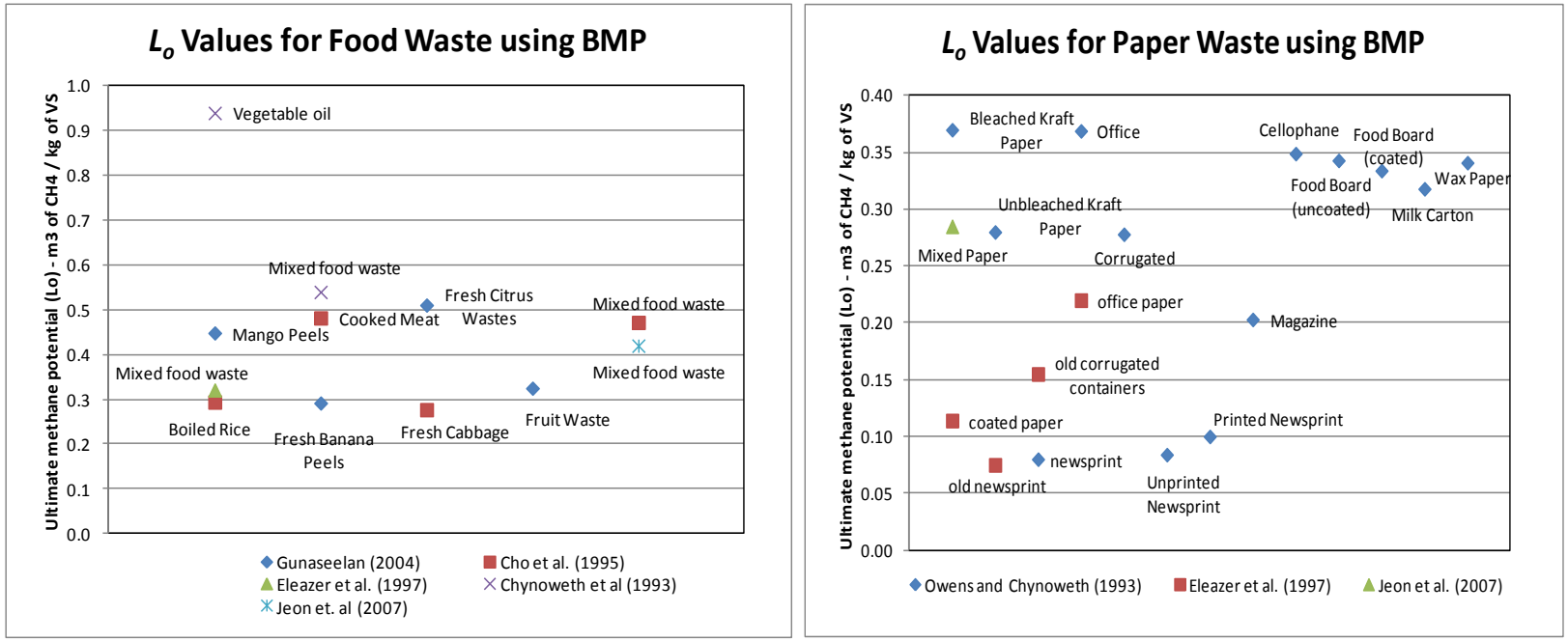

(a) (b)

NOTE: 1- BMP values are converted in mL/g of VS to get consistent units. Conversions are done using Volatile Solids values reported in the paper.

Figure 2.2: Ultimate Methane Potential using BMP and Lab-Scale Simulations for (a) Food Waste, (b) Paper Waste.

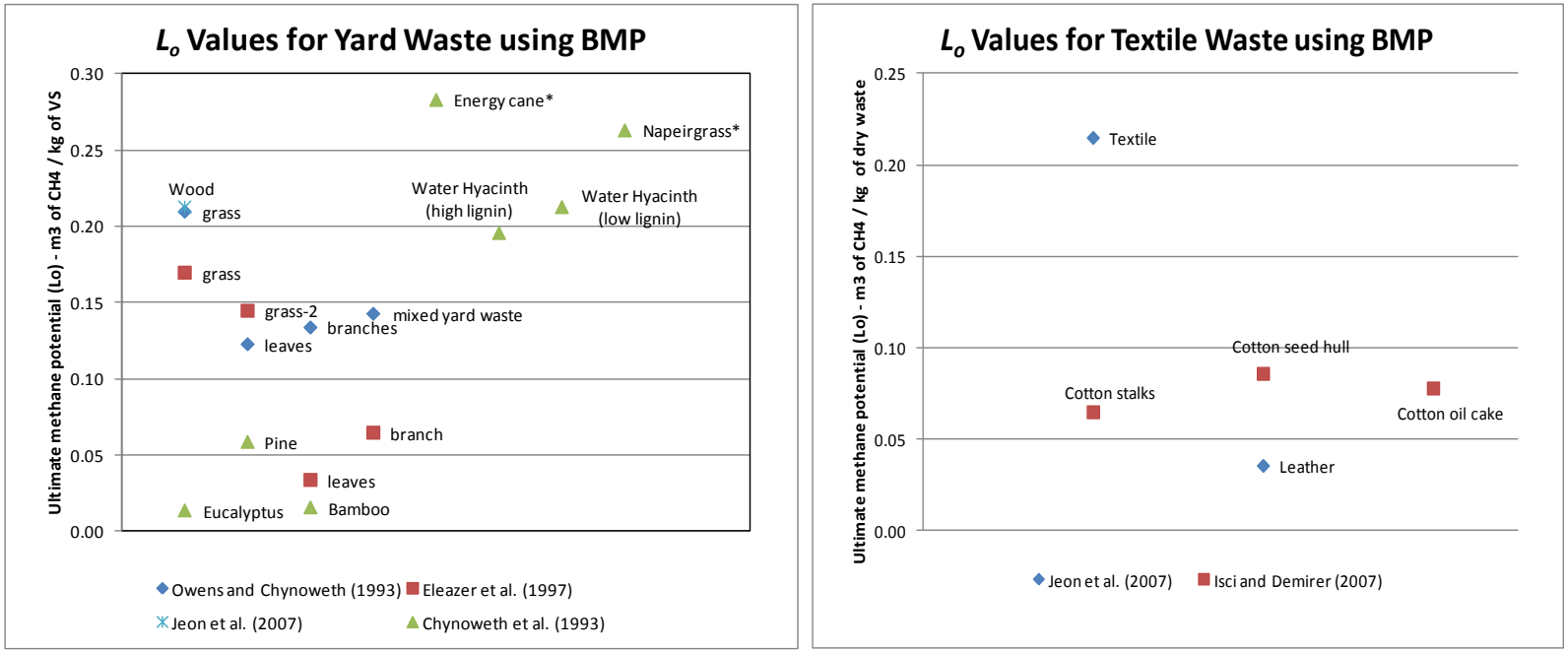

(a) (b)

NOTE: 1- BMP values are converted in mL/g of VS to get consistent units. Conversions are done using Volatile Solids values reported in the paper.
2- BMP for textile waste is represented in mL of CH_4/g of dry waste, because the Volatile Solids value was not available in some papers

Figure 2.3: Ultimate Methane Potential using BMP and Lab-Scale Simulations for (a) Yard Waste, and (b) Textile Waste

2.4.5 Comparison of Methods for Determining Ultimate Methane Potential

While the stoichiometric analysis method and C, H, L determination methods are faster, they often yield very high methane potential values, because methane potential calculated from these methods assumes that the entire carbon would be converted to methane. However, the extent of carbon conversion to methane under anaerobic conditions is limited; hence, the biodegradation factors need to be incorporated in each case to account for the recalcitrant carbon. Barlaz et al. (1997) and Jeon et al. (2007) reported the difference between the stoichiometrically calculated methane potential and BMP values. The ratio of methane potential obtained from BMP (or from lab scale studies) to the methane potential calculated using the stoichiometric or C, H, L analysis was reported as the biodegradability factor (Jeon et al. 2007; Barlaz et al. 1997).

Machado et al. (2009) performed a literature review of the biodegradability factors reported by different researchers. The biodegradability factors reported by Machado et al. (2009) and Jeon et al. (2007) are tabulated in Table 2.9.

It must be noted that the biodegradation factors were computed by researchers using lab scale anaerobic degradation studies (e.g. BMP, lab scale simulated landfills), thereby creating "ideal" conditions for biodegradation through shredding, controlling pH or by optimizing C/N ratio. Using these factors can help to compute the maximum amount of methane that can be generated from solid waste under anaerobic conditions. However, in practice the actual conditions may differ from the ideal conditions and hence an uncertainty in modeling efficiency is introduced.

While BMP tests provide the best guess for the ultimate methane potential of the solid waste, the tests are time-consuming and require 30-60 days for completion. Moreover, given

the heterogeneity of solid waste, it is very difficult to obtain a "representative sample" of solid waste. Hence, multiple samples need to be analyzed to gain an estimate of the ultimate methane potential of waste. Researchers have attempted to study the relationship between other faster and simpler methods (such as cellulose, hemicellulose, lignin, volatile solids, and total carbon) and BMP of solid waste samples.

Table 2.9: Biodegradability factors Reported in the Literature (adopted from Machado et al. (2009) and Jeon et al. (2007)

Source	Paper	Card-board	Food waste	Garden Waste	Wood	Textiles	Plastics
Tchobanoglous et al. (1993) and Bonori et al. (2001)	0.44	0.38	0.58	0.45	0.61	0.4	
Barlaz et al. (1997)	0.19-0.56	0.39	0.7	0.70-0.34	0.14		
Harries et al. (2001)	0.30-0.40	0.44		0.20-0.51	0.30-0.33	0.17-0.25	
Lobo (2003) - adopted	0.4	0.41	0.64	0.35	0.17	0.32	
Jeon et al (2007) - adopted for stoichiometric analysis	0.69		0.68		0.43	0.45	0.06

Wang et al. (1994) attempted to correlate (C+H)/L content of 10 samples collected from a Berkeley, California landfill with BMP measured in the lab. The authors found that the data had a low R^2 value (0.67), indicating that cellulose and hemicellulose is not well correlated with measured BMP. Eleazer et al. (1997) assessed the ultimate methane potential of MSW components in 2 litre reactors. They observed that the cellulose and hemicelluloses were not well correlated with methane production (R^2=0.49).

However, some studies contradict with the above results. Godley et al. (2005) carried out a review of different methods used for estimating biodegradability of wastes. The different

methods studied included biological and non-biological tests such as Dry Matter (DM), Loss on Ignition (LOI), Total Organic Carbon (TOC), Total Nitrogen (TN), cellulose, lignin, water-extractable dissolved organic carbon, chemical oxygen demand, biochemical oxygen demand, dynamic respiration index (DRI), specific oxygen uptake ratio (SOUR), BMP and cellulose hydrolysis method. It was found that cellulose and hemicelluloses tests provided useful information on waste composition but were not reliable indicators of waste biodegradability, because experiments with certain waste materials, e.g. wool gave unreasonable C/L ratio. In contrast, Ivanova et al. (2008) found that (C+H)/L was well correlated with BMP (R^2 = 0.84), and concluded that the cellulose and hemicellulose data for fresh MSW could be a valuable indicator of its biodegradability.

Shanmugham and Horan (2009) suggested that stoichiometric methane potential (SMP) together with Adenosine triphosphate can be used as an indicator for BMP of solid waste. Francois et al. (2006) studied the correlation between physical characteristics of waste (particle size and composition) and chemical characteristics (organic matter, organic carbon, and nitrogen content) as indicators of the methane potential of stabilized waste. They reported good correlation between BMP of degraded waste (stabilized waste) and paper cardboard (PC) content of the waste (R^2 = 0.91).

To summarize, studies correlating short term chemical analysis test with BMP test results have been inconclusive. Hence BMP, although time-consuming, is considered as the most reliable estimate of the ultimate methane potential of waste (L_0) (Wang et al. 1994; Francois et al. 2006; Godley et al. 2003; Kelly et al. 2006).

However, BMP of a solid waste sample provides the maximum amount of methane that can be produced if the waste is allowed to decompose in a landfill. The conditions in the BMP

test are optimal for methanogenesis (shredded waste, presence of macro and micro nutrients, controlled pH, optimum availability of microorganisms), while conditions in a landfill are mostly not optimum for growth.

The ultimate methane potential of a landfill (L_0) is affected by the moisture content (rainfall). IPCC mentions that L_0 is dependent on moisture, but fails to account for the rainfall effect on L_0. LandGEM ignores the effect of moisture on L_o values. Kamalan et al. (2011) performed a review of landfill gas models used worldwide, and found that only a couple of models suggest default values for L_0 with respect to moisture. BMP and all other techniques described above in this section ignore the effect of moisture and temperature on L_0.

2.5 Rate of Degradation (*k* value)

The rate of degradation of solid waste in landfills depends on waste composition, waste particle size, moisture, ambient temperature, and pH (Barlaz et al. 1990). As the *k* value increases, the methane generation rate from landfills increases. Alternative term used to denote the rate of degradation is half life ($t_{1/2}$), which is the amount of time required for the degradable organic matter in waste to decay to half of its initial mass. The relationship between *k* and $t_{1/2}$ is given in Eq. 2-17.

$$k = \frac{Ln\,(2)}{t_{1/2}} \tag{2-17}$$

The defaults for *k* values suggested by LandGEM and IPCC are shown in Tables 2.3 and 2.4, respectively. In this section the factors affecting rate of degradation (*k* value) and the methods of determination of *k* value are discussed.

2.5.1 Factors Affecting Methane Generation Rate in Landfills

Waste composition, waste particle size, moisture content, ambient temperature, and pH have been observed to impact methane production rates, and thus need to be accounted for in methane generation models (Barlaz et al. 1990). pH inside a landfill is typically unknown, and hence is not included in landfill gas generation models (Stege 2009). Reduction in particle size has been found to be favorable for methane generation from landfills. Shredded and well-mixed refuse is expected to permit greater contact to moisture and microorganisms. However, shredding of waste is seldom applied for landfills, and hence is also excluded while modeling. The key parameters that affect the methane generation rate constant (*k* value) are thus waste composition, moisture and temperature.

2.5.1.1 Waste Composition

Waste composition changes with geographical location, depending on economic conditions, lifestyle, industrial structure and waste management techniques. Guermond et al. (2009) compiled the waste composition information published for various countries (See Table 2.10).

Table 2.10: Waste Composition Found in Different Countries
(Adopted from Guermond et al. (2009))

Country	City	Organic Matter	Cardboard	Plastics	Metals	Glass
Morocco	Agadir	65-70	18	2-3	5.6	0.5-1
Jordan	Amman	63	11	16	2	2
Turkey	Istanbul	36.1	11.2	3.1	4.6	1.2
Tunisia	Tunis	68	11	7	4	2
Mauritania	Nouakchott	48	6.3	20	4.2	4
Guinea	Labe	69	4.1	22.8 (+textile)	1.4	0.3
France	Paris	28.8	25.3	11.1	4.1	13.1
Portugal		35.5	25.9	11.5	2.6	5.4
Greece	Palermo	31.7	23.1	11.8	2.7	8.3
Canada	Toronto	30.2	29.6	20.3	2.1	2

It is evident from Table 2.10, that the percent of organic matter in waste is higher in developing nations than developed nations (Guermoud et al. 2009).

The waste composition also changes over time due to changes in waste management practices, and the economic development of the region. The change in waste composition found in the U.S. over the last few decades is shown below (See Figure 2.4).

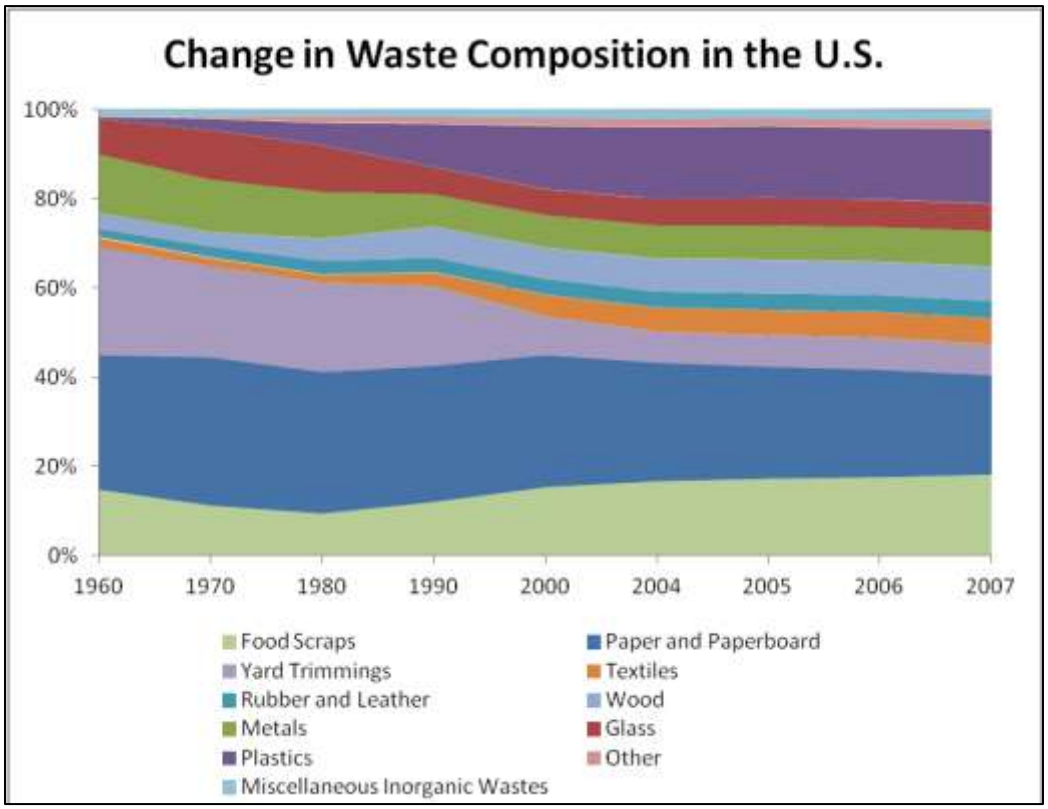

Figure 2.4: Change in Waste Composition in the U.S.

The amount of methane generated from a landfill depends on the organic content of the waste. Further, different types of waste degrade at different rates. Hence, the rate at which methane is generated from landfills also depends on the waste composition.

Owens and Chynoweth (1992) and Chynoweth et al. (1993) evaluated L_0 and k of various waste components using the Biochemical Methane Potential (BMP) test. While the BMP method

is a reliable test for finding the ultimate methane potential L_0, the conditions in a BMP reactor cannot be considered truly representative of conditions in a landfill; hence, the *k* estimates are not realistic and cannot be applied in a landfill scenario. However, the Owens and Chynoweth (1992) study is helpful for understanding the relative rates of degradation of different waste components.

Tchobanoglous et al. (1993) divided waste components into 2 categories (rapidly-degrading, and slowly-degrading). Cooper et al. (1992) conducted a review of the rates of degradation used for different waste components, and additionally went a step further by defining a category of moderately-degrading wastes to be considered in multiphase models (See Table 2.11).

Table 2.11: Relative Degradation Rates for Waste Components
(Source: Cooper et al. 1992)

MSW Component	**Findikakis (1988)**	**Tchobanoglous (1992)**	**EMCON (1982)**	**Ham (1979)**	**EMCON**	**Cooper et. al. (1992)**
Food	R	R	R	R	R	R
Paper	M	R	M	M	M	R,M,S
Cardboard	M	R	M	M	M	S
Plastics	S				S	S
Textiles	S	S	M		M	S
Rubber		S			S	S
Leather	S	S				S
Yard Waste	M	R,S	R	M	R	M,S
Wood	S	S	M	M	M	S
Mic. Organics		S				

US EPA's Landfill Methane Outreach Program (LMOP) in conjunction with U.S. Agency for International Development has developed model parameters (L_0 and *k*) for countries such as China, Colombia, Ecuador, Mexico, Philippines, Thailand, Ukraine, and for countries in Central America. The model parameters were developed by working with each country to gather data

to develop L_0 and k values. Out of the 8 landfill models developed under the LMOP program, models for 3 countries (namely Columbia, Mexico and Ukraine) divided the waste in 4 categories; L_0 and k values were suggested for each category. However, LMOP uses the equations suggested by LandGEM for computing the methane generation rates from the landfills. As mentioned earlier (See Section 2.3.1), LandGEM uses a simple first-order decay equation and thereby assumes that the waste is homogenous. The provision of including different waste degradation rates for different waste components is not included in LandGEM. Hence, the total landfill methane generation rate is calculated as the sum of methane generated by each waste category. This approach assumes that the individual waste components do not affect each other's degradation. Moreover, the process of finding field specific L_0 and k values for individual countries is time consuming (Stege 2009). The degradation rates suggested by LMOP for waste components are compared against the default k's recommended by IPCC and are shown in Table 2.13.

Oonk and Boom (1995) attempted to find the model parameters for a multiphase model for waste using data from nine Dutch landfills. The waste was divided into 3 categories; rapidly, moderately and slowly degrading wastes. The values for k were determined by trial and error method using SAS. The values suggested by Oonk and Boom (1995) are k_{rapid}= 0.185 yr^{-1}, $k_{moderate}$ =0.1 yr^{-1}, and k_{slow} = 0.03 yr^{-1}.

IPCC (2006) suggested default k values for the multiphase model for 4 different waste categories: rapidly, moderately and slowly degrading waste (See Table 2.13). As mentioned earlier in Section2.3.2, IPCC mentions that the information for k values for tropical conditions is limited, and default values were suggested based on the assumptions and values obtained from the studies conducted temperate conditions.

Cruz and Barlaz (2010) attempted to find *k* for different waste components based on an earlier published work by Eleazar et al. (1997). Laboratory scale *k* values were computed for 7 waste components based on the rates of degradation observed in 2 liter capacity laboratory scale bioreactors operated at conditions suitable for enhanced degradation. A *k* value for combined waste was computed using a weighted average. Further, the *k* values for combined waste from lab studies were scaled to match the values recommended by USEPA (2005) for field scale *k* values. A scaling factor (*f*) was computed for each waste component using the field scale *k* values. The lab scale and field scale *k* values for waste components and scaling factor (*f*) computed by the authors is shown in Table 2.12. The authors observed that the field scale *k* values for waste components used in this study are applicable only if the k_{field} value of combined waste is known. Secondly, this study assumes that the waste components do not influence each other's degradation. In addition, this study does not incorporate the effect of moisture and temperature on the rates of degradation, since the lab scale study was conducted on bioreactors with leachate recirculation at 37^{o}C. Hence, the values computed in this study have significant uncertainty (Eleazer et al. 1997; Cruz and Barlaz 2010).

A number of studies have developed *k* values for mixed waste, but not as functions of waste composition, and hence have not been included in the discussion here (Oonk and Boom 1995a; Brown et al. 1999; Solid Waste Association of North America 1998). It is evident from Tables 2.11 and 2.13 that the method of combining waste categories for gas modeling is not clear. There is a lot of variation in *k* values for each category; hence studies for estimating *k* values as functions of waste composition are needed, particularly as functions of rainfall/moisture content and ambient temperature.

Table 2.12: Lab Scale and Field Scale *k* Values Reported by Cruz and Barlaz (2010)

MSW component	discarded composition[a] (wet wt %)	k_{lab} (yr^{-1})	comments	$k = 0.04$ $k_{field} = k_{lab} \times f$ (yr^{-1})	$k = 0.12$ $k_{field} = k_{lab} \times f$ (yr^{-1})
textiles (cotton)[b]	0.71	3.08	equal to office paper	0.020	0.059
wood (non-C&D)	7.02	1.56	equal to branches	0.010	0.030
food waste	12.10	15.02		0.096	0.289
leaves	7.18	17.82		0.114	0.343
grass	5.43	31.13		0.200	0.600
branches	5.30	1.56		0.010	0.030
miscellaneous organics	1.40	13.68[b]	equal to average of food, wood, grass, leaves, and branches	0.088	0.263
newspaper	5.17	3.45		0.022	0.066
office paper	4.97	3.08		0.020	0.059
coated paper	1.47	12.68		0.081	0.244
corrugated containers/ Kraft bags	7.26	2.05		0.013	0.040
mixed paper	11.66	3.27	equal to average of office paper and newsprint	0.021	0.063
total biodegradable fraction	69.66[c]				
assumed bulk MSW decay rate				0.040	0.120
correction factor, *f*				0.0064	0.0192

[a] The composition of the waste discarded was calculated from the difference in waste generation and recovery as given in ref (*11*). [b] Roughly ~23.7% of textiles consumed in the United States from 2001 to 2005 were made of cotton ref (*22*). [c] Other components are inert (e.g., plastic and glass) and therefore the total does not sum 100%.

A number of studies have developed *k* values for mixed waste, but not as functions of waste composition, and hence have not been included in the discussion here (Oonk and Boom 1995a; Brown et al. 1999; Solid Waste Association of North America 1998). It is evident from Tables 2.10 and 2.11 that the method of combining waste categories for gas modeling is not clear. There is a lot of variation in *k* values for each category; hence studies for estimating *k* values as functions of waste composition are needed, particularly as functions of rainfall/moisture content and ambient temperature.

2.5.1.2 Moisture Content

A number of studies have confirmed that methane generation rate increases with an increase in waste moisture content (Barlaz et al. 1990; Mehta et al. 2002; Wreford et al. 2000; Alvarez and Martinez-Viturtia 1986; Chan et al. 2002; Lay et al. 1998). This may be due to increased contact between microbes and waste, as well as mobilization of nutrients, buffer and dilution of inhibitors. Lab scale studies concluded that leachate recirculation and neutralization

can be beneficial for methane generation, since it not only helps in distributing the nutrients, but also facilitates faster degradation due to dilution of carboxylic acids which accumulate at the end of phase one (See Section 2.1.2) (Barlaz et al. 1990; Rees 1980; Buivid et al. 1981; Sanphoti et al. 2006).

Faruquhar and Rovers (1973) conducted a critical review of the factors affecting methane generation in landfills, and found that maximum methane production was reported at moisture contents of 60% to 80% on wet weight basis. Rees (1980) plotted the methane generation and moisture content data published in research papers and found that the log of methane generation rate produced from landfills is directly proportional to the moisture content (See Figure 2.5a).

Solid Waste Association of North America (SWANA) (1997) also developed a curve of methane generation rate vs. moisture content of waste and observed a linear relationship between log of methane generation rate and moisture content of waste until the waste reaches saturation limit. However, thereafter methane generation rate is assumed to be constant, irrespective of the moisture content of waste. Although the graphs presented in SWANA (1997) and Rees (1980) are useful for calculating a relationship between methane generation rate (or rate constant *k*) with moisture content of waste, they were based on data from different landfills with different mixtures of waste, and are thus not useful for predicting methane generation as a function of waste composition (See Figure 2.5b).

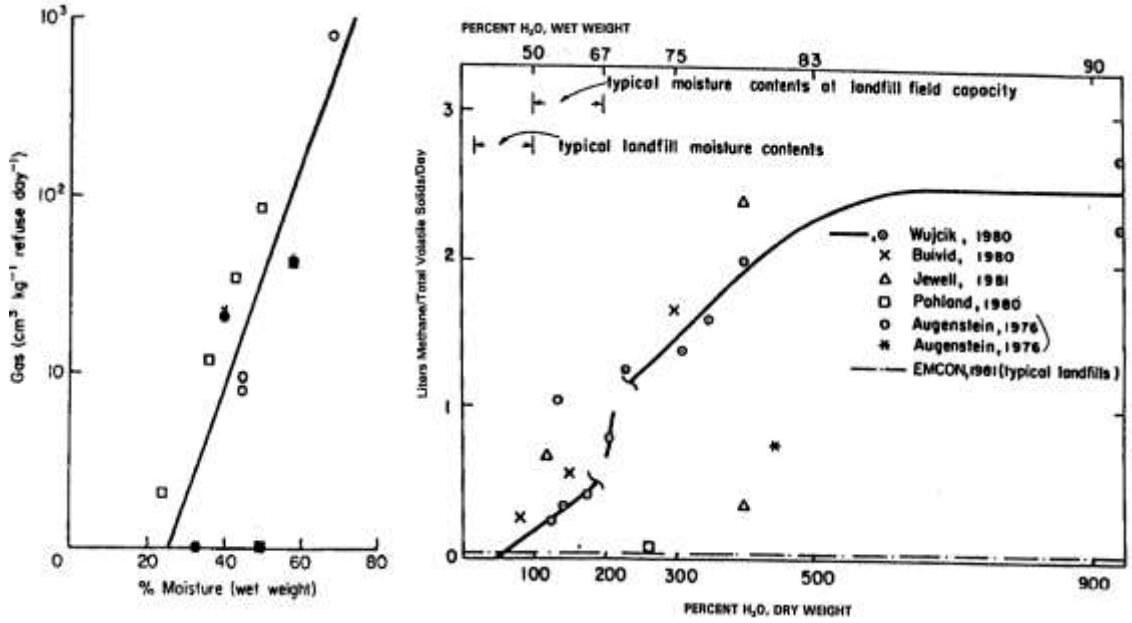

(a) (b)

Figure 2.5: Plots of Moisture Content vs. Methane Generation Rate by (a) Rees (1980) and (b) SWANA (1998)

However, some studies contradict the relationship presented by SWANA (1998). Hernandez-Berriel et al. (2008) studied the effect of moisture content of solid waste on methane generation rate using 6 columns of 14.5 L each. Water addition was done to simulate rainfall such that the moisture content of waste was maintained at 70% and 80%, respectively. The authors found that the methane generation rate was higher in reactors with 70% moisture content than in the reactors with 80% moisture content. Further, Hernandez-Berriel et al. (2010) studied the effect of various moisture regimes on the methane generation rate and leachate characteristics on laboratory scale bioreactors operated with leachate recycle. Four moisture content regimes were studied with 50%, 60%, 70% and 80% moisture content, respectively. It was found that the methane generation rate increased as the moisture content increased from 50% to 70%, with 70% moisture content producing the maximum amount of methane. However,

the methane generation rate dropped in the 80% moisture content reactor, presumably due to washout of nutrients.

Filipkowska and Agopsowicz (2004) also studied the effect of different water conditions on methane generation rate. 6 laboratory scale lysimeters were used at different rates of water addition, as well as variable rates of leachate recirculation. It was observed that the methane generation rate increased with increase in moisture content; however, when the reactor was flooded with water, the methane generation rate dropped sharply due to flooding.

It is evident from these lab scale studies that there may be optimum moisture content above which adding water may actually hinder methane generation, unlike what was suggested by SWANA (1997). However, it must be noted that the type of waste considered in Hernandez-Berriel et al. (2008) and Hernandez-Berriel et al. (2010) is quite different than the type of waste considered in the studies summarized by SWANA (1997): while the former used Mexican waste with higher food and yard waste, the latter used US waste with a higher percentage of paper waste. Paper being water absorbent and moderately-degrading waste, it is likely that the increase in moisture content may increase the methane generation rate. Hence it is important to find a relationship between methane generation rate constant with moisture content along with waste composition to see if any such interactions exists.

IPCC (2006), Stege (2009) and Stege (2010) have recommended default values for *k* values for different rainfall rates as well as different waste components based on the rainfall in the region (See Table 2.13). U.S. EPA considers rainfall effect implicitly by considering 2 regions with rainfall > 25 mm/yr and rainfall < 25 mm/yr for default *k*'s (See Table 2.3). However, a conclusive relationship has not yet been reported.

Table 2.13: Comparison of Default *k* Values Suggested in Different Multiphase Models

Source	Rainfall	Waste Components									
		Food	**20% Diapers**	**Toilet Paper**	**Garden waste green)**	**Paper**	**Card board**	**Textile**	**Wood**	**Straw**	**Rubber**
Stege (2009), M2M for Ukraine		Fast			Medium Fast	Medium Slow			Slowly		
	360-429 mm/yr	0.11			0.055	0.022			0.011		
	430 - 499 mm/yr	0.12			0.06	0.024			0.012		
	500 -599 mm/yr	0.14			0.07	0.028			0.014		
	600 -699 mm/yr	0.15			0.075	0.03			0.015		
Stege (2010), M2M for Columbia		Fast		Medium Fast		Medium Slow			Slowly		
	> 2000 mm/yr	0.4		0.17		0.07			0.035		
	1500-1999 mm/yr	0.34		0.15		0.06			0.03		
	1000-1499 mm/yr	0.26		0.12		0.048			0.024		
	500-999 mm/yr	0.18		0.09		0.036			0.018		
	< 500 mm/yr	0.1		0.05		0.02			0.01		
IPCC (2006)		Fast			Moderate	Slow			Slow		
	Temperate Region MAP/PET < 1	0.05-0.05			0.04-0.06	0.03-0.05			0.01-0.03		
	Temperate Region MAP/PET > 1	0.1-0.2			0.06-0.1	0.05-0.07			0.02-0.04		
	Tropical Region (MAP < 1000)	0.07-0.1			0.05-0.08	0.02-0.04			0.02-0.04		
	Tropical Region (MAP >1000)	0.17-0.7			0.15-0.2	0.06-0.085			0.03-0.05		

Few field scale studies have also confirmed that increase in moisture content of waste (through leachate recirculation) can help to increase the methane generation rate. Mehta et al. (2002) studied the effect of leachate recirculation on methane generation on two 8000 metric ton test cells and found the moisture content in the test cell with leachate recirculation was higher (38.8, 31.7 and 34.8%) than that without leachate recirculation (14.6, 19.2%). Also the methane generation rate in test cells with leachate recirculation was also higher than that without leachate recirculation.

Wreford et al. (2000) studied the effect of precipitation on methane generation rate and gas composition at the Burns Bog Landfill in Vancouver, Canada. It was found that the methane generation rate well correlated with the 14 day precipitation episode with a $R^2 = 0.88$. Gurijala and Sufilta (1993) obtained samples from the Fresh Kills Landfill and incubated them in laboratory scale reactors. Higher endogenous methane generation rates were observed from samples with higher moisture content. Further, supplemental moisture addition led to higher methane generation rates.

Wang-Yao et al. (2006) studied the effect of moisture movement on methane generation rate from 3 sanitary landfills and 4 open dumps in Thailand. Thailand being a tropical country, there was considerable difference in the moisture movement during the wet season as compared to the dry season. The authors found significantly higher methane flux during wet months than in dry months. The authors used the field scale methane data for compute *k* values using USEPA's LandGEM. The *k* values computed by the authors are shown in Table 2.14.

Table 2.14: Change in *k* Values According to the Wet and Dry Season in Thailand
(Source: Wang-Yao et al., 2006)

Site	Landfilling Condition	*k*- wet season (yr^{-1})	*k* dry season (yr^{-1})
Pattaya	Managed Deep	0.192	0.020
Cha-Am	Managed-Shallow	0.040	0.005
Nakomprathom	Unmanaged-Deep	0.005	0.002
Hua-Hin	Managed-Deep	0.138	0.016
Nontaburi	Unmanaged-Deep	0.0003	0.0001
Rayound	Unmanaged-Shallow	0.013	0.004
Samutprakan	Unmanaged- Deep	0.013	0.001

Barlaz et al. (2010) studied the performance of 5 bioreactor landfills in the US. The authors observed that the methane generation rate increases as the amount of moisture added to waste increases. *k* values ranging from 0.08-0.21 yr^{-1} were found in this study, as compared to AP-42's recommended *k* value of 0.04 yr^{-1}. The authors found a good correlation (R^2 =0.66) between *k* and the water added in the horizontal trenches during filling. However, the correlation between *k* and moisture content of the waste was not significant, and hence a definite relationship could not be developed.

Faour et al. (2007) attempted to find *k* values for wet landfills based on data from 29 operating bioreactor landfills. This study concluded that a conservative value of *k* =0.3 yr^{-1} would be reasonable and conservative for bioreactor landfills. However, the model is sensitive to moisture, temperature within the landfill and capture efficiency, which are often difficult to obtain.

It is evident that landfill scale studies confirmed the results obtained from lab scale studies: that the increase in moisture content of waste through leachate recirculation increased the methane generation rate from landfills, and resulted in higher *k* values than traditional landfills. However, a definite relationship between moisture content and *k* values has not been reported. Moreover, these *k* values were dependent on the type of waste in landfills. Hence, the

k value used for a landfill in Thailand for particular moisture content cannot be used for a landfill in the United States. Studies that quantitatively predict methane generation as a function of rainfall/moisture content, however, are lacking, particularly as functions of waste composition.

Gurijala et al. (1997) tried to develop a regression equation based on factors that influence landfill methane generation rate, using various samples collected at the Fresh Kills landfill. This research provided a statistical relationship of moisture content with methane generation rate for mixed waste, but not as a function of waste composition (Gurijala et al. 1997).

Moisture content of landfilled waste depends on initial moisture content of fresh solid waste, evaporation rates (functions of temperature and relative humidity), and annual rainfall. Moisture content of fresh solid waste ranges between 15-40% in the United States. Developing countries like India, Bangladesh and China have reported higher values of moisture content for fresh MSW, which may be due to the higher percentage of food in the waste (Taufiq, 2010). The temperature, relative humidity and annual rainfall further affect the moisture content of the waste in a landfill. The rainfall continuously keeps percolating through the intermediate temporary soil cover until the final cover of the landfill is in place. The water movement through landfilled waste mainly depends on the compaction of the waste. Buivid et al. (1981) showed that the moisture content of landfilled waste decreases with increase in level of compaction. Thus it is difficult to accurately predict the moisture content of waste within a landfill. Hence this study considers annual average rainfall (instead of moisture content of waste) as a parameter for predicting methane generation rate constant *k*.

2.5.1.3 Ambient Temperature

Most microbial processes are affected by temperature. Higher temperatures increase microbial activity, which boosts methane generation rates. Anaerobic degradation is considered to be an exothermic reaction, although the heat generated during anaerobic degradation is only 7% of that generated during aerobic degradation. Hence the temperature in a landfill is expected to be higher than the atmospheric temperature (Christensen and Kjeldsen 1989; Rees 1980; Bingemer and Crutzen 1987).

Faruquhar and Rovers (1973) found that the temperature of waste inside a landfill primarily depends on the temperature at which the waste was placed and also on the landfill management practices. The temperature is often found to be higher in the landfills if the aerobic phase was extended due to air leaks (or poor compaction) or if there was excessive moisture movement in the landfill. Attal et al. (1992) studied the temperature variation from borehole samples collected from Villeparisis technical landfill, France, where the waste age was about 6-8 years. It was found that the temperature inside the landfill increased steadily from 26^{o}C to 50^{o}C as the depth increased from 2 to 10 m. After 10 m to about 50 m below the ground level, the temperature within the landfill was found to stable at around 50^{o}C. Chiampo et al. (1996) also conducted a similar study based on borehole samples collected from an Italian landfill. It was found that the temperature increased from 15^{o}C to 50^{o}C in the upper 6 meters of waste and thereafter was constant at between 50-60^{o}C. Jones et al. (1983) also found a similar temperature distribution at Aveley landfill, UK. The waste temperature stabilized at 40-50^{o}C 6 m below the ground level. Maurice et al (1997) studied temperature variation in solid waste test cell for a period of 1 year, and found that the waste temperature is often higher than the ambient temperature and varies only ±1^{o}C over the winter and summer period.

While Attal et al. (1992), Chiampo et al. (1996) and Jones et al. (1983) study results were based on one time sampling events, Maurice (1997) included long term temperature measurement at relatively low depths.

Yesiller et al. (2003) studied the spatial distribution of temperature over time in a landfill located in Michigan, US. The authors concluded that temperature of waste is significantly affected by seasonal variations, placement of waste, age of waste, depth and location of waste together with available moisture. The waste temperature was observed to increase due to leachate recirculation.

Hansen et al. (2005) studied long term spatial and temporal variation in temperature in landfilled waste located in Alaska, British Columbia, Michigan and New Mexico. The authors recorded the highest temperature at the central location within the landfill and lower temperatures were observed above and below the central zone. The authors found that the temperatures were affected by the temperature during placement of the waste. Waste temperature was also affected by waste age. During the first few years after waste placement (0-10 yrs), temperature increased rapidly; however, thereafter it reduced and stabilized. Time-averaged waste temperature ranges were 0.9-33.0^{o}C for Alaska, 14.4-49.2^{o}C for British Columbia, 14.8-55.6^{o}C Michigan, and 20.5-33.6^{o}C for New Mexico. The highest temperature fluctuations were found in Michigan due to high precipitation/ moisture content, whereas lower temperature variation was found in New Mexico was due to dry climatic conditions.

It can be concluded that it is extremely difficult to guess the temperature within a landfill, which is affected by a number of factors such as waste age, depth, proximity to the landfill's edges, temperature during placement, and moisture content. However, the temperature acts as both a stimulator and response to biodegradation. The higher temperature

measurements observed in the landfills may be due to the presence of anaerobic microorganisms. It is, however, crucial to study the effect of temperature increase on the rate of biodegradation, and whether temperature together with moisture affects the rate of biodegradation.

Laboratory scale studies observed that the methane production rate increases when the temperature is raised from 20 to 30 and 40^{o}C (Christensen and Kjeldsen 1989). Significant reduction in methane generation was observed with temperature less than 20^{o}C and greater than 70^{o}C (Tchobanoglous et al. 1993). Buivid et al. (1981) also studied the effect of temperature on waste degradation in laboratory scale landfill reactors. Three temperatures were chosen, 25^{o}C, 37^{o}C and 60^{o}C. The authors reported that 37^{o}C was the most favorable temperature for enhanced methane generation.

Alvarez and Martinez-Viturtia (1982) conducted lab scale studies on Spanish waste with leachate recycle at 5 different temperatures (30, 34, 38, 44, and 46^{o}C). The authors concluded that the optimum ambient temperatures for methane production to be between 36- 38^{o}C. In addition, Arrehnius's equation was used to determine the effect of temperature on waste degradation in this study. Activation energy (E_a) = 13.27 kcal/mole was reported; however, this value was computed using saturation kinetics instead of first-order degradation kinetics (Alvarez and Martinez-Viturtia 1986; Hartz et al. 1982). El-Fadel et al. (1995) developed a model to predict methane generation rate from landfills based on temperature. However this model incorporated the Monod's kinetics for the model development (El-Fadel 1999).

Thus, it can be inferred from the studies mentioned above that there may be an optimum temperature for methane generation from landfills. SWANA (1998) developed a curve of k vs.1/T (See Figure 2.6); it was, however, developed from data from different landfills with

different mixtures of waste, and is thus not useful for predicting methane generation as a function of waste composition (Solid Waste Association of North America 1998).

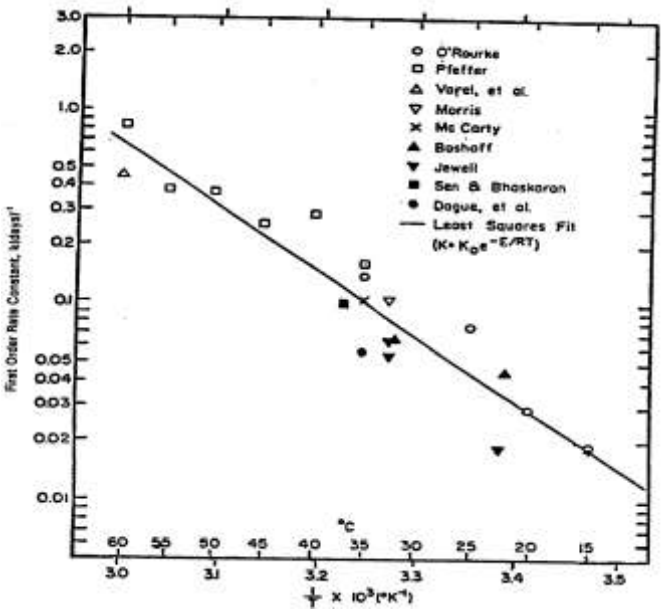

Figure 2.6: Plot of Temperature vs. *k* Value Reported by SWANA (1997)

IPCC (2006) suggests *k* values for different waste components based on the climatic conditions of MAP/PET ratio. However, a definite relationship between *k* values and waste composition, combined with moisture and temperature has not yet been reported.

Another factor that is often considered for predicting methane generation from landfills is ambient pressure. However, ambient pressure is mainly responsible for gas transport rather than methane generation unlike waste composition, temperature and moisture content. Spokas et al. (2009) have developed a field validated methodology for predicting methane generation from landfills, which was based on diffusion based equations which help predicting methane transport due to pressure gradient between landfill and the atmosphere.

2.5.2 Methods for Determining First Order k Values for Landfills

Several studies were performed in lab scale landfills as well on field scale landfill data to find the *k* values. This section gives a brief overview of the computations methods and equations used in literature for determining the first-order decay rate constant.

Faour et al. (2007) used actual landfill scale data obtained from 29 wet landfills across the US. The following equation was used for curve fitting.

$$V_s = \sum_{i=1}^{n} L_0(1 - e^{-kt}) \quad (2\text{-}18)$$

where V_s = specific cumulative methane volume (m^3/mg), and L_0 = Ultimate Methane Potential (m^3/mg). The authors found the model parameters using regression analysis with SAS employing the Gauss-Newton Method. The lag time was ignored while computing *k* values; however, during the lag phases, certain amounts of methane are produced. The cumulative methane produced during the lag phase ($V_{storage}$) was also determined.

Owens and Chynoweth (1993) found L_0 and *k* values using BMP data. Although the *k* values used in this study are not realistic, the method used for finding was Non-Linear Regression fit using Marquardt-Levenberg algorithm in SigmaPlot 4.0.

Tolaymat et al. (2010) used landfill gas emissions from 2 bioreactor landfill cells and one conventional for modeling methane. L_0 was determined using BMP, and was found to be 48.4 m^3/wet Mg. A decay rate of 0.06 yr^{-1} was found for the conventional landfill and 0.11 yr^{-1} was found for the bioreactor landfill. *k* was estimated by optimizing the LandGEM equation using statistical software package R. The following equation was used for optimization, which primarily depended on minimization on sum of squared errors using a quasi-Newton method.

$$SSE = \sum_m \left(\frac{kL_0}{12} \sum_{i=0}^{m} M_i e^{-k\left(\frac{m-i}{12}\right)} - Q_m \right)^2 \quad (2\text{-}19)$$

where Q_m = Amount of methane measured from the landfills during any particular year. This paper does not specifically mentions how the initial lag period was treated (Tolaymat et al. 2010).

Cruz and Barlaz (2010) used laboratory data previously published by Eleazer et al. (1997) for determining lab scale *k*'s. k_{lab} were computed for waste components using the first order decay equation as shown in Eqs. 2-20 to 2-23.

$$\frac{dm}{dt} = -km \quad (2\text{-}20)$$

$$\ln\frac{m}{m_0} = -kt \quad (2\text{-}21)$$

$$m = m_o - m_{CH4} - m_{CO2} \quad (2\text{-}22)$$

$$\ln(m_0 - m_{CH4} - m_{CO2}) = -kt + ln\,(m_0) \quad (2\text{-}23)$$

where, *m* = mass of reactive carbon remaining, kg;

m_0 = Initial mass of reactive carbon in the waste computed using the measured methane yield, kg; m_{CH4} and m_{CO2}= Mass of methane generated from the waste, kg; *k* = first-order decay rate constant, yr^{-1}; *t*= time, yr.

The authors used Simple Linear Regression (SLR) for curve fitting. It is also important to note that the authors ignored the initial lag time for computing *k*'s and lag times were removed since the equation was expected to be used in LandGEM. Also, carbon lost as COD in leachate was not accounted for because the lab scale reactors were bioreactors (leachate was recirculated).

Bigilli et al. (2009) used lab scale reactors with and without leachate recirculation for finding *k* values. Samples were withdrawn from the reactors every 100 days for a reactor life of 800 days. BMP analysis was done on each sample to find the rate of degradation. L_0 was

obtained from BMP studies and *k* was computed by fitting the methane generation curve using MATLAB.

Machado et al. (2009) found L_0 and *k* values for a landfill in Brazil using two methods. In the first method, waste samples were obtained from the landfill at different depths. Change in waste composition and moisture was studied with waste age. The L_0 values were computed from the waste composition data using the computation method suggested by IPCC (2006). *k* values were determined using the following equation.

$$\frac{L_0 t}{L_0} = e^{-kt} \tag{2-24}$$

In the second approach, curve fitting was done on landfill methane emissions for determining *k* using Eq. 2.18. L_0 of fresh waste was computed using IPCC (2006) guidelines and was used in Eq. 2.18. The authors concluded that the L_0 and *k* values found using these two methods were comparable and close, indicating that either could be used for further research.

To summarize, Faour et al (2007) and Owens and Chynoweth (1993) used non-linear regression methods for determining L_0 and *k* values. Cruz and Barlaz (2010), Tolaymat et al. (2010), Bigilli (2009), Oonk and Boom (1995) and Machado et al. (2009) fixed L_0 either by finding BMP or using the waste composition data and then used either curve fitting or simple linear regression for determining the *k* value.

Amini et al. (2012) conducted a review of methods used for determining L_0 and *k* in literature. The authors identified 4 approaches for determining the model parameters, and studied the impact of approach used for calculating L_0 and *k* on the model performance using actual landfill scale data from Florida landfills. The authors concluded that the model was insensitive to the approach taken for identifying the model parameters. However, the authors

commented that fixing L_0 using waste composition or BMP and the finding k using model fitting or regression is the simplest method of determining L_0 and k for landfills.

Biochemical Oxygen Demand (BOD) studies also use an equation similar to Eq. 2-18 for determining the "Ultimate BOD". The most commonly used for determining ultimate BOD and rate of BOD exertion are Fujimoto's method, Thomas's Slope method, Least Squares method and Non-Linear Regression method. Oke and Akindahunsi (2005) conducted a comparison to study the method of determination with the best goodness of fit and found that the non-linear regression method was better than the other methods used for finding the model parameters.

2.6 Lab Scale Studies vs. Field Scale Studies

Controlling moisture, temperature, and waste composition under field conditions is difficult. Lab studies allow control of these factors, but tend to over predict field rates due to ideal conditions: nutrients such as nitrogen and phosphorous may be added, and waste is shredded, which presumably increases decomposition by increasing surface area for contact between microbes and substrate (Ress et al. 1998; Barlaz 2006). In lysimeter tests, Ham and Bookter (1982) confirmed that shredding produced higher methane concentrations. Buivid et al. (1981) however, in landfill test cell experiments found that methane generation rate increased with particle size.

Barlaz et al. (1990) reviewed these contrasting results, and believed that this may be due to inoculum addition and the larger particle size range in Buivid's experiments (1 cm to 35 cm). Further research needs to be done to confirm the effect of shredding on methane generation from laboratory scale reactors. The small size of lab scale reactors may also accelerate methane production, due to more uniform ideal conditions. Larger lab scale reactors would allow use of un-shredded wastes, and more heterogeneous conditions that come closer

to those in an actual landfill. Cruz and Barlaz (2010) found that the lab scale *k* values were high compared to the field scale *k*s, and formulated a scaling factor (*f*) for determining the field scale degradation rates (See Section 2.5.1.1 for detailed description).

2.7 Summary

The efficiency of a model to predict methane generation from landfills depends on its input parameters (L_0 and *k*). Literature shows that *k* values depend on the waste composition, moisture and ambient temperature. However, the studies for finding *k* values based on waste composition particularly with respect to moisture and ambient temperatures have not yet been conducted. Therefore, the aim of this study was to find a relationship between first order decay rate constant (*k* values) with respect to waste composition, rainfall and temperature and also to study any interactions among these predictor variables.

CHAPTER 3

MATERIAL AND METHODS

3.1 Introduction.

The goal of this research was to develop a model for predicting methane generation rates for any landfill with basic information about waste composition, annual rainfall, and ambient temperature. The proposed Capturing Landfill Emissions for Energy Needs (CLEEN) model enables predicting methane generation rates from landfills worldwide; it can be used by any country to estimate methane potential of its landfills, regardless of waste composition or climate.

The methodology for this research was divided in 5 tasks.

Task 1: Developing an experimental design for studying the effect of rainfall, ambient temperature and waste composition on the first-order degradation rate constant (*k*).

Task 2: Setting up laboratory scale simulated landfill reactors based on the experimental design. This task included waste collection and storage, as well as designing and constructing gas tight laboratory scale landfill reactors.

Task 3: Operating and monitoring laboratory scale simulated landfill reactors. This step involved measuring parameters such as moisture content, volatile solids, gas volume and percentage of methane (CH_4), carbon dioxide (CO_2) and oxygen (O_2) in gas; and measuring leachate volume and pH.

Task 4: Analysis and Model Development. A comprehensive multiple linear regression (MLR) model was developed to predict first order decay constant (*k*) using rainfall, ambient temperature and waste composition.

Task 5: Incorporating the MLR equation into the CLEEN model and finding scale-up factor using landfill scale data.

Each of these tasks will be discussed in detail in the next sections.

3.2 Task 1: Experimental Design

3.2.1 Rainfall Rates

To study the effect of average annual rainfall on the methane generation rate constant, rainfall rates of 2, 6, and 12 mm/day were used, corresponding to 60, 180, and 360 mm/month. These rates encompass monthly precipitation rates for most developing countries in Central America, South America, Africa (with the exception of the Sahara countries), and the Far East (India, China, Thailand, and Indonesia). The average monthly rainfall across the world is shown in Figure 3.1 (Pidwirny 2010).

It is evident from Figure 3.1 that some regions in the world receive rainfall beyond the range considered in this study. However, extremely low rainfall rates would mean extremely slow waste degradation, and hence were avoided in this study. Likewise, simulating higher rainfall rates could lead to flooding conditions in the simulated landfills, and hence were eliminated from this study. Although testing a larger number of rainfall rates would better characterize methane variation with respect to rainfall, the time involved in measuring gas production for each reactor is extensive. Therefore, only three rainfall rates were incorporated into the design to limit the overall number of reactors.

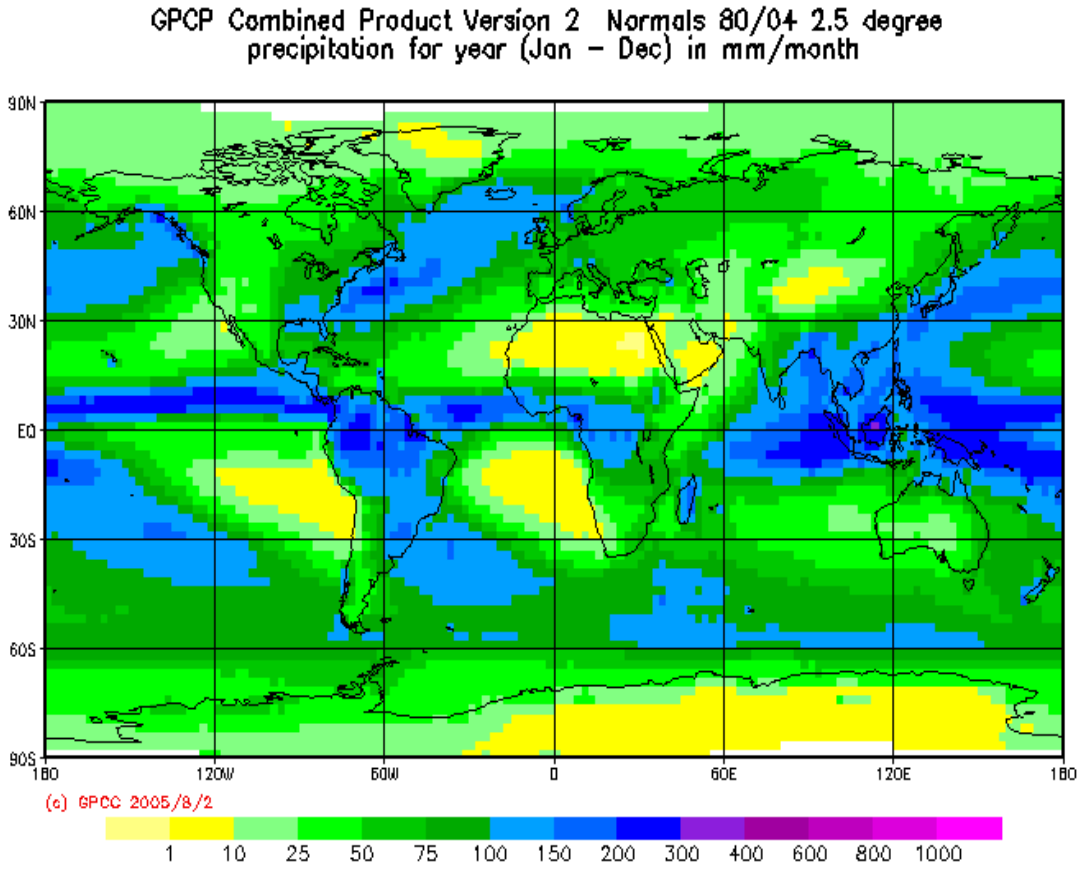

Figure 3.1: World Map Depicting Average Monthly Precipitation (Source: Pidwirny 2010)

3.2.2 Ambient Temperatures

To determine the effect of ambient temperature on methane generation rate, tests were conducted at 3 temperatures, 20°C, 30°C and 37 °C (corresponding to 68°F, 86°F, and 98°F, respectively) as representative ambient temperatures. These temperatures were selected because annual mean temperatures for most of South America, Central America, Africa, India, and Indonesia range between 20°-35°C. Average monthly summer temperatures in these regions can range up to 40°C. The rate of degradation is lower at lower temperature; hence, to

limit the duration of this study, temperatures lower than 20°C were not considered. Annual average ambient temperatures observed across the world are shown in Figure 3.2.

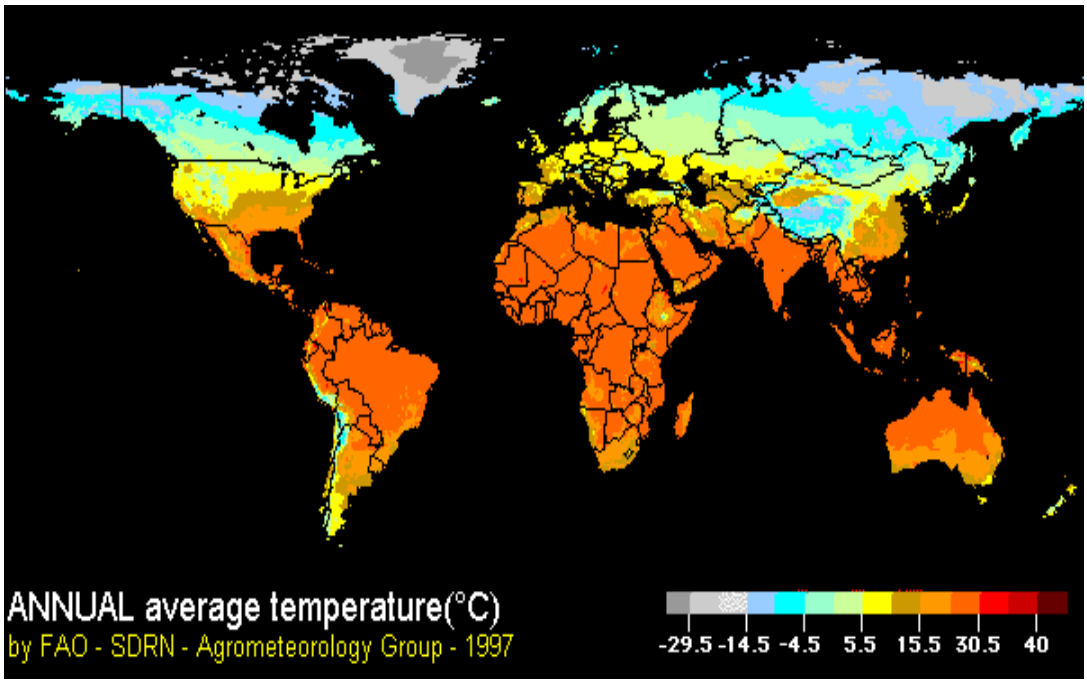

Figure 3.2: World Map Depicting Average Annual Ambient Temperatures.
(Source: Sustainable Development Department (SD), Food and Agriculture Organization of the United Nations)
(http://www.fao.org/WAICENT/FAOINFO/SUSTDEV/EIdirect/CLIMATE/EIsp0002.htm)

Laboratory scale landfill reactors were placed in 2 constant temperature rooms at 30°C and 37°C. In order to incorporate the lower temperature range, reactors were placed in the laboratory, where the temperature is approximately 20°C (70°F).

3.2.3 Waste Composition

Methane generation from landfills mostly occurs due to anaerobic degradation of the organic portion of the solid waste. Hence solid waste components considered in this research were highly biodegradable wastes: food, paper, yard, and textile (Weitz et al. 2002), as well as inert inorganic waste. Although inorganic waste is not biodegradable, it may interfere with

microbial access to organics, which can impact the first-order decay constant (*k*); hence, it was considered as a variable in the design.

3.2.4 Experimental Design

A cyclic incomplete block design (Dean and Voss 1999) was used for the experimental setup to minimize the number of reactors. Since the time involved in monitoring the reactors was enormous and the space available in the constant temperature rooms was limited, the number of laboratory scale reactors had to be limited to 30.

As described above, temperatures of 20^{o}C, 30^{o}C and 37^{o}C, and average rainfall rates of 2, 6 and 12 mm/day, were considered in this research. Thus, temperature and rainfall were the two factors of primary interest, each studied at 3 levels and in all combinations; hence, all $3^2 = 9$ combinations of temperature and rainfall were used in the experimental design. It is known that the effect of these 2 factors on *k* also depends on the composition of the waste, which is represented by 5 waste components.

Considering the factors mentioned above, the experimental design could be conducted using a complete factorial design, a complete block design or an incomplete block design.

Complete Factorial Design: A complete factorial design enabled exploration of all main effects and interaction effects. However, if 3 levels were assumed for each of the 7 factors mentioned above (temperature, rainfall, % food,% paper, % textile, % yard and %Inorganic waste) then 3^7 = 2187 combinations (reactors) were required. With a restriction of 30 reactors, it would have been impossible to analyze more than one waste component using the complete factorial design; hence this design was not used in this study.

Complete Block Design: In experimental design, so-called “blocking” factors are used to model the variability due to factors that affect the response, but are not of primary interest. The

interaction effects between temperature and rainfall were anticipated to be more significant; hence these were given priority, and the waste composition effect was treated as a "blocking" factor. With the regression modeling approach, it is possible to explore interactions with waste composition and potentially include a few of these in the model to predict *k*.

A complete block design required a reactor assigned to all combinations of the waste composition (blocking factor) and the 9 combinations of temperature and rainfall, i.e., if there are *b* blocks, then we need 9*b* reactors. With the restriction of 30 reactors, at most *b* = 3 blocks are possible, which means that only three waste combinations could be explored in the experimental design. Given the wide variety of possible waste compositions, it was pertinent to maximize the waste combinations to study their impact of methane generation rates. Hence, an incomplete block design was chosen to allow the inclusion of more waste combinations because not all waste combinations will be tested under all temperature-rainfall conditions. A complete block design is orthogonal, while an incomplete block design is not; hence, analysis of an incomplete block is mathematically more complex, but can be easily handled with a regression based approach.

Balanced Incomplete Block Design: In a Balanced Incomplete Block (BIB) design, the number of treatments and blocks are designed in such a way that the following three conditions are satisfied:

1. $v*r = b*k$
2. $r*(k-1) = \lambda*(v-1)$ where λ is an integer.
3. $b \geq v$

Where,

v = No. of Treatments = combinations of rainfall and temperatures 3^2 = 9 combinations

b = No. of Blocks = Waste compositions

r = number of times a treatment appears in the design.

k = block size (number of times the blocks appear in the design.

n = number of experiments = $b*k = v*r$

To satisfy these conditions the following assumptions were made:

v=9, λ =1, r =4, k=3, b =12

Using these assumptions the total number of reactors required was:

$n = vr$ (or kb)= 4*9 = 36

As mentioned earlier, it was necessary to restrict the number of reactors to 30, due to practical considerations; hence a cyclic incomplete block design was used in this study.

3.2.5 Constructing a Cyclic Incomplete Block Design

To construct an incomplete block design, 9 combinations of waste components were selected with varying waste compositions. The following assumptions were made for the cyclic incomplete block design:

Number of treatments (v) = rainfall and temperature combinations 3^2=9

Number of blocks (b) = combinations of waste components = 9

Block size (k) = number of times a block appears in the design = 3

Number of times a treatment appears in the design (r) = 3

Total no. of reactors = $vr = bk$ = 27

The specific combined waste cases were determined by a mixture design (Mason et al. 1989), such that each biodegradable waste component (food, yard, textile, and paper) could be observed in a range of 0-100%. Since inorganic waste does not have a potential to generate gas by itself, its range was selected between 0 to 40%. Table 3.1 summarizes the 9 waste

combinations used in the experimental design. These combined waste cases serve as 9 blocks for the cyclic incomplete block design.

Table 3.1 Component Percent by Weight for Each Waste Combination

	Component % by Weight for each Waste Combination								
Component	**A**	**B**	**C**	**D**	**E**	**F**	**G**	**H**	**I**
Food	**100**	0	0	0	0	**60**	**30**	**10**	**20**
Paper	0	**100**	0	0	**60**	0	**10**	**30**	**20**
Textile	0	0	**100**	0	0	**30**	0	**60**	**20**
Yard	0	0	0	**100**	0	**10**	**60**	0	**20**
Inorganic	0	0	0	0	**40**	0	0	0	**20**

The percentages of waste components in the 9 blocks were selected chosen such that the following three conditions were satisfied:

a. The sum of all components in a reactor was equal to 100.

b. The correlation between the percentages of waste components was minimized. This was done to ensure that the correlation between the rates of degradation for any waste components was not induced due to the design. For example, if the results indicated that food waste influences the degradation of paper waste, it should not be due to the correlation between the percentages of waste components chosen in the design. Figure 3.3 shows the box plots depicting the correlation between waste components.

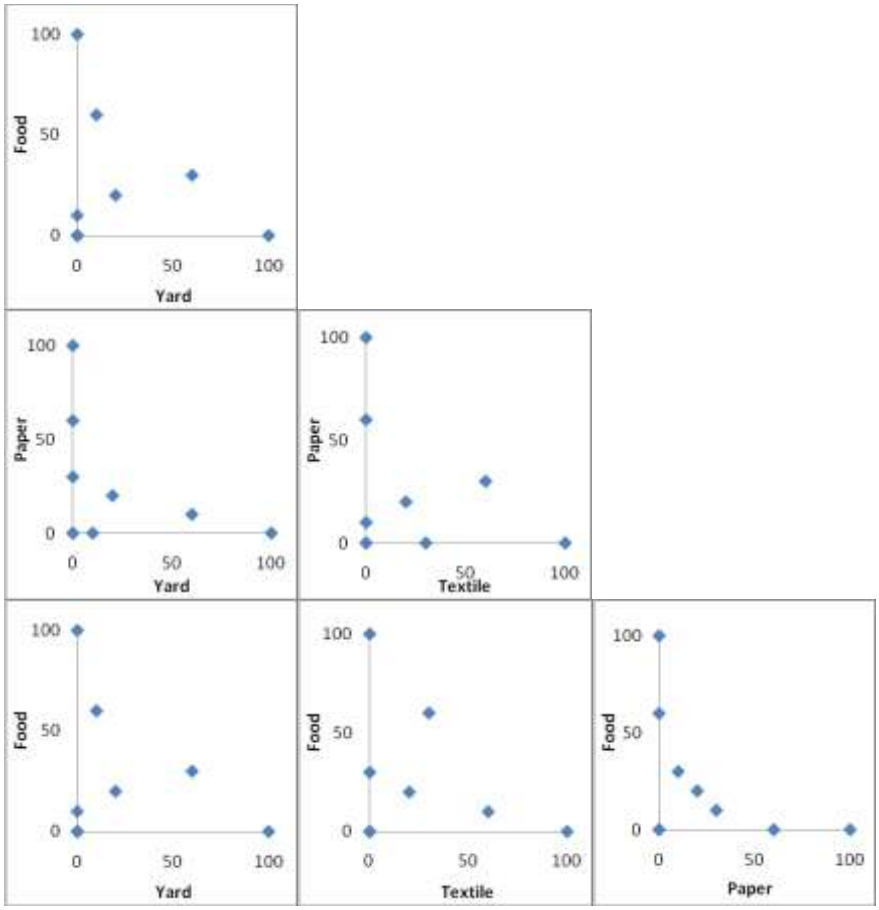

Figure 3.3: Correlation Between Percentages of Waste Components Chosen for the Experimental Design.

c. Euclidean distance of components in the 5-dimensional waste component space (percentages of food, yard, textile, paper and inorganic waste) was maximized. As mentioned above it was necessary to vary the waste components from 0-100% (except inorganic waste varied between 0-40%). While the design required the 9 blocks to cover the 5 dimensional waste component spaces, it was also necessary to ensure that the points were not too close to each other. Hence Euclidean distances of waste components were computed.

For satisfying these conditions multiple combinations were chosen by trial and error. The combination which had maximum Euclidean distance was chosen (Chen et al. 2006). Table 3.2 shows the Euclidean distances computed for the percentages of waste components chosen for the 9 blocks.

Table 3.2: Euclidean distances Computed for the Percentages of Waste Components Chosen for the 9 Blocks.

Distance w.r.t	**Distance between a_{ij} in five dimensional space**									
point	**1**	**2**	**3**	**4**	**5**	**6**	**7**	**8**	**9**	Min Distance
1		141.42	141.42	141.42	123.29	50.99	92.74	112.25	89.44	**50.99**
2			141.42	141.42	56.57	120.83	112.25	92.74	89.44	**56.57**
3				141.42	123.29	92.74	120.83	50.99	89.44	**50.99**
4					123.29	112.25	50.99	120.83	89.44	**50.99**
5						98.99	92.74	78.74	56.57	**56.57**
6							66.33	66.33	50.99	**50.99**
7								89.44	50.99	**50.99**
8									50.99	**50.99**
Performance metric value (least distance between any two points)										**50.99**

Table 3.3 shows the matrix with treatment and block combinations used in the experimental design for setting up the laboratory scale landfill reactors. Practical considerations were required while designing this, e.g. a high percentage of slow degrading waste was avoided with the lowest temperature and rainfall combination, because of its slow degradation process. For example, reactor 1 was installed with 2 mm/day rainfall at an ambient temperature of 20°C, and contained waste combination corresponding to combination **a**, which according to Table 3.1

is 100% paper waste. Methane emissions were measured over time for 27 lab scale landfills with varying waste compositions, rainfall and temperature.

Table 3.3: Rainfall, Temperature, and Waste Component Combinations for the Simulated Landfill Reactors

Rainfall, mm/day	Temperature, °C (°F)	Waste Component Combination								
		A	B	C	D	E	F	G	H	I
2	**20 (68)**		1					2		3
2	**30 (86)**	4		5					6	
2	**37 (98)**		7		8					9
6	**20 (68)**	10		11		12				
6	**30 (86)**		13		14		15			
6	**37 (98)**			16		17		18		
12	**20 (68)**				19		20		21	
12	**30 (86)**					22		23		24
12	**37 (98)**	25					26		27	

Note: Each blue number denotes the number of the lab-scale landfill reactor.

In addition, Reactors 28-30 were control reactors with seeding but no waste installed at 20°C, 30°C, and 36°C, respectively. Methane generated from the control reactors was subtracted from that generated by other reactors to account for the methane emissions from the seed.

3.3 Task 2: Setting up Laboratory Scale Simulated Landfill Reactors.

3.3.1 Waste Collection

As mentioned earlier in Section 2.2.3, food, paper, yard, and textile were the major biodegradable waste components considered in this study. In addition, inert inorganic waste was included to study the impact of non-biodegradable waste on the decay rate constant (*k*). Waste components were collected from individual sources instead of a waste transfer station or landfill in order to obtain “pure” waste. “Pure” waste is a commonly used term, which indicates that the waste components are not mixed. For example, paper waste being absorbent, quickly

absorbs the moisture and nutrients from food waste. To avoid such mixtures, waste components were obtained from individual waste sources.

Food waste was obtained from the University of Texas at Arlington's (UTA) cafeteria, and from Indian and Thai restaurants near Arlington, TX, as examples of food from developing countries. The waste from UTA cafeteria mostly contained fruits, vegetable skin, bread, and processed meat. The waste from Indian and Thai restaurants contained fruit and vegetable leftovers and mostly unprocessed meat. The waste was mixed well and stored in air-tight containers at 4^{o}C for a period of 7 days.

A mixture of grass, leaves, and tree/bush trimmings was obtained from the university's vicinity and is representative of the variety particularly found in Texas. The species of trees found in Texas are mostly Live Oak, Post Oak, Red Oak, American Elm, Pecan, Bald Cypress, and Creepy Myrtle. The waste was collected in a period from July to November and stored in air-tight bags at 4^{o}C.

A mixture of textiles was obtained from local tailors. The waste contained a mixture of cut textiles, mostly made of polyester and cotton, or a blend of the two. Large pieces of textiles were discarded, but the cut pieces of textiles were not shredded further, and were directly loaded in the reactor.

Paper waste was obtained from the university's recycling bins (office paper), and faculty and student's personal recycling bins (newspapers, mail, magazines, tissues and towels, diapers), and local stores (corrugated boxes and milk cartons). Individual waste components were mixed together to replicate the percentages found in the US (USEPA 2007). Although it would be better to replicate the percentages found in the developing countries, very little information was available related to the actual composition of paper waste in the developing

countries. Large pieces of waste were cut in order to fit into the reactors. The average paper size in the reactor was 4" x 6". Paper was not cut into finer pieces or shredded because it has been reported to become bio-available due to shredding, which can lead to faster degradation and larger *k* values (Buivid et al. 1981). Hence the course structure of waste was maintained in the reactors to try to replicate the actual conditions in the landfills.

Inerts, including sand, dust, stones, glass bottles, metal cans, and plastic bottles, were obtained from the university's recycling facility. Cut glass and metals were discarded to avoid injuries in the laboratory. Construction and demolition waste was collected from the Department of Civil Engineering's concrete testing facility. The waste components were then stored in air-tight bags in a constant temperature room (Environmental Growth Chamber) at 4^{o}C.

3.3.2 Reactor Setup

Experiments were conducted in 16-L HDPE wide-mouth plastic buckets (United States Plastic Corporation, OH) modified for gas and leachate collection and for water addition (See Figure 3.4).

Before filling the reactors with waste, all reactors were leak-checked. Leak tests were conducted using a simple U-tube manometer (Dwyer Instruments Inc., Michigan City, IN) after proper sealing of reactors. To verify that there was no significant leakage; reactors were monitored for 1-2 days. The head difference at 12 and 48 hours was recorded to confirm that it was within permissible limits of 0.5 in. and 3 in. of water column, respectively (Mohammad Adil Haque 2007). Once the reactors were leak-tested, their empty weight was measured.

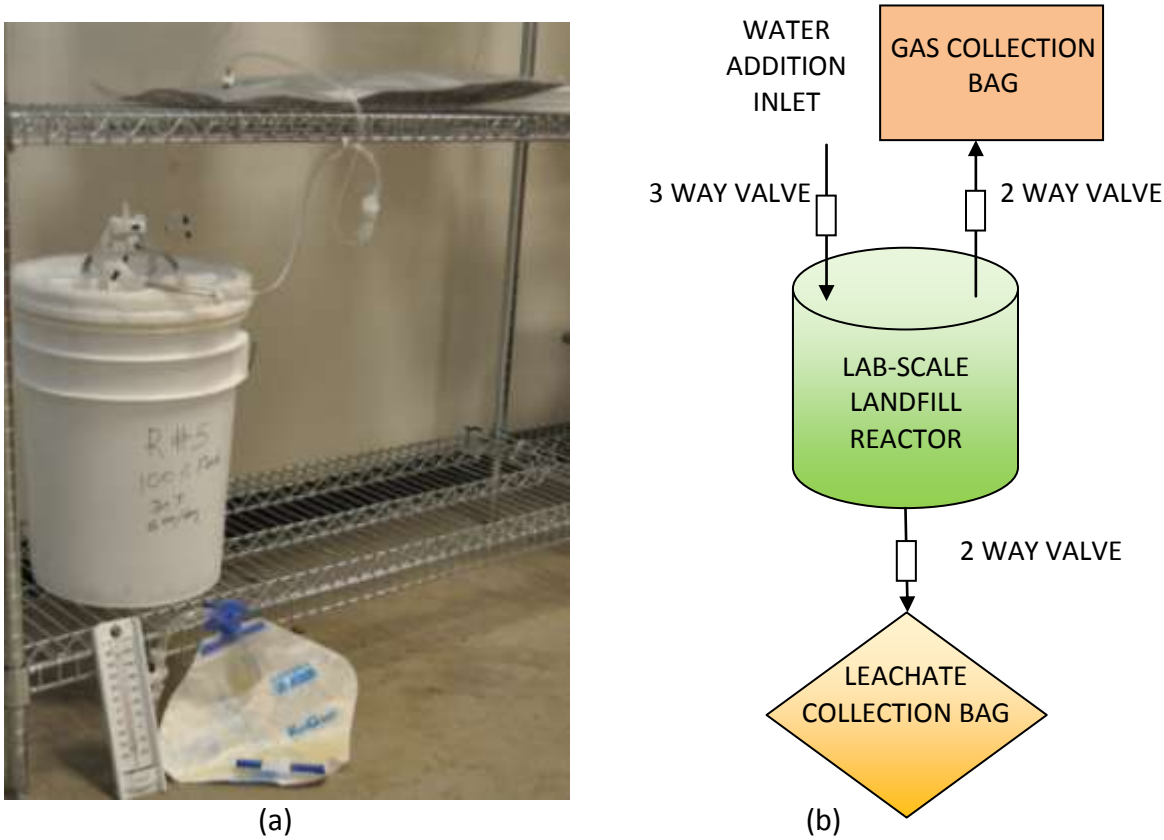

Figure 3.4: Laboratory Scale Landfill Reactor Setup (a) Photograph and (b) Schematic

Reactors were then filled with refuse components, as described in the Experimental Design section. A 10 inch diameter piece of filter fabric (Geotextile) was placed at the bottom of the reactor and overlain with waste. Seed was obtained from a continuously-stirred anaerobic sludge digester operated at a hydraulic loading rate of 19 days at 20^{o}C and added to each reactor to achieve 10-12 % by weight. Sludge was obtained from the Village Creek wastewater treatment plant, Fort Worth, TX.

In addition, tap water was added to the waste to make sure that the waste was near saturation limit. In a landfill, lack of moisture affects acclimatization of micro-organisms to the waste, which results in a longer lag phase. LandGEM assumes a lag phase extending to about 0-1 years, and the gas produced (if any) during this period is neglected. Although saturating the

waste with water ensures that the reactors overcome the lag phase faster, it does not affect its overall rate of degradation (*k* value). Moreover, leachate is produced only when the waste has moisture exceeding its saturation limit. It was crucial to study the pH during the initial stages of the reactors, because there is a possibility of acid accumulation during the acidogenic phase (Christensen and Kjeldsen 1989). Hence, to ensure good microbial contact, and to reduce the lag period, water was added, such that the waste was near saturation limit. The amount of water required for each waste component (food, paper, textile, yard and inorganic) to reach saturation was calculated based on values reported by Stone and Kahle (1972).

Each reactor was then weighed and placed in its position in one of the constant temperature locations (see Experimental Design section), and connected to a leachate collection bag (2-L Kendall-KenGuard Drainage Bag) and gas collection bag (22-L Cali 5-Bond Bag, Calibrated Instruments, Inc.). A schematic of the reactor installation process is shown in Figure 3.5.

27 laboratory scale landfill reactors were filled with various proportions of waste components and operated at various rainfall-temperature combinations, as discussed in the Experimental Design section (See Section 3.2.5). Three reactors, with seeding but no waste, served as controls to determine methane production from the seed.

Figure 3.5: Reactor Installation Process

3.4 Task 3: Reactor Operation and Measurements

3.4.1 Average Rainfall

As mentioned earlier, rainfall rates of 2, 6, and 12 mm/day were used to study the effect of rainfall on the methane generation rate constant. Tap water was added to the reactors to simulate rainfall. Distilled or deionized water was not used for rainfall simulation, because distilled water has a tendency to absorb more contaminants than tap water and which could result in higher carbon washout. The amount of water to be added to the reactors was computed using the bucket dimensions.

Recirculation rates for rainfall intensities of 2, 6 and 12 mm/day were calculated as 100, 300 and 600 mL/day, respectively. Water addition was done using the three way valve attachment shown in Figure 3.6.

Figure 3.6: Water Addition for Rainfall Simulation

Potassium hydroxide (KOH) addition was required in 100% food reactors during the initial period to avoid excessive acid accumulation as observed in previous studies (Vavilin et al. 2004; Wang et al. 1997).

3.4.2 Gas Generation Measurement

Gas production was measured by pumping gas out of the collection bag through a standard SKC grab air sampler (SKC Aircheck sampler model 224-44XR) at 1.0 L/min connected to a calibrator (Bios Defender 510M) to get a minute by minute gas pumping rate. LANDTEC-GEM 2000 PLUS with infrared gas analyzer (±3% accuracy) was used for measuring % Methane (CH_4), % Carbon Dioxide (CO_2), %Oxygen (O_2), and percentage of other gases. In addition, Hydrogen Sulfide (H_2S) and Carbon Monoxide (CO) were recorded. The frequency of gas sampling depended on the amount of gas generated. During the initial stages of degradation, the gas bags were emptied twice a day, to avoid excessive buildup in the gas bags. As degradation progressed, the rate of gas production decreased and the frequency of sampling was reduced accordingly. Gas production rate was reported in STP.

Figure 3.7 shows instruments used for gas volume and composition measurement. Each reactor was destructively sampled when gas production dropped to a low constant value.

(a) (b)

Figure 3.7: Gas Measurements (a) Composition using Landtec GEM 2000 and (b) Volume using SKC Sampler & Calibrator

Methane readings from Landtec GEM 2000 were compared with those from a gas chromatograph (SRI 8610) with flame ionization detector equipped with Hayesep D packed column. It was found that the % methane found by Landtec GEM 2000 was within $\pm$7% of that found by the gas chromatograph.

3.4.3 Leachate Volume and pH

Leachate volume generated was recorded daily. pH (HQD 40 Hach meter) was measured daily as an indicator for the degradation stage (Barlaz et al., 1990). Leachate collection and pH measurement procedure is shown in Figure 3.8.

Figure 3.8: Leachate Collection, and pH Measurement Procedure

3.4.4 Moisture Content

The initial moisture content of the waste components in each reactor was determined to understand the moisture content of each component. However, before installing each reactor, anaerobic sludge and water were added to the waste to ensure good microbial contact. Hence, a sample was withdrawn from each reactor for finding the moisture content before putting it into operation, and is hereafter referred to as initial moisture content of the reactor. Each sample was analyzed in triplicate for determining moisture content on a wet weight basis, as summarized below according to Standard Methods APHA 2540B (AWWA-APHA, 2005).

Approximately 500 g of waste (except food waste) was dried in an oven at 105^{o}C (±5 ^{o}C) until a constant weight was achieved. The duration of drying was separate for each waste sample; yard waste samples reached constant weight within 24 hours, while textile wastes required 48-54 hours to reach constant weight. Extra care was taken while finding the moisture content of samples containing higher percentages of food waste (for e.g. waste composition a- 100% food, and f- 60% food, 30% Textile and 10% Yard), because it was reported that some of the organic matter from food waste volatilizes at 105^{o}C (Angelidaki et al. 2009). Hence, food

waste samples were dried at 65°C (± 5°C) for about 5-7 days, until the samples reached constant weight.

Moisture content on a wet weight basis (w_w) was determined using the following relationship.

$$w_w = \frac{weight\ of\ water\ (g)}{wet\ weight\ of\ waste\ \ (g)} \quad (3\text{-}1)$$

At the end of the reactor operation, samples were taken from the top, middle and bottom layer of each reactor and moisture content was determined for each of these samples. This was done to examine the effect of rainfall rates on the moisture content of the waste and to detect if there was unequal distribution of moisture in the reactors.

The ongoing probable moisture content of waste in each reactor was computed using a water balance (Tchobanoglous et al. 1993), as shown below:

$$\Delta F_{SW} = W_{SW} + W_A - W_L \quad (3\text{-}2)$$

where

ΔF_{SW} = Solid waste field capacity or variation of water content (L/kg)

W_{SW} = Initial moisture content of the refuse (L/kg)

W_A = Water added (L/kg)

W_L = Percolated water (leachate) (L/kg)

3.4.5 Volatile Solids Determination

Volatile solids are an indicator of the organic content in the waste samples. Organic content of the waste is expected to decrease as the waste decomposes. Initial volatile solids were determined in triplicate for each reactor. Once the gas production had reached a low constant value, the reactors were destructively sampled and the volatile solids concentration in

the degraded waste was also measured in triplicate, according to Standard Method APHA 2540-E.

Dried waste samples were ignited in a muffle furnace at 550^{o}C (± 10^{o}C) for about 2 hours, or until it reached constant weight. The percent weight lost during ignition was the volatile solids in the waste. The biodegradable portions of waste (food, paper, textile, and yard) were used for finding the volatile solids. Plastics and metal were avoided because they may cause dioxin emissions and volatilize easily, thus inducing an error into the computation. The volatile solids content of inorganic waste (including plastic, metals, concrete and soil) was assumed to be negligible. Figure 3.9 shows the samples after burning, and the muffle furnace.

(a) (b)

Figure 3.9: Volatile Solids Determination (a) Samples after Burning (b) Muffle Furnace

3.4.6 L_0 Determination

Ultimate methane generation capacity (L_0) of the waste components was determined using the Biochemical Methane Potential (BMP) method (I. Angelidaki, M. Alves, D. Bolzonella, L. Borzacconi, J. L. Campos, A. J. Guwy, S. Kalyuzhnyi, P. Jenicek and J. B. van Lier 2009; U.S. EPA 1998; Bogner 1990b). For the BMP test, the samples from all reactors were ground using a

Thomas Wiley Mini mill, and sample passing through a 2 mm sieve was used for the study. Since the ultimate methane potential is a property of the waste composition or the degradable organic content of the waste, the samples with the same composition were mixed together. For example, reactor nos. 8, 19, and 14 had the same composition; hence, they were mixed in equal quantities. Thus, 9 samples corresponding to the 9 blocks were analyzed using BMP. BMP was carried out in 125 mL Wheaton Serum Bottles with rubber stoppers and crimps (Sigma Aldrich Co. LLC, St. Louis, MO). The procedure followed for the BMP test was as specified in Wang et al. (1994), except that the inoculums were obtained from an anaerobic CFSTR operated at a residence time of 20 days.

BMP bottles were incubated at 37^{o}C for a period of 60-80 days. Gas volume was measured by equilibrating pressure using a 60 mL ground glass syringe, followed by a 5 mL ground glass syringe to ensure that all the excess pressure is removed. The gas composition was measured in a GC (SRI 8610) equipped with FID detector. The samples were tested in triplicate for BMP, to obtain a mean and standard deviation.

3.4.7 Data Analysis

Methane production rate was recorded versus time for each reactor. The ultimate methane potential and *k* value for each reactor were computed using non-linear regression analysis with Guass-Newton method using SAS software. Three methods were used for finding the parameters L_o and *k*:

1. Assuming L_0 = Total amount of methane generated from the reactor, and substituting it into Equation 3-3.

$$V = L_0(1 - e^{-kt}) \quad (3\text{-}3)$$

$$Ln\left(1-\frac{V}{L_0}\right)=-kt \quad (3\text{-}4)$$

where,

V= Cumulative volume of methane generated from reactor (m^3/kg),

L_0 = Ultimate methane potential (m^3/kg),

k = first order methane generation rate constant (yr^{-1}),

t = time (year).

k and L_0 were computed from Eq. 3-4 using Simple Linear Regression (SLR) analysis using SAS software.

2. Thomas Method used to find parameters for BOD (Thomas, 1937).
3. Non Linear Regression Analysis.

   Guass-Newton method was used for computing the parameters L_0 and *k* for each reactor using SAS software.

A comparative analysis was conducted to find the best method for finding the model parameters. The goodness of fit was tested using the following criteria:

1. Sum of Square of Errors (SSE) should be minimized.

   $SSE = (Y_{calculated} - Y_{obs})^2$ (3-5)

   Where,

   $Y_{calculated}$ = Predicted cumulative methane generation (m^3/kg),

   Y_{obs} = Observed cumulative methane generation from reactors (m^3/kg)

2. Coefficient of Determination (CD) value should be maximized.

   $$CD=\frac{\sum_{i=1}^{n}(Y_{obs_i}-\bar{Y}_{obs})^2-\sum_{i=1}^{n}(Y_{obs_i}-Y_{calc_i})^2}{\sum_{i=1}^{n}(Y_{obs_i}-\bar{Y}_{obs})^2} \quad (3\text{-}6)$$

The comparative analysis was performed for 5 reactors and is presented in Appendix A. The comparative analysis showed that Non-Linear Regression provided the best fit; hence, it was used for finding L_0 and k values for all the reactors.

3.5 Task4: Developing Multiple Linear Regression Model

Using SAS software, a comprehensive statistical model was developed that incorporates all of the above 7 factor variables (temperature, rainfall, and proportions of 5 waste components) in predicting the response variable (methane generation rate constant, k). Based on data collected, a multiple linear regression model was developed to predict k as a function of waste composition, annual rainfall, and temperature, as shown in Eq. 3-7.

$$k = \beta_0 + \beta_1 R + \beta_2 T + \beta_3 F + \beta_4 P + \beta_5 TX + \beta_6 Y + \beta_7 I + \varepsilon \quad (3\text{-}7)$$

where

k = first-order methane generation rate constant (yr^{-1})

βs = parameters to be determined through multiple linear regression, using the lab data

R = annual rainfall (mm/day)

T = average annual temperature at the landfill location (K)

F = fraction of landfilled waste that is food (%)

Y = fraction of landfilled waste that is yard waste (%)

TX = fraction of landfilled waste that is textiles (%)

P = fraction of landfilled waste that is paper (%)

I = fraction of landfilled waste that is inorganic (%)

ε = error uncertainty, modeled as a random variable.

βs were determined through multiple linear regression, using data from the laboratory experiments. With the regression function, the expected value of k was estimated using

statistical confidence intervals, and *k* was predicted using statistical prediction intervals (Kutner et al., 2005). These intervals provided information on model's uncertainty.

3.6 Task 5: Developing CLEEN Model

The CLEEN model was developed by incorporating the MLR equation in the first order decay based model for predicting methane generation rates from landfills. It was anticipated that the lab scale data would yield higher *k* values than those found in the landfills. Hence scale-up factors were developed using the methane recovery data from City of Denton landfill. Ambient temperature, rainfall rate, and waste composition data was acquired from the City of Denton's landfill and were used in the statistical model (Eq. 3.7) to determine field scale *k* values. L_o values for various waste components developed using the BMP test were used to calculate a weighted-average L_o using the waste composition information. Methane recovery estimates were compared to the actual recovery rates from the landfill and scale-up factor (*f*) was developed by computing a ratio of the actual *k* value to the computed *k* value.

CHAPTER 4

RESULTS AND DISCUSSION

4.1 Introduction

The experimental results are presented and discussed in this chapter, which is divided into three sections. The first section includes the characteristics of municipal solid waste components (moisture content, volatile solids and biochemical methane potential). The gas generation data from the laboratory scale landfill reactors, along with leachate volume, pH and probable moisture content inside the reactor, are presented in the second section. The methane generation data from laboratory scale reactors was then used for computing the first order decay constant (k) for each reactor. The last section of this chapter includes details about modeling the ultimate methane potential (L_o) and the rate constant (k).

4.2 Characteristics of Municipal Solid Waste Components

4.2.1 Moisture Content of Waste

As discussed in Chapter 3, individual waste components (food, paper, textile, yard, and inorganic waste) were obtained directly from their sources, not allowed to be mixed and stored at 4^{o}C. Moisture content of each waste component was determined and the results are presented in Table 4.1. Food waste had the maximum moisture content (82.85 %), followed by yard waste (56.91%). Textile waste did not have much moisture, since it was collected from local tailors and was not allowed to be mixed with any other components. Similarly, paper waste collected from UTA's paper recycling bins was not expected to have much moisture. However, paper waste also contained food packaging cardboard, paper cups and milk cartons which were

collected from local grocery stores, along with toilet tissues and paper towels collected from UTA's trash cans. The moisture content of paper waste (8.52%) can be attributed to these sources.

Table 4.1: Moisture Content of Waste Components

Waste Combination*1	**A**	**B**	**C**	**D**
Composition	**100% Food**	**100% Paper**	**100% Textile**	**100% Yard**
Sample1	80.46	10.39	4.339	54.00
Sample2	85.27	6.540	4.396	59.82
Average	**82.87**	**8.465**	**4.367**	**56.91**

Note 1: Waste combination nomenclature can be found from Table 3.1

The waste components were then mixed according to the weights specified in the experimental design (See Section 3.2). The moisture content of waste after mixing is presented in Table 4.2. The paper and textile wastes have the maximum moisture absorption capacities. The inorganic waste contained metal cans and plastic bottles along with construction and demolition (C&D) waste. In some cases, the plastic bottles and cans had some liquid residue, which was responsible for higher moisture content of waste combination E- 60% paper and 40% inorganic as compared to waste combination B- 100% paper.

Table 4.2: Moisture Content of Waste after Mixing

Waste Combination	**E**	**F**	**G**	**H**	**I**
Composition	**60%Paper + 40% Inorganic**	**60% Food +30% textile +10% Yard**	**60%Yard +30% Food + 10% Paper**	**60% Textile +30% Paper + 10% food**	**20% each**
Sample 1	13.88	47.99	64.32	12.06	20.52
Sample 2	10.39	52.80	58.72	7.535	29.00
Sample 3	10.31	64.58	50.69	5.139	32.97
Average	**11.53**	**55.13**	**57.91**	**8.245**	**27.50**
Std. Dev.	**2.038**	**8.532**	**6.848**	**3.515**	**6.358**

Moisture contents of fresh waste observed in this study were compared with those reported in the literature (See Table 4.3). It can be observed that the moisture content values found in this study were close to the values found in the literature.

Table 4.3: Comparison of Moisture Content Observed in this Study with Previous Studies

	Moisture Content (% wet wt)	**Author**	**Moisture Content (% wet wt) found in this study**
Food Waste			
Mixed Food Waste	68.30	Qudias (2000)	82.86
Boiled Rice	65.00	Cho et al. (1995)	
Cooked Meat	47.00	Cho et al. (1995)	
Fresh Cabbage	95.00	Cho et al. (1995)	
Mixed food waste (Korean)	74.00	Cho et al. (1995)	
Bean Sprouts	80.00	Cho et al. (1995)	
Fried Egg	78.00	Cho et al. (1995)	
Food Waste	50-80%	Tchbanoglous (1993)	
Paper Waste			
Paper	4-10	Tchobanoglous (1993)	8.466
Cardboard	4-8	Tchobanoglous (1993)	
Yard Waste			
Yard Wastes	30-80	Tchobanoglous (1993)	56.91
Wood	15-40	Tchobanoglous (1993)	
Textile Waste			
Textiles	6-15	Tchobanoglous (1993)	4.368
Other Waste			
Plastic	2.75	Qudias (2000)	Not Determined
Plastic	1-4	Tchobanoglous (1993)	
Tin Cans	1-4	Tchobanoglous (1993)	

4.2.2 Initial Moisture Content of Waste

As mentioned earlier in Chapter 3, the reactors were filled with waste components according to the experimental design. Sludge was added to the reactors to ensure microbial contact. Additional water was also added in all reactors, except 100% food reactors, to saturate the waste. Since 100% food waste reactors were already saturated with moisture (with 82.86% moisture content); no additional water was added in these reactors. Instead, 100% food waste reactors were allowed to drain excess moisture during the first few days.

Solid waste samples were collected after mixing sludge and water with waste, for determining the initial characteristics of waste inside the reactor. Hereafter, this moisture content will be referred as the initial moisture content of the waste. The initial moisture content of waste was used for calculating the methane yield and for finding the probable moisture content within the reactor. The initial moisture content data for each reactor is tabulated in Table 4.4. The average initial moisture content of waste after sludge and water addition for all reactors is plotted in Figure 4.1.

Table 4.4: Initial Moisture Content within the Reactors

Moisture Content of 20°C Reactors (% on wet weight basis)									
Waste Combination	**A**	**B**	**C**	**D**	**E**	**F**	**G**	**H**	**I**
Sample 1	87.47	21.08	76.33	78.82	59.00	84.70	64.60	33.56	62.62
Sample 2	84.21	27.81	74.85	82.25	58.01	85.89	74.77	47.69	51.58
Sample 3									45.28
Average	**85.84**	**24.45**	**75.59**	**80.53**	**58.51**	**85.30**	**69.69**	**40.63**	**53.16**

Moisture Content of 30°C Reactors (% on wet weight basis)									
Waste Combination	**A**	**B**	**C**	**D**	**E**	**F**	**G**	**H**	**I**
Sample 1	88.20	50.26	54.13	63.96	39.36	61.51	68.73	55.40	50.84
Sample 2	85.96	70.39	52.86	71.76	43.29	67.10	63.73	55.26	53.89
Sample 3	90.44	70.03	53.19	69.67	43.54	64.50	63.63	60.32	50.47
Average	**88.20**	**63.56**	**53.39**	**68.47**	**42.06**	**64.37**	**65.37**	**56.99**	**51.73**
Std. Dev	**2.239**	**11.52**	**0.656**	**4.041**	**2.347**	**2.798**	**2.913**	**2.881**	**1.879**

Moisture Content of 37°C Reactors (% on wet weight basis)									
Waste Combination[*1]	**A**	**B**	**C**	**D**	**E**	**F**	**G**	**H**	**I**
Sample 1	93.70	48.11	44.59	79.88	42.83	72.34	74.59	46.25	60.00
Sample 2	93.00	56.58	42.23	81.96	39.55	75.14	74.20	52.79	61.34
Sample 3	94.36	52.65	45.96	76.40	48.14	75.79	75.63	53.51	50.85
Average	**93.68**	**52.45**	**44.26**	**79.41**	**43.51**	**74.42**	**74.81**	**50.85**	**57.40**
Std. Dev	**0.6816**	**4.238**	**1.891**	**2.810**	**4.335**	**1.834**	**0.7409**	**4.001**	**5.709**

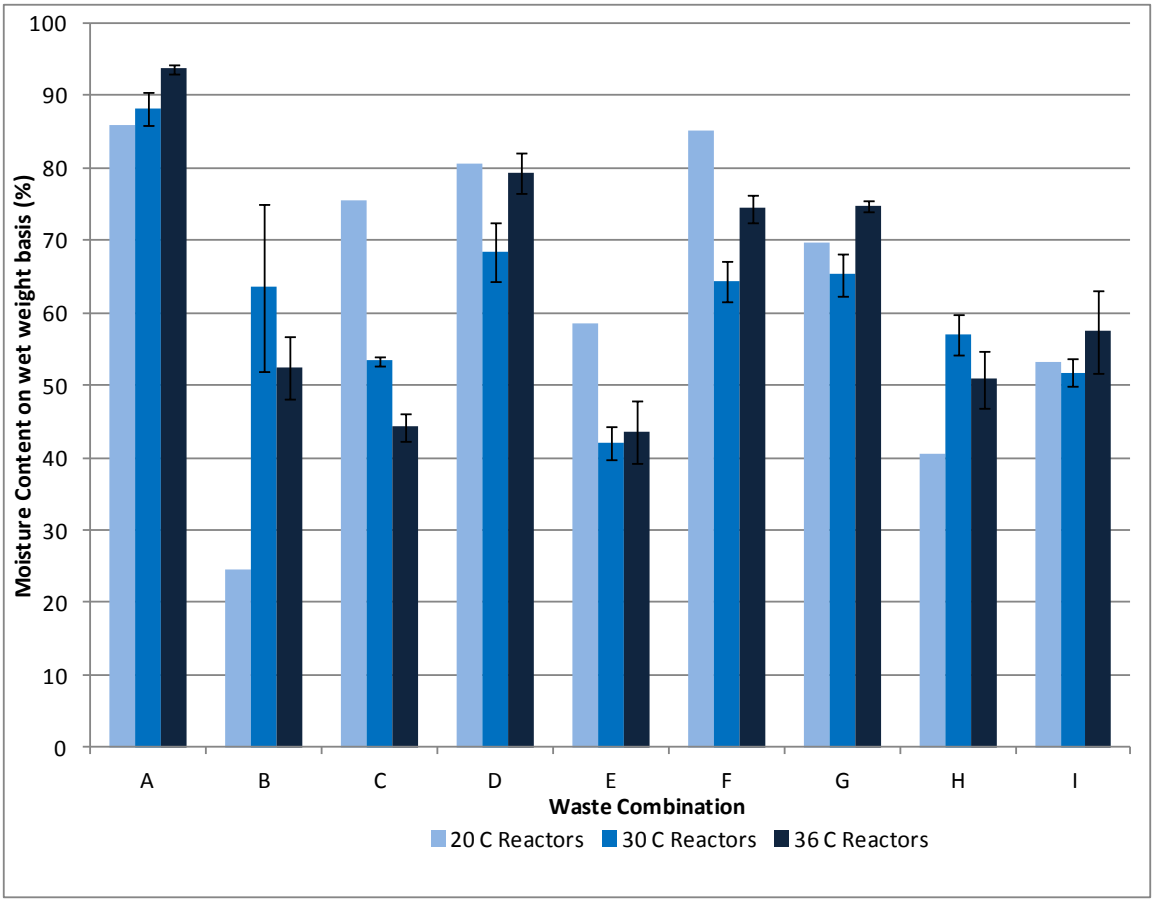

*Note: The waste composition and reactor numbers can be found in Table 3.1 and 3.2
Error bars are not shown for reactors at 20°C because the tests were carried out in duplicates.

Figure 4.1: Average Initial Moisture Content on Wet Weight Basis within the Reactors.

4.2.3 Initial Volatile Solids

Volatile Solids (VS) of the waste combinations (A to I) were determined before the reactors were put into operation and hereafter will be referred as initial volatile solids. The volatile solids test was performed for each reactor, and the results are tabulated in Table 4.5. Since the volatile solid is a property of the waste, it was expected to be similar for reactors with identical composition. Hence the average values and standard deviations were computed with respect to waste combinations, and are graphically represented in Figure 4.2. Waste combination "E- 60% paper and 40% inorganic" and "I = 20% each" had inorganic waste in it.

Since plastic waste is highly volatile, the inorganic portion of the waste was segregated and the volatile solids test was performed on the organic portion only. The values were then adjusted using a weighted average, assuming the volatile solids of inorganic waste to be equal to zero.

Table 4.5: Volatile Solids Results for Waste Combinations (A to I)

Volatile Solids (%)									
Waste Combination [*1]	**A**	**B**	**C**	**D**	**E** [*2]	**F**	**G**	**H**	**I** [*2]
20°C	92.73	89.42	94.97	80.39	53.74	92.64	82.68	92.53	72.00
	92.49	88.83	99.85	80.95	55.46	93.48	87.56	90.56	64.08
30°C	88.12	89.75	98.85	86.51	53.57	91.26	88.75	94.74	71.53
	90.82	91.21	98.22	88.52	54.00	93.94	87.59	97.01	71.42
	91.96			86.20		95.55	87.97		70.23
37°C	89.38	91.44	98.84	86.86	54.70	95.00	86.50	96.06	72.95
	88.97	90.38	99.11	85.68	55.90	88.57	86.84	95.97	72.03
	86.77	84.87				93.53	87.46		
		88.85					82.94		
AVG	**90.16**	**89.34**	**98.31**	**85.02**	**54.56**	**93.00**	**86.71**	**94.48**	**70.61**
Std Dev	2.183	2.057	1.718	3.101	0.9586	2.226	2.176	2.464	2.992

NOTE:

1- The waste combination details and reactor numbers can be found in Table 3.1 and 3.2
2- Volatile solids for waste combination with inorganic waste was adjusted using weighted average.
3- Blanks indicate that the number of replicates for each reactor were not constant.

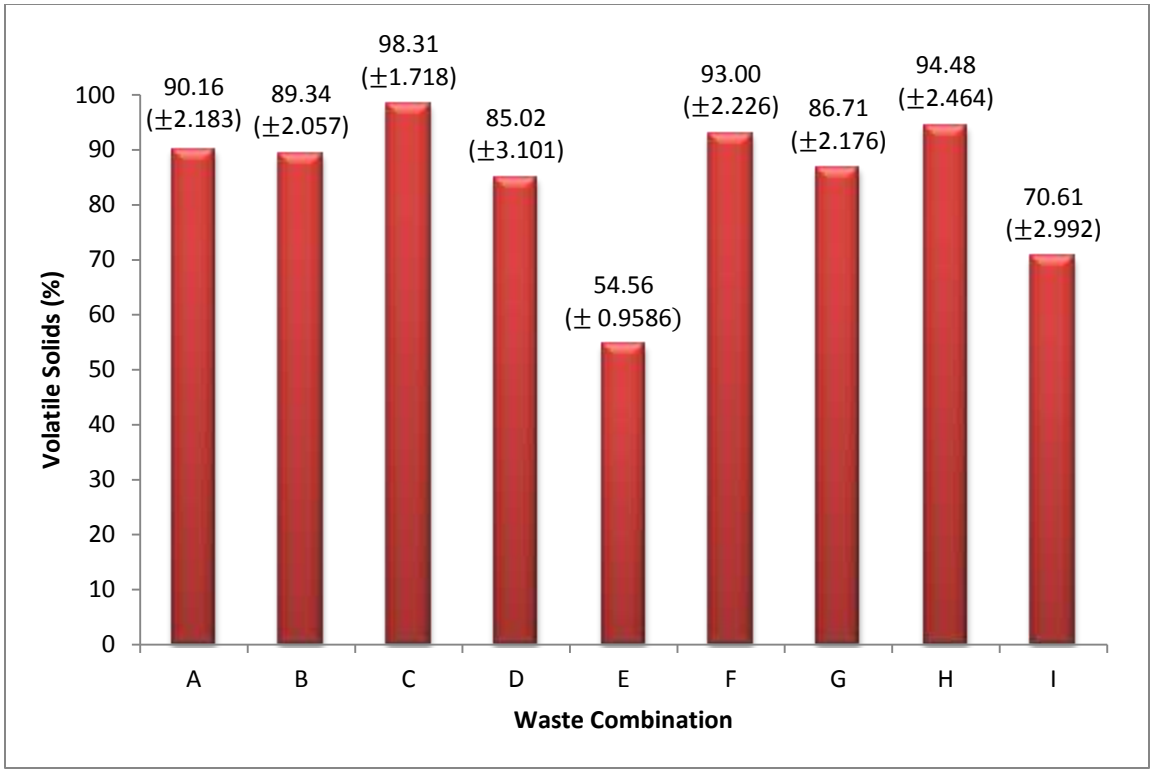

NOTE: Volatile solids for waste combination (E and I) with inorganic waste was adjusted using weighted average. Values in parenthesis are standard deviations.

Figure 4.2: Average Volatile Solids Content for Waste Combinations (A to I).

The initial volatile solids data was used for computing the Biochemical Methane Potential (BMP). The initial volatile solids for 100% waste combinations were compared to the values reported in the literature. (See Table 4.6) Volatile solids found in this study were comparable to those reported in the literature. The volatile solids for yard waste found in this study, however, were less than those reported in literature. It must be noted that the values listed in Table 4.6 were for waste components e.g. grass, leaves. Since the yard waste considered in this study included all components such as grass, leaves, and branches, there was some variability observed in this study.

Table 4.6: Comparison of Volatile Solids Found in This Study with Literature

Waste Composition	Volatile Solids (% wt)	Author	VS (%) found in this study
Food Waste			
Mixed Food Waste	88.34	Qudias (2000)	90.16 (± 2.183)
Boiled Rice	99.00	Cho et al. (1995)	
Cooked Meat	97.00	Cho et al. (1995)	
Fresh Cabbage	84.00	Cho et al. (1995)	
Mixed food waste (Korean)	95.00	Cho et al. (1995)	
Fruits and Vegetable waste	81.7 - 98.4	Gunaseelan (2004)	
Food	93.80	Eleazer et. al. (1997)	
Paper Waste			
Paper and Cardboard	83.65	Qudias (2000)	89.34 (±2.057)
Office Paper	96.20	Owens and Chynoweth (1993)	
Corrugated Paper	94.80	Owens and Chynoweth (1993)	
Newsprint (unprinted)	91.40	Owens and Chynoweth (1993)	
Newsprint (printed)	92.20	Owens and Chynoweth (1993)	
Magazine	97.10	Owens and Chynoweth (1993)	
Food Board (uncoated)	98.60	Owens and Chynoweth (1993)	
Food Board (coated)	93.30	Owens and Chynoweth (1993)	
Milk Carton	99.40	Owens and Chynoweth (1993)	
Wax Paper	98.40	Owens and Chynoweth (1993)	
Coated Paper	74.30	Eleazer et. al. (1997)	
Old News Print	98.50	Eleazer et. al. (1997)	
Old Corrugated Containers	98.20	Eleazer et. al. (1997)	
Office Paper	98.60	Eleazer et. al. (1997)	
Office Paper	88.40	Wu et. al. (2001)	
Newsprint	98.00	Wu et. al. (2001)	
Yard Waste			
Grass	88.10	Owens and Chynoweth (1993)	85.02 (± 3.101)
Leaves	95.00	Owens and Chynoweth (1993)	
Branch	93.90	Owens and Chynoweth (1993)	
Mixed Yard Waste	92.00	Owens and Chynoweth (1993)	
Grass	85.00	Eleazer et. al. (1997)	
Grass 2	87.80	Eleazer et. al. (1997)	
Leaves	90.20	Eleazer et. al. (1997)	
Branch	96.60	Eleazer et. al. (1997)	

4.2.4 Biochemical Methane Potential of Waste

Biochemical Methane Potential (BMP) test was performed on dried and ground waste samples collected for all 9 waste combinations (A to I). The BMP test results are indicative of the total amount of methane that can be generated from a particular type of waste. Since the ultimate methane potential is a property of the waste composition or the degradable organic content of the waste, the samples with the same waste combination were mixed together. Thus, 9 samples corresponding to the 9 blocks (e.g. A to I) were analyzed using BMP. The tests were performed in triplicate and the results are represented as mL of CH4 corrected at STP/g of VS. Average BMP values are tabulated in Table 4.7 and the BMP exerted is graphically represented in Figure 4.3.

According to the procedure, BMP samples were analyzed every 7-10 days until the change in BMP was less than 5%. It was found that the BMP was fully exerted by most samples within 60-70 days of operation. However, samples with yard waste were incubated for about 80-100 days until the change in BMP was less than 5%. A standard of office paper was tested with the other samples. The BMP of ground office paper (not shown in the figure) was found to be 364.7 mL of CH_4/g of VS.

The BMP values were compared with those reported in literature. The BMP values for food, paper, yard and textiles wastes are shown in Figure 2.2. Table 4.8 summarizes the BMP values from literature, which were compared with the BMP observations from this study. Previous studies listed in Table 4.8 studied “pure” waste which was not mixed with other types of waste. However, in certain cases the BMP values were grouped to represent the type of waste. For example, BMP values for banana peels, fresh cabbage, and mixed cooked meat were combined to obtain a BMP range for food waste.

Table 4.7: Biochemical Methane Potential Values for Waste Combinations (A to I)

Biochemical Methane Potential									
Waste Combination	**A**	**B**	**C**	**D**	**E**	**F**	**G**	**H**	**I**
Waste Composition	**100% Food**	**100% Paper**	**100% Textile**	**100% Yard**	**60%Paper + 40% Inorg**	**60% Food +30% textile +10% Yard**	**60%Yard +30% Food + 10% Paper**	**60% Textile +30% Paper + 10% food**	**20% each**
Average BMP (mL of CH_4/g VS)	389.76	336.18	184.45	188.58	241.58	279.96	276.96	259.68	293.95
Std. Dev.	29.24	7.165	28.61	17.46	6.758	48.32	20.26	12.57	9.761

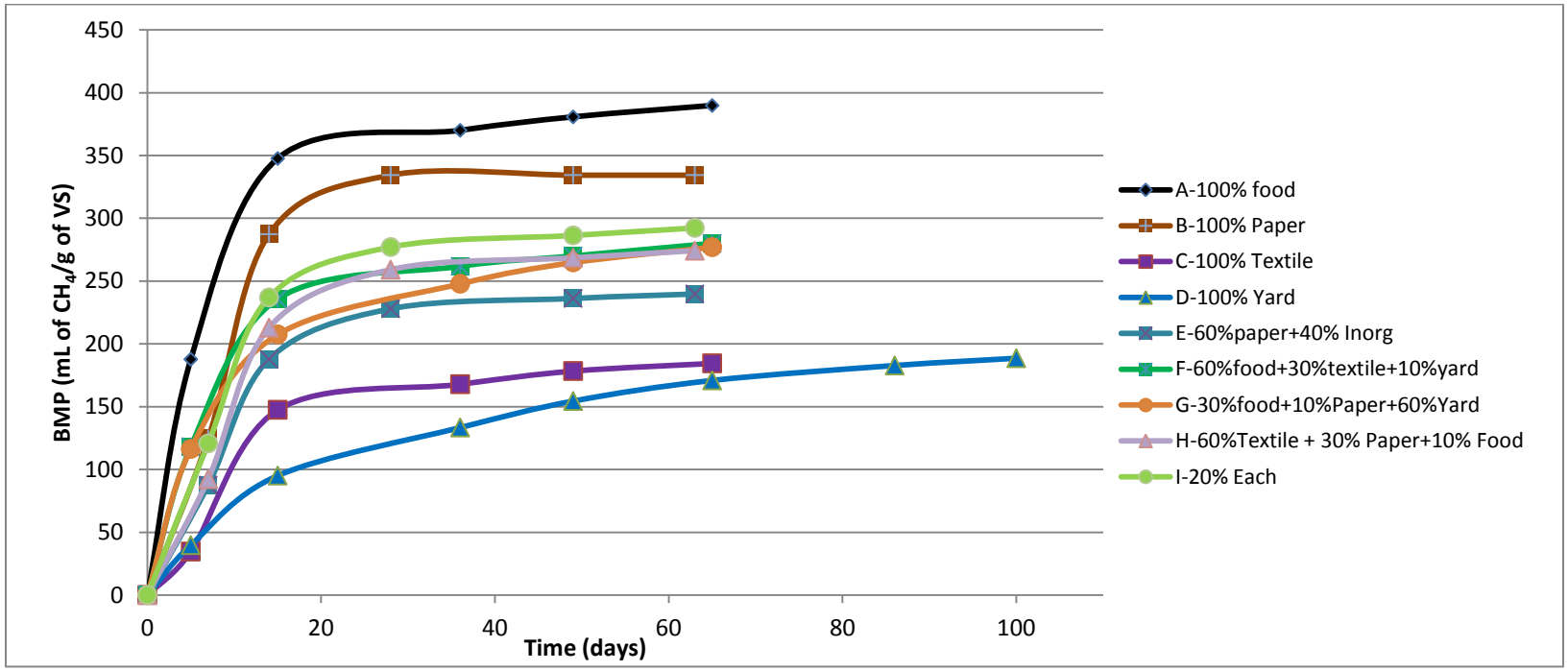

Figure 4.3: Biochemical Methane Potential (BMP) of Waste Combinations (A to I)

Table 4.8: Comparison of Biochemical Methane Potentials Found in this Study with Literature

Waste	**BMP range (m^3 of CH_4/kg of VS)**	**Authors**	**BMP found in this study**
Food Waste	0.292 – 0.54	Gunaseelan (2004) Cho et al. (1995) Eleazer et al. (1997) Jeon et. al (2007) Chynoweth et al (1993)	0.389 (± 0.0292)
Paper Waste	0.075 – 0.370	Owens and Chynoweth (1993) Eleazer et al. (1997) Jeon et. al (2007)	0.336 (±0.0071)
Textile Waste	0.035-0.21 m^3/kg of dry waste	Jeon et. al (2007) Isci and Demirer (2007)	0.181 (± 0.028) m^3/kg of dry waste
Yard Waste	0.014 – 0.283	Owens and Chynoweth (1993) Eleazer et al. (1997) Chynoweth et al. (1993) Jeon et. al (2007)	0.188 (±0.017)

From Table 4.8, it can be observed that the values observed in this study were within the range reported in literature. However, the BMP of paper waste appeared to be on the higher side. It should be noted that the values from literature were taken from studies conducted on individual components of paper waste such as office paper, corrugated paper, food board, coated paper. In the present study, all types of paper were mixed together to replicate the US paper composition reported in EPA (2007). Hence the BMP values found in this study were for the combined waste category, and hence could be directly compared to the values listed in Table 4.8, and Figure 2.2 and 2.3. Overall, the BMP values found in this study were consistent with those reported in the literature.

4.3 Reactor Data

Gas composition, gas volume and leachate pH act as indicators of microbial activity in the reactors. This section discusses the gas composition, volume and pH results from three

100% yard waste composition reactors (8, 14, and 19) at varying temperature and rainfall conditions as examples. The operating parameters for the reactors are summarized in Table 4.9 and the results are illustrated in Figure 4.4. The gas composition is shown in %, and the methane generation rate is represented in mL of methane at STP/ kg of dry solids/day.

Table 4.9: Operating Parameters for 100% Yard Reactors no. 8, 14, 19

Reactor no.	Waste Composition	Ambient Temperature	Rainfall
8	100% Yard	37^{o}C	2 mm/day
14	100% Yard	30^{o}C	6 mm/day
19	100% Yard	20^{o}C	12 mm/day

Anaerobic decomposition of solid waste in a typical landfill occurs in four stages: (i) aerobic phase, (ii) acidogenesis (acid formation), (ii) methanogenesis (methane formation), (iv) decelerating methane phase. From Figure 4.4 it can be observed that initially the percent oxygen in the reactors was high (about 20%), and reduced rapidly. This being the aerobic phase, gas mainly consisted of carbon dioxide and other gases (H_2S, and nitrogen compounds). In this phase, methane content in all the reactors was less than 20%.

In the acidogenic phase, the leachate pH started dropping, typically below 7.0. If the leachate pH was found to be below 5.5, potassium hydroxide (KOH) was added to the reactors, to avoid excessive acid accumulation. The methane content in gas increased in the third phase, methanogenesis, and stabilized around 50-60%. During methanogenesis the leachate pH was found to be between 6.0-8.5.

Reactor no. 8 - 100% Yard - 37°C - 2 mm/day

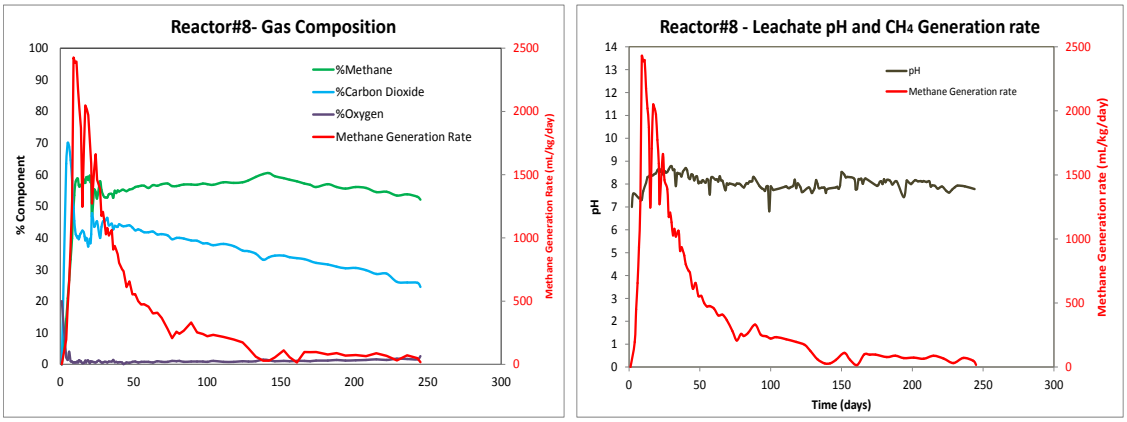

Reactor no. 14 - 100% Yard - 30°C - 6 mm/day

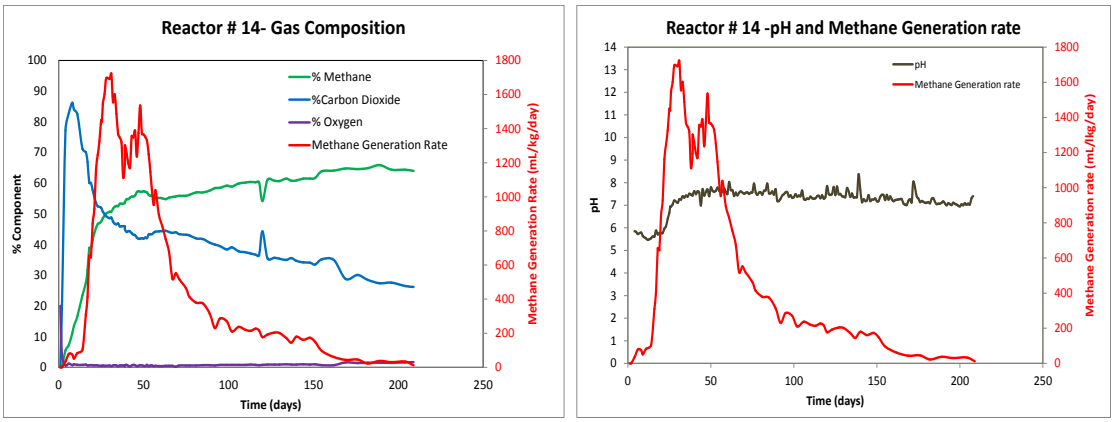

Reactor no. 19 - 100% Yard - 20°C -12 mm/day

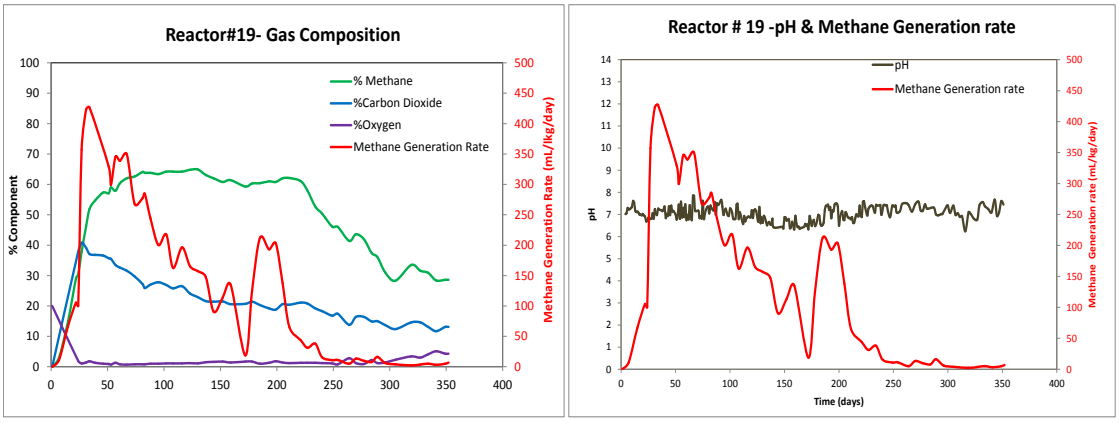

Figure 4.4: Gas Composition, Methane Generated and Leachate pH in 100% Yard Reactors

In the declining methane phase, the volume of gas generation decreased; hence the methane generation rate reduced. Similar trends were observed in all other reactors. Methane generation graphs and pH observations for all 27 reactors are shown in Appendix B.

Reactor no. 10, a 100 % food waste reactor, was set up at 20^{o}C, according to the experimental design. It was observed that the leachate pH dropped to 4.3 within 24 hours after installing the reactor. Shao et. al (2005) reported that excessive volatile fatty acid accumulation and sudden pH drop occur when waste with high food waste content is landfilled. Hence to neutralize the waste, KOH was dissolved into water and added in the reactor. However, even after running the reactor for 80 days, substantial improvement in the leachate pH was not observed. Further, the methane content in gas was close to zero. Hence the reactor was perceived to have failed and was dismantled. The data for reactor no. 10 is shown in Appendix B.

Subsequently, to avoid excessive acid accumulation, KOH was added in all food waste reactors while installing the reactors. Similar observations were reported by Wang et al. (1997) where food waste reactors with 30% seed failed due to acid accumulation; however when the seed percentage was increased to 70%, the reactors were successful, due to dilution effect. In this study additional seed was not added to avoid an increase in methane generation rate (*k* value) due to the presence of additional micro-organisms (seed). The percentage of seed in all reactors was maintained between 15-20% by weight to avoid variability.

4.3.1 Comparison of Methane Generation Rates and Cumulative Methane Generation:

Comparison of methane generation rates from reactors is presented in this section. Since each type of waste was expected to exhibit similar trends for methane generation, these results were compiled with respect to waste combinations (A to I). The methane generation rate

is expressed in terms of mL of methane at STP/kg of dry waste/ day. The cumulative methane generation rate is computed by adding the daily methane generation rate and is expressed in terms of liters of methane at STP / kg of dry waste.

A - 100 % Food Waste: Operating parameters for waste combination A- 100% food waste reactors were as follows.

Reactor no.	Waste Composition	Ambient Temperature	Rainfall
4	100% Food	30^{o}C	2 mm/day
10	100% Food	20^{o}C	6 mm/day
25	100% Food	37^{o}C	12 mm/day

The methane data from 100% food waste reactors is shown in Figure. 4.5. As mentioned earlier, reactor no. 10, at 20^{o}C and 6 mm/day rainfall failed due to excessive acid accumulation; hence the data from reactor no. 10 is not included in Figure 4.5.

It can be observed that the cumulative methane generation from food reactors is significantly influenced by the rainfall. The total amount of methane generated from R25 (37^{o}C, 12 mm/day) was considerably lower than R4 (30^{o}C, 2 mm/day), indicating that the carbon leaching was signifcantly higher in R25 due to the higher rainfall condition. Further, it was observed that the duration of the lag phase was longer in case of food waste as compared to other 100% reactors operated at similar temperature. A longer lag phase was also observed in reactors with higher percentage of food (Waste combination F: 60% food waste). These longer lag phases can be attributed to VFA generation in reactors with high food content. Shao et al. (2005) conducted studies for solid waste in China, comprised of about 50-60% food waste, reported that rapid hydrolysis and volatile fatty acid accumulation in waste with a high percentage of food waste caused an increased lag phase before methanogenesis started. It was observed on dismantling that food reactors had the maximum amount of settlement, and

considerable loss in weight, which could be due to degradation of waste (since food is the most easily degraded of the waste categories tested) and high amount of carbon leaching.

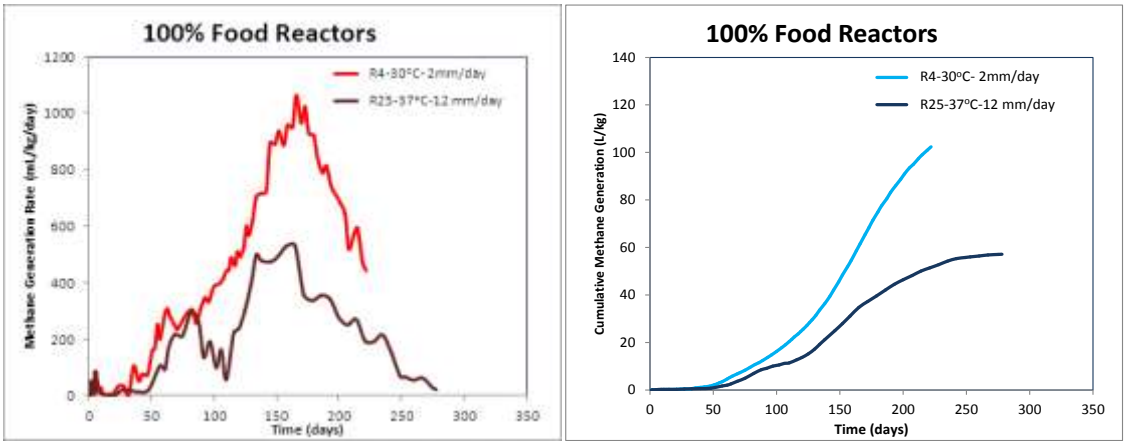

(a) (b)

(c)

Figure 4.5: 100% Food Waste Reactors (a) Methane Generation Rate, (b) Cumulative Methane Generated (c) Reactor pictures

B- 100 % Paper Reactors: Operating parameters for waste combination B- 100% paper waste reactors were as follows:

Reactor no.	Waste Composition	Ambient Temperature	Rainfall
1	100% Paper	20°C	2 mm/day
7	100% Paper	37°C	2 mm/day
13	100% Paper	30°C	6 mm/day

Methane generation data for 100% paper reactors is shown in Figure 4.6. It can be seen from the methane generation rate curve that the methanogenesis initiated slowly in the 20°C reactor. The 37°C reactor shows the highest initial methane generation rate, which then dropped quickly. As the temperature increased, the initiation of methanogenesis was faster in case of 100% paper waste reactors.

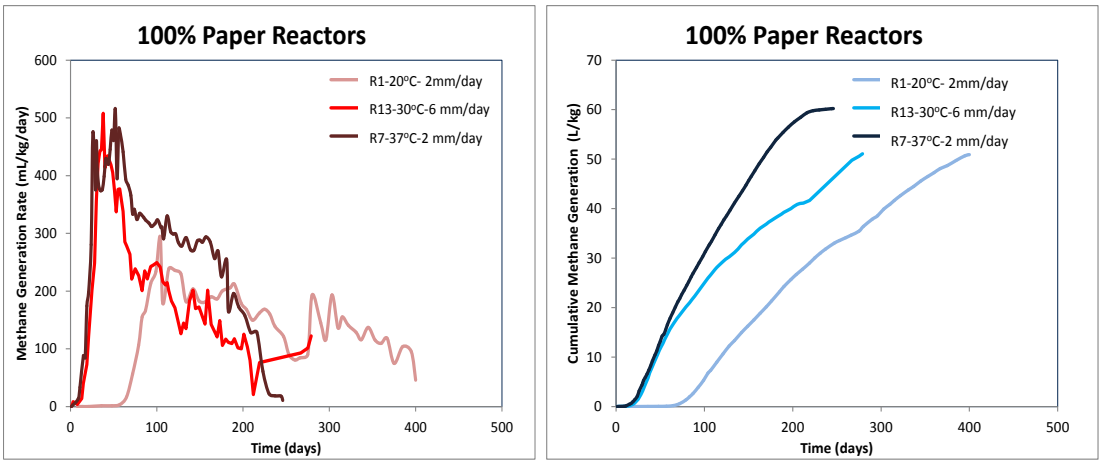

Figure 4.6: 100% Paper Waste Reactors (a) Methane Generation Rate, (b) Cumulative Methane Generated (c) Reactor Pictures

It should also be noted that reactor no. 1 and reactor no. 7 – both received the same amount of rainfall (2 mm/day); while the former was placed at 20°C, the latter was at 37°C. The cumulative methane generated from reactor no. 1 was 50.64 L/kg and reactor no. 7 was 59.94

L/kg. It would be safe to say that the total amount of methane generated from these two reactors receiving the same amount rainfall was very close. However, the cumulative methane generated from reactor no. 13 was less than that produced from other reactors (R#1 and R#7) with lesser rainfall. Thus, an increase in rainfall decreased the total methane generated from the 100% paper reactors. This could be due to carbon leaching, since the amount of carbon leached out of the reactor would be higher at higher rainfall rates.

Previous studies (Barlaz, 2006; Eleazer et.al., 1997) have mentioned that paper waste typically has lesser ammonical-nitrogen content, which serves as a nutrient for methanogens. Hence the paper reactor may be nutrient starved and may need additional nutrients for complete degradation. However, in this study nutrients were not added to the reactors in order to replicate the field conditions in the lab scale reactors. Thus the lesser amount of methane generated from these reactors could also be a result of nutrient deficiency.

After dismantling the reactors, it was found on visual observation that the paper towels and office paper from the paper reactors had mostly degraded. However, the printed paper waste was quite legible, while cardboard and milk cartons remained unchanged.

C- 100% Textile Reactors: Operating parameters for waste combination C- 100% textile waste reactors were as follows.

Reactor no.	Waste Composition	Ambient Temperature	Rainfall
5	100% Textile	30^{o}C	2 mm/day
11	100% Textile	20^{o}C	6 mm/day
16	100% Textile	37^{o}C	6 mm/day

Methane generation rates from 100% textile reactors are shown in Figure 4.7. The methane generation data from reactor no. 11- 20^{o}C, 6 mm/day is not shown here, because the total amount of methane generated from this reactor was very low. Even after operating the

reactor for 352 days, the methane generation rate was not significant. It was observed that there was excessive leachate production on the first day of reactor operation, which could have caused microbial washout. To confirm this hypothesis, additional sludge was added in R11 on day 230, and again on day 234. There were significant increases in methane generation after microbe (sludge) addition. Hence it can be concluded that the reactor was microbe deficient for the first 230 days. Since the effect of sludge addition on the methane generation rate constant (*k* value) could not be quantified, the data from this reactor was not considered for further analysis.

Mutiple peaks were typically observed in 100% textile waste; this could be due to different types of textile wastes degrading at different rates. The textile waste used in this study included all types of textiles: cotton, jeans, polyester, spandex, blends, etc. Hence each type of waste could be degrading at different rates. Overall, the rate of degradation of textile wastes was very slow; hence the reactors were still producing methane after about 300 days. Further, textile wastes had relatively lower rates of degradation (as compared to other waste categories); hence rainfall and temperature did not seem to substantially impact methane generation. The leachate was often colorful, probably due to to the leaching of dyes used in the textiles.

After dismantling the reactors it was observed that 100% textile reactors had very little or no settlement. The colors of some textiles were still intact and identifiable. However, on drying, certain types of textiles (jeans and cotton waste) had become brittle and would crumble upon touch. Polyester and blended textiles were mostly unchanged.

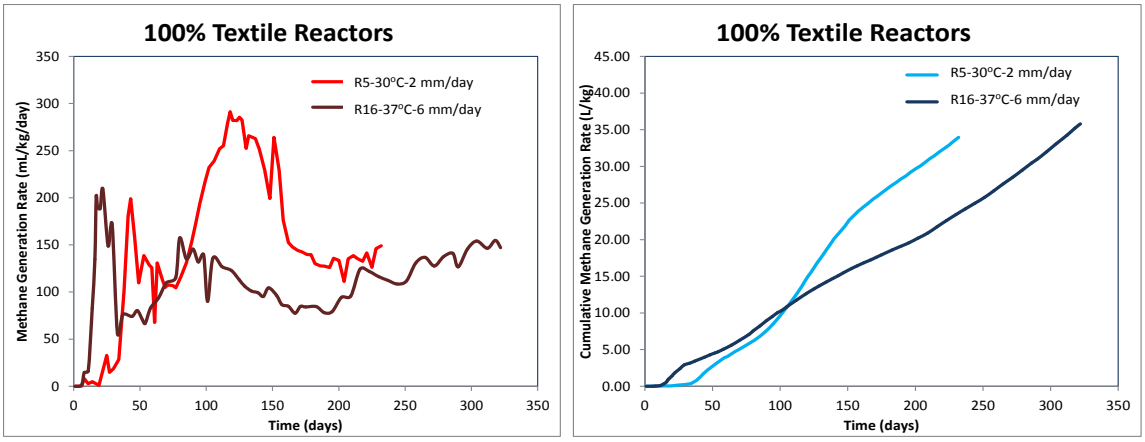

(a) (b)

(c)

Figure 4.7: 100% Textile Waste Reactors (a) Methane Generation Rate, (b) Cumulative Methane Generated (c) Reactor Pictures

D- 100% Yard Reactors: The comparison between methane generation rates from 100% yard reactors is shown in Figure 4.8. The operating parameters for waste combination D: 100% yard reactors is shown below:

Reactor no.	Waste Composition	Ambient Temperature	Rainfall
8	100% Yard	37°C	2 mm/day
14	100% Yard	30°C	6 mm/day
19	100% Yard	20°C	12 mm/day

From Figure 4.8, it can be observed that methanogenesis initiated slowly in the 20°C reactor. The 37°C reactor showed the highest initial methane generation rate, which then dropped quickly. The 30°C reactor had an intermediate methane generation rate, which then gradually started decreasing. Thus, methane generation was faster as the temperature

increased, even though the rainfall was infact increasing as the temperature decreased. It can be seen from the cumulative methane generation graph (Figure 4.8(b)) that the total methane generated from reactor no. 19 was significantly less than that from reactor nos. 8 and 14. This could be due to higher carbon leached out due to higher rainfall rate.

Yard waste showed very high peaks, as compared to other reactors. However, visual observation of the remaining waste upon dismantling the reactors showed that the grass from the yard waste was probably responsible for the higher peaks. The leaves, twigs and branches in the yard waste did not show significant degradation.

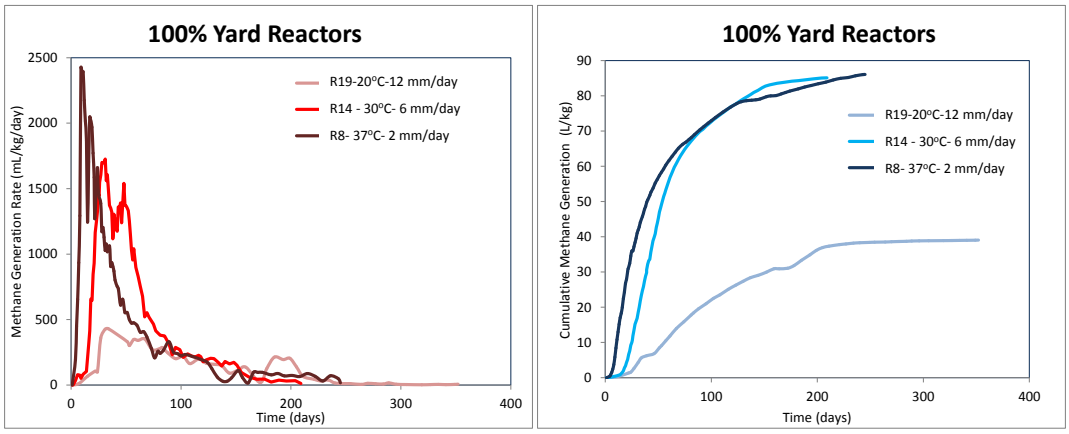

(a) (b)

(c)

Figure 4.8: 100% Yard Waste Reactors (a) Methane Generation Rate, (b) Cumulative Methane Generated (c) Reactor Pictures

E: 60% Paper and 40% Inorganic Reactors: The methane generation data from 60% paper and 40% inorganic waste reactors is shown in Figure 4.9. The operating parameters for waste combination E: 60% paper and 40% inorganic reactors is shown below:

Reactor no.	Waste Composition	Ambient Temperature	Rainfall
12	60% Paper + 40% Inorganic	20^{o}C	6 mm/day
17	60% Paper + 40% Inorganic	37^{o}C	6 mm/day
22	60% Paper + 40% Inorganic	30^{o}C	12 mm/day

Although inorganic waste does not produce methane, it was important to study the effect of inorganics, including plastic, metals, C&D waste, on degradation of waste. Methane generation data showed considerable fluctuations in daily methane generation rates. It was found that the leachate would often get locked in these reactors, which could be due to the presence of plastics. Initiation of methanogenesis was faster as the temperature increased.

Reactors no. 12 & 17 received same amount of rainfall; however the cumulative methane generated from these two reactors had considerable difference. The cumulative methane generation was similar for reactors 12 and 22, receiving 6 mm and 12 mm per day rainfall, respectively. Thus, these reactors did not follow the trend observed for the 100% paper reactors of increased rainfall decreasing cumulative methane generation.

When the reactors were dismantled, the paper waste from these reactors appeared to have degraded more than that from the 100% paper reactors. This could be due to the additional water due to the presence of plastics in these reactors. Inorganic waste from these reactors was mostly unchanged; however, the plastic bottles had water accumulated inside them.

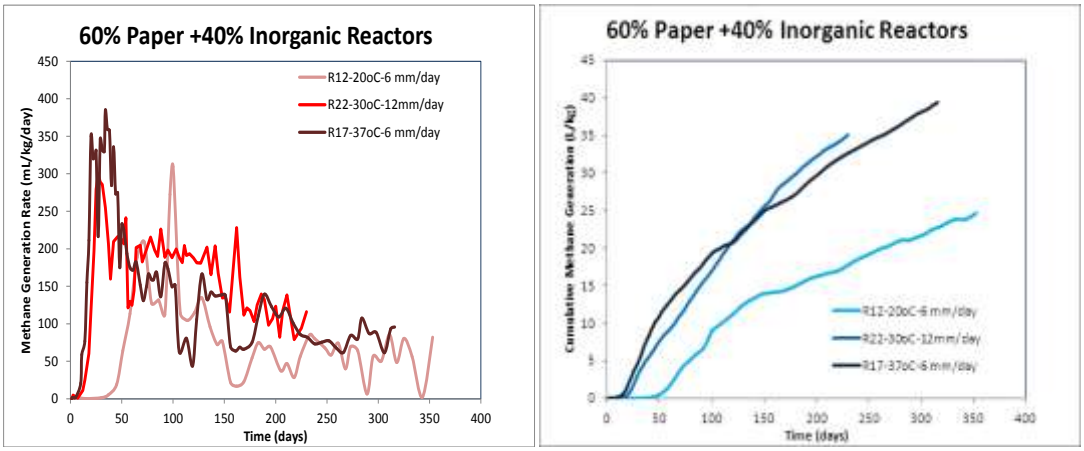

(a) (b)

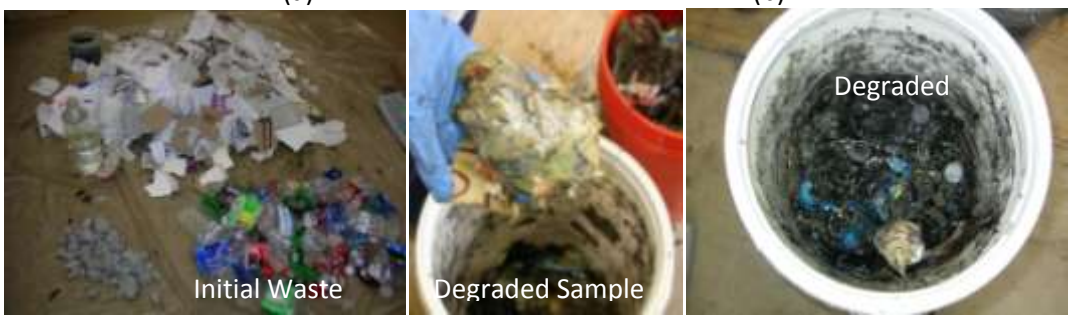

(c)

Figure 4.9: 60% Paper+ 40% Inorganic Waste Reactors (a) Methane Generation Rate, (b) Cumulative Methane Generated (c) Reactor Pictures

F: 60% Food + 30% Textile +10% Yard Reactors: The methane generation data and cumulative methane generated from 60% food+30% textile +10% yard reactors is shown in Figure 4.10. The operating parameters for waste combination F: 60% food + 30% textile +10% yard were as follows:

Reactor no.	Waste Composition	Ambient Temperature	Rainfall
15	60% Food + 30% Textile +10% Yard	30°C	6 mm/day
20	60% Food + 30% Textile +10% Yard	20°C	12 mm/day
26	60% Food + 30% Textile +10% Yard	37°C	12 mm/day

These reactors displayed more than one peak. This could be due to different types of waste degrading at different rates. The overall rate of degradation was slow due to the presence of textile waste in the reactors. Even after operating reactor no. 26 at 37°C for 320 days, it was still producing gas, and had not dropped to a low constant value. Similar behavior was found in reactors no. 20 and 15, which were operated at lower temperatures.

Reactors no. 20 and 26 received same amount of rainfall (12 mm/day) and the cumulative methane generated from these reactors was comparable. After dismantling it was found that the food waste in these reactors had mostly disappeared; however the textile waste was mostly unchanged. The settlement in 60% food reactors was also high, second only to the 100% food reactors.

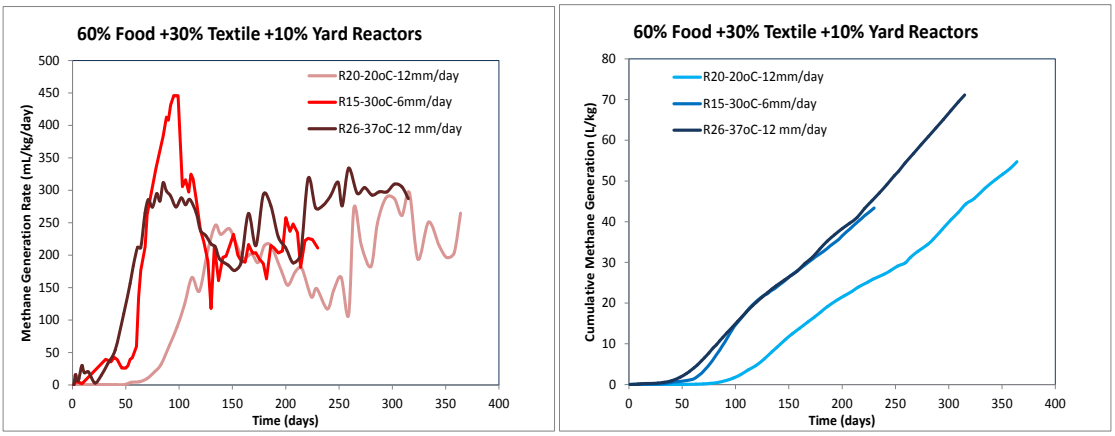

(a) (b)

(c)

Figure 4.10: 60% Food + 30% Textile + 10% Yard Waste Reactors (a) Methane Generation Rate, (b) Cumulative Methane Generated (c) Reactor pictures

G: 60% Yard + 30% Food + 10% Paper: The methane generated rates from 60% yard+30% food+ 10% paper reactors are shown in Figure 4.11. The operating parameters are summarized below.

Reactor no.	Waste Composition	Ambient Temperature	Rainfall
2	60% Yard + 30% Food + 10% Paper	20^{o}C	2 mm/day
18	60% Yard + 30% Food + 10% Paper	37^{o}C	6 mm/day
23	60% Yard + 30% Food + 10% Paper	30^{o}C	12 mm/day

It can be seen that lag period was longest in 20^{o}C reactor. However, the lag period in 30^{o}C is observed to be lesser than that for the reactor at 37^{o}C. The smaller lag period for reactor no. 23 compared to reactor no. 18 at higher temperature could be because of higher rainfall. The total amount of methane generated from reactors no. 2, 23 and 18 was almost similar, indicating that the effect of rainfall was not significant on the cumulative methane generated from the reactors. This contradicts the observations from other reactors. On dismantling the food waste within these reactors was not identifiable. However, the leaves were identifiable, but grass had mostly disappeared, or was lumped into an unidentifiable mass.

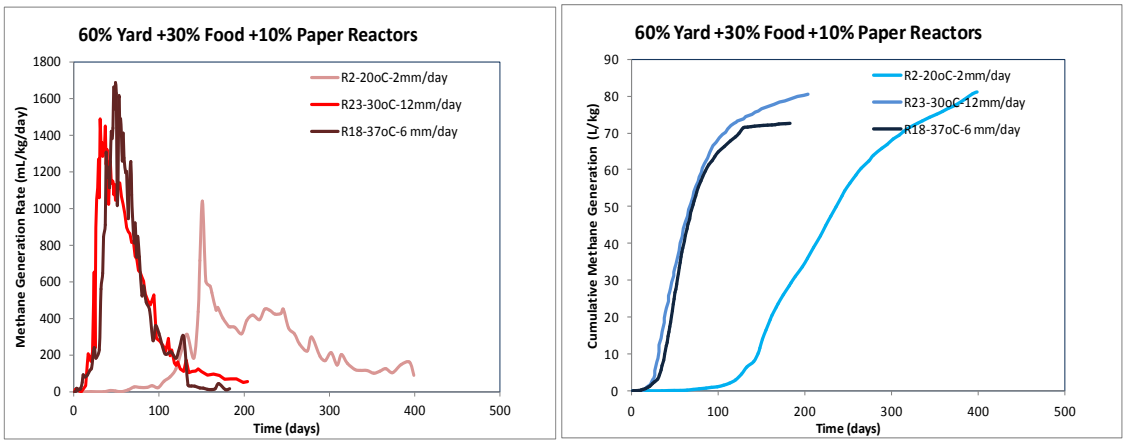

(a) (b)

(c)

Figure 4.11: 60% Yard + 30% Food + 10% Paper Waste Reactors (a) Methane Generation Rate, (b) Cumulative Methane Generated (c) Reactor Pictures

H- 60% Textile + 30 % Paper + 10% Food Reactors: The methane generated from 60% textile+30% paper and 10% food reactors is shown in Figure 4.12. The operating parameters are listed below.

Reactor no.	Waste Composition	Ambient Temperature	Rainfall
6	60% Textile + 30 % Paper + 10% Food	30°C	2 mm/day
21	60% Textile + 30 % Paper + 10% Food	20°C	12 mm/day
27	60% Textile + 30 % Paper + 10% Food	37°C	12 mm/day

It can be observed that the lower the temperature, the longer was the lag phase in these reactors. Multiple peaks were observed due to the presence of a combination of wastes, as well as high percentage of textile waste. There was considerable variability in the cumulative

methane generated from reactors no. 21 and 27, although both of them received the same amount of rainfall, which contradicts the observations from other reactors. The cumulative methane generated from reactor no. 27 was lower than reactor no. 6; this could be due to higher amount of rainfall in reactor no. 27 is higher than reactor no. 6, which would mean higher carbon washout. However, R21 and R6 had almost same amount of total methane generation, while the R6 received lesser rainfall than R21. This again contradicts the results from other reactors, where increase in rainfall reduced the total amount of methane generated from the reactors.

Upon dismantling, the textile wastes did not appear to have changed much. However, after drying it was observed that certain types of textile waste like cotton fabrics had turned brittle and would turn into powder on touch. The food waste was not identifiable in these reactors. Paper waste was lumped with the textile and was difficult to separate, indicating degradation of paper waste.

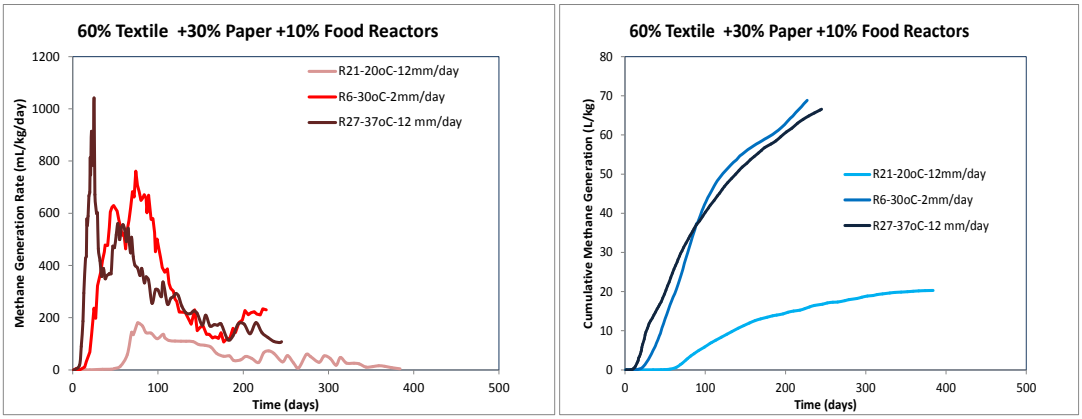

(a) (b)

(c)

Figure 4.12: 60% Textile + 30% Paper + 10% Food Waste Reactors (a) Methane Generation Rate, (b) Cumulative Methane Generated (c) Reactor pictures

I – 20% each: The methane generated from 20% each reactors is shown in Figure 4.13. The operating parameters for waste combination I: 20% each are shown below.

Reactor no.	Waste Composition	Ambient Temperature	Rainfall
3	20% each	20°C	2 mm/day
9	20% each	37°C	2 mm/day
24	20% each	30°C	12 mm/day

The lag phase was longest at 20°C. However, the lag phase in reactor no. 24 at 30°C was shorter than that observed in reactor no. 9 at 37°C. This could be due to the presence of a higher amount of rainfall in reactor no. 24. Reactor no. 24 showed faster initiation of methanogenesis and the methane generation rate dropped gradually. However, reactor no. 9

showed the highest peak and the rate dropped rapidly thereafter. Reactor no. 3 was still producing considerable amount of gas after 370 days of operation. This behavior could be due to interaction effects.

The cumulative methane generation from reactors no. 9 and 3 was expected to be similar. However, since reactor no. 3 was still producing gas when it was dismantled, it is possible that amount of methane generated from it would eventually be comparable.

On dismantling these reactors, it was found that the food waste, tissues, office paper and grass had mostly degraded. Textile waste, cardboard, milk cartons, leaves and inorganic waste were mostly unchanged on visual examination.

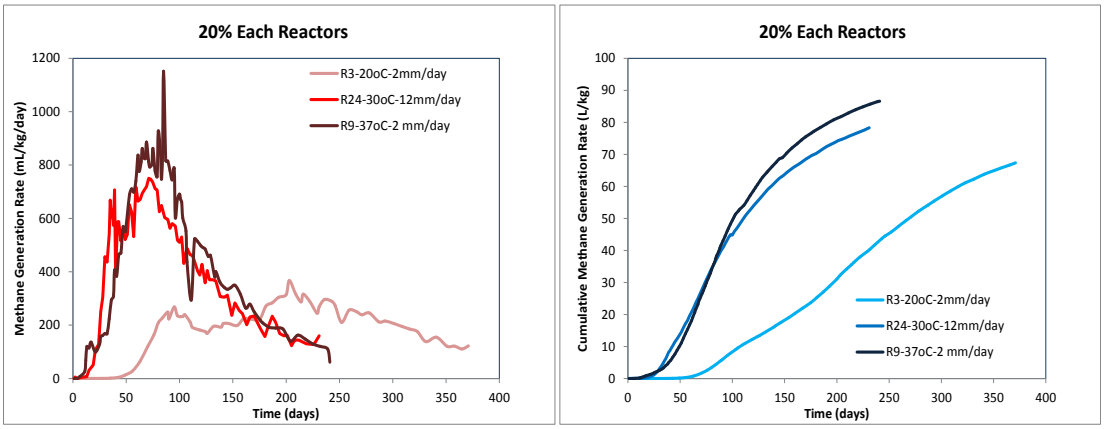

(a) (b)

(c)

Figure 4.13: 20% Each Waste Reactors (a) Methane Generation Rate, (b) Cumulative Methane Generated (c) Reactor Pictures

4.3.2 Effect of Waste Composition on Methane Generation Rate

To study the effect of waste composition on methane generation rate, the methane generated from all reactors was plotted against time at a particular temperature (See Figure 4.14-4.16). Waste composition affects methane generation rate significantly. From Figures 4.14-4.16, it can be observed that 100% yard wastes showed a relatively early high peak and asymptotic decrease, following classic first-order decay. 60% yard waste reactors followed a similar trend. Methane generation curve from paper waste reactors also showed first-order decay curve; however, the total amount of methane generated from 100% paper reactors was low, compared to the other reactors. This could be due to the nutrient deficiency in paper reactors. 100% food reactors showed a late peak, compared to other reactors, which could be due to the enhanced lag phase due to rapid hydrolysis. Due to the late peak, the cumulative methane generation curve from 100% food waste reactors did not follow exactly a first-order curve. Further, 100% textile waste reactors showed the lowest cumulative methane generation, with multiple and relatively low peaks. Thus 100% textile waste reactors did not follow the first-order decay curve. However, for the 20% each reactors, and in cases where there was a mixture of different types of wastes, the cumulative methane generation curve generally followed classic first-order decay. This behavior could be because the presence of a mixture of wastes supplemented nutrients, which enhanced the methane generation rates. The 60% food reactors showed a substantial lag phase, similar to the 100% food reactors.

It should be noted again that in each case the amount of rainfall received was different; hence the duration of lag phase and the peak intensity depended on the rainfall. The effect of temperature, rainfall and waste composition on rate of degradation can only be quantified using a multiple linear regression equation.

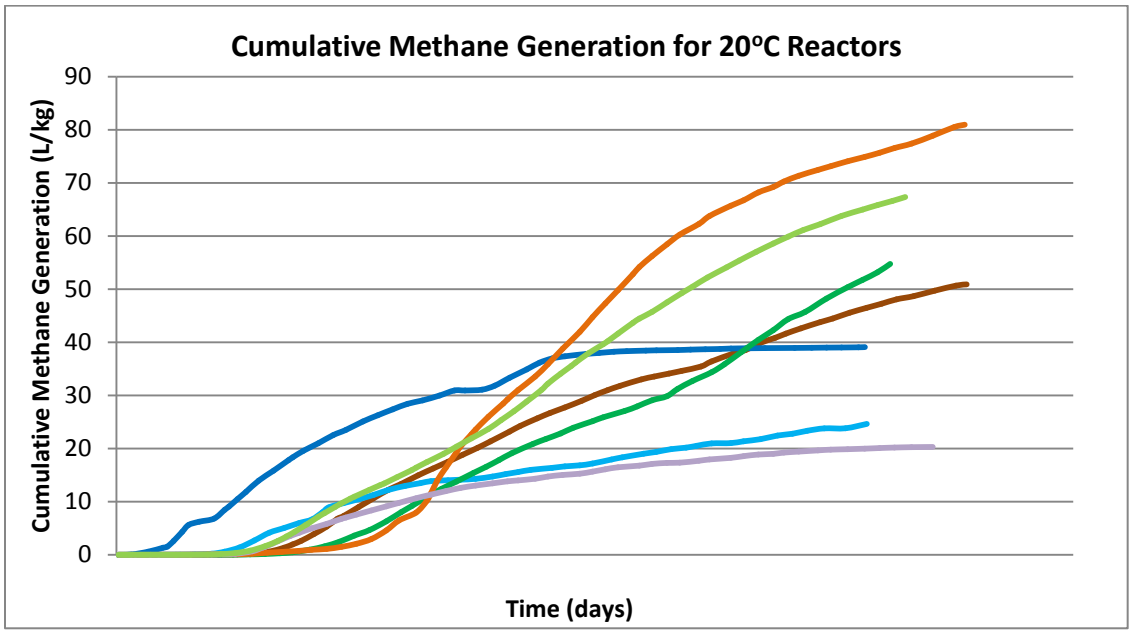

(a)

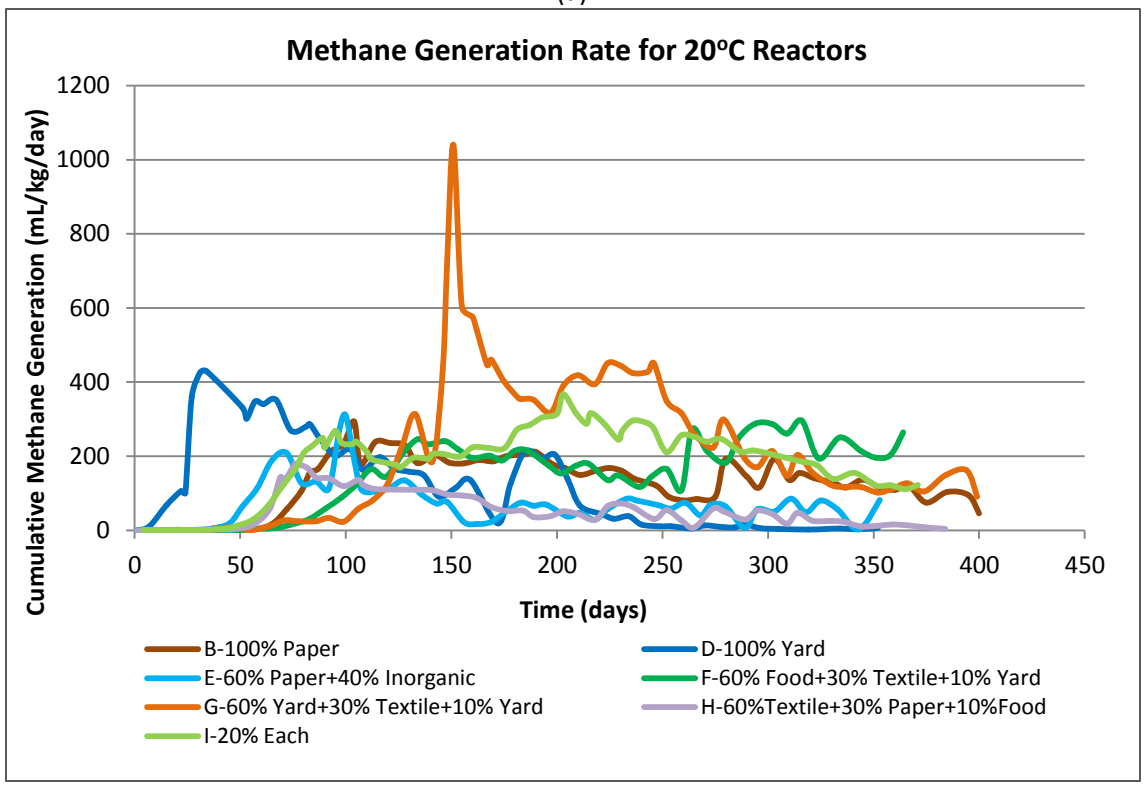

(b)

Figure 4.14: Gas Generation Rates for 20°C Reactors (a) Cumulative Methane Generation Curve (b) Methane Generation Rate Curve

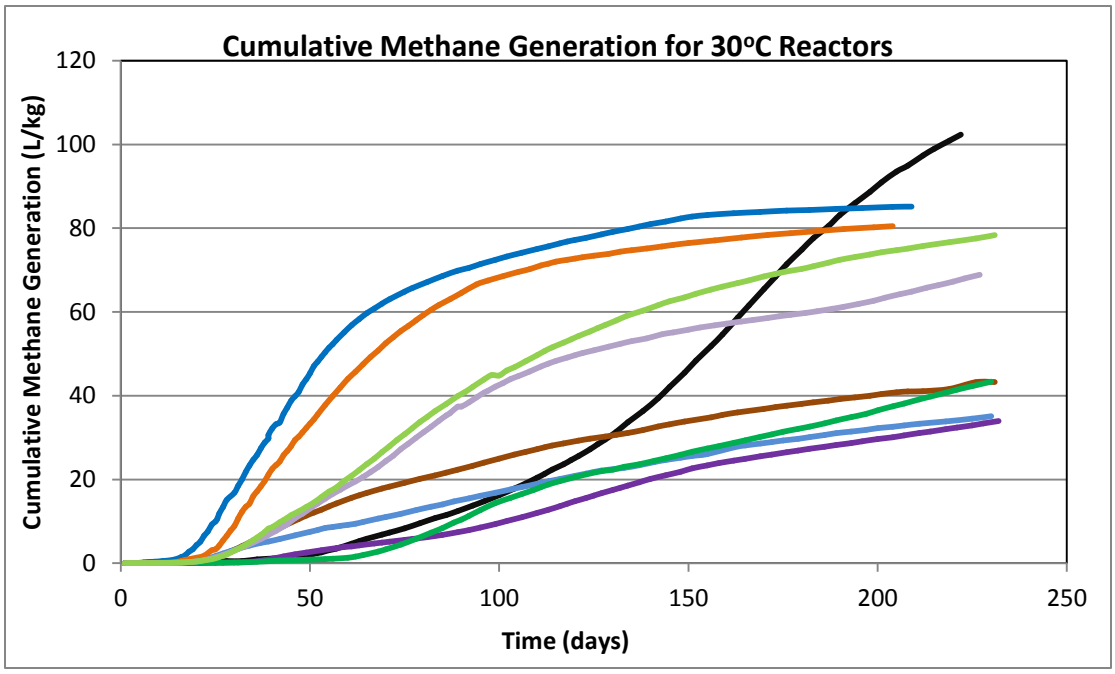

(a)

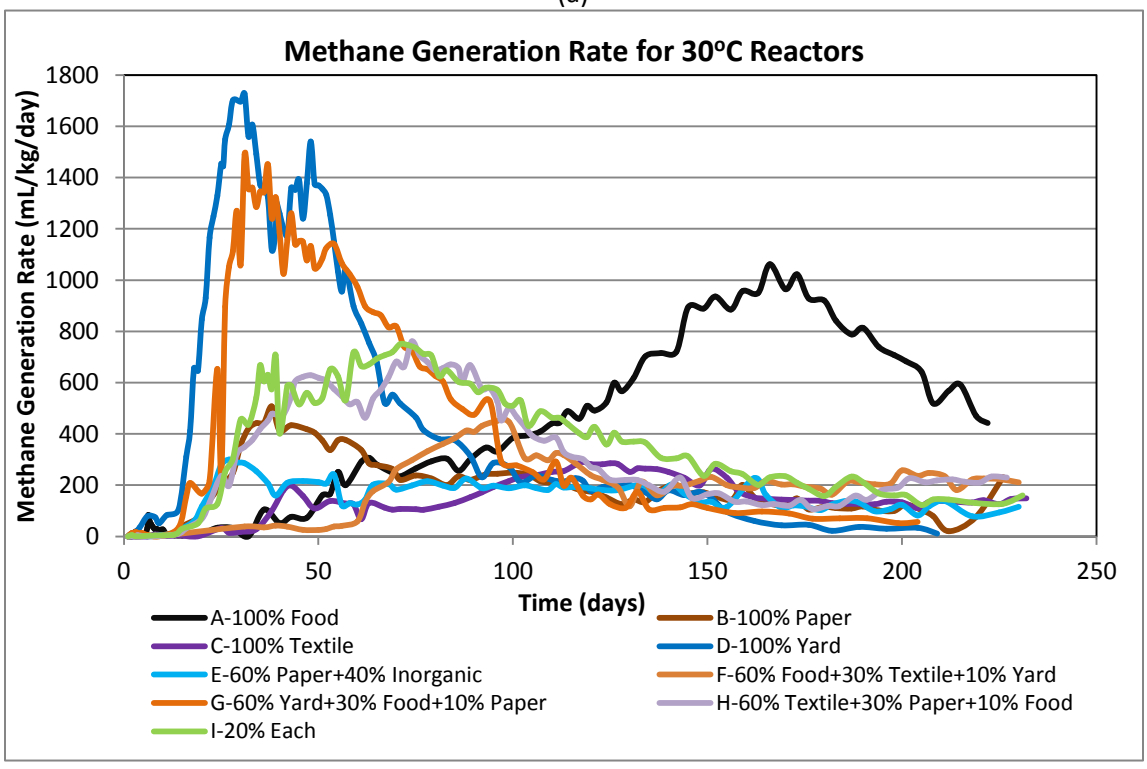

(b)

Figure 4.15: Gas Generation Rates for 30°C Reactors (a) Cumulative Methane Generation Curve (b) Methane Generation Rate Curve

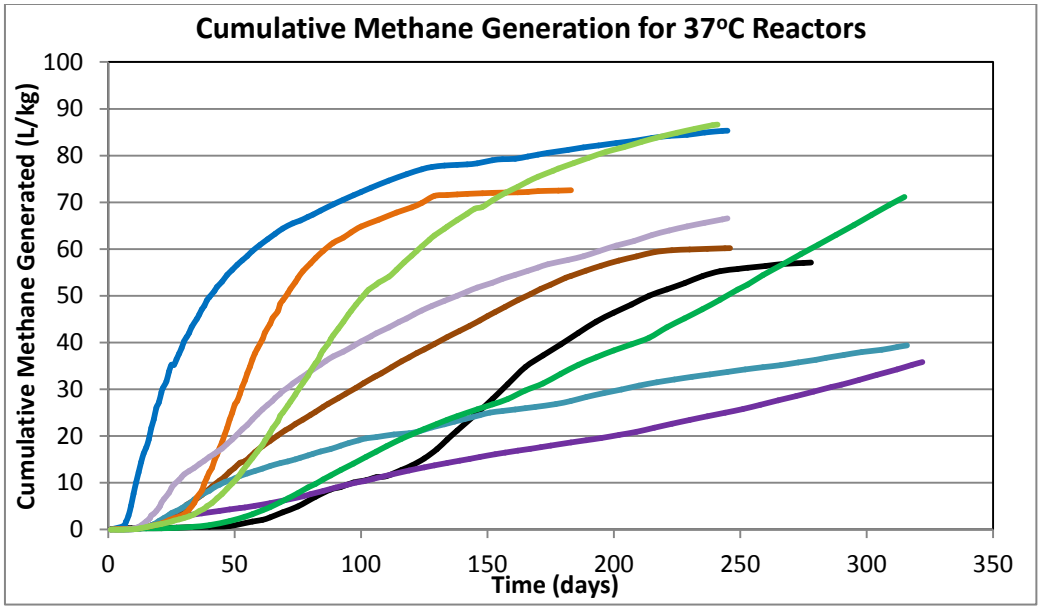

(a)

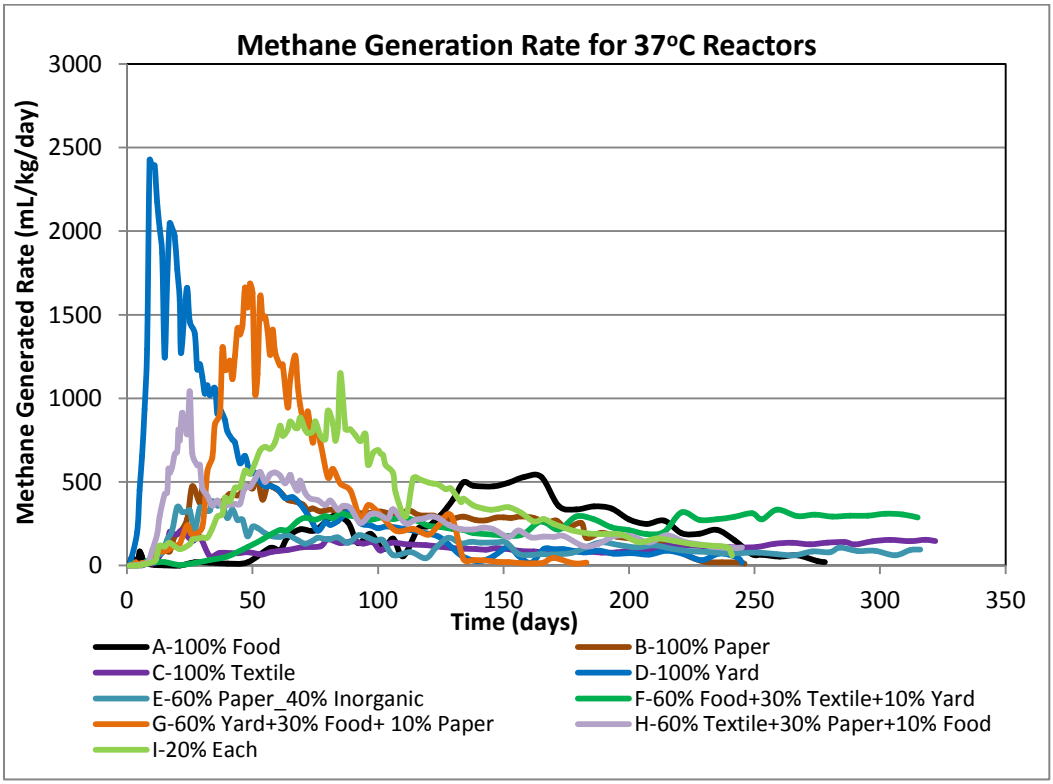

(b)

Figure 4.16: Gas Generation Rates for 37°C Reactors (a) Cumulative Methane Generation Curve (b) Methane Generation Rate Curve

4.3.3 Probable Moisture Content

The probable moisture content inside the reactor was computed based on the initial moisture content, amount of water added and leachate produced. The probable moisture content in the reactors was plotted with respect to time to study the variation in moisture content within the reactors (See section 3.4.4). The probable moisture content inside the reactors is shown in Figure 4.17.

During the first few days after reactor installation, there was no leachate production from reactors until the waste reached its saturation limit. Thereafter, the amount of leachate produced was mostly equal to the amount of water added in the reactor. The probable moisture content was fairly constant for most reactors. However, there were two exceptions: reactors with a high percentage of food waste, and reactors with a high percentage of textile waste. 100% food waste (reactors no. 4 & 25) reactors typically had very high initial moisture content; hence they lost water faster until the waste reached a stable moisture content. This also led to faster carbon washout from food reactors. Reactors with a higher percentage of textile waste however kept absorbing water; hence the moisture content within reactor no. 11, 16 and 5 kept increasing. Inorganic waste, especially plastic waste, obstructed water flow; hence there was considerable fluctuation observed in the probable moisture content in reactor no. 12 and 17.

It must be noted that that the probable moisture content of waste was computed using the initial weight of the waste. However, there was considerable weight loss within the reactor during its lifetime. The weight loss was especially significant for reactors with high food content. Hence this method of computing moisture content is only approximate.

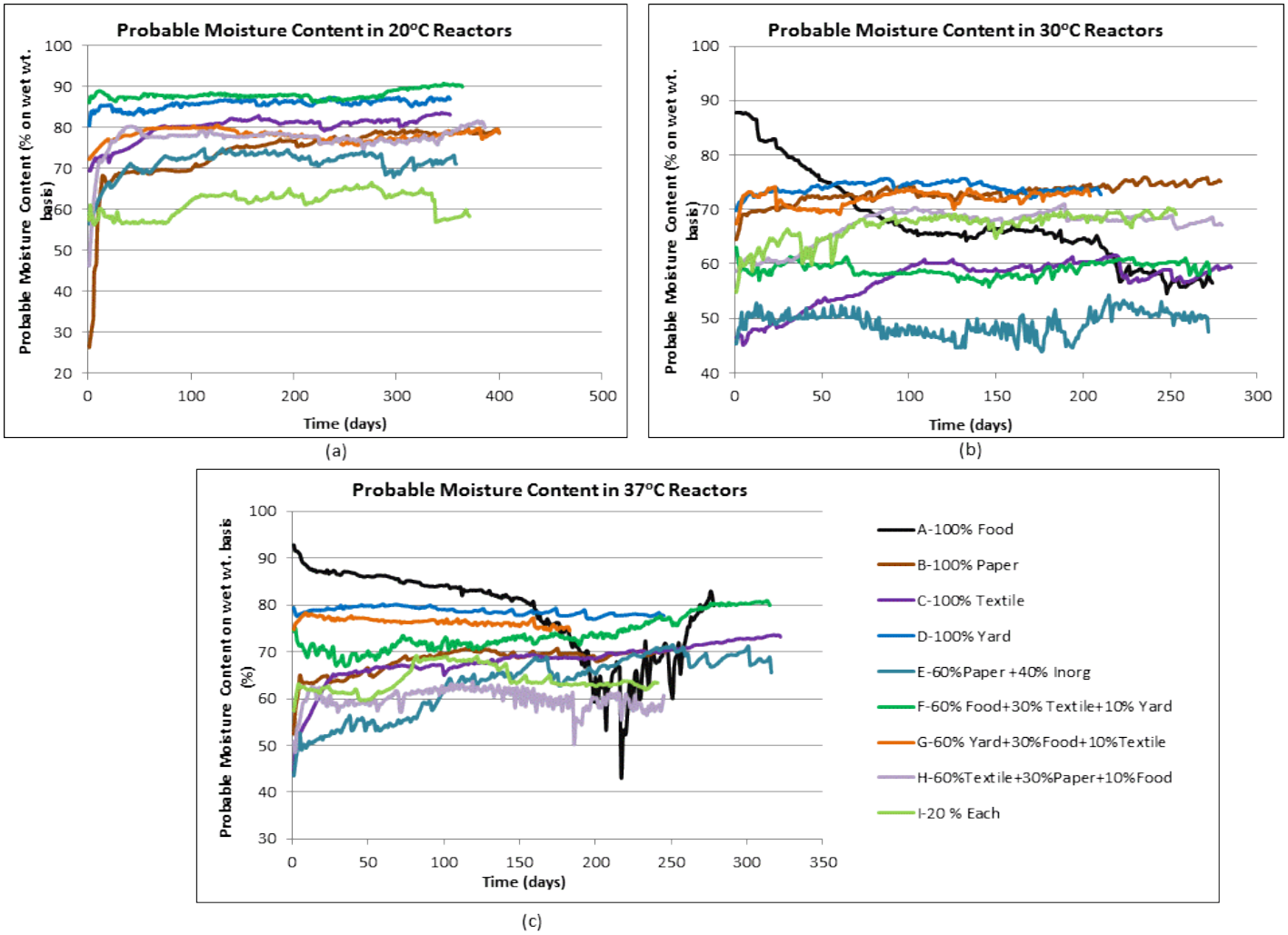

Note: The reactor no.s can be found in Table 3.1 and 3.2

Figure 4.17: Probable Moisture Content in (a) 20°C, (b) 30°C and (c) 37°C Reactors

4.3.4 Final Moisture Content of Waste

After dismantling each reactor, degraded waste samples were collected from the top, middle and bottom of the reactor. Moisture content was determined for these 3 samples to study if there was differential moisture content in the reactor. Observed final moisture contents were plotted with respect to depth for every reactor. It was observed that the bottom layer had higher moisture content than the rest of the reactor. This explained the variation in saturated moisture content of waste with the same waste composition. The moisture variation within reactors is shown in Figure 4.18.

These moisture contents indicate that the reactors were unintentionally operating in the moisture content range typical of bioreactor landfills, although leachate was not recirculated. This could be due to the rainfall calculations which were done based on the rainfall received per surface area. Future studies could consider rainfall per waste volume, rather than rainfall per area. This could help reduce the moisture content of waste in the lab, and help replicate the typical moisture content in the landfill.

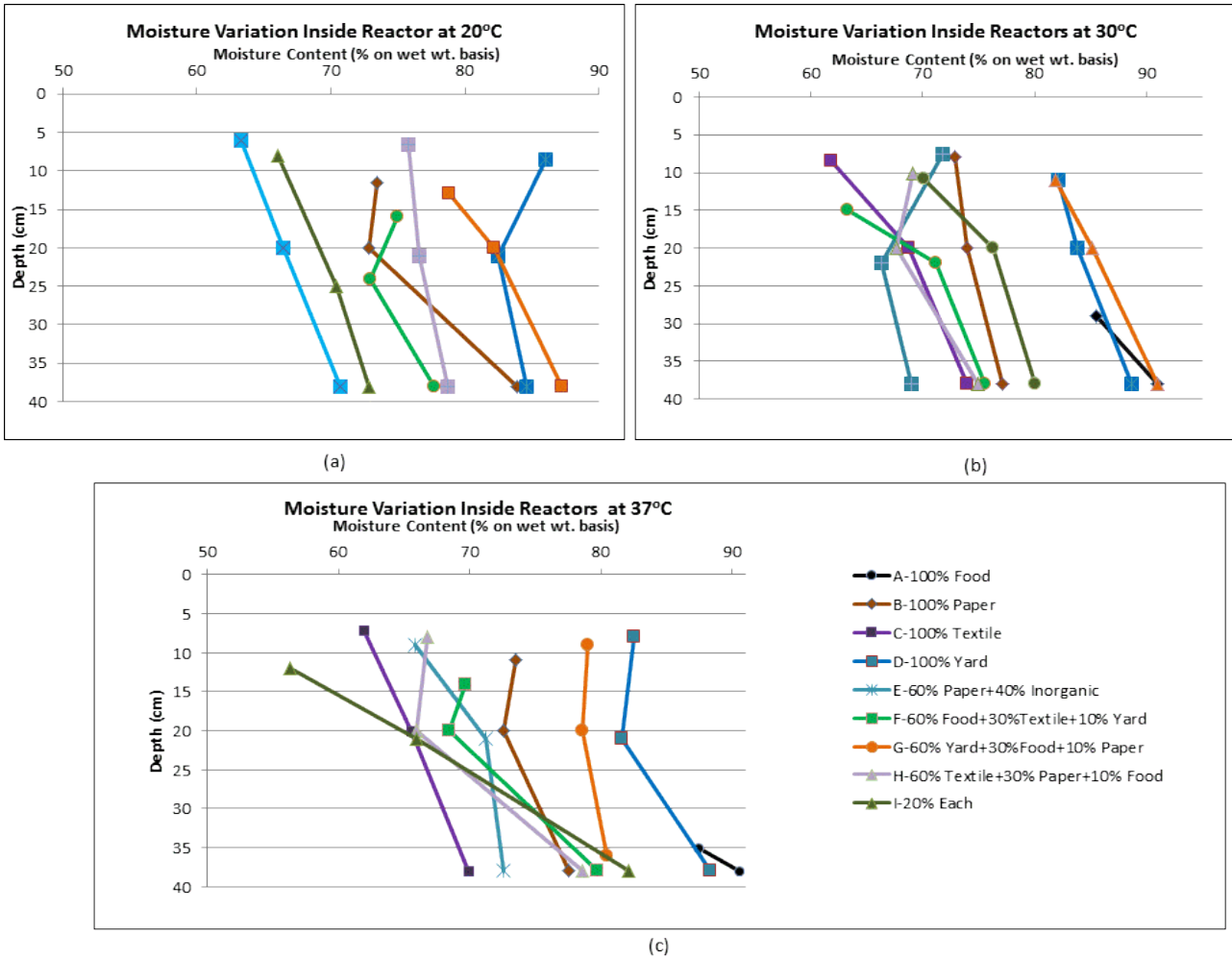

Note: The reactor no.s can be found in Table 3.1 and 3.2

Figure 4.18: Moisture Variation Inside (a) 20°C (b) 30°C (c) 37°C

Table 4.10: Comparison of Observed and Calculated Moisture Content within the Reactor

Reactor	Observed Degraded M.C.		Calculated Probable M.C.	Difference (Observed-Calculated)
	%	Std Dev	%	
1	76.70	6.240	78.73	2.03
2	82.73	4.254	78.78	-3.95
3	69.76	3.455	58.35	-11.41
4	88.29	NA	56.52	-31.77
5	68.20	6.057	59.28	-8.92
6	70.57	3.902	67.14	-3.43
7	74.49	2.648	69.94	-4.55
8	84.15	3.652	77.75	-6.40
9	66.10	15.884	63.35	-2.75
12	62.91	5.862	83.12	20.21
13	66.78	3.722	71.16	4.38
14	74.67	2.216	75.12	0.45
15	84.84	3.417	72.71	-12.13
16	69.96	6.232	58.21	-11.75
17	65.76	4.000	73.22	7.46
18	69.86	3.590	65.54	-4.32
19	79.34	0.974	74.58	-4.76
20	83.01	1.560	86.97	3.96
21	75.21	2.353	89.99	14.78
22	77.03	1.533	80.02	2.99
23	69.05	2.752	47.37	-21.68
24	86.05	4.627	72.38	-13.67
25	75.45	5.015	69.02	-6.43
26	88.92	NA	79.89	-9.03
27	72.55	6.185	79.95	7.40

Further, the average observed moisture content was also compared against the computed probable moisture content, as shown in Table 4.10. The average observed values and probable moisture content values seemed to agree in most cases. The probable moisture content values were also within the error range in most cases. However, as mentioned earlier,

the change in weight of the reactor affected the probable moisture content significantly; hence this method gave an “approximate” estimate of the moisture content.

4.3.5 Degraded Volatile Solids of Waste

Volatile solids (VS) of degraded waste were determined to study the effect of degradation on volatile solids. The volatile solids content of degraded waste (hereafter called “final volatile solids”) are tabulated in Table 4.11. Further, the change in the volatile solids was calculated and is shown Figure 4.19.

It was found that there was considerable loss in the dry weight of the reactors after degradation. However, the volatile solids percent was only reduced from -0.5 to 19%. Since the waste studied in this case was “pure” waste, the loss in volatile solids was relatively small. In a mixed solid waste sample from a landfill, some portion of the waste is comprised of inorganics such as soil. Over time, as the degradation increases, the amount of organic waste decreases, while the inorganic portion remains same. Hence, the percent volatile solids decreases. In this study, the reactors were filled with organic waste only (except in certain cases where inorganic wastes were present). Hence, although the waste was degrading, and recalcitrant carbon percentage was increasing, the inorganic portion was not actually increasing; hence, the volatile solids did not change much in these reactors. These results are consistent with those observed by Wu et al. (2001). The change in volatile solids in a reactor with office paper was found to be 26.80% and for a newsprint reactor was found to be only 4.40% even after operating the reactors for a period of 9 months.

Table 4.11: Change in Volatile Solids in Reactors (All Values in Percent)

		100% Food	100% Paper	100% Textile	100% Yard	60 % Paper +40% Inorganic	60% Food + 30% Textile+ 10% Yard	60% Yard +30% food +10% paper	60% Textile +30% Paper +10% Food	20% each
		A	**B**	**C**	**D**	**E**	**F**	**G**	**H**	**I**
20°C	**Initial VS**	92.61	89.13	97.41	80.67	54.60	93.06	85.12	91.55	68.04
	Final VS		85.43		70.79	50.77	81.00	82.93	91.65	64.88
	Change in VS		**3.69**		**9.88**	**3.83**	**12.06**	**2.19**	**-0.11**	**3.16**
30°C	**Initial VS**	90.30	90.48	98.54	87.08	53.78	93.58	88.10	95.88	71.06
	Final VS	87.18	84.74	98.17	80.09	51.43	86.98	80.86	95.67	66.42
	Change in VS	**3.12**	**5.74**	**0.36**	**6.99**	**2.36**	**6.60**	**7.24**	**0.20**	**4.65**
37°C	**Initial VS**	88.38	88.89	98.98	86.27	55.30	92.37	86.50	96.02	72.49
	Final VS	84.70	82.27	99.48	67.25	52.41	87.98	77.51	89.19	61.12
	Change in VS	**3.68**	**6.62**	**-0.51**	**19.02**	**2.89**	**4.39**	**8.99**	**6.83**	**11.37**

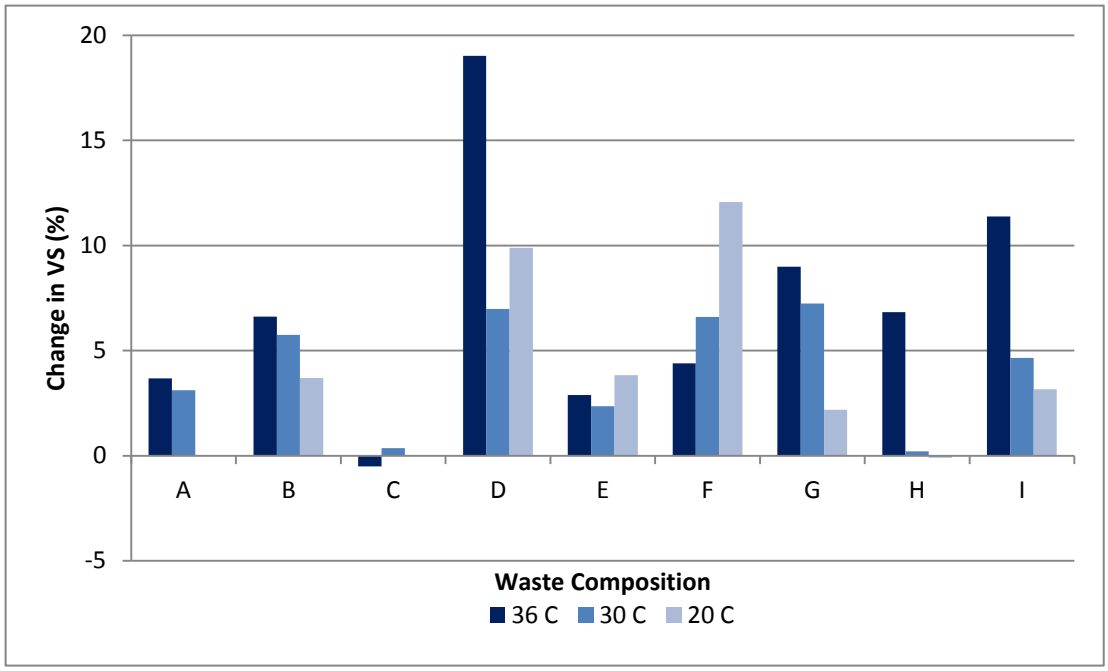

Figure 4.19: Change in Volatile Solids after Degradation

4.4 *k* Computation

4.4.1 Lag Phase Removal

The first phase in degradation was the lag phase, during which the microbes become acclimatized to the waste, and hydrolyze it into simpler substrates. The lag phase needs to be eliminated while curve fitting the data. The amount of methane produced during the lag phase was not included when calculating the ultimate methane potential of waste. Faour et al. (2007) attempted to model the methane generated during the lag phase for the first time. According to the nomenclature used by Faour et al. (2007), the methane produced during the lag phase was called "Storage Volume- V_{sto}". In the case of actual full-scale landfills, the lag phase may extend for several years and V_{sto} may be significant.

The lag phases and V_{sto} found in this study are tabulated in Table 4.12. The lag phase is also plotted with respect to waste combinations in Figure 4.20.

Table 4.12: Lag Phase and Storage Volume for Each Reactor

Reactor no.	Lag Phase (days)	V_{sto} (m^3/kg)	Reactor no.	Lag Phase (days)	V_{sto} (m^3/kg)	Reactor no.	Lag Phase (days)	V_{sto} (m^3/kg)
1	79	1.34	9	30	2.51	19	22	1.36
2	120	2.97	12	58	1.4	20	91	0.97
3	63	0.79	13	19	0.44	21	45	0.06
4	47	1.6	14	11	0.56	22	14	0.11
5	34	0.37	15	60	1.28	23	16	0.53
6	20	0.39	16	17	0.88	24	24	0.94
7	21	1.38	17	10	0.11	25	48	0.74
8	5	0.84	18	30	3.19	26	48	1.79
						27	12	0.63

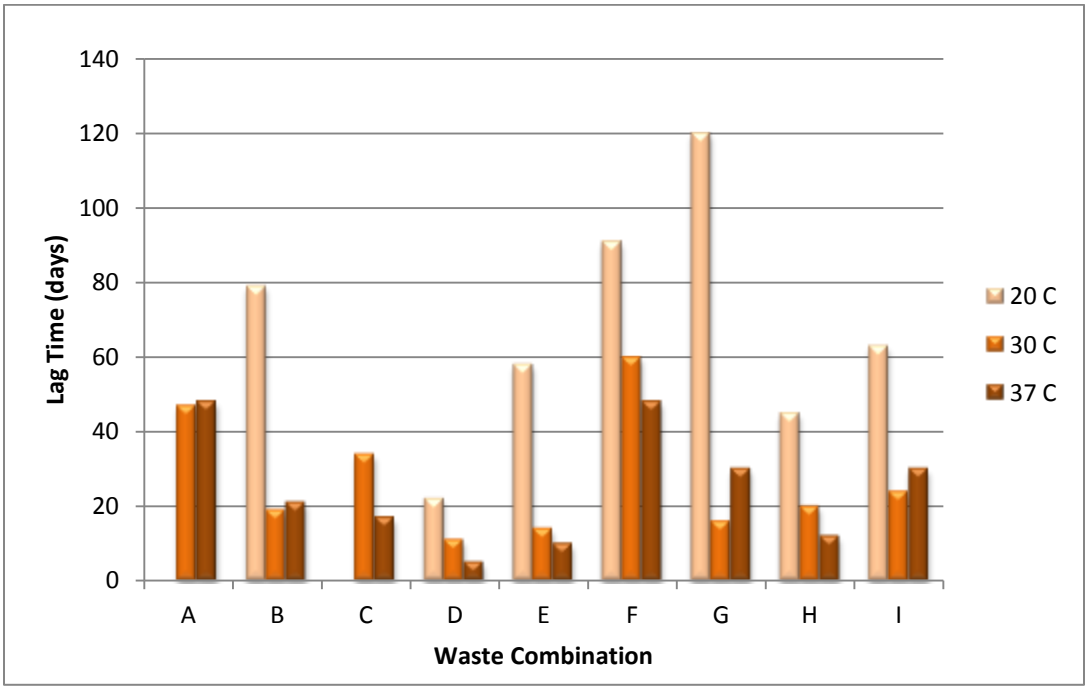

Figure 4.20: Lag Phase Duration with respect to Time

Certain types of waste had shorter lag times compared to other wastes. For example, yard waste (D-100% yard) had the shortest lag time. However, temperature had significant impact on the duration of the lag phase. For any particular waste combination, the lag phase was longest for lower temperature (20^{o}C). Likewise, the lag phase at 30^{o}C was expected to be longer than that at 37^{o}C. However, in some cases the duration lag phase was reduced due to higher rainfall rates (waste combination G and I). However, at 20^{o}C, irrespective of the rainfall received by the reactor, the lag phase duration was observed to be the longest.

4.4.2 Non-Linear Regression

k values were calculated for all reactors using non-linear regression applying the Newton-Gauss method. Statistical software SAS was used for conducting the non-linear regression analysis. In most cases the non-linear regression was able to converge using the first-order decay equation. However, the residual plot showed a curvature for most reactors, which indicates non-constant variance. This could be because in many cases the waste did not follow a first-order decay equation properly. Other relationships (second-order or saturation kinetics) were not implemented because it was beyond the scope of this study. An example of a fitted curve and residual plot is shown in Figure 4.21.

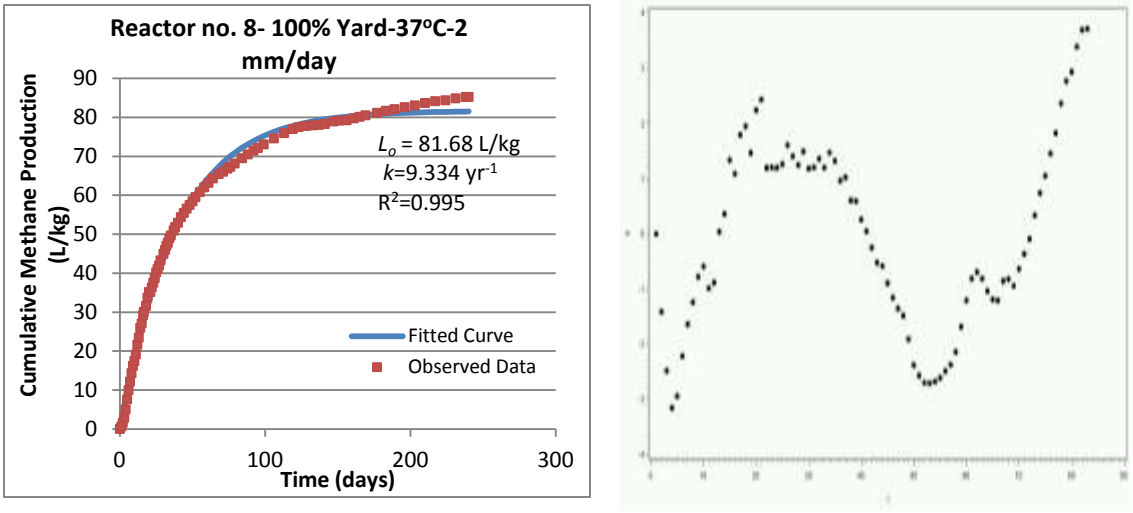

(a) (b)

Figure 4.21: Reactor no. 8 (a) Fitted Curve and (b) Error Plot

However, for some reactors the non- linear regression was not able to converge. The data for reactors such as 100% food waste and 100% textile waste typically could not converge. Reactors no. 20 and 26 had 60% food waste+30% textile waste+10% yard waste; these reactors also could not converge. This could be because these two types of wastes did not follow a first-order decay relationship. Food waste for example had a very long lag phase, and showed multiple peaks. It was not practical to remove this lag phase for modeling, because a considerable amount of gas had been produced in this phase. Secondly, it was necessary to have an average *k* value for the reactor. If a certain portion of the gas production was neglected, it would have led to high and unreasonable *k* values.

Table 4.13: L_o and k values based on Laboratory Scale Data

Reactor	L_o	k
	m^3/kg	/yr
1	83.46	1.026
2	113.6	1.617
6	89.39	2.602
7	102.8	1.580
8	81.68	9.344
9	118.4	2.409
12	25.43	2.504
13	53.40	2.767
14	93.02	5.731
15	76.79	1.628
17	44.92	2.178
18	75.92	7.811
19	41.42	3.24
21	24.70	2.008
22	78.47	1.033
23	91.88	5.037
24	108	2.416
27	77.59	2.924

Textile wastes showed multiple peaks in the methane generation rate graphs. Further, textile waste degraded at a very slow rate and even after monitoring the reactors for 250-400 days, the reactors were still producing considerable gas. Hence the reactors had not reached the final stabilization phase. In such cases the non-linear regression approach did not work. An attempt was made to use a simple linear regression equation. This method involved using the final observed cumulative methane generation value as L_o. This assumption could be justified, because if the reactor had been operated further, the L_o values could have been different. Hence the data from 9 reactors out of 27 could not be used for model development. The converged values of L_o and k are presented in Table 4.13.

4.4.3 Comparison with Values Presented in Literature

Eleazer et al. (1997) observed that yard waste and coated paper showed a classic first-order methane production with a peak followed by asymptotic decline. However, food waste showed multiple peaks, which the authors believed could be because of the presence of different types of substrates. The authors also reported that office paper exhibited a nearly constant methane production for about 300 days, which could be because of its near uniform composition. Similar observations were found in the present study. In this study, yard waste and paper waste showed the classic first-order decay. Food waste and textile waste showed multiple peaks. The paper waste considered in this study was mixed paper waste, with coated, non-coated, office paper mixed together. Hence as a combined effect, the classic first-order peak followed by a decline was observed in this study.

In the present study, it was observed that the *k* values were considerably higher than those observed in the landfills. Typical landfill *k* values are in the range of 0.02-0.7 yr-1. Although this study aimed at recreating landfill like conditions by not adding nutrients and using larger reactors (16L instead of the typical 2L), which allowed for not shredding waste, the higher *k* values could be a result of controlled environment and greater microbial access compared to the conditions in a landfill. This observation is consistent with the results published in Cruz and Barlaz (2010). The *k* values found in the lab scale bioreactor study published by Cruz and Barlaz (2010) are compared with those found the present study in Table 4.14.

Table 4.14: Comparison of L_o and k values with Literature

Cruz and Barlaz (2010)			Present Study		
Waste	**k (yr^{-1})**	**L_o (m^3/dry Mg)**	**Waste**	**k (yr^{-1})**	**L_o (m^3/dry Mg)**
Food Waste	15.02	300.7	Food Waste	NA[*1]	NA[*1]
Office Paper	3.08	217.3	Paper Waste	1.02-2.76[*2]	53-102.8[*2]
Newspaper	3.45	74.3			
Corrugated Container	2.05	152.3			
Coated Paper	12.68	84.4			
Grass	31.13	144.4	Yard Waste	3.24- 9.34[*2]	45-93.02[*2]
Branches	1.56	62.6			
Leaves	17.82	30.6			

NOTE: [*1]Non linear regression did not converge for food waste reactors. Hence L_o and k values are not enlisted here.

[*2] L_o and k values are dependent on temperature and rainfall. Hence a range is presented here.

From Table 4.14, it can be seen that there is some variability in the values reported in the lab scale studies published by Cruz and Barlaz (2010) and the present study. This could be attributed the fact the studies conducted by Cruz and Barlaz (2010) were at ideal conditions (shredded waste, with leachate recycle and nutrient addition at 40^{o}C). Further, the effects of rainfall and temperature were not considered in the previous studies.

The curve fitting done by Cruz and Barlaz (2010) is shown in Figure 4.22. It can be observed that the errors were non-constant, which indicates that the waste degradation did not exactly follow first-order degradation.

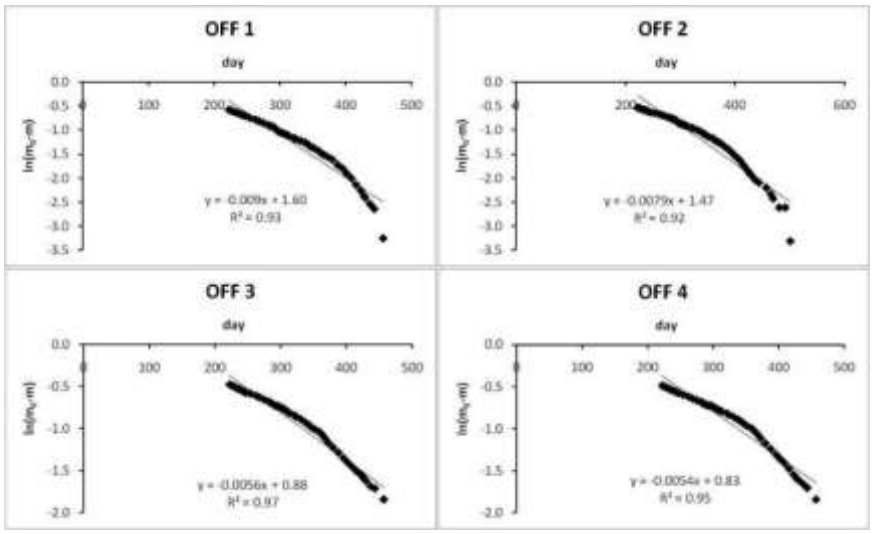

Figure 4.22: Curve Fitting plots (Source: Cruz and Barlaz,2010)

Error plots from the present study also followed similar trend (See Figure 4.21). However, since the *k* values were higher than those found in field-scale landfills, it was necessary to use scale-up factors to adapt the model for field scale conditions.

4.4.4 L_o and Biochemical Methane Potential Comparison

The modeled ultimate methane potential (L_o) was compared with the Biochemical Methane Potential (BMP) found in this study (See Table 4.15). Biochemical Methane Potential (BMP) was found to be higher than the ultimate methane potentials computed from the laboratory scale data. This could be due to the fact that BMP test involved ideal conditions for degradation (ground samples, presence of buffering agent, presence of macro and micro nutrients). However, in the lab scale reactors, solid waste was not ground, there were pH fluctuations, nutrients to enhance degradation were not added, and carbon lost in leachate was not recycled. It was expected that the amount of carbon lost would also increase as the rainfall increases.

Table 4.15: Comparison between BMP and Modeled L_o

Reactor	Initial VS	BMP	Modeled L_o	
	%	m^3/VS	m^3/kg of DS	m^3/kg of VS
1	89.13	334	83.46	93.64
2	85.12	277	113.60	133.46
6	96.02	268	89.39	93.10
7	90.48	390	102.80	113.62
8	87.08	182	81.68	93.80
9	71.06	286	118.40	166.62
12	54.60	236	25.43	46.57
13	90.48	390	53.40	59.02
14	87.08	182	93.02	106.82
15	93.58	280	76.79	82.06
17	53.78	236	44.92	83.52
18	88.10	277	75.92	86.18
19	87.08	182	41.42	47.57
21	91.55	268	24.70	26.98
22	53.78	236	78.47	145.91
23	88.10	276	91.88	104.29
24	71.06	286	108.00	151.98
27	96.02	268	77.60	80.81

Figure 4.23 shows the effect of rainfall on the BMP/L_o ratio. On preliminary observation, it can be seen that as the rainfall increased, the BMP/L_o values increased, which indicates that the L_o values decreased as the rainfall increased. However, it must be noted that this was based on the lab scale data where the composition and temperature were different in each case. Hence further analysis is necessary to study the effect of rainfall on the ultimate methane potentials from landfills.

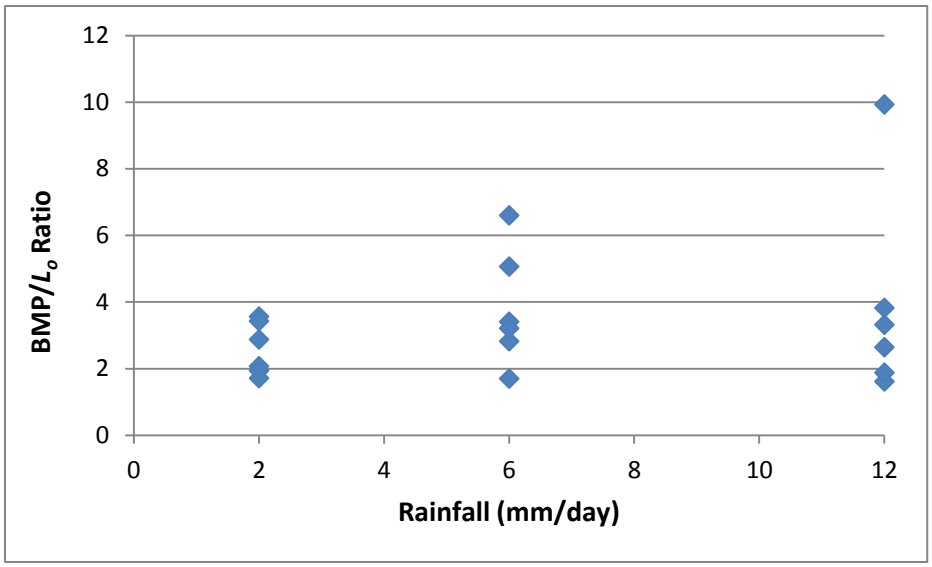

Figure 4.23: Change in BMP/L_o Ratio with respect to Rainfall

CHAPTER 5

MODEL DEVELOPMENT AND VALIDATION

5.1 Introduction

This chapter describes the procedure for developing the proposed Capturing Landfill Emissions for Energy Needs (CLEEN) model. This chapter is divided into 2 sections. The first section describes the procedure for developing the multiple linear regression (MLR) equation for predicting *k* values using 7 predictor variables: rainfall, temperature, and waste composition (% food, % paper,% textile, % yard and % inorganic). The assumptions made for developing the CLEEN model are presented in the second section.

5.2 Multiple Linear Regression Analysis

This section gives a detailed description of the steps involved in a multiple linear regression analysis. Based on the laboratory scale data, a MLR equation was developed to predict the first-order decay constant (*k*) as a function of rainfall, temperature and waste composition. As mentioned earlier in Chapter 4, curve fitting using a non-linear regression method was successful for 18 reactors out of 27. The data from these 18 reactors was used for developing the MLR equation. Statistical software SAS was used for the analysis. The raw data used for developing the MLR equation is presented in Table 5.1. The steps followed for developing the statistical relationship were:

1. Studying raw data plots and correlation analyses,
2. Developing preliminary MLR model and checking model assumptions,

3. Conducting remedial actions, such as transformations, until the model assumptions for regression analysis were satisfied,
4. Exploring possible interaction terms,
5. Searching for good fitted MLR models,
6. Selecting the best fitted MLR model.

Table 5.1: Raw Data for Developing the MLR Equation

Rainfall	Ambient Temperature	% Food	% Paper	%Textile	%Yard	% Inorganic	Computed *k* value
mm/day	K						yr^{-1}
2	293	0	100	0	0	0	1.03
2	293	30	10	0	60	0	1.62
2	303	10	30	60	0	0	2.60
2	310	0	100	0	0	0	1.58
2	310	0	0	0	100	0	9.34
2	310	20	20	20	20	20	2.41
6	293	0	60	0	0	40	2.50
6	303	0	100	0	0	0	2.77
6	303	0	0	0	100	0	5.73
6	303	60	0	30	10	0	1.63
6	310	0	60	0	0	40	2.17
6	310	30	10	0	60	0	7.81
12	293	0	0	0	100	0	3.24
12	293	10	30	60	0	0	2.01
12	303	0	60	0	0	40	1.03
12	303	30	10	0	60	0	5.04
12	303	20	20	20	20	20	2.42
12	310	10	30	60	0	0	2.92

5.2.1 Raw Data Plots and Correlation Analysis

5.2.1.1 Response vs. Predictor Plots

The response vs. predictor plots are used for studying if a multiple linear regression form would be suitable for fitting the data. The response vs. predictor plots are presented in Figure 5.1.

It was observed that the *k* vs. rainfall graph showed a decreasing trend, while *k* vs. temperature showed an increasing trend. Thus increase in rainfall decreased the rate of degradation, and increase in temperature increased the rate of degradation. An increasing trend was also found in the *k* vs. yard waste plot, indicating that the presence of a higher amount of yard waste increased the rate of degradation. In case of *k* vs. food, *k* vs. paper, *k* vs. textile, and *k* vs. inorganic plots, a slight curved downward trend was observed.

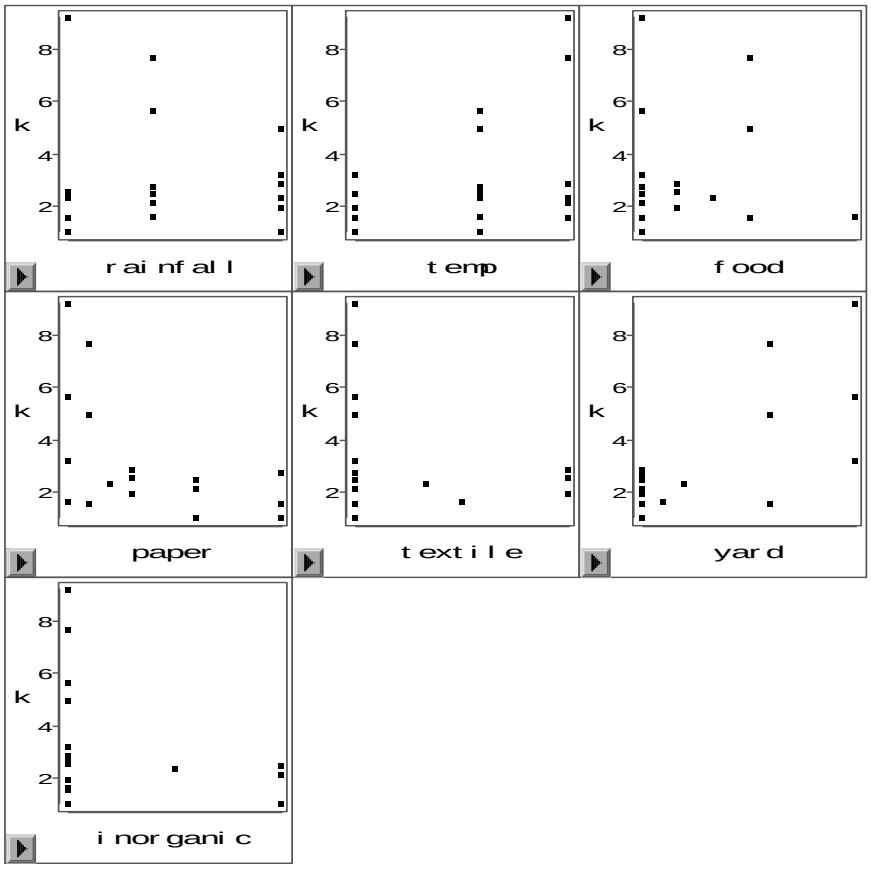

Figure 5.1: Response vs. Predictor Plots

5.2.1.2 Predictor vs. Predictor Plots

The predictor vs. predictor plots; shown in Figure 5.2, helps in exploring if any predictors are linearly correlated with each other. Presence of downward or upward trends in the plots indicate that the predictors are linearly correlated with each other. A slight downward trend was observed in food vs. paper, paper vs. yard, and textile vs. yard, paper vs. textile plots. Hence, mullticollinearity was present in the data.

Complications in the MLR analysis can occur when there is high multicollinearity in the relationship. Extremely high multicollinearity indicates that two or more predictors are explaining the same variation in the response variable, leading to numerical issues in

computing least squares to estimate the parameters for the MLR model. These numerical issues correspond to an inability to precisely determine the appropriate estimated parameters, i.e., the variance of the least squares estimators is inflated.

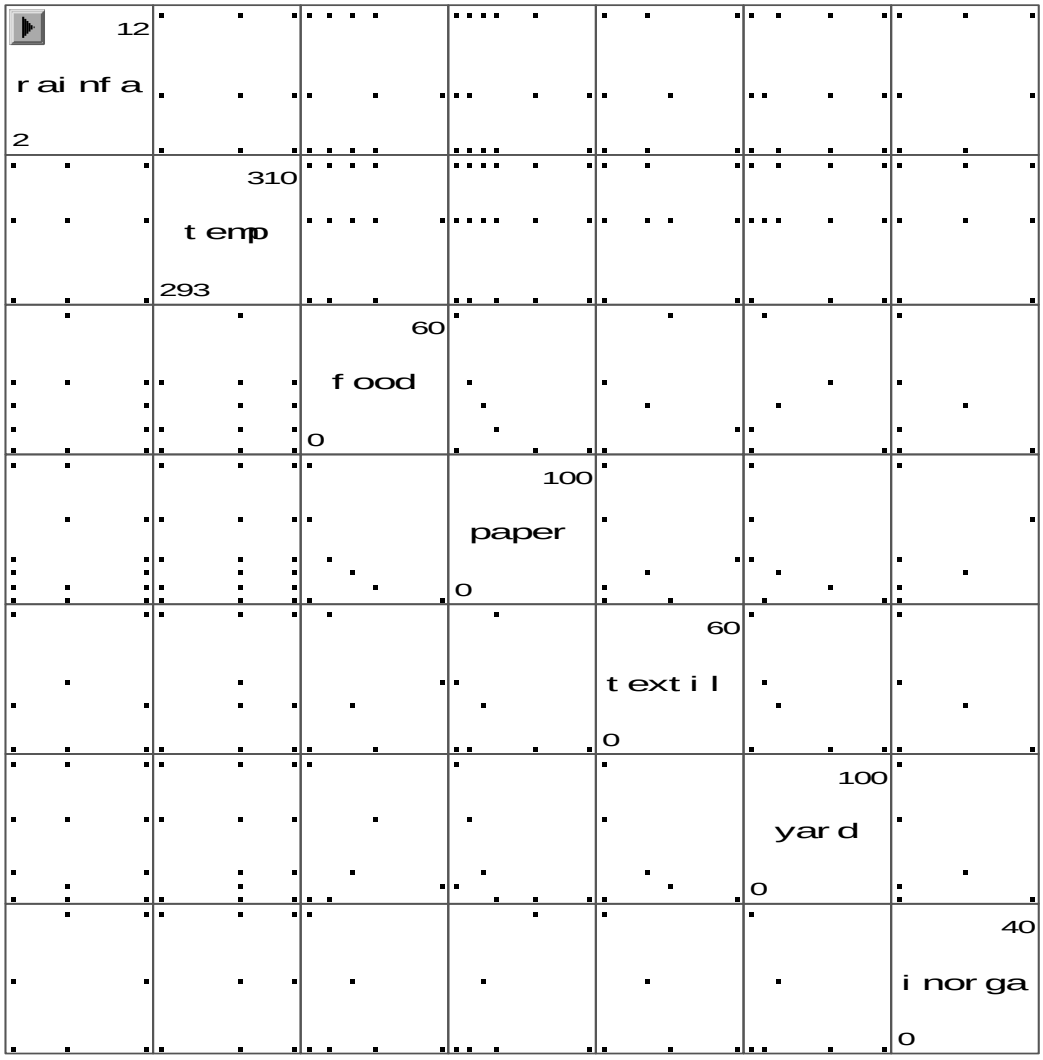

Figure 5.2: Predictor vs. Predictor Plots

5.2.1.3 Correlation Analysis

Correlation analysis helps in quantifying the linear association between two variables. Table 5.2 shows the Pearson's correlation coefficients computed for all response vs. predictor and predictor vs. predictor combinations. Pearson's correlation coefficient (r) ranges from -1 to +1. While positive values of r indicate strong positive linear relationship, negative values of r indicate a presence of a negative linear relationship. When $r = 0$, it indicates that there is little or no correlation between the variables. From Table 5.2, it can be observed that k and % yard was highly correlated, with a correlation coefficient of 0.721. All other correlation coefficients were non-zero, which indicated that there was some correlation between all predictors and response variables.

Presence of a non-zero value in the correlation matrix between predictor variables shows multicollinearity. However, if $r < 0.7$ it can be assumed that the multicollinearity problems would not be very serious. Due to the mixture design that was necessary for this study, multicollinearity was inherent in the data. From Table 5.2, it can be observed that correlation coefficients for predictors had a non-zero value. However, since the correlation coefficients were less than 0.7 in all cases, it was concluded that their correlations were not high. However, correlation between paper and yard waste was equal to 0.6804, which was close to 0.7 but less than 0.7.

Table 5.2: Correlation Analysis for Raw Data

Pearson Correlation Coefficients, N = 18								
Prob > |*r*| under H_0: Rho=0								
	k	**rainfall**	**temp**	**food**	**paper**	**textile**	**yard**	**inorganic**
k	1	-0.0779	0.39396	-0.0055	-0.5045	-0.2278	0.72102	-0.3077
rainfall	-0.0779	1	-0.1564	0.02785	-0.2199	0.21328	0.00237	0.15381
temp	0.39396	-0.1564	1	0.06103	-0.0423	0.02662	-0.023	0.05014
food	-0.0055	0.02785	0.06103	1	-0.5148	0.20615	0.02906	-0.2605
paper	-0.5045	-0.2199	-0.0423	-0.5148	1	-0.1915	-0.6804	0.24192
textile	-0.2278	0.21328	0.02662	0.20615	-0.1915	1	-0.4079	-0.2316
yard	0.72102	0.00237	-0.023	0.02906	-0.6804	-0.4079	1	-0.3746
inorganic	-0.3077	0.15381	0.05014	-0.2605	0.24192	-0.2316	-0.3746	1

5.2.1.4 Evaluating the Impact of Missing Data

At this point, additional investigation was conducted to explore the high correlation between paper and yard waste. Initially, when the original experiment was designed using the cyclic incomplete block with mixture design for waste composition, the correlation between waste components was not significant (See Table 5.3).

Table 5.3: Correlation Analysis for the Original Experimental Design

Pearson Correlation Coefficients, N = 27					
Prob > |r| under H_0: Rho=0					
	food	**paper**	**textile**	**yard**	**inorganic**
food	1	-0.45526	-0.17619	-0.12863	-0.23911
paper	-0.45526	1	-0.35063	-0.409	0.26245
textile	-0.17619	-0.35063	1	-0.37169	-0.25
yard	-0.12863	-0.409	-0.37169	1	-0.21571
inorganic	-0.23911	0.26245	-0.25	-0.21571	1

In a mixture design if % food waste was to be increased, other waste components had to be reduced. Hence, in most cases, there was a negative correlation between waste

components. This negative correlation was unavoidable in a mixture design. Due to this correlation, multicollinearity arises in regression analysis resulting from mixture designs. To further investigate this multicollinearity effect, variance inflation factors (VIF's) were calculated for the original design of experiments (See Table 5.4). It can be observed that the VIF's were greater than 5 for all waste components, which indicates that there may be serious multicollinearity in the data.

Table 5.4: Variance Inflation Factors for the Original Experimental Design

Variable	Variance Inflation Factors
food	5.90
paper	10.11
textile	7.11
yard	7.39

As mentioned earlier, the *k* values from some reactors could not be calculated in this study. 100% food, 100% textile and 60% food + 30% textile + 10% yard reactors typically did not converge during the non-linear regression analysis. Hence, these data points were omitted. Due to this, the correlation between some waste components (e.g. paper and yard waste) was found to be higher than the original design.

5.2.2 Preliminary Multiple Linear Regression Equation

Initially an attempt was made to develop a MLR model as follows:

$$k = \beta_0 + \beta_1 R + \beta_2 T + \beta_3 F + \beta_4 P + \beta_5 TX + \beta_6 Y + \beta_7 I + \varepsilon \quad (5\text{-}1)$$

where,

k = first-order methane generation rate constant (yr^{-1}),

βs = parameters to be determined through multiple linear regression, using the lab data,

R = annual rainfall (mm/day),

T = average annual temperature (K),

F= % food, P = % paper, TX= % textile, and Y = % yard in landfilled waste,

ε = error uncertainty, modeled as a random variable.

After regressing k with all predictor variables, it was observed that the model was not appropriate, because the waste composition (% food, % paper, % textile, %yard and % inorganic) summed up to 100%. Thus one variable (out of the five) was a linear combination of the other 4 variables, such that X_5 = 100% $-X_1-X_2-X_3-X_4$. This is again a property of a mixture design. Hence, it was necessary to employ an alternate model form. It was decided to use 4 out of the 5 variables for developing the MLR model. Since inorganic waste does not contribute to methane production, the effect of inorganic waste on the k values was expected to be minimal. Hence, % inorganic waste was not used for building the MLR equation.

The preliminary MLR model was developed using SAS, and the estimates for the model parameters (β's) are presented in Table 5.5.

Table 5.5: Parameter Estimates for the Preliminary MLR Model

Parameter Estimates							
Variable	**DF**	**Parameter Estimate**	**Standard Error**	**t Value**	**Pr > |t|**	**Type I SS**	**Variance Inflation**
Intercept	**1**	-40.975	17.9921	-2.28	0.0437	185.908	0
rainfall	**1**	-0.0115	0.09976	-0.11	0.9106	0.55035	1.22426
temp	**1**	0.13992	0.05731	2.44	0.0327	13.5418	1.05061
food	**1**	-0.0037	0.03602	-0.1	0.9191	0.07594	2.47363
paper	**1**	0.00736	0.03186	0.23	0.8215	33.6252	8.9725
textile	**1**	0.0148	0.02857	0.52	0.6145	6.66803	2.98122
yard	**1**	0.05124	0.02686	1.91	0.0829	8.99278	7.61798

Based on the SAS output (Table 5.5), the preliminary fitted MLR equation is shown in Eq. (5-2)

$$\hat{k} = -43.0181 - 0.0149R + 0.14721T - 0.00464F + 0.00706P + 0.0148TX + 0.0511Y \quad (5\text{-}2)$$

Where, $\hat{k}$ = predicted rate of degradation (yr^{-1}), R= rainfall (mm/day), T= temperature (K), *F*= % food, *P* = % paper, T*X*= % textile, and *Y* = % yard in landfilled waste.

5.2.2.1 Checking Assumptions for the MLR Equation

The following assumptions underlie any multiple linear regression (MLR) analysis:

1. The MLR model form is reasonable.
2. The residuals (errors) have constant variance.
3. The residuals (errors) are normally distributed.
4. The residuals are not auto-correlated.

These assumptions can be verified by performing residual analysis. Residuals are the errors terms or the difference between the predicted value of *k* ($\hat{k}$) and the observed *k* (from the lab data).

5.2.2.2 MLR Model Form Is Reasonable

The MLR model form is assumed to be adequate when all the residuals versus predictor plots have no curvature in them (See Figure 5.3). Curvature was observed in residuals vs. rainfall and residuals vs. paper plots. Further, a slight curvature was found in the residuals vs. yard plot.

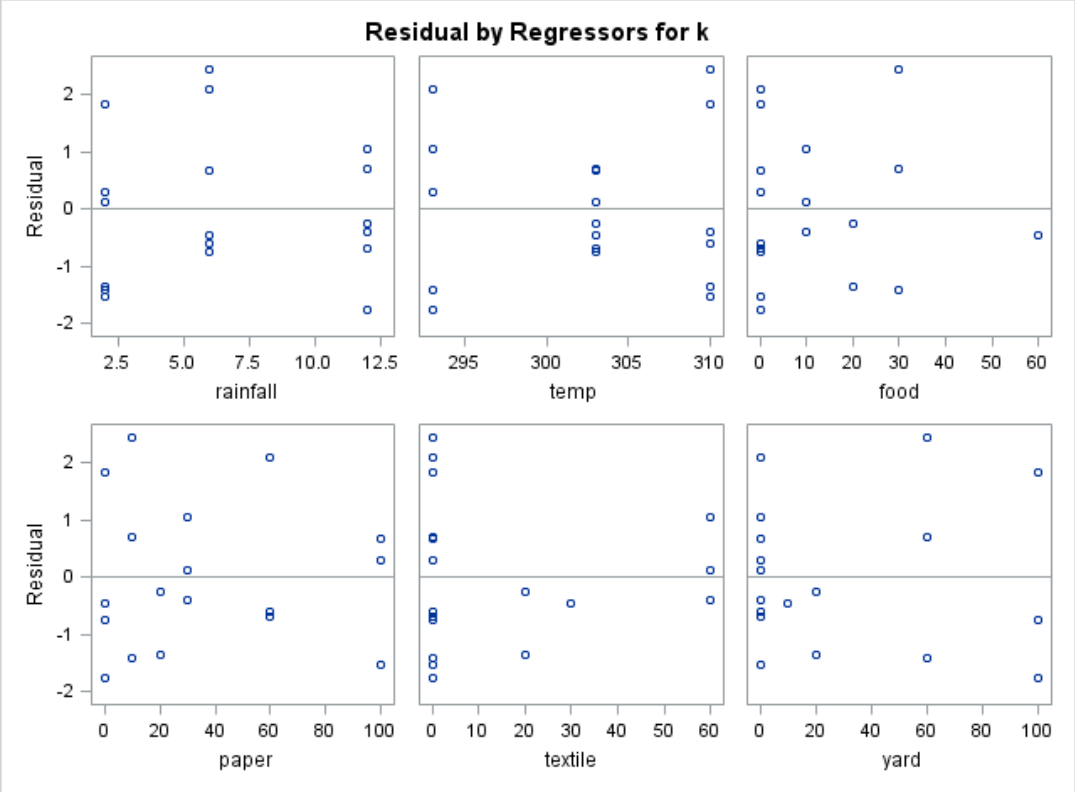

Figure 5.3: Residuals vs. Predictor Plots for the Preliminary Model

5.2.2.3 Residuals Have Constant Variance

A regression based model assumes that the errors have constant variance. This means that when the residuals are plotted against the predicted value of *k* ($\hat{k}$), they should be randomly scattered. Presence of a funnel shape in the residuals vs. $\hat{k}$ plot (see Figure 5.4) indicates that the residuals have a non-constant variance. A curved funnel shape was observed in Figure 5.4. This indicates that the residuals had a non-constant variance in the MLR model.

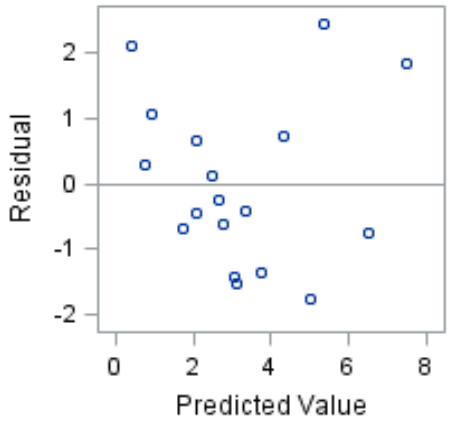

Figure 5.4: Residuals vs. Predicted $\hat{k}$ Plot for the Preliminary Model

5.2.2.4 Residuals Are Normally Distributed

The MLR model assumes that the residuals are normally distributed. To check this assumption, residuals vs. normal scores were plotted (See Figure 5.5). A linear trend in residuals vs. normal score plot indicates that the residuals are normally distributed. From Figure 5.5, the residuals displayed an S-shaped curve, which indicates that the residuals had shorter tails relative to the normal distribution. Therefore, it can be concluded that the normality assumption was violated in the current MLR model.

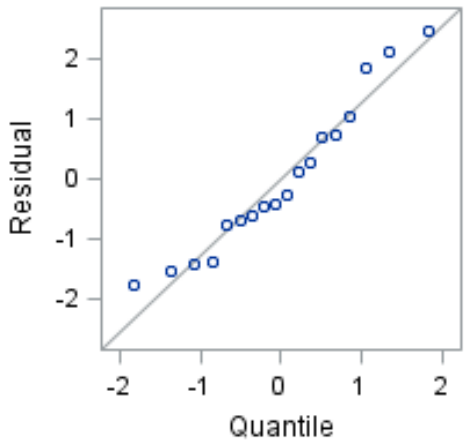

Figure 5.5: Normal Probability Plot for Preliminary Model

5.2.2.5 Residuals Are Not Serially Correlated

MLR analysis requires that errors are uncorrelated (independent) with each other. The time series plot is used to check if the residuals are uncorrelated. If there is an identifiable increasing or decreasing trend in the time series plots, it indicates that the errors are correlated. In this case all the reactors were operated at the same point of time, and the *k* values were computed from these reactors. Hence, the *k* values were not expected to be correlated and time series plots were not plotted.

5.2.2.6 Discussion on the Preliminary MLR Model

From the residual analysis, it was evident that the current model form was not adequate, the error variance was not constant, and the errors were not normally distributed. The recommended remedial actions to address this violated model assumptions required transformations. Specifically, a variance stabilizing transformation on the response is required to stabilize the error variance (i.e., make it constant), and additional transformations on predictor variables may be needed to address curvature. Normality often improves once the other assumptions are satisfied, but normality is not a required assumption. The model assumptions were revisited after performing transformations.

5.2.3 Transformations

5.2.3.1 Transformations on the Response Variable (*k*)

A variance stabilizing transformation, such as square root or logarithm, compresses high response variable values. Slight curvature in the response-predictor plots also indicated a need to compress high *k* values to linearize the relationships. To explore the possibility of using a transformation on the response variable (*k* value), three different compression transformations were tested in the sequence mentioned below.

1. Square-root transformation ($\sqrt{k}$)
2. Log transformation ($\log_{10} k$)
3. Inverse square-root transformation ($1/\sqrt{k}$)

The comparative analysis for these three transformations is shown in Table 5.6. The SAS outputs with all residual plots are shown in Appendix D. It was evident from Table 5.6 that the log transformation on *k* performed better than other two transformations in terms of the response vs. predictor plots, residuals vs. predicted ($\hat{k}$) plots and normal probability plots. Hence, it was decided to use the log transformation on the response variable. However, there was some curvature observed in the residuals vs. rainfall and residuals vs. temperature plots even after the log transformation was conducted. Hence, it was necessary to explore some additional transformations on the predictors for this MLR model.

Table 5.6: Comparison of Different Y- Transformations

	Preliminary Model	$\sqrt{k}$ **Transformation**	**Log *k* Transformation**	$1/\sqrt{k}$ **Transformation**
Response Variable	*k*	Sqrt (*k*)	$Log_{10}(k)$	1/sqrt (*k*)
Predictor variables	rainfall, temp, food, paper, textile, yard	rainfall, temp, food, paper, textile, yard	rainfall, temp, food, paper, textile, yard	rainfall, temp, food, paper, textile, yard
Y vs X	Curvature with temp and paper	Curvature with rainfall, temperature, textile and paper	Slight curvature with rainfall. Others mostly had linear trends	Curvature with rainfall, temperature, paper, textile, yard
R^2	0.6986	0.7087	0.6879	0.634
Adj. R^2	0.5342	0.5498	0.5176	0.4358
VIF	paper=8.96	paper = 8.97	paper = 8.97	paper = 8.97
	yard=7.61	yard = 7.62	yard =7.62	yard = 7.61
	all others < 5	others <5	others <5	others<5
e vs. yhat	Slight curvature (curved funnel)	Curved funnel	No funnel	Funnel Shape
e vs. x	Curvature in residuals vs. rainfall, paper and yard	Curvature in residuals vs. rainfall, temperature and textile	Curvature in residuals vs. rainfall and temp	Curvature in residual vs rainfall and residuals vs. temperature
Normality	Shorter tails than normal probability plots	S shaped-shorter tails than normal probability plot	Almost normal	Longer left tail. Not normal

5.2.3.2 Transformations on X- Variables

From the $\log_{10}k$ transformation plots (see Appendix D), it was observed that the residuals vs. rainfall and residuals vs. temperature plots showed curvature. Based on the raw data plots and residual plots, it was necessary to use transformations on rainfall and temperature terms. First, quadratic transformations were used on rainfall and temperature.

The squared terms were added in the model only after standardizing them. Standardization is a procedure where the mean is centered by assigning it to zero, and the variance is scaled to one. Standardization helps in understanding a model which has predictors with different scales. The variables were standardized using Eq. (5-3).

$$X_1{}^2 = \left(\frac{X_1 - Mean}{Standard\ Deviation}\right)^2 \quad (5\text{-}3)$$

After adding the quadratic terms for rainfall and temperature it was observed that the residuals vs. textile and yard showed some curvature. Hence, quadratic terms were added for textile and yard waste, and the residual analysis were repeated in each case. Comparisons of the X-transformations performed in this study are shown in Table 5.7. The SAS outputs along with raw data plots and residual plots are shown in Appendix D.

From Table 5.7, it was observed that as the number of variables increased, the R^2 value of the model improved. However, the VIF's were also increasing, indicating problems of variance inflation due to the multicollinearity among the predictors. Further, the residual analysis showed curvature in the residuals vs. predictor plots. After conducting the correlation analysis, it was found that some of the squared terms had very high correlation with the original predictors, despite the standardization; e.g. correlation between textile and the square of textile standardized was equal to 0.90. This induced high multicollinearity in the model. It must also be noted that the residuals vs. textile plot had one single point which gave the plot the appearance of curvature, and hence, it was decided that curvature was not present in that plot. As mentioned earlier, the observations for 60% food + 30% textile + 10% yard and 100% textile reactors were omitted. If the complete data for textile waste were available, such anomalies would have been avoided.

Further, it was observed that the curvature in residuals vs. yard waste plot grew worse as the quadratic terms for textile and yard waste were added. Hence it was concluded that the model with quadratic terms for rainfall and temperature terms did an overall better job than the other MLR models.

Table 5.7: Comparison of X- Transformations

	Without Quadratic Transformation on X	**Quadratic Transformations on Rainfall and Temp**	**Quadratic Transformations for Rainfall, Temp and Textile**	**Quadratic Transformations for Rainfall, Temp, Textile and Yard**
Response Variable	$Log_{10}k$	$Log_{10}k$	$Log_{10}k$	$Log_{10}k$
Predictor Variables	ainfall, temp, food, paper, textile, yard	rainfall, temp, food, paper, textile, yard	rainfall, temp, food, paper, textile, yard	rainfall, temp, food, paper, textile, yard
Quadratic Terms	None	$rainfall^2$, $temp^2$	$rainfall^2$, $temp^2$, $textile^2$	$rainfall^2$, $temp^2$, $textile^2$, $yard^2$
Y vs X	Slight curvature with rainfall. Others mostly had linear trends	Mostly Linear Curvature with $temp^2$	Curvature with rainfall, $temp^2$, paper and textile	Mostly linear. Curvature with $temp^2$ and paper
R^2	0.6879	0.7778	0.7881	0.8417
Adj. R^2	0.5176	0.5803	0.5497	0.6155
VIF	paper = 8.96 yard =7.61 Others <5	paper =9.22 yard =7.95	paper=10.85 textile=19.31 $textile^2$=11.59 yard=9.75	paper = 11.27 textile=22.78 $textile^2$=12.25 yard=22.81 $yard^2$=10.22
e vs. yhat	No funnel	No funnel	Funnel Shape	No Funnel
e vs. x	Curvature in residuals vs. rainfall and temp	Slight curvature in residuals vs. textile	Curvature in residuals vs. $temp^2$, textile and yard	Curvature temp, $temp^2$ and yard
NPP	Almost normal	S shaped Shorter Tails than NPP	S shaped (shorter tails than NPP)	S shaped Not normally distributed

5.2.3.3 MLR Model after Transformations

Since a log transformation was conducted on the rate of decomposition (*k* value), the transformation was expected to affect all the response-predictor trends. Hence, the response vs. predictor plots were reviewed again (See Figure 5.6).

From Figure 5.6, temperature and yard showed an increasing linear trend with the logarithm of rate of decomposition (*k*); which indicated that, as temperature and % yard was increased, the rate at which waste degraded in the landfill also increased. Rainfall showed a decreasing trend. No other trends were obvious in the response vs. predictor plots. It appeared that high response values in the raw data plots were compressed and linearized due to the log transformation on the response variable.

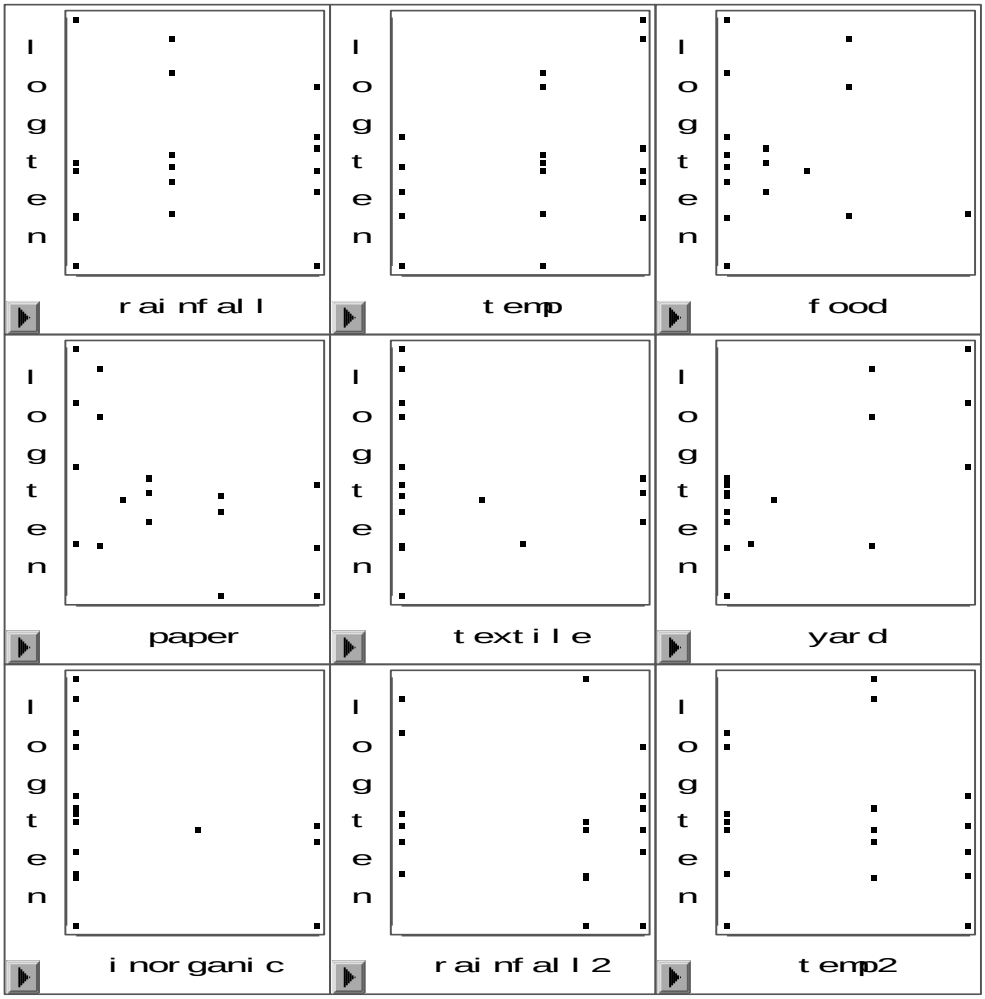

Figure 5.6: Response vs. Predictor Plots for the Transformed Model

The MLR model after performing the necessary transformations was as follows.

$$\widehat{log_{10}k} = \beta_0 + \beta_1 R + \beta_2 R^2 + \beta_3 T + \beta_4 T^2 + \beta_5 F + \beta_6 P + \beta_7 TX + \beta_8 Y + \varepsilon \quad (5\text{-}4)$$

The estimates of the model parameters (βs) calculated by SAS are shown in Table 5.8.

Table 5.8: Parameter Estimates for the Transformed MLR Model

Parameter Estimates							
Variable	**DF**	**Parameter Estimate**	**Standard Error**	**t Value**	**Pr > |t|**	**Type I SS**	**Variance Inflation**
Intercept	**1**	-4.6731	2.28151	-2.05	0.0708	3.21284	0
rainfall	**1**	0.01096	0.01217	0.9	0.3913	0.00069	1.49
rainfall^2	**1**	-0.1375	0.07205	-1.91	0.0886	0.06616	1.38
temp	**1**	0.01593	0.00717	2.22	0.0535	0.16363	1.34
temp^2	**1**	0.02053	0.06107	0.34	0.7445	0.01163	1.45
food	**1**	-0.0008	0.00409	-0.2	0.8456	0.00029	2.60
paper	**1**	0.00149	0.00357	0.42	0.6869	0.535	9.22
textile	**1**	0.00476	0.00336	1.42	0.1897	0.01499	3.36
yard	**1**	0.00698	0.00303	2.3	0.047	0.15987	7.95

5.2.4 Rechecking Model Assumptions for the Transformed Model

5.2.4.1 MLR Model Form is Reasonable

The MLR model form is assumed to be adequate when all the residual versus predictor plots have no curvature in them. This assumption was rechecked by plotting the residuals vs. predictor plots for the transformed model (See Figure 5.7). The appearance of slight curvature was seen in the residuals vs. textile plot, as mentioned earlier, due to a single point. Hence it was decided that curvature was not genuinely present in this plot. No other residuals vs. predictor plots showed curvature. Hence it was concluded that the transformed MLR model form was adequate.

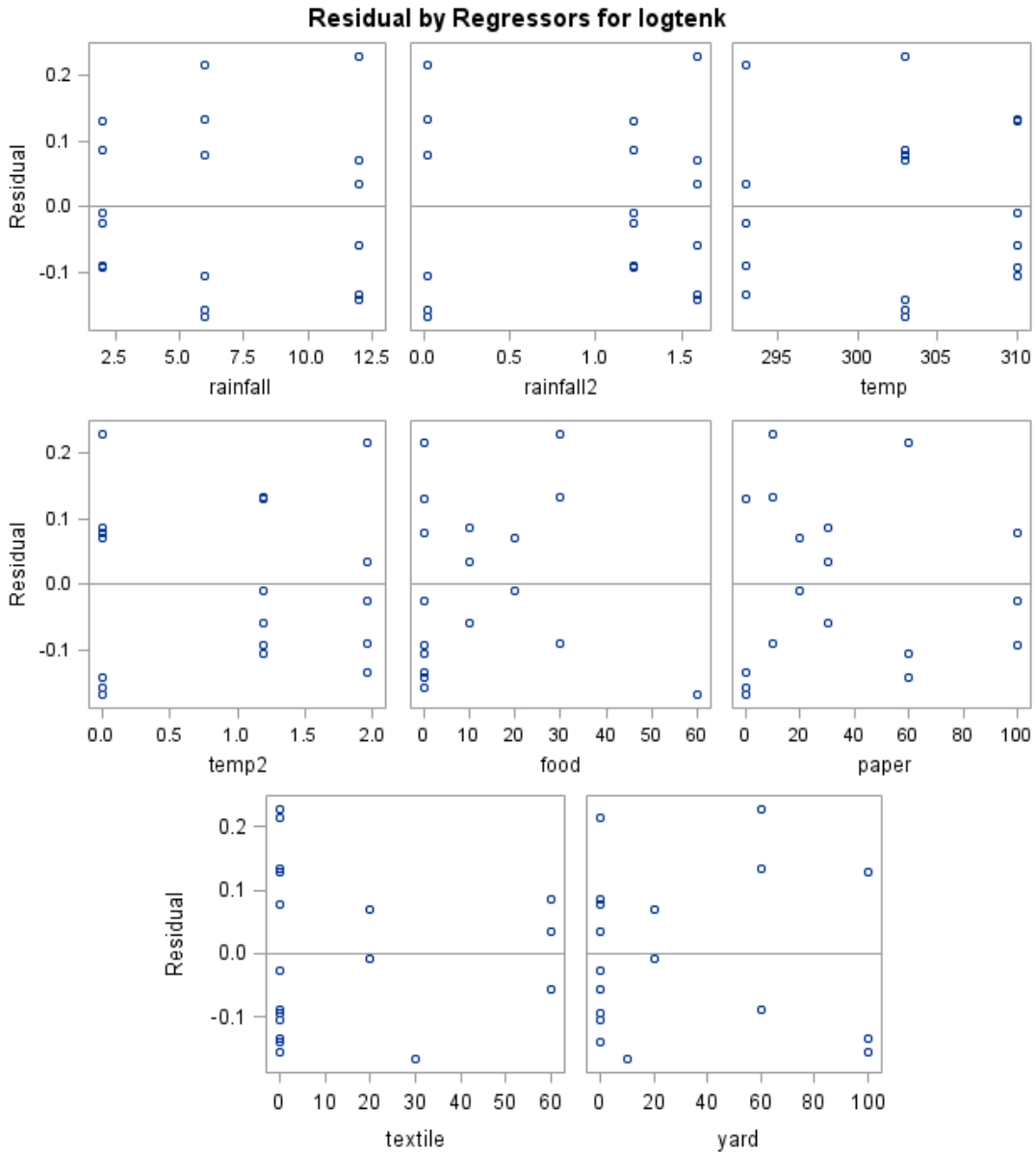

Figure 5.7: Residuals vs. Predictor Plots for the Transformed MLR Model

5.2.4.2 Residuals Have Constant Variance

For a MLR model to be satisfactory, it has to satisfy the assumption that its residuals have constant variance. This assumption was rechecked for the transformed MLR model using residuals vs. predicted value of $\log_{10}k$ ($\widehat{log_{10}k}$) plot (See Figure 5.8). A funnel shape was not

observed in this plot. This indicates that the residuals had a constant variance. This assumption was re-verified later using the Modified-Levene test.

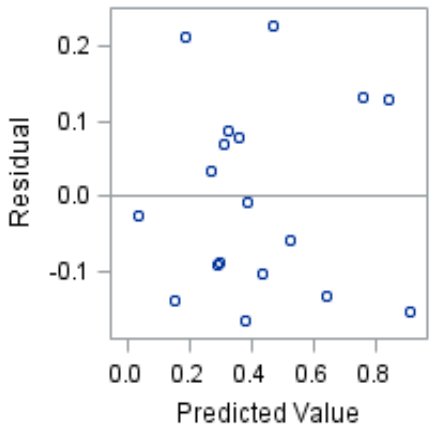

Figure 5.8: Residuals vs. Predicted Response Plot for the Transformed MLR Model

5.2.4.3 Residuals Are Normally Distributed

This assumption was re-verified for the transformed MLR model using the normal probability plot (See Figure 5.9). The residuals vs. normal scores plot showed an 'S" shaped curve. This indicated that the residuals followed a distribution with shorter tails than the normal distribution. Hence, the assumption that the errors are normally distributed was violated. This conclusion was verified using the normality test.

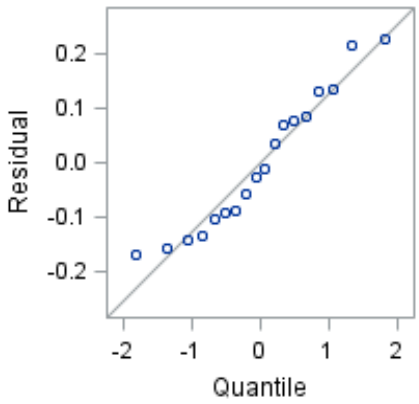

Figure 5.9: Residuals vs. Normal Scores Plot for the Transformed MLR Model

5.2.4.4 Modified-Levene Test for Checking Constant Variance

This test is performed to detect non-constant variance even when there is serious departure from normality. In order to conduct the test, the dataset is divided into two groups based on the fitted values, such that the number of observations in both the groups were approximately equal. In this case, the dividing point was chosen to be $\widehat{log_{10}k}$ = 0.37. This value was chosen as a dividing value because the numbers of observations in each group were equal to nine. The absolute deviations (d_{i1} , d_{i2}) of residuals around the medians were calculated for each group The SAS output for the conducting the Modified–Levene test, which uses the two sample t-test, is shown in Table 5.9.

Table 5.9: SAS Output for the Modified-Levene Test for the Transformed MLR Model

Obs		**group**		**meand**		
1		1		0.08835		
2		2		0.1155		
The TTEST Procedure						
Group	**N**	**Mean**	**Std Dev**	**Std Err**	**Minimum**	**Maximum**
1	9	0.0883	0.0643	0.0214	0	0.1792
2	9	0.1155	0.0895	0.0298	0	0.2851
Diff (1-2)		-0.0272	0.0779	0.0367		
Method		**Variances**		**DF**	**t Value**	**Pr > |t|**
Pooled		Equal		16	-0.74	0.4706
Satterthwaite		Unequal		14.525	-0.74	0.4717
Equality of Variances						
Method		**Num DF**		**Den DF**	**F Value**	**Pr > F**
Folded F		8		8	1.94	0.3695

The following hypotheses are considered for the Modified-Levene test.

F- test- Hypothesis

H_0: Variances of the two populations (d_1 , d_2)are equal

H_1: Variances of the two populations (d_1 , d_2) are unequal

Considering $\alpha = 0.05$

From Table 5.9, p-value from f-test = 0.3695 > α. Hence, we fail to reject H_0, which means that the variances of d_1 and d_2 are equal. Hence the "equal" variance output from the t-test was referred for further analysis.

T-test- Hypothesis

H_0: Means of d_1 and d_2 populations are equal- Hence the constant error variance assumption is satisfied.

H_1: Means of d_1 and d_2 populations are not equal- Hence the constant error variance assumption is violated.

From Table 5.9, p- value = 0.4706 > α. Hence we fail to reject H_0. Given that this verified the conclusion from the residuals vs. predicted values plot, we can say that the constant variance assumption was satisfied by the transformed MLR model. The same conclusion was reached when $\alpha = 0.01$, and 0.1.

5.2.4.5 Test for Normality

For testing normality, the following hypotheses are considered.

H_0 : Normality is satisfied.

H_1 : Normality is not satisfied.

The SAS output for correlation between residuals and normal scores is shown in Table 5.10.

From Table 5.10, $\hat{\rho}$ (e,z) = 0.97571

Considering $\alpha = 0.1$, c (α, n) = c (0.1, 18) = 0.957

According to the decision rule, if $\hat{\rho} < c$ (α, n), then reject H_0.

From Table 5.10, $\hat{\rho}$ =0.97571 > c (α, n) = 0.957; hence, we fail to reject H_o. In this case, the test was unable to detect nonnormality, although deviation from normality was visible in

the normal probability plot. Usually in practice the normal probability plots are considered more reliable than the normality test. Hence, we can conclude that the normality was not satisfied by the transformed MLR model. However, normality is not a required assumption of the MLR model.

Table 5.10: SAS Output for Testing Normality in the Transformed MLR Model

Pearson Correlation Coefficients, N = 18		
Prob > |r| under H_0: Rho=0		
	e	**enrm**
e	1	0.97571
enrm	0.97571	1

5.2.4.6 Variance Inflation Factor (VIF)

This factor is used to assess if there is serious multicollinearity between predictors. The VIF value identifies cases of high variance inflation due to the complications caused by high multicollinearity. If a VIF value is more than one, that means that multicollinearity exists; however, the multicollinearity may not be serious. As a guideline, if a VIF value exceeds 5, it means serious multicollinearity exists between the predictors. More directly, it means that the variance for that estimated model parameter is inflated more than 5 times. In this case, from SAS output shown in Table 5.8, the VIF's for paper and yard waste were greater than 5; therefore, there was serious multicollinearity between predictors. However, this could be due to the correlation between yard and paper waste (See Section 5.2.1.4). The issue of high multicollinearity often resolves itself in when considering subset models during the model search task.

5.2.4.7 Outliers

These are single data points that affect the trend of grouped data by pulling it toward its position. The SAS output for checking outliers is shown in Table 5.11.

Table 5.11: SAS Output for Checking Outliers in the Transformed MLR Model

Obs	Residual	RStudent	Hat Diag Hii	Cov Ratio	DFFITS
1	-0.0257	-0.1926	0.4745	5.2689	-0.183
2	-0.0884	-0.6766	0.4697	3.2989	-0.6368
3	0.0863	0.8589	0.6755	4.0214	1.2393
4	-0.0928	-0.722	0.4824	3.16	-0.6971
5	0.1297	1.0258	0.4679	1.7839	0.962
6	-0.0092	-0.0633	0.3791	4.6282	-0.0495
7	0.2135	2.2246	0.5615	0.0863	2.5172
8	0.0783	0.6492	0.5493	4.0347	0.7167
9	-0.1547	-1.4847	0.5928	0.793	-1.7912
10	-0.1668	-1.7927	0.6432	0.3872	-2.4067
11	-0.1032	-0.7843	0.4516	2.7023	-0.7116
12	0.1328	1.0173	0.4336	1.7052	0.89
13	-0.1337	-1.0947	0.4952	1.6281	-1.0843
14	0.0343	0.27	0.5218	5.5627	0.2821
15	-0.1405	-1.2194	0.5368	1.3438	-1.3128
16	0.2277	1.9868	0.423	0.1354	1.7011
17	0.0696	0.453	0.2877	3.2262	0.2879
18	-0.0574	-0.4724	0.5544	5.0569	-0.5269

Outliers may be X-outliers or Y-outliers. The X-outliers are identified by assessing the diagonal elements of the Hat-matrix (h_{ii}), which are also called leverage values. The cut-off point for h_{ii} is $2p/n$, where p = number of parameters in the model and n = total number of observations. In this MLR model, the $h_{ii} > 0.888$ meant that the observation '*i*' was X-outlying. Based on the cut-off point and the SAS output shown in Table 5.11, there were no X-outliers detected in the transformed MLR model.

The Y-outliers are identified by assessing the studentized deleted residuals, t_i, and the cut-off are calculated based on the Bonferroni Outlier test at α =0.1,0.05 . According to the Bonferroni outlier test, the cut-off points for Y outliers were $|t_i| > t(1-\alpha/2n, n-p-1) = 3.690$ and 4.29005 at α = 0.1 and 0.05, respectively. Based on the cut-off points and the SAS output shown in Table 5.11 , no Y-outliers were detected.

5.2.5 Exploring Possible Interaction Terms

Interaction terms arise due to a combined effect of two predictor variables on the response. 15 possible interaction terms were considered in this study to explore the interactions between the 6 predictor variables. However, only a few interaction terms may be helpful for the model performance, by explaining any of the variability in the response that remained unexplained by the current MLR model. Hence to explore if an interaction term may help the model, partial regression plots are used. Alternately, the standardized interaction term is plotted against the residuals to detect if any interaction terms can help the model. For this the predictors must first be standardized. As mentioned earlier, standardization is a procedure where the mean is centered by assigning it to zero, and the variance is scaled to one. Standardization helps in understanding a model which has predictors with different scales.

If a linear trend is observed in residuals vs. standardized interaction term plot, then that interaction term is considered to be helpful to the MLR model. However, if the points are randomly scattered in the residuals vs. standardized interaction plots, then the interaction term may not be helpful. Figure 5.10- 5.12 shows the residuals vs. interaction plots.

From Figure 5.10-5.12, it was observed that the interaction terms stdx1x3 (standardized rainfall x food) and stdx2x6 (standardized temperature x yard) showed an

upward linear trend with the residuals. Further, variable stdx2x4 (standardized temperature x paper) showed a downward linear trend with the residuals. Other than these, the other interaction terms did not exhibit any trends. Hence these three interaction terms (stdx1x3, stdx2x4 and stdx2x6) were included in the MLR model.

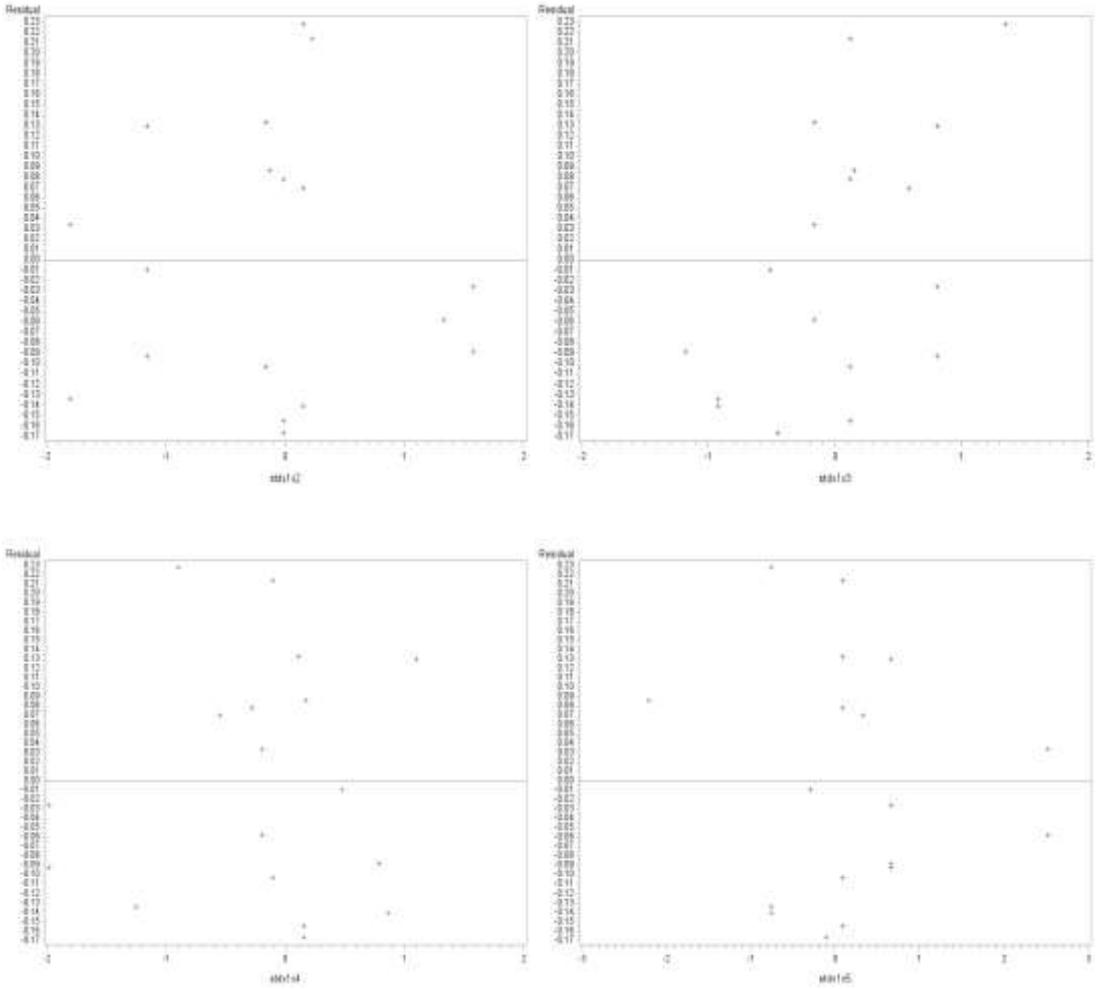

Figure 5.10: Interaction Plots for the Transformed MLR Model

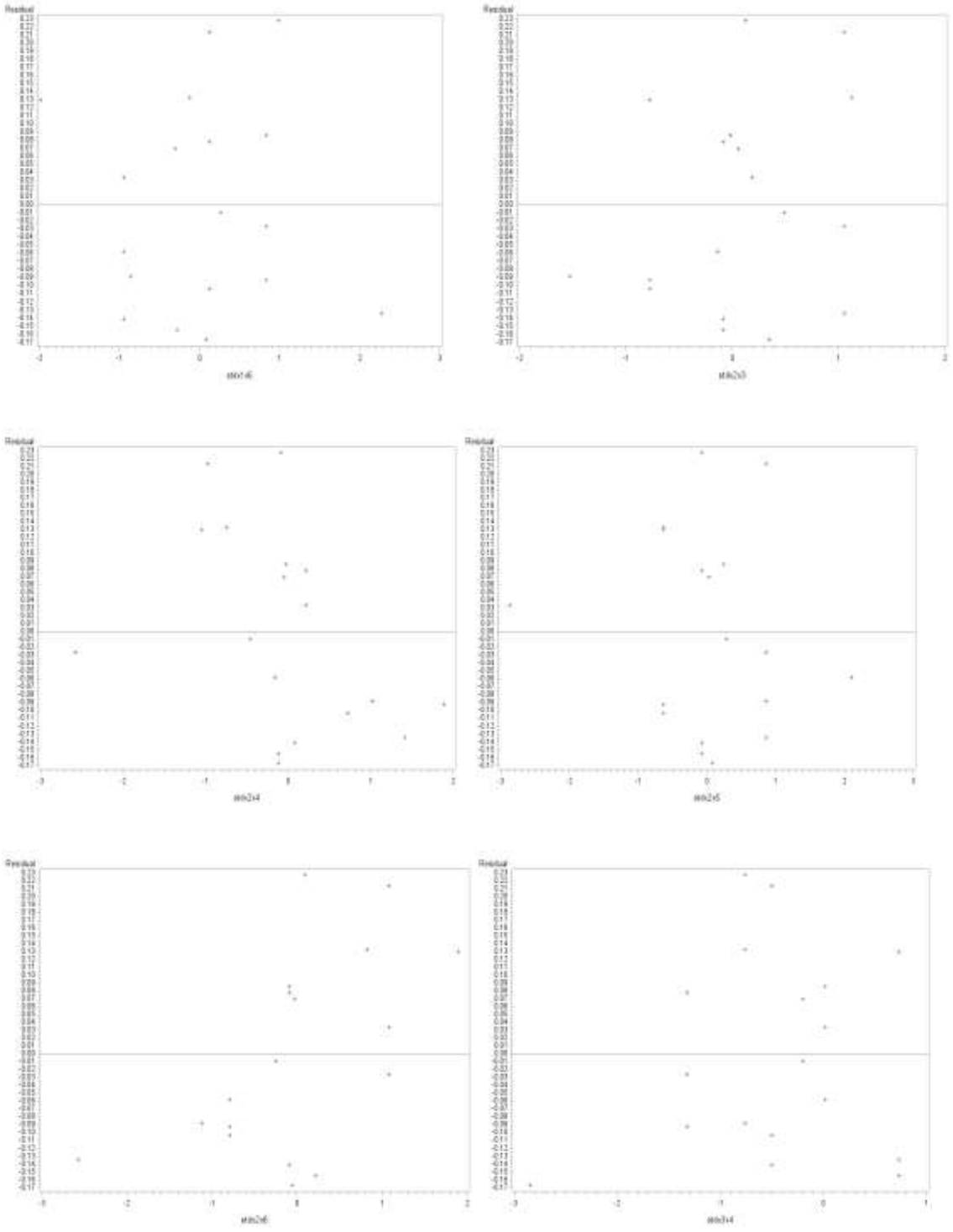

Figure 5.11: Interaction Plots for the Transformed MLR Model

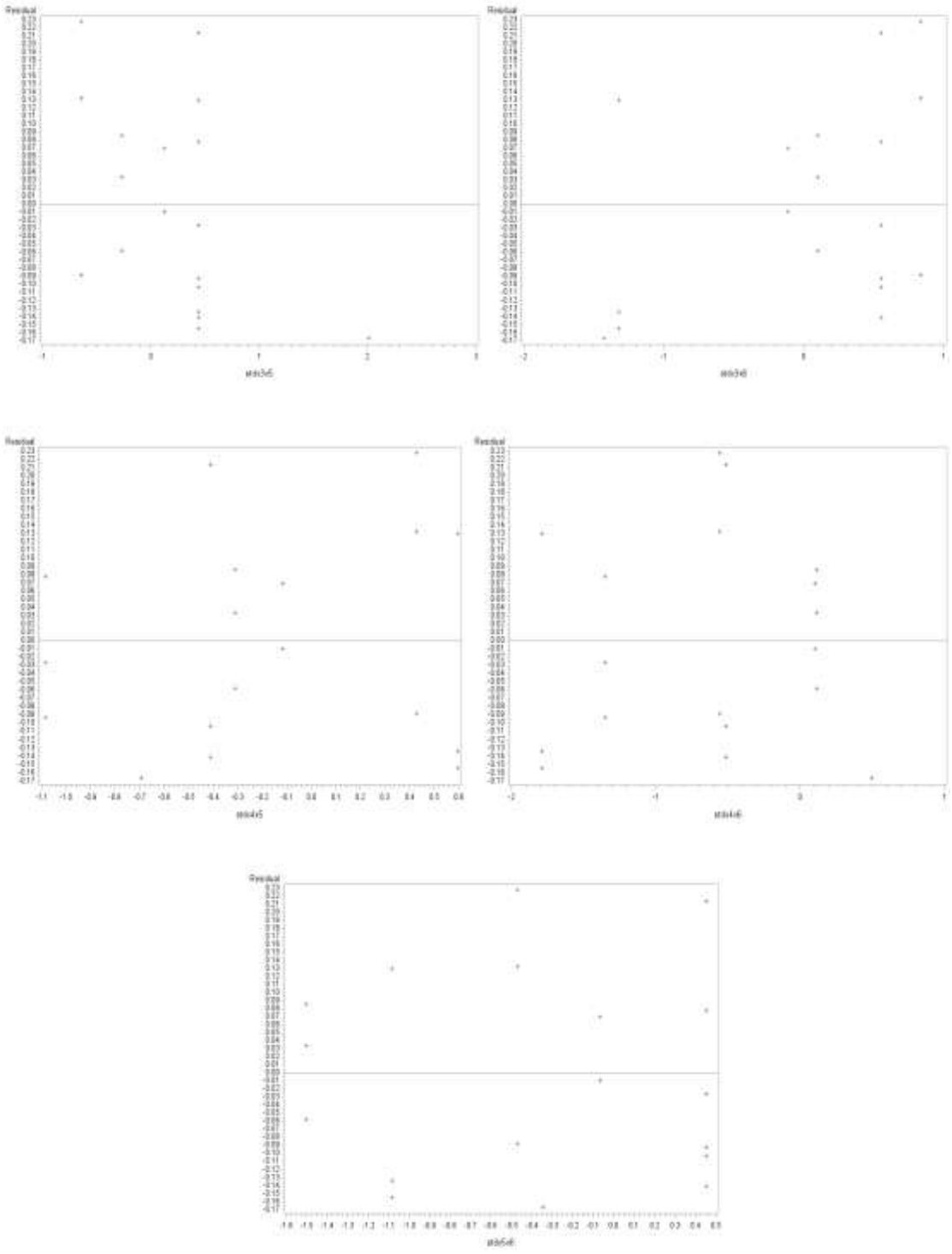

Figure 5.12: Interaction Plots for the Transformed MLR Model

The presence of interaction terms in a model typically induces high multicollinearity, because the interaction terms may be correlated with the original predictors. Hence it was necessary to check the correlation matrix (see Table 5.12). If the correlation coefficient (*r*) had a value greater than 0.7, it meant that the variables were highly correlated and could induce high multicollinearity. From Table 5.12, it can be observed that the following predictors were highly correlated with the interaction terms added.

1. food with x1x3 (temperature x food),
2. paper with x2x4 (temperature x paper), and
3. yard waste with x2x6 (temperature x yard).

Table 5.12: Correlation Analysis for the Added Interaction Terms before Standardization

Pearson Correlation Coefficients, N = 18												
Prob > |r| under H0: Rho=0												
	$Log_{10}k$	**rainfall**	**rainfall2**	**temp**	**temp2**	**food**	**paper**	**textile**	**yard**	**x1x3**	**x2x4**	**x2x6**
$Log_{10}k$	1	0.0237	-0.2108	0.3790	-0.1289	0.0132	-0.5588	-0.1230	0.7030	0.1355	-0.5540	0.7166
rainfall	0.0237	1	0.3381	-0.1564	-0.1769	0.0279	-0.2199	0.2133	0.0024	0.4015	-0.2196	-0.0055
rainfall2	-0.2108	0.3381	1	-0.1482	0.1399	-0.1086	-0.1039	0.3148	0.0201	0.0549	-0.1044	0.0132
temp	0.3790	-0.1564	-0.1482	1	-0.4210	0.0610	-0.0423	0.0266	-0.0230	0.0872	-0.0180	-0.0051
temp2	-0.1289	-0.1769	0.1399	-0.4210	1	-0.2431	0.1016	-0.0690	0.0524	-0.3751	0.0911	0.0446
food	0.0132	0.0279	-0.1086	0.0610	-0.2431	1	-0.5148	0.2062	0.0291	**0.8442**	-0.5143	0.0296
paper	-0.5588	-0.2199	-0.1039	-0.0423	0.1016	-0.5148	1	-0.1915	-0.6804	-0.4515	**0.9995**	-0.6807
textile	-0.1230	0.2133	0.3148	0.0266	-0.0690	0.2062	-0.1915	1	-0.4079	0.2311	-0.1912	-0.4076
yard	0.7030	0.0024	0.0201	-0.0230	0.0524	0.0291	-0.6804	-0.4079	1	0.0126	-0.6806	**0.9996**
x1x3	0.1355	0.4015	0.0549	0.0872	-0.3751	0.8442	-0.4515	0.2311	0.0126	1	-0.4512	0.0156
x2x4	-0.5540	-0.2196	-0.1044	-0.0180	0.0911	-0.5143	0.9995	-0.1912	-0.6806	-0.4512	1	-0.6808
x2x6	0.7166	-0.0055	0.0132	-0.0051	0.0446	0.0296	-0.6807	-0.4076	0.9996	0.0156	-0.6808	1

Further, the correlation between the interaction terms x2x4 (temperature*paper) and x2x6 (temperature*yard) was also high. This could be due to correlation between paper and yard waste. The correlations can be reduced if the interaction terms are calculated using

standardized predictors. Table 5.13 shows the correlation matrix with standardized interaction terms.

From Table 5.13, it can be observed that the correlation coefficients decreased in most cases. Since the correlation coefficients are non-zero, it means that the predictors are still correlated with each other, but not highly correlated. However, the correlation between stdx2x6 and stdx2x4 was still higher than 0.7. This indicated that there may be serious multicollinearity if all these terms are included in the MLR model.

Table 5.13: Correlation Analysis for the Added Interaction Terms after Standardization

Pearson Correlation Coefficients, N = 18												
Prob > |r| under H0: Rho=0												
	$Log_{10}k$	**rainfall**	**rainfall2**	**temp**	**temp2**	**food**	**paper**	**textile**	**yard**	**stdx1x3**	**stdx2x4**	**stdx2x6**
$Log_{10}k$	1	0.0237	-0.2108	0.3790	-0.1289	0.0132	-0.5588	-0.1230	0.7030	0.2932	-0.1204	0.2616
rainfall	0.0237	1	0.3381	-0.1564	-0.1769	0.0279	-0.2199	0.2133	0.0024	-0.1098	0.1885	-0.2290
rainfall2	-0.2108	0.3381	1	-0.1482	0.1399	-0.1086	-0.1039	0.3148	0.0201	0.0282	0.1317	-0.1938
temp	0.3790	-0.1564	-0.1482	1	-0.4210	0.0610	-0.0423	0.0266	-0.0230	0.2522	0.0853	0.0428
temp2	-0.1289	-0.1769	0.1399	-0.4210	1	-0.2431	0.1016	-0.0690	0.0524	-0.2118	-0.0562	-0.0291
food	0.0132	0.0279	-0.1086	0.0610	-0.2431	1	-0.5148	0.2062	0.0291	-0.1734	0.0017	-0.0230
paper	-0.5588	-0.2199	-0.1039	-0.0423	0.1016	-0.5148	1	-0.1915	-0.6804	0.2678	-0.0589	0.0667
textile	-0.1230	0.2133	0.3148	0.0266	-0.0690	0.2062	-0.1915	1	-0.4079	-0.1128	0.0007	0.0249
yard	0.7030	0.0024	0.0201	-0.0230	0.0524	0.0291	-0.6804	-0.4079	1	-0.0375	0.0685	-0.0736
stdx1x3	0.2932	-0.1098	0.0282	0.2522	-0.2118	-0.1734	0.2678	-0.1128	-0.0375	1	-0.3074	0.4694
stdx2x4	-0.1204	0.1885	0.1317	0.0853	-0.0562	0.0017	-0.0589	0.0007	0.0685	-0.3074	1	**-0.7481**
stdx2x6	0.2616	-0.2290	-0.1938	0.0428	-0.0291	-0.0230	0.0667	0.0249	-0.0736	0.4694	-0.7481	1

5.2.6 MLR Model Search

MLR model search is the step where potential good models are identified. Parameters which have insignificant effect on the model are removed in this step. Three methods, backwards deletion, best subsets and stepwise regression, were used for the MLR model search. The best MLR model was identified based on the results from all three methods.

Based on the previous analysis, eleven predictor variables (Rainfall, Rainfall^2, Temperature, Temperature^2, Food, Paper, Textile, Yard, StdX_1X_3, StdX_2X_4, and StdX_2X_6) were considered to find the good models for predicting the rate of degradation (Log_{10} k) for any landfill.

5.2.6.1 Backward Elimination Method for MLR Model Search

Backward elimination method for MLR model search uses an iterative process, where regression is conducted by including all possible variables in the model and the predictor variables are eliminated (one by one) if they are not significant at the specified confidence level. A potential good model is the one in which all remaining predictor variables are statistically significant.

In this study, a cutoff α value of 0.1 was chosen for the backward elimination method. Eleven predictor variables were considered in the model initially. From the regression equation obtained from the full model, p-values were calculated for testing the following hypotheses:

$H_0 : \beta_k = 0$, $H_1 : \beta_k \neq 0$

The predictor variable with largest p-value (if p was greater than α = 0.1) was removed. The remaining parameters were regressed again, until all the remaining predictor variables were significant at α = 0.1. The SAS output for last two iterations using the backward elimination method and the summary are shown in Table 5.14. A model with 5 predictor variables (highlighted in yellow) was chosen by the backward elimination method.

Table 5.14: SAS output for Backward Elimination Method for MLR Model Search

Backward Elimination: Step 6					
Variable rainfall Removed: R-Square = 0.8262 and C(p) = 3.1211					
Analysis of Variance					
Source	**DF**	**Sum of Squares**	**Mean Square**	**F Value**	**Pr > F**
Model	5	1.01147	0.20229	11.41	0.0003
Error	12	0.21278	0.01773		
Corr. Total	17	1.22425			
Variable	**Parameter Estimate**	**Standard Error**	**Type II SS**	**F Value**	**Pr > F**
Intercept	-2.86596	1.51834	0.06318	3.56	0.0835
rainfall2	-0.12125	0.05142	0.09859	5.56	0.0362
temp	0.01046	0.005	0.07771	4.38	0.0582
textile	0.00418	0.00168	0.11008	6.21	0.0284
yard	0.00598	0.00092255	0.74519	42.03	<.0001
stdx1x3	0.12165	0.05014	0.10436	5.89	0.032
Backward Elimination: Step 7					
Variable temp Removed: R-Square = 0.7627 and C(p) = 4.4523					
Analysis of Variance					
Source	**DF**	**Sum of Squares**	**Mean Square**	**F Value**	**Pr > F**
Model	4	0.93376	0.23344	10.45	0.0005
Error	13	0.29049	0.02235		
Correct Total	17	1.22425			
Variable	**Parameter Estimate**	**Standard Error**	**Type II SS**	**F Value**	**Pr > F**
Intercept	0.30999	0.0695	0.44459	19.9	0.0006
rainfall2	-0.14215	0.05662	0.14083	6.3	0.0261
textile	0.00461	0.00187	0.13642	6.11	0.0281
yard	0.00607	0.00103	0.76921	34.42	<.0001
stdx1x3	0.15058	0.05411	0.17303	7.74	0.0155
All variables left in the model are significant at the 0.0500 level.					
Summary of Backward Elimination					

Step	**Variable Removed**	**No. Vars In**	**Partial R-Square**	**Model R-Square**	**C(p)**	**F Value**	**Pr > F**
1	paper	10	0	0.8857	10.000	0	0.9772
2	stdx2x4	9	0.0001	0.8856	8.0036	0	0.9565
3	food	8	0.0041	0.8815	6.2206	0.29	0.6054
4	temp2	7	0.0152	0.8663	5.0177	1.15	0.3108
5	stdx2x6	6	0.0216	0.8447	4.1505	1.61	0.2327
6	rainfall	5	0.0185	0.8262	3.1211	1.31	0.2767
7	temp	4	0.0635	0.7627	4.4523	4.38	0.0582

5.2.6.2 Stepwise Regression Method for MLR Model Search

The stepwise regression method uses backward elimination and forward selection methods for evaluating best MLR model. This method also uses an iterative approach, starting with no variables in the model. The variables are added or deleted using the p-value to test the hypothesis: H_0: β_k= 0. With a step by step approach the predictors in the model are removed, beginning with the predictor with largest p value, if $p > \alpha_{out.}$ If no predictors are removed, the predictors which are not in the model are added, starting from the predictor with the smallest p-value, if $p < \alpha_{in}$. This procedure is repeated until no predictor variables can be added or removed from the model yielding one potentially good model. The SAS output for stepwise regression is shown in Table 5.15. In this case, the α_{in} and α_{out} were set at 0.1. The best model suggested by stepwise regression method had three variables (highlighted in green). However, the selected model was not the same as with the one selected by the backward elimination method. Hence this model (with three variables) was also short-listed for further comparison.

Table 5.15: SAS Stepwise Regression Method for MLR Model Search

Stepwise Selection: Step 1					
Variable yard Entered: R-Square = 0.4941 and C(p) = 12.5470					
Analysis of Variance					
Source	**DF**	**Sum of Squares**	**Mean Square**	**F Value**	**Pr > F**
Model	1	0.60496	0.60496	15.63	0.0011
Error	16	0.6193	0.03871		
Corrected Total	17	1.22425			
Variable	**Parameter Estimate**	**Standard Error**	**Type II SS**	**F Value**	**Pr > F**
Intercept	0.28071	0.05862	0.88756	22.93	0.0002
yard	0.00481	0.00122	0.60496	15.63	0.0011

Table 5.15- *Continued*

Stepwise Selection: Step 2					
Variable temp Entered: R-Square = 0.6504 and C(p) = 6.3465					
Analysis of Variance					
Source	**DF**	**Sum of Squares**	**Mean Square**	**F Value**	**Pr > F**
Model	2	0.79626	0.39813	13.95	0.0004
Error	15	0.42799	0.02853		
Corrected Total	17	1.22425			
Variable	**Parameter Estimate**	**Standard Error**	**Type II SS**	**F Value**	**Pr > F**
Intercept	-4.42925	1.81967	0.16905	5.92	0.0279
temp	0.01556	0.00601	0.19131	6.7	0.0205
yard	0.00488	0.00105	0.62038	21.74	0.0003

Stepwise Selection: Step 3					
Variable stdx2x6 Entered: R-Square = 0.7393 and C(p) = 3.6813					
Analysis of Variance					
Source	**DF**	**Sum of Squares**	**Mean Square**	**F Value**	**Pr > F**
Model	3	0.90509	0.3017	13.23	0.0002
Error	14	0.31916	0.0228		
Corrected Total	17	1.22425			
Variable	**Parameter Estimate**	**Standard Error**	**Type II SS**	**F Value**	**Pr > F**
Intercept	-4.28537	1.62786	0.15799	6.93	0.0197
temp	0.01508	0.00538	0.17928	7.86	0.0141
yard	0.00503	0.000937	0.65535	28.75	0.0001
stdx2x6	0.07895	0.03613	0.10883	4.77	0.0464

All variables left in the model are significant at the 0.1000 level								
No other variable met the 0.1000 significance level for entry into the model.								
Summary of Stepwise Selection								
Step	**Variable Entered**	**Variable Removed**	**Number Var In**	**Partial R-Sq**	**Model R-Sq**	**C(p)**	**F Value**	**Pr > F**
1	yard		1	0.4941	0.4941	12.547	15.63	0.0011
2	temp		2	0.1563	0.6504	6.3465	6.7	0.0205
3	stdx2x6		3	0.0889	0.7393	3.6813	4.77	0.0464

5.2.6.3 Best Subset Method for MLR Model Search

The best subsets method helps to evaluate which predictor variables should be included in the MLR model. This method provides the specified number of best models with one or more variables. In this case, the best subsets method was run several times, starting from one predictor variable until all eleven variables were included in the MLR model.

The following criteria were used for selecting the best models:

1. R^2 should be high. The coefficient of determination (R^2) is a measure used to describe how well a particular model fits the data. Usually, R^2 never decreases as the number of predictors in the MLR model increases, giving a potentially false impression that one should have as many predictors in the model as possible. In practice, the smallest model that yields a high R^2 is desired.
2. Adjusted R^2 should be high. Adjusted coefficient of determination (R_{adj}^2) penalizes the addition of useless variables. Again, in practice, the smallest model that yields a high adjusted R^2 is desired.
3. Mallows C_p value should be small or close to the number of parameters in the model. If it has no bias, or if the model has all the significant parameters included in it, then the C_p value is small; hence it is used as a criterion for best MLR model selection.
4. Akaike Information Criterion (AIC) or Schwarz Bayesian Criterion (SBC) should be minimized. AIC and SBC are the measures of relative goodness of fit for any MLR model. Hence, AIC and SBC are considered for model selection.

Table 5.16 shows the output for the best subsets method for MLR model selection. The models selected by backward elimination method and stepwise regression method are highlighted in yellow and green, respectively.

Table 5.16: SAS Output for Best Subsets Method for MLR Model Selection

No. of Var	R_{adj}^2	R^2	C_p	AIC	SBC	Variables in Model
1	0.4625	0.4941	12.547	-56.652	-54.871	yard
1	0.2693	0.3123	22.0896	-51.124	-49.343	paper
2	0.6038	0.6504	6.3465	-61.302	-58.631	temp yard
2	0.5426	0.5964	9.1811	-58.716	-56.045	yard stdx1x3
3	0.6834	0.7393	3.6813	-64.584	-61.022	temp yard stdx2x6
3	0.6384	0.7022	5.6267	-62.191	-58.629	temp yard stdx1x3
4	0.6986	0.7695	4.0958	-64.801	-60.349	temp textile yard stdx2x6
4	0.691	0.7637	4.3998	-64.354	-59.902	rainfall temp yard stdx2x6
5	0.7538	0.8262	3.1211	-67.882	-62.539	rainfall^2 temp textile yard stdx1x3
5	0.7251	0.806	4.1823	-65.901	-60.558	rainfall2 temp textile yard stdx2x6
6	0.76	0.8447	4.1505	-67.907	-61.674	rainfall rainfall^2 temp textile yard stdx1x3
6	0.754	0.8408	4.3548	-67.461	-61.229	rainfall^2 temp textile yard stdx1x3 stdx2x6
7	0.7727	0.8663	5.0177	-68.6	-61.477	rainfall rainfall^2 temp textile yard stdx1x3 stdx2x6
7	0.765	0.8618	5.2542	-68.004	-60.881	rainfall rainfall^2 temp temp^2 textile yard stdx1x3
8	0.7761	0.8815	6.2206	-68.771	-60.757	rainfall rainfall^2 temp temp^2 textile yard stdx1x3 stdx2x6
8	0.7639	0.875	6.56	-67.814	-59.801	rainfall rainfall^2 temp food textile yard stdx1x3 stdx2x6
9	0.7569	0.8856	8.0036	-67.41	-58.506	rainfall rainfall^2 temp temp^2 food textile yard stdx1x3 stdx2x6
9	0.7525	0.8835	8.1113	-67.09	-58.186	rainfall rainfall^2 temp temp^2 paper textile yard stdx1x3 stdx2x6
10	0.7223	0.8857	10.001	-65.418	-55.624	rainfall rainfall^2 temp temp^2 food textile yard stdx1x3 stdx2x4 stdx2x6
10	0.7222	0.8856	10.002	-65.412	-55.618	rainfall rainfall^2 temp temp^2 food paper textile yard stdx1x3 stdx2x6
11	0.6761	0.8857	12	-63.421	-52.736	rainfall rainfall^2 temp temp^2 food paper textile yard stdx1x3 stdx2x4 stdx2x6

It was found that the R^2 and C_p kept improving as the number of variables was increased in the model. On the contrary, R_{adj}^2 increased initially and reached a maximum value of 0.7728 (for model with 8 variables), and then dropped thereafter. The AIC decreased initially, reached a minimum of -68.505 (for model with 8 variables), and increased thereafter. The lowest SBC value was found for the model with maximum number of variables. It was difficult to find a model which fits all the criteria; hence the models selected by the two other methods (Stepwise regression and Backward Elimination) were short-listed and checked for all the criteria mentioned above.

5.2.6.4 Best MLR Model Selection

Based on all three methods mentioned above, the MLR models in Table 5.17 were short-listed. The model with 5 variables, selected by the backward elimination method, had much better R^2 and adjusted R^2 values than the three variable model selected by the stepwise regression method. Further, the *C*, AIC and SBC values were lower in case of the 5-variable model. Hence, the model with 5 variables was selected as the best MLR model.

Table 5.17: Shortlisted Models for MLR Model Selection

No. of Var.	R_{adj}^2	R^2	C_p	AIC	SBC	Variables in Model
3	**0.6834**	0.7393	3.6813	-64.584	-61.022	temp yard stdx2x6
5	**0.7538**	0.8262	3.1211	-67.882	-62.539	rainfall2 temp textile yard stdx1x3

5.2.7 Re-verifying Assumptions for the Selected MLR Model

The selected MLR model is shown below:

$$\widehat{log_{10}k} = -2.866 - 0.1212*\text{Std. Rainfall}^2 + 0.01046*\text{Temp} + 0.00418*\text{Textile} + 0.00598*\text{Yard} + 0.12165*\text{Std. (Rainfall*Food)} \quad (5\text{-}5)$$

The parameter estimates for the selected MLR model (Eq. 5-5) are shown in Table 5.18. All variables were significant at α = 0.1. The Variance Inflation Factors (VIF's) were less than five, which indicates that this model likely did not have serious multicollinearity.

Table 5.18: Parameter Estimates for the Selected MLR Model

Parameter Estimates							
Variable	**DF**	**Parameter Estimate**	**Standard Error**	**t Value**	**Pr > |t|**	**Type I SS**	**Inflation**
Intercept	**1**	-2.86596	1.51834	-1.89	0.0835	3.21284	0
rainfall^2	**1**	-0.12125	0.05142	-2.36	0.0362	0.05439	1.19706
temp	**1**	0.01046	0.005	2.09	0.0582	0.15141	1.11354
textile	**1**	0.00418	0.00168	2.49	0.0284	0.00936	1.43008
yard	**1**	0.00598	0.000923	6.48	<.0001	0.69196	1.2525
stdx1x3	**1**	0.12165	0.05014	2.43	0.032	0.10436	1.11355

5.2.7.1 Checking the MLR Model Form

The SAS output for residuals vs. predictors is shown in Figure 5.13. It was observed that residuals vs. rainfall^2 showed possible curvature. An attempt was made to add the rainfall term in the model to check whether it would help eliminate the possible curvature in the plots. However, adding rainfall in the model adversely affected the curvature in residuals vs. temperature and yard waste plots; hence, it was removed. Since the curvature is not clear and possible not genuine, it was concluded that the current MLR model form is acceptable.

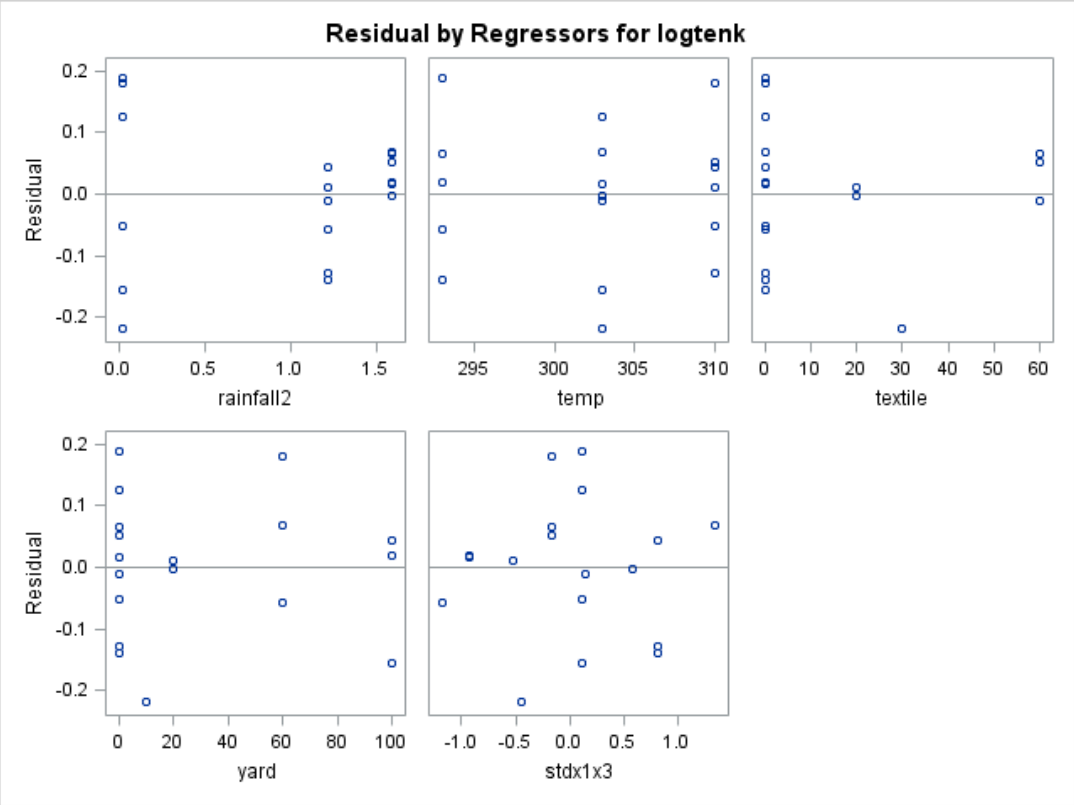

Figure 5.13: Residuals vs. Predictor Plots for the Selected MLR Model

5.2.7.2 Checking Constant Variance Assumption

The SAS output for residuals vs. predicted response variable ($\widehat{logk}$) is shown in Figure 5.14. A funnel shape was not observed in this plot. Hence it can be concluded that the current MLR model satisfied the constant variance assumption. This conclusion was re-verified using the Modified-Levene test.

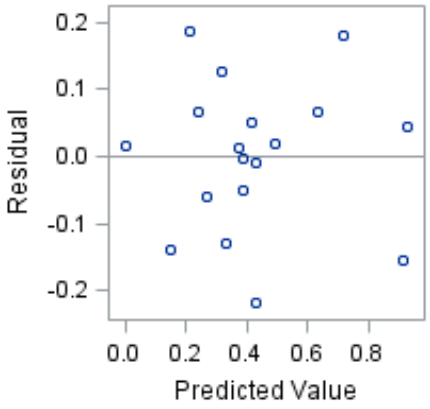

Figure 5.14: Residuals vs. Predicted Response Plot for the Selected MLR Model

5.2.7.3 Checking If Residuals Are Normally Distributed

Figure 5.15 shows the SAS output for residuals vs. normal scores plot. Longer or shorter tails were not observed in Figure 5.15. It can be concluded that the residuals followed a distribution close to the normal distribution. This assumption was re-verified using the test for normality,

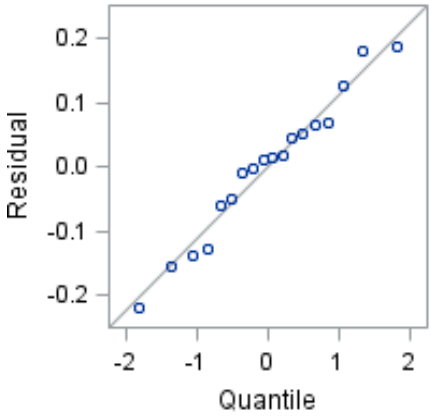

Figure 5.15: Residual vs. Normal Score Plot for the Selected MLR Model

5.2.7.4 Test for Normality

For checking normality the following hypotheses are considered.

H_0 : Normality is satisfied.

H_1 : Normality is not satisfied.

The SAS output for the correlation between the residuals and normal scores is shown in Table 5.19.

Table 5.19: SAS Output for Testing Normality for the Selected MLR Model

Pearson Correlation Coefficients, N = 18		
Prob > |r| under H_0: Rho=0		
	e	**enrm**
e	1	0.98639
enrm	0.98639	1

From Table 5.19, $\hat{\rho}$ (*e,z*) = 0.98639

Considering α = 0.1, *c* (α, *n*) = *c* (0.1, 18) = 0.957

According to the decision rule, if $\hat{\rho} < c$ (α, *n*), then reject H_0. In this case $\hat{\rho}$ =0.986 > c (α, *n*) = 0.957, hence we fail to reject H_o. Therefore it can be concluded that normality was not violated by the current MLR model, which verifies the observations from the normal probability plot.

5.2.7.5 Test for Constant Variance Assumption

The Modified Levene's test was used for testing non-constant variance. According to the procedure, the dataset it divided into two groups, based on $\widehat{Log_{10}k}$ such that each group had the same number of observations. The absolute deviations (d_{i1} , d_{i2}) of residuals around the medians were calculated for each group (See Table 5.20).

Table 5.20: SAS output for Modified Levene Test for the Selected MLR Model

Obs	group	meand
1	1	0.08074
2	2	0.086615

The TTEST Procedure

Variable: d

group	N	Mean	Std Dev	Std Err	Minimum	Maximum
1	9	0.0807	0.0676	0.0225	0	0.1763
2	9	0.0866	0.0831	0.0277	0	0.238
Diff (1-2)		-0.00588	0.0757	0.0357		

group	Method	Mean	95% CL Mean		Std Dev	95% CL Std Dev	
1		0.0807	0.0288	0.1327	0.0676	0.0457	0.1295
2		0.0866	0.0227	0.1505	0.0831	0.0561	0.1592
Diff (1-2)	**Pooled**	-0.00588	-0.0816	0.0698	0.0757	0.0564	0.1153
Diff (1-2)	**Satterthwaite**	-0.00588	-0.0818	0.0701			

Method	Variances	DF	t Value	Pr > |t|
Pooled	Equal	16	-0.16	**0.8714**
Satterthwaite	Unequal	15.363	-0.16	0.8715

Equality of Variances

Method	Num DF	Den DF	F Value	Pr > F
Folded F	8	8	1.51	0.5725

Two sample t-tests were conducted on d_{i1} and d_{i2} of observations as follows. The following hypotheses were considered for the Modified-Levene test:

F- test- Hypothesis

H_0: Variances of the two populations (d_1 , d_2) were equal

H_1: Variances of the two populations (d_1 , d_2) were unequal

Considering α = 0.05

Considering α = 0.05, from Table 5.20, p-value from f test = 0.5725 > α. Hence, we failed to reject H_0, which indicates that the variances of d_1 and d_2 were equal. Hence the "equal" variance output from the t-test was used.

T-test- Hypothesis

H_0: Means of d_1 and d_2 populations are equal- Hence the constant error variance assumption is satisfied.

H_1: Means of d_1 and d_2 populations are not equal- Hence the constant error variance assumption is violated.

From Table 5.20, p- value = 0.8716 > α. Hence, we failed to reject H_0. Therefore, the constant variance assumption was satisfied. The same conclusion was reached when α = 0.01, and 0.1. Hence, it can be concluded that the constant error variance assumption was satisfied by the selected model.

5.2.7.6 Checking for Outliers

The X-outliers are identified by assessing the diagonal elements of the Hat-matrix (h_{ii}), which are also called leverage values. The cut-off point for h_{ii} is $2p/n$, where p = number of parameters in the model and n = total number of observations. In this MLR model, if h_{ii} > 0.555 meant that the observation 'i' was X-outlying. Based on the cut-off point and the SAS output (see Table 5.21), X-outliers were not detected in the current MLR model.

The Y-outliers are identified by assessing the studentized deleted residuals, t_i, and the cut-off was calculated based on the Bonferroni Outlier test at α =0.1,0.05 . According to the Bonferroni's outlier tests, the cut-off points for Y outliers were $|t_i| > t(1-\alpha/2n, n-p-1)$ = 3.428 and 3.9175 at α = 0.1 and 0.05, respectively. Based on cut-off points and the SAS output (see Table 5.21), no Y-outliers were detected.

Table 5.21: SAS Output for Checking Outliers in the Selected MLR Model

Obs	*e*	tres	cook id	h_{ii}	dffitsi
1	-0.1396	-1.3405	0.19001	0.38818	-1.1087
2	-0.0588	-0.551	0.02807	0.35683	-0.398
3	-0.0098	-0.0882	0.00058	0.30813	-0.0564
4	-0.1297	-1.1641	0.09667	0.29975	-0.7742
5	0.04397	0.42302	0.01911	0.39058	0.32668
6	0.0115	0.09845	0.00048	0.23066	0.05163
7	0.18783	1.78463	0.31888	0.37528	1.54515
8	0.12655	1.07027	0.05124	0.2116	0.55817
9	-0.1553	-1.4999	0.24526	0.39546	-1.2885
10	-0.2198	-1.9174	0.21442	0.25923	-1.3039
11	-0.0519	-0.4541	0.01237	0.26466	-0.2631
12	0.17977	1.57162	0.14624	0.26213	1.00638
13	0.01826	0.18638	0.0049	0.45845	0.16442
14	0.06573	0.64945	0.05138	0.42226	0.54118
15	0.01523	0.15751	0.0037	0.47244	0.14286
16	0.068	0.6468	0.04213	0.37662	0.48996
17	-0.0032	-0.0256	0.00002	0.14859	-0.0102
18	0.05113	0.48732	0.02417	0.37914	0.36827

5.2.8 Selected MLR Equation

The complete ANOVA table, including parameter estimates for the selected model, is shown in Table 5.22.

It can be observed that all predictor terms included in the MLR model were significant at α=0.1 level. % paper was dropped from the model because the effect of paper waste on the rate of degradation constant (*k* values) was not found to be significant at α =0.1. This can be confirmed from the raw data plots (See Figure 5.6). The *k* value did not change much as the % paper in the waste was increased. The parameter estimates show that *k* values increase when the % textile and % yard waste increase in the landfilled waste. % Food waste was not

significant for predicting the logarithm of *k* value at α=0.1 level. However, the interaction term of food and rainfall was found to be significant. This indicates that the impact of food was enhanced when % food was combined with rainfall. The impact of this interaction term will be explained in the section 5.2.9. The intercept β_0 = -2.8658, was the estimated logarithm of *k* value when rainfall was equal to 0 mm/day, temperature was equal to 0 K, and all waste components in the landfilled waste were also assigned to 0. This value is irrelevant in this case, since the data did not extend to zero, and methane generation cannot be expected from a landfill if there were no biodegradable waste in it.

Table 5.22: ANOVA Table for the Selected MLR Model

Analysis of Variance							
Source		**DF**	**Sum of Squares**	**Mean Square**	**F Value**	**Pr > F**	
Model		5	1.01147	0.20229	11.41	0.0003	
Error		12	0.21278	0.01773			
Corrected Total		17	1.22425				
Root MSE			0.13316	R-Square		0.8262	
Dependent Mean			0.42248	Adj R-Sq		0.7538	
Coeff Var			31.5187				
Parameter Estimates							
Variable	**DF**	**Parameter Estimate**	**Standard Error**	**t Value**	**Pr > |t|**	**Type I SS**	**Variance Inflation**
Intercept	1	-2.866	1.51834	-1.89	0.0835	3.21284	0
rainfall2	1	-0.1213	0.05142	-2.36	0.0362	0.05439	1.19706
temp	1	0.01046	0.005	2.09	0.0582	0.15141	1.11354
textile	1	0.00418	0.00168	2.49	0.0284	0.00936	1.43008
yard	1	0.00598	0.00092	6.48	<.0001	0.69196	1.2525
stdx1x3	1	0.12165	0.05014	2.43	0.032	0.10436	1.11355

It can be observed that the coefficient of determination R^2 for predicting logarithm of the rate of degradation *k* value was 0.8262. This means that 82.6% of the variability of the logarithm of *k* value was explained by the predictors in the selected MLR model. From Table 5.22, it can be observed that the VIF's were less than 5; hence, it can be concluded that the multicollinearity was not serious for this model. Based on the residual analysis, it can be concluded that the model form was reasonable; residuals had constant variance and were almost normally distributed. Further, there were no outliers detected by the model. Hence the selected MLR model is hereafter used for building the CLEEN model.

5.2.9 Final MLR Model

The final MLR equation is as follows:

$$\widehat{Log_{10}}k = -2.86596 - 0.12125 \times R^2 + 0.01046 \times T + 0.00418 \times TX + 0.00598 \times Y + 0.12165 \times R \times F \quad (5\text{-}6)$$

Where,

k = Rate of degradation in terms of first order decay constant (yr^{-1}),

R = Average annual rainfall (standardized) (mm/day),

T= Ambient temperature (K),

TX = % Textile in landfilled waste,

Y= % Yard in landfilled waste,

F = % Food in landfilled waste (standardized).

As mentioned earlier, the squared terms and interaction terms were standardized to minimize multicollinearity. Standardization was conducted by subtracting the mean and scaling the variance to one. In the final MLR model, the squared term $rainfall^2$ and the interaction term rainfall*food was standardized as follows:

$$Rainfall^2 = \left(\frac{Rainfall - 6.667}{4.22875}\right)^2 \quad (5\text{-}7)$$

$$Rainfall \times Food = \left(\frac{Rainfall - 6.667}{4.22875}\right) \times \left(\frac{Food - 12.222}{16.64705}\right) \quad (5\text{-}8)$$

Substituting the standardized terms, the final MLR equation (Eq. 5-6) can be expressed as follows:

$$\widehat{log_{10}k} = -3.02658 - 0.0067282R^2 + 0.069313R + 0.00172807(R \times F) + 0.01046T - 0.01152F + 0.00418\,TX + 0.00598Y \quad (5\text{-}9)$$

Thus it can be concluded that the logarithm of *k* can be predicted using the average annual rainfall, ambient temperature, and %food, % textile, and % yard of the landfilled waste. 3D plots were generated to further study the effect of rainfall and temperature on the estimated *k* values using the comprehensive regression equation (Eq. 5-9). Figure 5.16 shows the 3D plots depicting the effect of rainfall and temperature on *k* values for a constant waste composition. EPA's national average waste composition was used for generating the 3D plot (USEPA, 2007). Similar plots can be generated for any other waste composition. The 3D plots can help to visualize the effect of change in atmospheric conditions on the rate of degradation, even if the biodegradable portion of the waste is exactly the same.

The waste composition found in Mexico was very different compared to that found in the United States. Typically, the % food waste in Mexican waste was higher than that found in the United States. Hence, a 3D plot was also generated for studying the effect of rainfall and temperature on Mexican waste composition (See Figure 5.17). It can be observed that due to the presence of a higher amount of food waste, the surface plot for Mexican waste was considerably different as compared to the surface plot made for US waste composition.

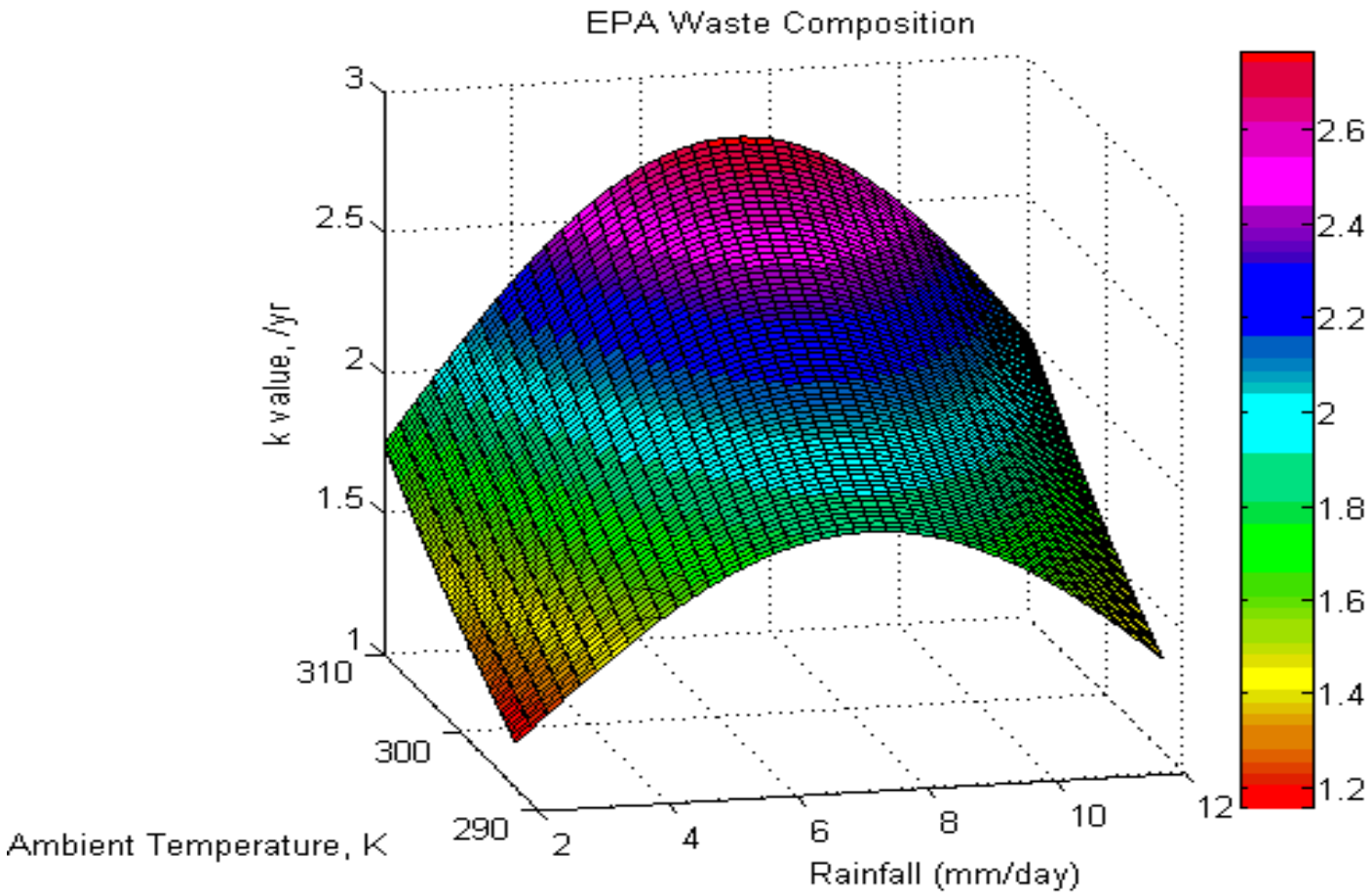

Figure 5.16: 3D Plots Showing Effect of Rainfall and Temperature on *k* Values for Typical Waste Composition Found in the United States (EPA, 2007)

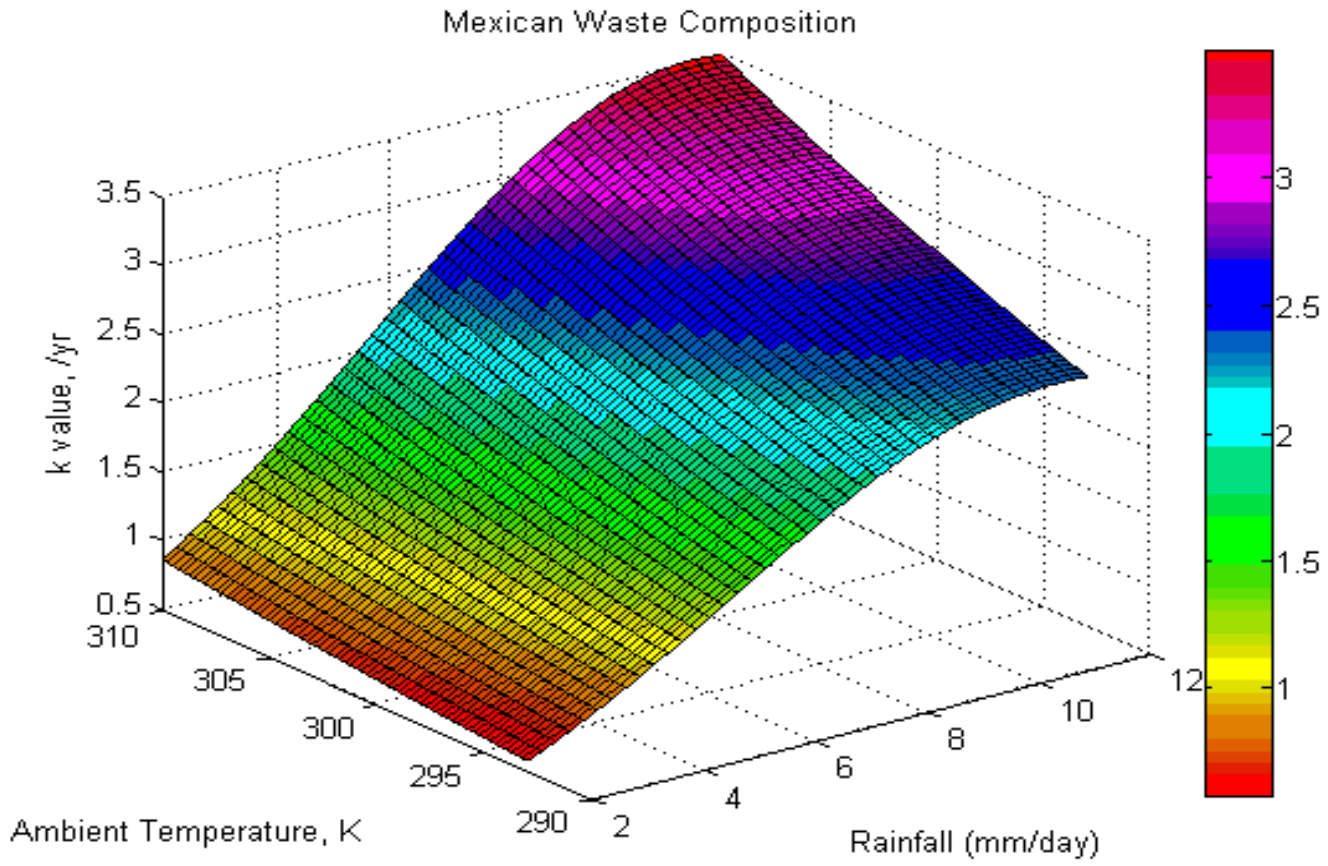

Figure 5.17: 3D Plots Showing Effect of Rainfall and Temperature on *k* Values for Typical Waste Composition Found in Mexico (Hernandez-Berriel, 2008)

Further, 2D plots were generated to study the effect of change in % food and rainfall on the rate of degradation (*k*) (See Figure 5.18). It must be noted that increasing the % food in waste would mean that % textile and % yard were reduced, such that the sum of all waste components would be equal to 100%. This would mean that the effect of change in % food should be plotted on a 4D plot, which is difficult to visualize. Hence, Figure 5.18 was generated by assuming the % textile and % yard components to be 10% each and the rest of the waste was assumed to be comprised of inorganic waste. A change in rainfall and % food in the waste seems to affect the *k* values significantly.

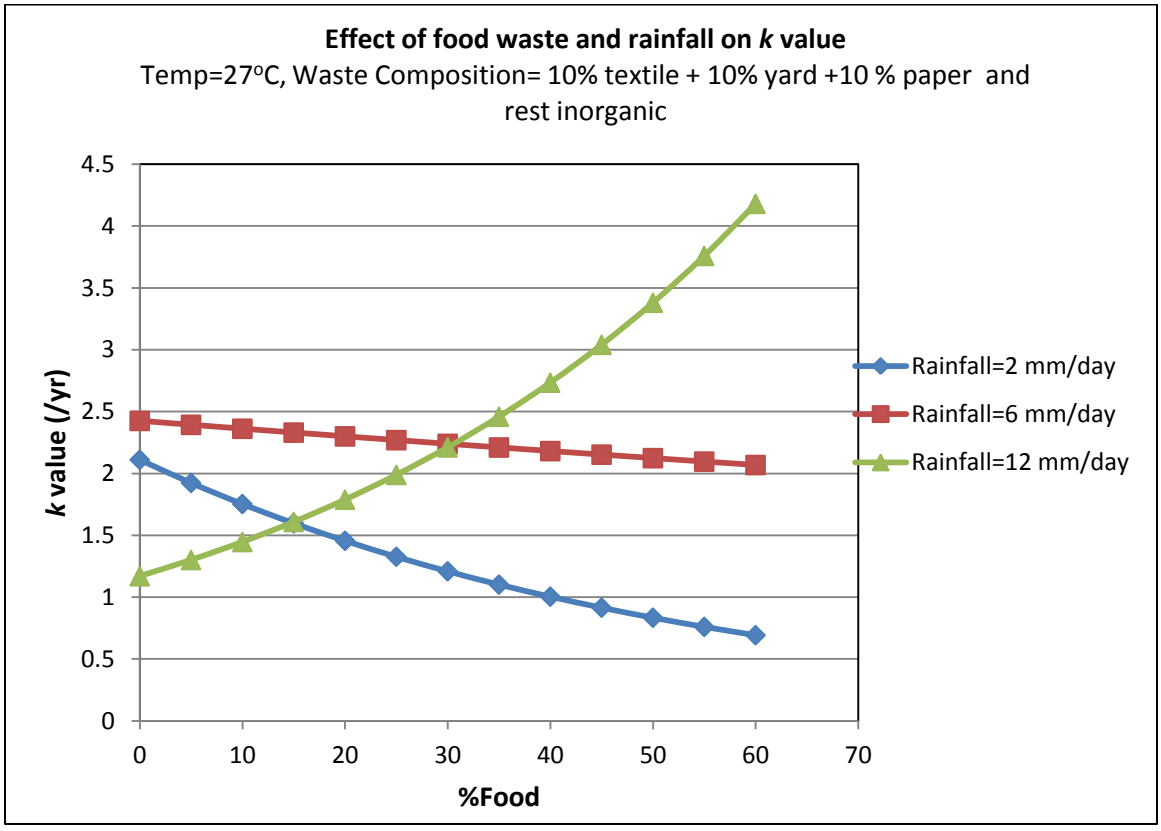

Figure 5.18: Effect of Change in % Food Waste and Rainfall on *k* value

5.2.10 Limiting Conditions for the Comprehensive Regression Equation

The MLR equation can be used for predicting methane generation rate from landfills receiving rainfall between 2 and 12 mm/day and annual ambient temperature from 20^{o}C to 37^{o}C. According to the design of experiments the equation would have been applicable for food, paper, textile and yard waste from 0-100%. However, as mentioned earlier some reactors with 60% and higher percentage of food waste and textile waste were not able to converge using non-linear regression. Hence, this data was not used for developing the comprehensive MLR equation. Thus, the applicability of the comprehensive MLR equation for predicting methane generation from waste is limited to 0-60% of food waste, and 0-60% of textile waste. The MLR equation can be used for waste with paper and yard waste between 0-100%. Further research is necessary to study the performance of the MLR equation for predicting methane generation beyond the limiting conditions.

5.3 CLEEN Model Development

5.3.1 Assumptions for CLEEN Model

The Capturing Landfill Emissions for Energy Needs (CLEEN) model is an Excel-based model using a simple first-order decay equation for predicting methane generation rates from landfills. The assumptions involved in the CLEEN model are briefly discussed in this section. The following information is required as inputs to the CLEEN model:

1. Starting year of waste acceptance
2. Yearly Waste tonnage
3. Waste Composition
4. Average Annual Ambient Temperature
5. Average Annual Rainfall

5.3.1.1 First-Order Decay Equation

The first-order decay equation recommended by LandGEM (2005) for estimating methane generation from landfills is shown below:

$$Q_{CH_4} = \sum_{i=0}^{n} \sum_{j=0}^{10} k \frac{M_i}{10} L_0 e^{-kt_{ij}}$$

where

Q = Methane recovered from landfills (m^3/yr),

M= Mass of waste deposited in the year "i" within the landfill (Mg),

k= First-order decay constant (yr^{-1}),

L_0 = Ultimate methane generation potential (m^3/Mg),

t_{ij} = Age of the j^{th} section of waste mass M_i, accepted in the i^{th} year (decimal years)

The modification of using 1/10th of the mass for finding the methane generation was incorporated into LandGEM in 2005. This modification helped in dividing the integral division into several small parts, helping to lower the methane estimates by 1-25% (LandGEM, 2005).

CLEEN model proposed using the 1/12th of the mass instead of 1/10th as shown in the equation above. This will enable user to input monthly waste accepted if available. In addition, dividing the integral division can further improve the estimation efficiency. Hence the first order decay equation used in the CLEEN models is as follows

$$Q_{CH_4} = \sum_{i=0}^{n} \sum_{j=0}^{12} k \frac{M_i}{12} L_0 e^{-kt_{ij}}$$

where

Q = Methane recovered from landfills (m^3/yr),

M= Mass of waste deposited in the year "i" within the landfill (Mg),

k= First-order decay constant (yr^{-1}),

L_0 = Ultimate methane generation potential (m^3/Mg),

t_{ij} = Age of the j^{th} section of waste mass M_i, accepted in the i^{th} year

5.3.1.2 Methane Recovery and Oxidation

Typically in a landfill, it is assumed that out of the total amount of methane generated in the landfill, only a certain portion is recovered via the methane recovery system. The remaining methane migrates to the surface and may be emitted from the surface of the landfill. However, some portion of the methane is oxidized due to presence of methane-oxidizing bacteria in the cover soil. The CLEEN model being a generation based model, it was necessary to account for the losses due to recovery and oxidation. LandGEM (2005) does not account for the losses occurring due to the recovery and oxidation. IPCC (2006) uses 10% oxidation losses for managed landfills with oxidizing cover material. However, IPCC (2006) is a model estimating methane emissions from the landfill surface; hence, the amount of methane recovered needs to be input into the model.

In this study, an attempt was made to account for the recovery and oxidation losses, using the equation suggested by IPCC (2006).

Methane Generated = Methane Recovered + Methane Emitted + Methane Oxidized (5-12)

Methane Emissions = (Methane Generated – Methane Recovered)* (1 - % oxidized) (5-13)

In the CLEEN model, the amount of methane generated from the landfill can be calculated using a first-order decay equation. Further, methane recovered and methane surface emissions can be computed by providing % recovered and % oxidized in the model. However, it must be noted that the factors % methane recovered and % methane oxidized are sources of uncertainty in the model.

In case % recovered and % oxidized is not available, IPCC's default value of 10% oxidation has been adopted in the CLEEN model (IPCC, 2006). However, recent studies have however found that % methane oxidized ranges between 11 to 89 % with a mean value of 36 $\pm$ 6% (Chanton, 2009). The amount of methane oxidized is a function of type of cover soil, temperature of cover soil, moisture content of the cover soil, and amount of methane generated. CLEEN model allows the user to input site specific oxidation rates if available.

Percent methane recovered from a landfill, or methane recovery (% *R*), depends on several factors such as landfill cover (final, intermediate, daily), gas fluxes, permeability of covers and the operating vacuum pressures used while recovering gas from landfills. Researchers have reported % recovery (%*R*) to be in the range of 10-90% (IPCC, 2006). USEPA's AP-42 draft section 2.4 for Municipal Solid Waste suggested a modification to LandGEM by incorporating a default value for % recovery as 75%. This section is currently under review (as of May 2012). Using this guideline, 75% recovery was used as a recommended value in the CLEEN model (USEPA, 2006), however, users are allowed to input site specific % recovery if available.

5.3.1.3 Lag Period

Typically lag time is the time required for the methane to be generated from the solid waste after being deposited in the landfill. Barlaz (2004) reported the typical lag time in a landfill to be about 1 year. However, the lag time also depends on waste composition and climatic conditions of the landfill. IPCC (2006) suggested using 0-6 months as lag time as a good engineering practice. LandGEM (2005) does not specify the typical lag time considered in the model. However, LandGEM assumes that the waste deposited in a particular year starts producing methane in the following year, irrespective of the month in which the waste was deposited. Thus, the waste deposited from January 2010 to December 2010 is assumed to start

producing gas in January 2011. Hence it can be concluded that LandGEM assumes an average lag time of 6 months.

The structure of CLEEN model is similar to that of LandGEM; hence the average lag time was assumed to be 6 months. However, additional research is needed to identify the effect of waste composition and climatic conditions on the lag time, which will give an accurate estimate of the time required for methane to be generated from a landfill.

5.3.1.4 Ultimate Methane Potential (L_0)

The Biochemical Methane Potential (BMP) values were used for finding the ultimate methane potential in the CLEEN model. Chapter 2 gives a detailed literature review of the L_0 used in LandGEM and IPCC's models. In this study, it was found that the BMP values were larger than the cumulative methane produced in the lab scale reactors. This was primarily because the conditions in the BMP test were close to ideal conditions for degradation. Further, the cumulative methane generated from the reactors was influenced by the rainfall and waste composition. Theoretically, given enough time, the microbes should convert the organic matter in the waste to methane, if it is convertible, even if conditions are not ideal. Hence the BMP values were considered as reasonable estimates of L_0 in the CLEEN model.

The ultimate methane potential in the CLEEN model can be computed using an average of the BMP values weighted according to the waste composition. Thus, the L_0 value can be adjusted if the waste composition changes due to changes in the waste management practices such as recycling and composting. Table 5.24 shows the BMP values incorporated into the CLEEN model based on the observations in this study.

Table 5.24: BMP, Volatile Solids and Moisture Content values for Waste Components Found in this Research

Type of Waste	BMP	VS	BMP	Moisture Content	BMP
	m^3/Mg of Volatile Solids (VS) in waste	g of VS/100 g of dry solids	m^3/Mg of dry solids in waste	kg of water/ 100 kg of wet waste	m^3/Mg of wet waste
Food	389.8	90.16	351.4	82.87	60.19
Paper	336.2	89.34	300.3	8.456	274.9
Textile	184.5	98.31	181.3	4.367	173.4
Yard	188.6	85.02	160.3	56.91	69.08
Non- Biodegradables	0	0	0		0

Alternatively, the users can calculate L_0 values based on the BMP and moisture contents reported in the literature. The typical values of BMP and moisture content reported in the literature are summarized in Table 5.25.

Table 5.25: BMP and Moisture Content values for Waste Components Reported in Literature

Type of Waste	Biochemical Methane Potential (BMP)		Moisture Content*
	m^3/kg of VS in waste	Source	%
Food	292-540	Gunaseelan (2004), Cho et al. (1995), Eleazer et al. (1997), Jeon et. al (2007), Chynoweth et al (1993	50-80
Paper	75-370	Owens and Chynoweth (1993), Eleazer et al. (1997) Jeon et. al (2007)	4-8
Textile	35-210 m^3/kg of dry waste	Jeon et. al (2007), Isci and Demirer (2007)	6-15
Yard	14 – 283	Owens and Chynoweth (1993), Eleazer et al. (1997), Chynoweth et al (1993), Jeon et. al (2007)	30-80
Plastics			1-4

NOTE: * The moisture content values were adopted from Tchobanoglous et al. (1993)

5.3.1.5 *k* value

In the CLEEN model, *k* values were computed using the comprehensive regression equation Eq. 5-9.

$$\widehat{log_{10}}k = -3.02658 - 0.0067282R^2 + 0.069313R + 0.00172807(R \times F) + 0.01046T - 0.01152F + 0.00418\,TX + 0.00598Y$$

Where

R = Annual Rainfall (mm/day),

T = Annual ambient temperature (^{o}K),

F = % Food in landfilled waste,

TX = % Textile in landfilled waste,

Y = % Yard in landfilled waste

The CLEEN model was setup in such a way that *k* values could be computed for each year depending on the waste composition and climatic conditions. However, as mentioned above, the *k* values computed using the MLR equation were found to be higher than those typically found in the landfills. Hence a scale up factor '*f*' was computed to adjust the *k* values for the actual landfill conditions.

5.3.2 Computing Scale-up Factor (f)

The scale-up factor can be defined as the ratio of the actual *k* value found in the landfill to the *k* value computed using the comprehensive regression equation.

$$\text{Scale} - \text{up Factor}\ (f) = \frac{k_{field}}{k_{calculated}} \quad (5\text{-}14)$$

Where,

K_{field} = *k* value estimated using curve fitting for actual scale landfill data (yr^{-1}),

$k_{calculated}$ = *k* value calculated using the comprehensive MLR equation (yr^{-1}).

As an example, methane recovery data from the City of Denton's landfill was used for computing a scale up factor for the *k* values. The City of Denton's landfill started accepting waste in 1984. The landfill was divided into three cells. Cell 0, the oldest cell in the landfill, was accepting waste from 1984 to 1998; thereafter, the waste was diverted to Cell 1, which accepted waste until 2009. Currently, all the waste is being diverted to Cell 3. Final cover has not been installed on any of the three cells. The gas recovery system was installed at the landfill in 2008, and the gas flow rate is being measured at the outlet header. This gas flow rate combined with the gas composition data from the landfill, were used for estimating the k_{actual} value.

As mentioned earlier, the input parameters required for the CLEEN model were waste tonnage, waste composition, annual ambient temperature and annual average rainfall. The detailed description of these parameters is included in the following sections.

5.3.2.1 Waste Tonnage

The amount of waste accepted (or waste tonnage) in the City of Denton's landfill from 1984 to 2010 is shown in Table 5.26.

5.3.2.2 Waste Composition

The composition of fresh municipal solid waste was studied at the University of Texas at Arlington in 2009-2010. The waste composition was determined by collecting waste samples on site, and hand sorting each MSW component into the following categories: paper, plastic, food waste, leather and textile, wood & yard waste, metals, glass, Styrofoam and sponge, construction and demolition (C&D) waste and others (soils and fines) (Taufiq, 2010). The waste composition changes monthly and with seasons; hence a yearly average was used in the CLEEN model (See Figure 5.19). Further, the waste composition was not available from 1984 to 2009. Hence, the waste composition was assumed to be the same as that found in 2009.

Table 5.26: Waste Accepted in the City of Denton's Landfill

Year	Waste Accepted	Year	Waste Accepted
	Metric Tons		Metric Tons
1984	79792	1998	92019
1985	87053	1999	101241
1986	95584	2000	102536
1987	140641	2001	100080
1988	105139	2002	97295
1989	77999	2003	96635
1990	50860	2004	109436
1991	58764	2005	112933
1992	68717	2006	103049
1993	75061	2007	115933
1994	103370	2008	119084
1995	91083	2009	160596
1996	78797	2010	160580
1997	103406		

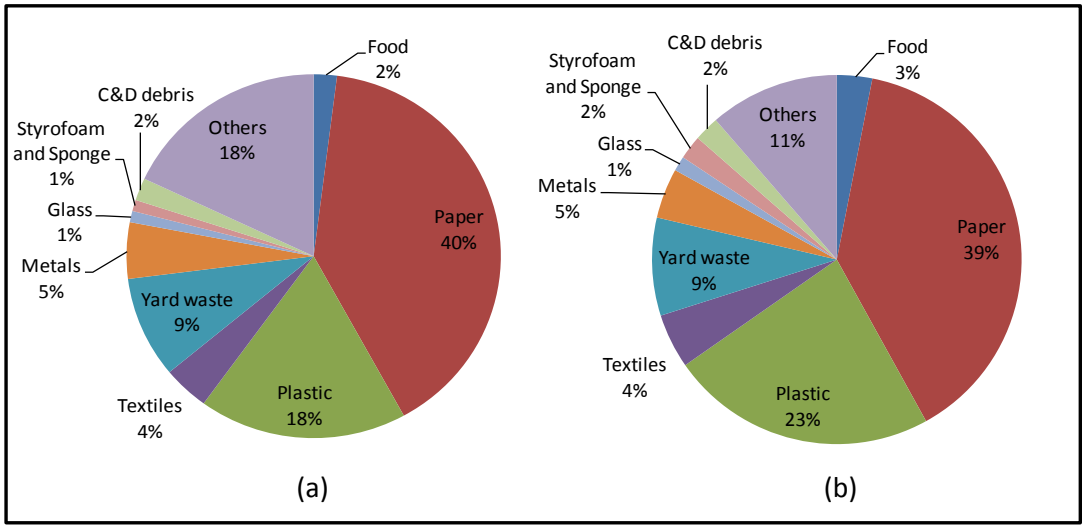

Figure 5.19: City of Denton Landfill Fresh Municipal Solid Waste Composition found in (a)2009 (b) 2010 (Source: Taufiq, 2010)

5.3.2.3 Annual Ambient Temperature

The average annual ambient temperature for the year 2010 was reported as 63.9^{o}F (17.72^{o}C) at the nearest weather station from Denton, TX (www.usclimatedata.org). This value was used for computing the *k* values in the CLEEN model, although the comprehensive regression equation only allowed interpolation of ambient temperatures between 20^{o}C to 37^{o}C.

5.3.2.4 Average Annual Rainfall.

The annual average rainfall recorded at the nearest weather station from the Denton, TX was found to be 34.34 inches (2.366 mm/day) (www.noaa.gov). According to NOAA, the average rainfall was computed based on the rainfall recorded from 1954 to 2010. Hence this value was used for computing the *k* value in the CLEEN model. However, since 2009, the City of Denton's landfill was operated as a bioreactor landfill, by reintroducing leachate/ stormwater in the waste. The water addition was done only in Cell 2 and Cell 3. Hence, it was necessary to apply a correction to the rainfall data, by adding the amount of leachate/ stormwater reintroduced into the landfill. Based on the recirculation data and the dimensions of the cells, it was found that 0.04 and 0.11 mm/day additional rainfall infiltrated into the waste due to the leachate recirculation in 2009 and 2010, respectively.

5.3.2.5 Ultimate Methane Potential

The ultimate methane potential was computed using a weighted average of the waste composition. Table 5.27 shows the sample calculations for computing the ultimate methane potential value.

Table 5.27: Ultimate Methane Potential Calculation for the City of Denton Landfill

Type of Waste	BMP	% in Denton Waste	Weighted Avg for BMP
	m^3/Mg of wet waste	on wet weight basis	m^3/Mg of wet waste
Food	60.19	2	1.204
Paper	274.9	40	109.9
Textile	173.4	4	6.936
Yard	69.08	9	6.218
Others	0	45	0
SUM			**124.330**

5.3.2.6 Estimating $k_{calculated}$

The k value was computed in the CLEEN model using the comprehensive MLR equation (Eq. 5-9).

$$\widehat{log_{10}k} = -3.02658 - 0.0067282R^2 + 0.069313R + 0.00172807(R \times F) + 0.01046T - 0.01152F + 0.00418\,TX + 0.00598Y$$

Where,

R = Annual Rainfall (mm/day) =34.34 mm/day

T = Annual ambient temperature (K) = 290.7 K

F = % Food in landfilled waste = 2 %

TX = % Textile in landfilled waste = 4 %

Y = % Yard in landfilled waste = 9 %

Using the above relationship, the $k_{calculated}$ was found to be 1.5835 yr^{-1}.

5.3.2.7 Estimating k_{field}

The monthly gas flow rate was obtained from the gas header for a period of three years from 2009 to 2011. The gas composition data was also obtained from the gas wells as well as the header line. It was found that the methane content was between 50-54% in the landfill gas.

The observed average methane flow rate recovered from the landfill was plotted along with the methane recovery curve computed from the CLEEN model. Trial and error was used to determine the *k* value which best-fit the methane recovery curve to the field scale data (See Figure 5.20). This resulted in a scale-up factor of 0.0121, and a k_{field} of 0.019 yr^{-1}.

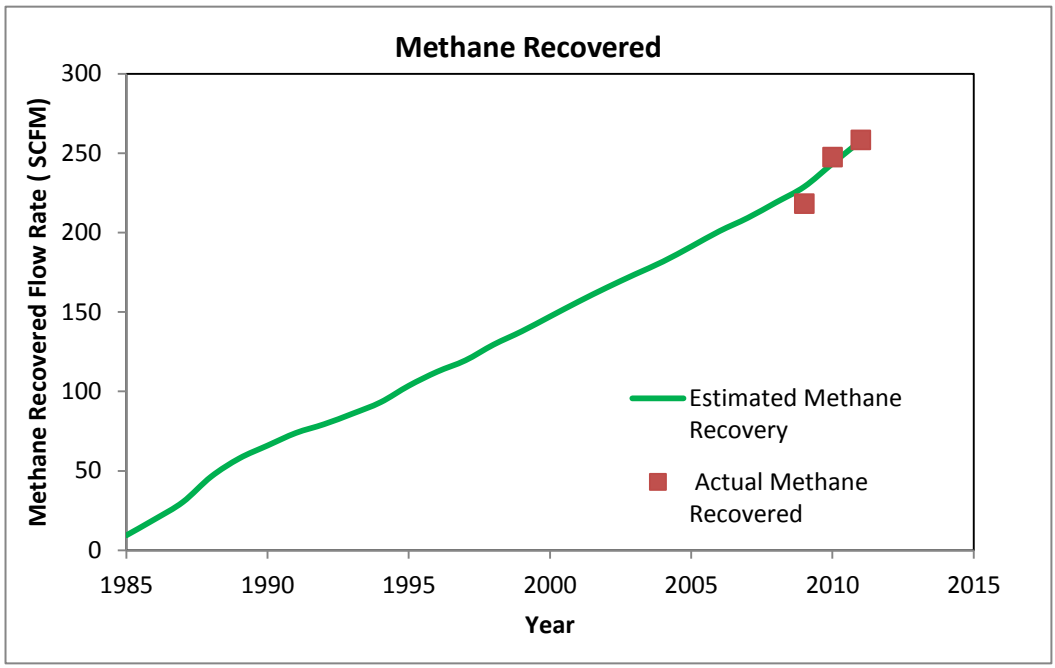

Figure 5.20: Graphical Representation of Methane Recovered from City of Denton Landfill

Cruz and Barlaz (2010) used lab scale bioreactor data to find the scale up factors for 2 conditions, first considering the bulk decay rates, k_{actual} = 0.04 for traditional landfills and k_{actual} = 0.12 for bioreactor landfills. Scale-up factors reported by Cruz and Barlaz (2010) were 0.064 for traditional landfills and 0.0192 for bioreactor landfills. The scale up factor computed in this study falls within the range reported by Cruz and Barlaz (2010). However, further research is necessary to study the impact of conditions such as rainfall and temperature on the scale-up factor found in this study. Methane recovery data from additional landfills should be studied.

5.3.3 Uncertainties in the CLEEN Model

The CLEEN model uses a first-order decay equation for computing the amount of methane generated from landfills. The comprehensive equation for *k* value was developed from lab scale data. Hence, it holds for conditions in the range studied in the lab: temperatures from 20 to 37^{o}C, and rainfall between 2 to 12 mm/day. Using the relationship beyond the temperature or rainfall range mentioned above would lead to extrapolation. Further studies are required for verify whether *k* behaves linearly beyond the range mentioned above.

The applicability of the comprehensive MLR equation for predicting methane generation from waste is limited to 0-60% of food waste, and 0-60% of textile waste. The MLR equation can be used for waste with paper and yard waste between 0-100%. Further research is necessary to study the performance of the MLR equation for predicting methane generation beyond the limiting conditions.

The methane recovered from the gas collection system depends on several factors such as landfill cover, permeability of cover soils, presence of preferential pathways and the operating parameters of landfill gas collection system. These factors affect the estimation of the % recovery in the landfills. Hence the variability in the amount of methane recovered from a landfill induces uncertainty in the estimation efficiency of the CLEEN model. Similarly, the % oxidation value affects the estimates of methane surface emissions from the CLEEN model. The scale-up factor was developed using the methane recovery data from the City of Denton landfill. The estimation of the scale-up factor depends on the % recovery assumed in the model. Further, the scale up factor may vary from landfill to landfill. Factors such as rainfall and temperature may also affect the scale-up factor, thus introducing an interaction between the scale-up factor and the predictor variables. A comprehensive study with landfill scale emission data from

landfills located worldwide with diverse climatic conditions must be conducted to study these interaction effects. Further, additional modifications can be done in the CLEEN model to incorporate monthly waste acceptance and monthly rainfall- temperature via computer software programming which can analyze such complex computation.

The estimation efficiency is also a function of the lag time considered in the model. It was observed in the lab scale reactor study that the lag-time was longest at the lowest temperature. Such effects must be quantified to improve the estimation efficiency. Further, the exact waste composition data for landfills is often not available. In addition, the sampling methodology for finding waste composition varies significantly. Hence a uniform sampling methodology needs to be implemented for overcoming the uncertainty in the model performance. Some of these uncertainties listed above such as lag time and waste composition data affect all other models. Hence additional research in this field can improve the overall estimations of methane emissions from landfills, irrespective of the models used.

CHAPTER 6

CONCLUSIONS AND RECOMMENDATIONS

Accurately estimating methane generation from landfills has always been a challenge for the solid waste industry. Current models use a first-order decay equation for estimating methane generated from landfills. The major limitation of the current models is their inability to adapt to the varying waste compositions and climatic conditions found worldwide. The main objective of this research was to study the effect of waste composition and climatic factors such as rainfall and ambient temperature on the overall rate of waste degradation.

The main thrust of this research was to develop a methodology through which the factors rainfall, ambient temperature and waste composition could be varied simultaneously in a laboratory-scale setup. An incomplete block design was used with rainfall and temperature as main predictor variables and waste composition as a blocking variable for the laboratory scale setup. The results from the laboratory scale setup were used for developing a comprehensive regression equation for estimating the rate of waste degradation. Further, an attempt was made to develop an improved model for predicting methane generation from landfills based on basic information about the waste composition, rainfall and ambient temperature.

6.1 Summary and Conclusions

The following results and conclusions are based on the findings from this study:

1. Reactors with yard waste (grass and leaves) showed classic first-order decay curves, with the shortest lag period and faster rate of degradation than the other types of waste. Further,

methane generation curves from yard waste reactors showed a relatively higher peak and asymptotic decrease, following a classic first-order decay curve. Currently, most countries prefer composting for yard waste rather than landfilling. Based on the short lag periods observed for reactors with higher amounts of yard waste (60% and above), it is likely that yard waste may start producing methane before the landfill gas collection system is installed. Hence diverting yard waste from landfills can help reduce the methane emissions from landfill surfaces.

2. The reactors with high amounts of food waste (60% and above) had longer lag periods compared to all other types of waste. In addition, methane generation curves from food waste reactors showed multiple peaks and did not follow a typical first-order degradation curve. The longer lag periods could be due to the accumulation of carboxylic acids in the acidogenesis phase, and the presence of multiple peaks could be due to different types of food waste degrading at different rates. The total amount of methane generated from food waste reactors depended on the rainfall, because the amount of carbon washed out increased with the rainfall.
3. Paper waste reactors degraded at a moderate rate. Typically, methane generation from paper reactors followed a first-order decay curve; however, the total amount of methane generated from 100% paper reactors was low, compared to other reactors. This could be due to the nutrient deficiency in paper reactors.
4. Reactors with higher amounts of textile wastes (60% and above) degraded at very slow rates, often displaying multiple and relatively low peaks in the methane generation curves. The presence of multiple peaks could be due to different types of textile wastes degrading

at different rates. Overall, textile waste reactors showed the minimum cumulative methane generation compared to other reactors.

5. Overall, reactors with high amounts of textile waste and food waste did not follow a typical first-order decay curve. However, in cases where the waste components were mixed together and in reactors with waste combination I-20% each waste, it was observed that the methane generation curve followed a first-order decay curve. This behavior could be because the waste mixture supplemented nutrients which enhanced the methane generation rates.
6. Overall, it was observed that an increase in temperature increased the rate of degradation. In most cases, the peaks in the methane generation rate curves were higher at higher temperatures.
7. After dismantling the reactors, it was found that the reactors with 100% food waste had maximum settlement (30-33 cm) as compared to 0-16 cm in other reactors. Food waste typically had higher initial moisture content as compared to other waste. Over the period of time of the study, the waste kept losing water until it reached a constant moisture content value. Hence a considerable amount of carbon leached out, thereby increasing the settlement in the reactor.
8. The lag period (time required for the methane generation to begin) was mostly dependent on the waste composition. Since the lag period is the time required for the microorganisms to hydrolyze the substrates, it makes sense that it was affected by the waste composition. For example, yard waste had the shortest lag period, while textile and food waste required a longer lag period.

9. For a particular waste composition, the lag period was found to be longest at the lowest temperature, 20^{o}C. Likewise, the lag period at 30^{o}C was expected to be longer than that at 37^{o}C. However, in some cases the lag period was reduced due to higher rainfall rates (waste composition G and I). However, irrespective of the rainfall, the lag period was found to be longest at 20^{o}C.
10. In all reactors it was found that the Biochemical Methane Potential (BMP) value was higher than then cumulative methane generated from the reactors. It was also observed that the difference between BMP and ultimate methane generated from reactors was larger as the rainfall was increased. This was because the amount of carbon washed out from the reactors increased as the rainfall was increased.
11. The probable moisture content in the reactor was estimated by performing a water balance. After dismantling the reactors, the average observed moisture content was compared with the probable moisture content. The calculated probable moisture content gave an approximate estimate (± 20%) of the moisture content within the reactor. The probable moisture content calculations were based on the initial dry weight of the waste; which decreased with degradation. Hence, it was found that the change in weight of the reactor due to degradation affected the probable moisture content significantly.
12. The volatile solids content of raw waste was compared with that of the degraded waste. It was found that the change in volatile solids content due to degradation was between -0.5 to 19%. Since the waste used in this study was “pure” waste, the loss in volatile solids was relatively small. While the waste was degrading in the reactor, the recalcitrant carbon percentage was increasing. However, the inorganic portion was not actually increasing; hence, the volatile solids did not change significantly in these reactors.

13. Multiple Linear Regression (MLR) analysis was used on the lab scale data to quantify the effect of waste composition, rainfall and ambient temperature on the first-order decay constant (*k*). The best model was selected using the backward elimination method, best subsets method and stepwise regression method, such that all parameter were significant at α =0.1. The best model was found to have an adjusted R^2 of 0.7538, and is given by:

$$\widehat{log_{10}}k = -3.02658 - 0.0067282R^2 + 0.069313R + 0.00172807(R \times F) + 0.01046T - 0.01152F + 0.00418\,TX + 0.00598Y$$

where *k* = rate of degradation in terms of first order decay constant (yr^{-1}), *R* = Average annual rainfall (mm/day), *T*= ambient temperature (K), *TX* = % textile in landfilled waste, *Y*= % yard in landfilled waste, *F* = % food in landfilled waste.

14. It can be observed from the MLR model that increasing the ambient temperature increases the rate of degradation. Likewise, increasing the amount of textile waste and yard waste can also help in increasing the rate of degradation. Textile wastes typically have higher moisture absorption capacity; hence, the presence of high amounts of textile waste can aid faster and uniform distribution of nutrients and microbes due to higher moisture content. The presence of high amount of yard wastes, especially grass and leaves which are easily degradable, help in hydrolysis of waste which aids microbial growth, thereby increasing the overall rate of degradation. It was observed that the rate of degradation was affected by the combined effect of food waste and rainfall since they interact with each other. Paper waste did not affect the rate of degradation. Overall, paper waste degrades at a moderate rate, as compared to other organics considered in this study. A change in the amount of paper waste affected the overall rate of degradation; however, that effect was not significant at 90% confidence level.

15. The MLR equation can be used for predicting methane generation rate from landfills receiving rainfall between 2 and 12 mm/day and annual ambient temperature from 20^{o}C to 37^{o}C. The applicability of the comprehensive MLR equation for predicting methane generation from waste is limited to 0-60% of food waste, 0-60% of textile waste, 0-100% of paper waste and 0-100% of yard waste.
16. The *k* values observed in the lab-scale study were higher than those observed in the landfills. Although this study aimed at recreating landfill like conditions by not adding nutrients and using larger reactors (16L instead of the typical 2L), which allowed for not shredding waste, the higher *k* values could be a result of a controlled environment and greater microbial access compared to the conditions in a landfill. Hence it was necessary to develop scale-up factors to adjust the model to field-scale conditions.
17. The Capturing Landfill Emissions for Energy Needs (CLEEN) model was developed by incorporating the comprehensive regression equation into first-order decay based model for estimating methane generation rates from landfills. In addition, the CLEEN model can be used to predict methane emissions from landfill surface by incorporating methane recovery and methane oxidation rates.
18. A scale-up factor for the CLEEN model was computed to adapt the model for field scale emissions using the City of Denton's landfill emissions data as follows:

$$\text{Scale up Factor } (f) = \frac{k_{actual}}{k_{calculated}}$$

Where, k_{actual} = *k* value estimated using curve fitting for actual scale landfill data (yr^{-1}), $k_{calculated}$ = *k* value calculated using the comprehensive MLR equation (yr^{-1}). Using the field scale data, the scale-up factor for the Denton Landfill was found to be 0.012.

6.2 Recommendations for Future Studies

The following recommendations are suggested for future studies:

1. Further research needs to be done to validate CLEEN's effectiveness in predicting methane generation rates from landfills compared to the current models (LandGEM and IPCC). A dataset with varying climatic conditions and waste compositions should be used for the validation. There should be additional research to identify the interaction (if any) between the scale-up factor (*f*) and the predictors.
2. Running experiments for temperature and rainfall ranges beyond the range used in this study can help towards improving the prediction efficiency of models. In addition, running laboratory scale landfill reactors longer so convergence may be achieved for some waste combinations for which it was not achieved in this work can help in overcoming the limiting conditions of the current model.
3. It was observed in this research that the methane generation curve from reactors with higher amount of food waste does not follow a first-order decay curve. Additional research is necessary to identify the kinetic model that fits the methane curves for waste streams with higher percentages of food waste. This research will particularly benefit countries like China, India, Bangladesh, and Mexico, which have about 50% or more food waste in their waste streams. Alternatively, exploring different rates of degradation for different types of food waste (cooked vs. uncooked, fruits and vegetables vs. meat) can further help future prediction models.
4. The model developed in this research can be used for life cycle analysis of municipal solid waste landfills. It may give a better picture of how long the carbon may stay in the landfills until it is completely degraded or removed.

5. Further research is necessary to understand the impact of actual temperatures within the landfill on waste degradation. Researchers have reported elevated temperatures inside the landfills higher than the ambient temperatures. As of now, it is difficult to predict the actual temperature inside the landfill. Further research is necessary to correlate the actual temperatures within the landfill with ambient temperatures, and the CLEEN model needs to be modified accordingly.
6. Additional research is necessary to identify the effect of cover material on methane emissions, recovery and oxidation.
7. Developing methods to better capture methane released early in the landfill, while waste is just being placed and studying factors affecting the lag duration before methane generation begins is necessary for improving the prediction efficiency of the current models.
8. Current research mainly focused on conventional landfills. The technology of operating landfills as "bioreactors" through leachate recirculation is currently being used more widely. In a bioreactor, landfill nutrients and carbon lost in leachate are reintroduced in the waste which enhances degradation rates. Hence, accounting for enhanced moisture content in a bioreactor landfill by adjusting rainfall rates for calculating *k* values may not be sufficient. Hence, additional research is necessary to identify the effect of operating landfills as bioreactors on the *k* values.
9. Adding rainfall at intervals other than daily may impact the *k* values. Hence further research is required to identify the impact of rainfall intervals on *k*. Further, a study of whether rainfall per waste volume rather than rainfall per landfill area may improve the prediction efficiency of the model.

APPENDIX A

COMPARATIVE ANALYSIS OF METHODS FOR FINDING *k* VALUES

A.1 Comparative Analysis of Methods for Finding k Values

Reactor	Simple Linear Regression				Thomas Method				Non Linear Regression			
	L_o	k	Error	C.D.	L_o	k	Error	C.D.	L_o	k	Error	C.D.
8	85.23	7.34	1217.00	0.98	96.44	6.59	3589.00	0.93	81.68	9.33	238.15	0.995
9	84.09	4.38	2814.90	0.95	296.80	0.74	2078.00	0.96	118.40	2.41	990.45	0.98
17	39.83	3.21	393.90	0.96	42.98	2.47	89.92	0.99	44.92	2.17	55.92	0.99
18	69.43	13.46	4467.28	0.85	98.03	4.41	2425.51	0.92	78.92	7.81	657.30	0.98
27	65.94	4.93	1831.29	0.94	94.69	2.17	282.83	0.99	77.60	2.92	25.81	0.999

APPENDIX B

pH and GAS GENERATION RATES FOR REACTORS

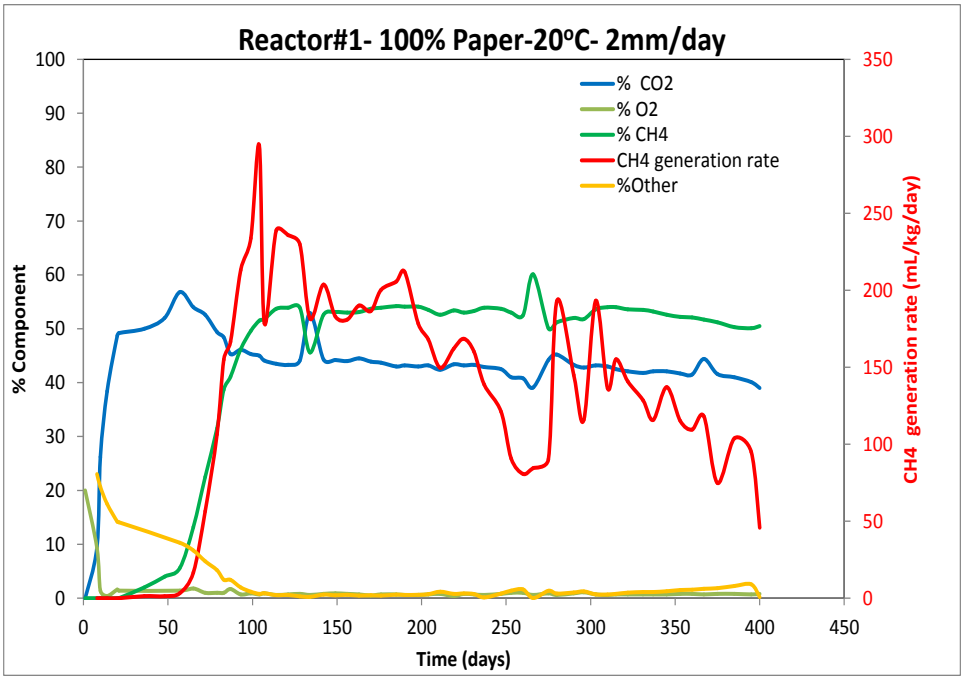

(a)

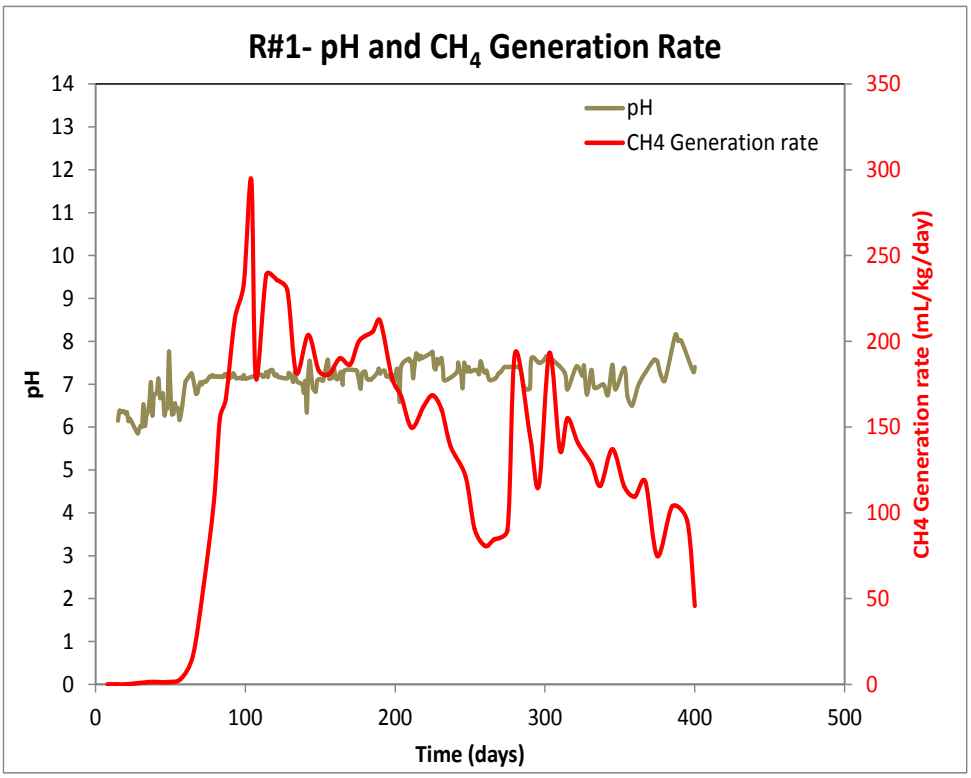

(b)

Figure B1: Gas generation rate and pH at 20°C from Reactor 1

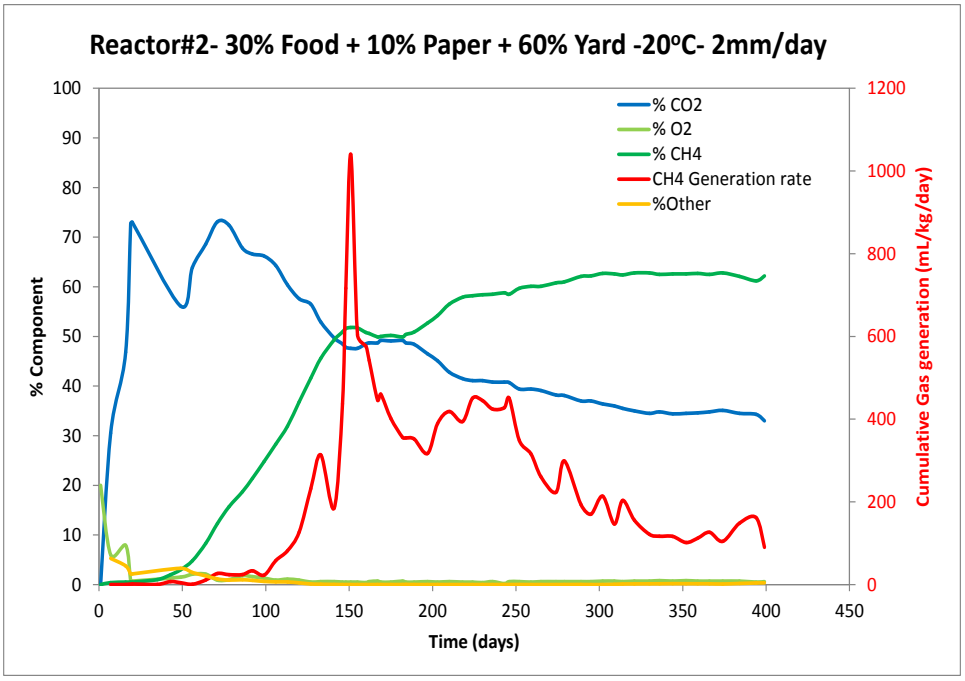

(a)

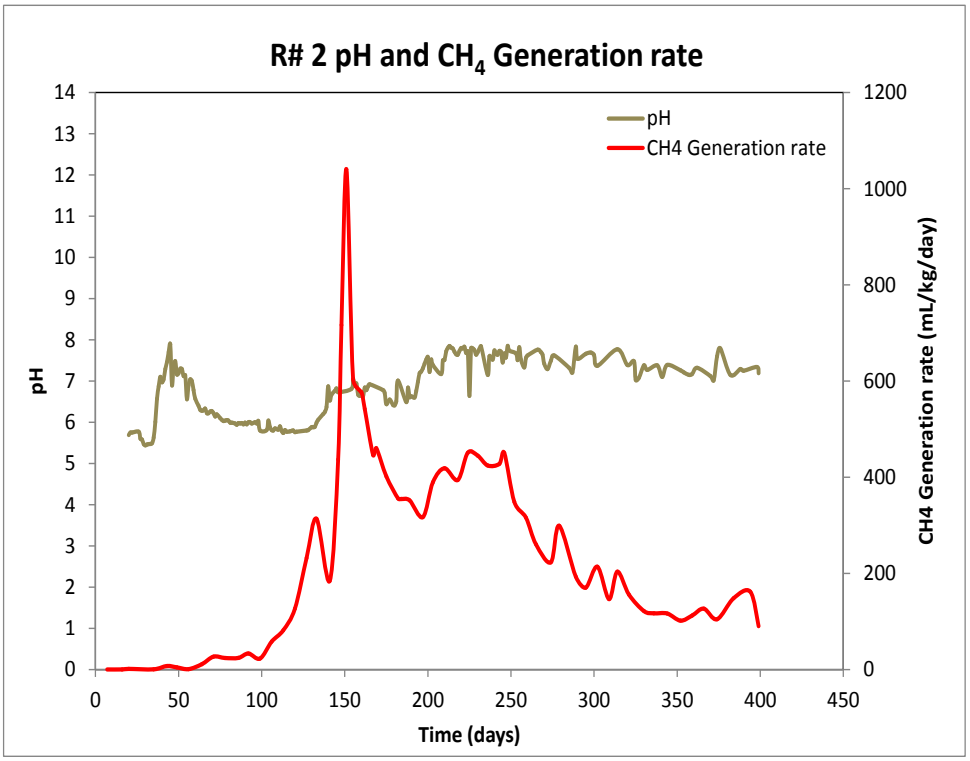

(b)

Figure B2: Gas generation rate and pH at 20°C from Reactor 2

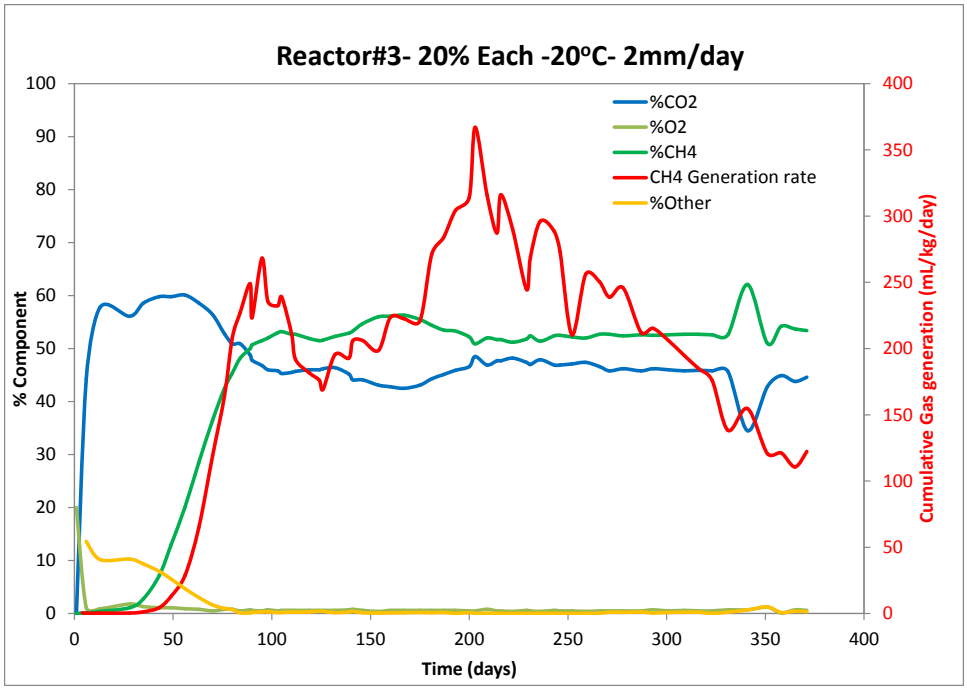

(a)

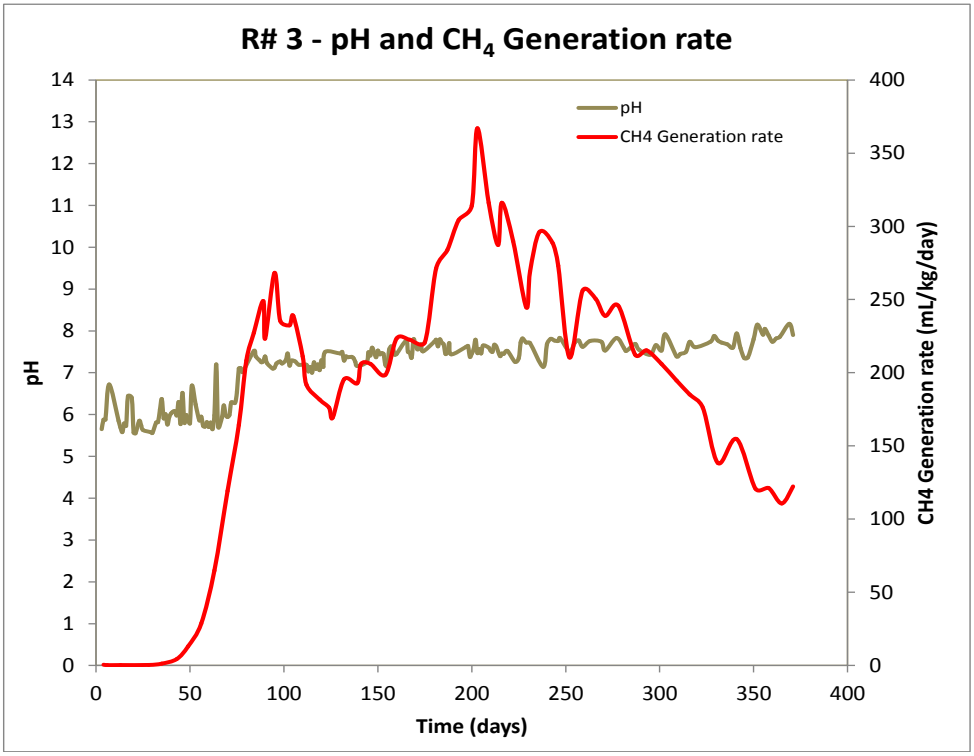

(b)

Figure B3: Gas generation rate and pH at 20°C from Reactor 3

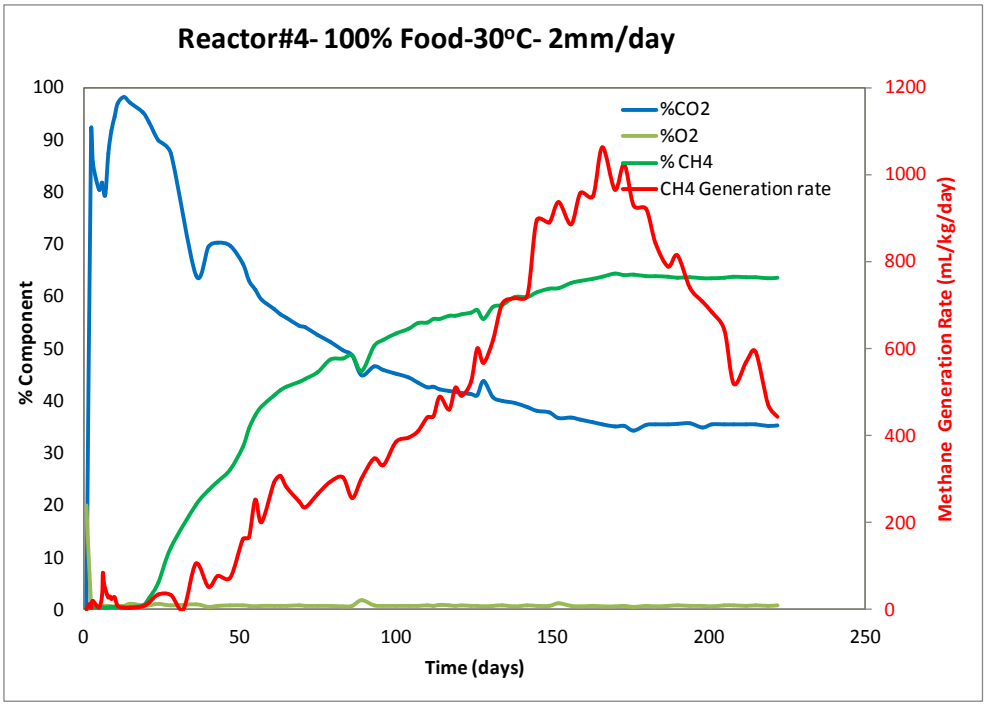

(a)

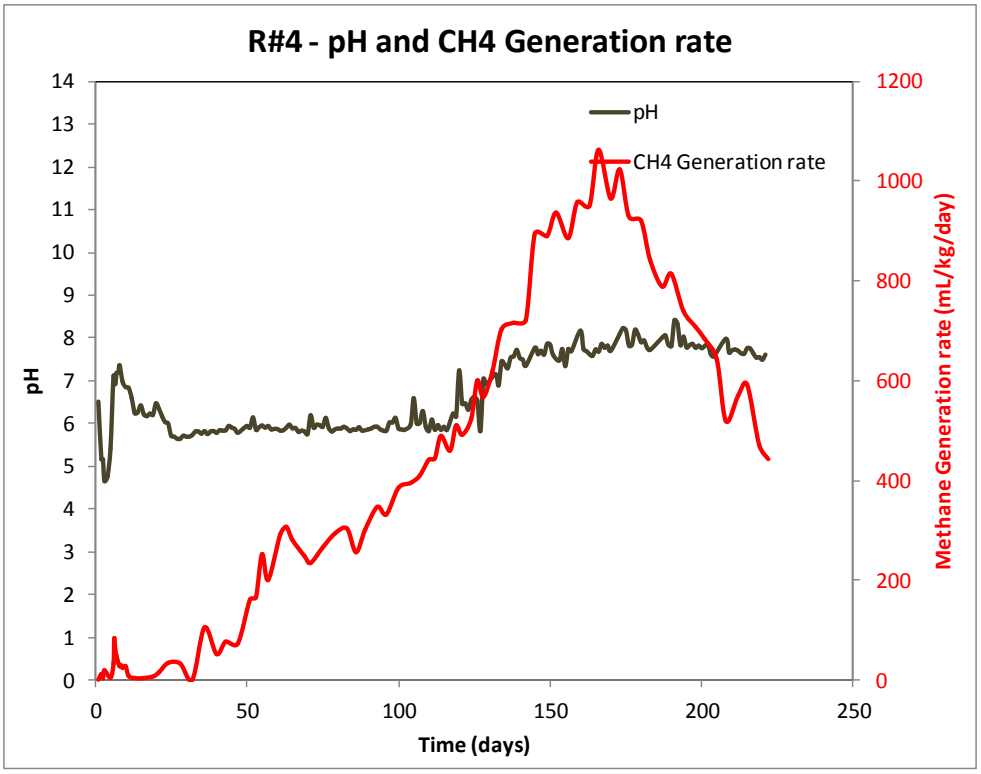

(b)

Figure B4: Gas generation rate and pH at 30°C from Reactor 4

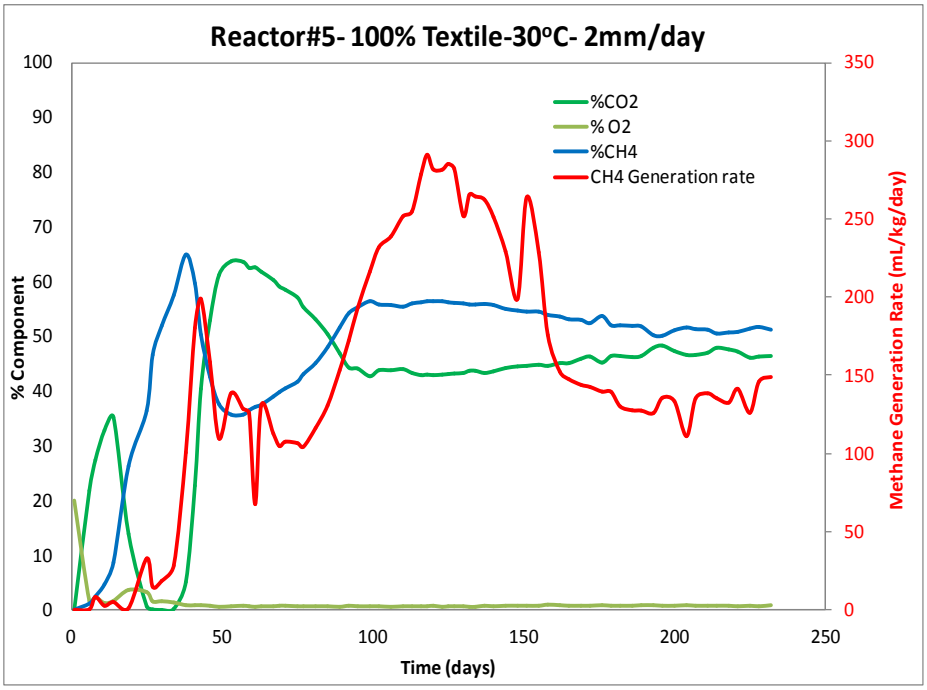

(a)

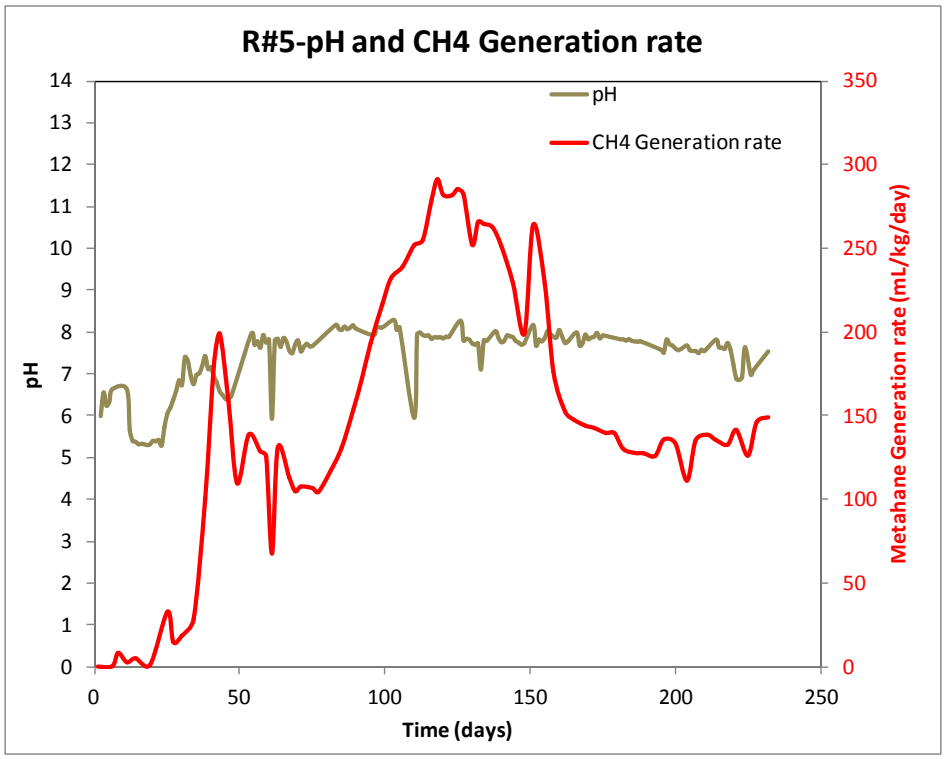

(b)

Figure B5: Gas generation rate and pH at 30°C from Reactor 5

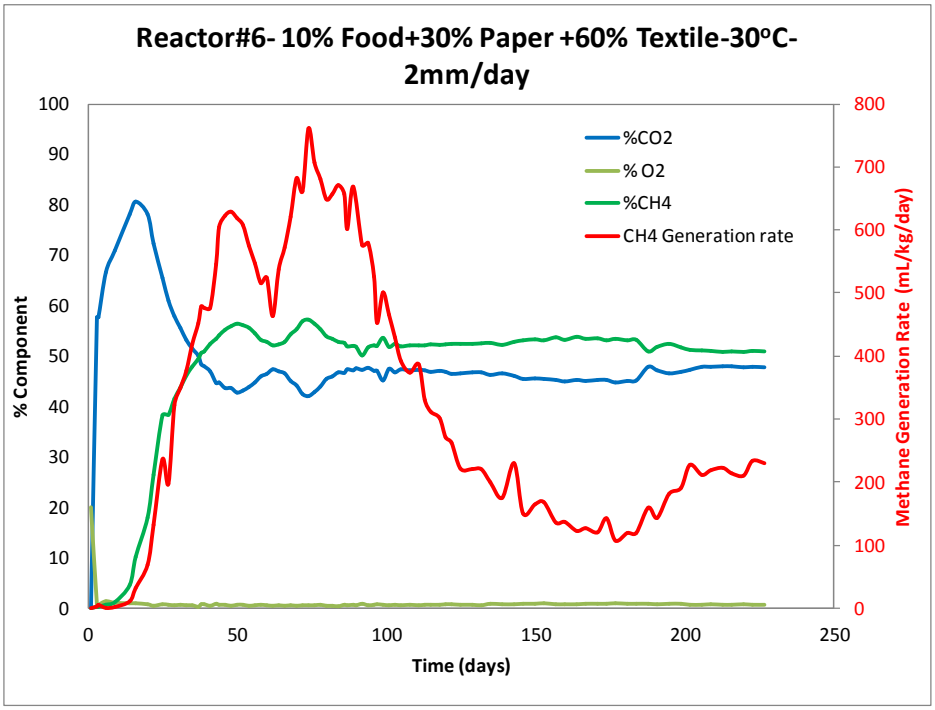

(a)

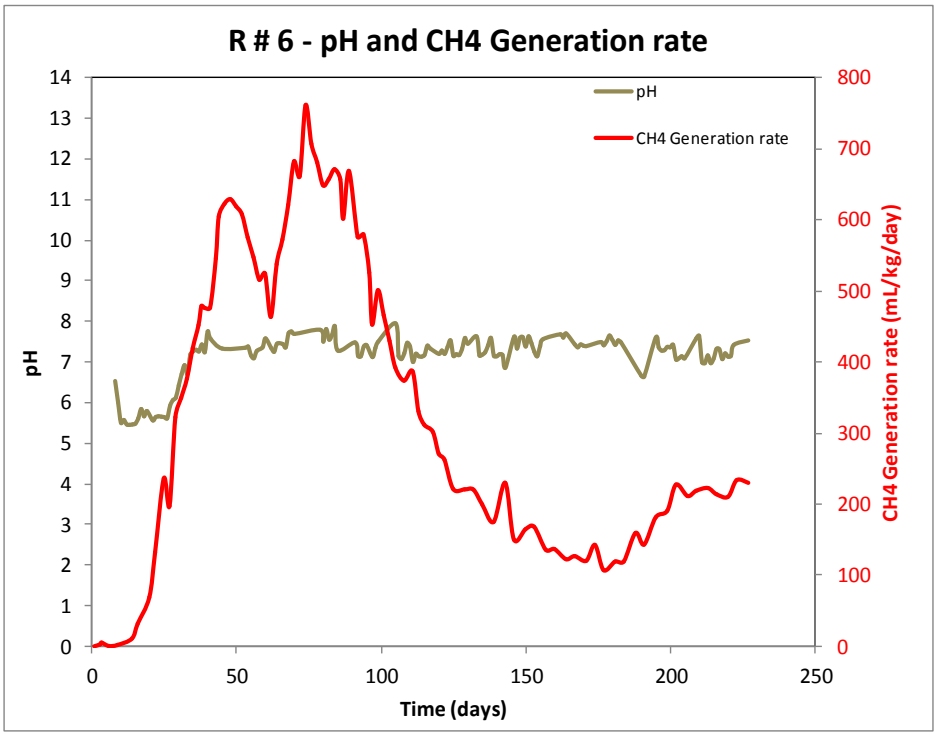

(b)

Figure B6: Gas generation rate and pH at 30°C from Reactor 6

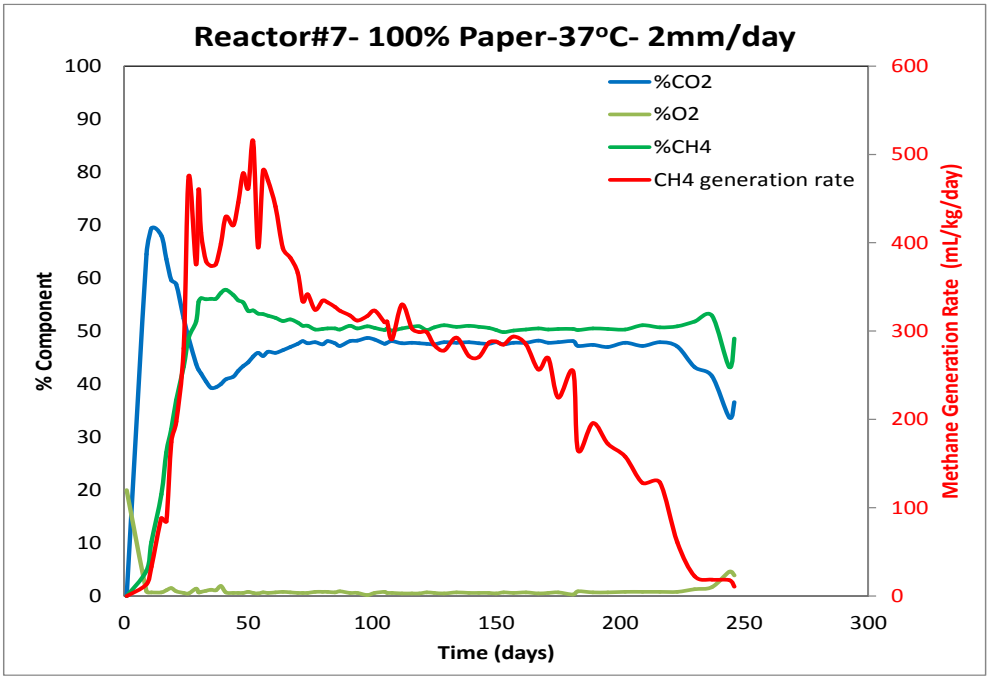

(a)

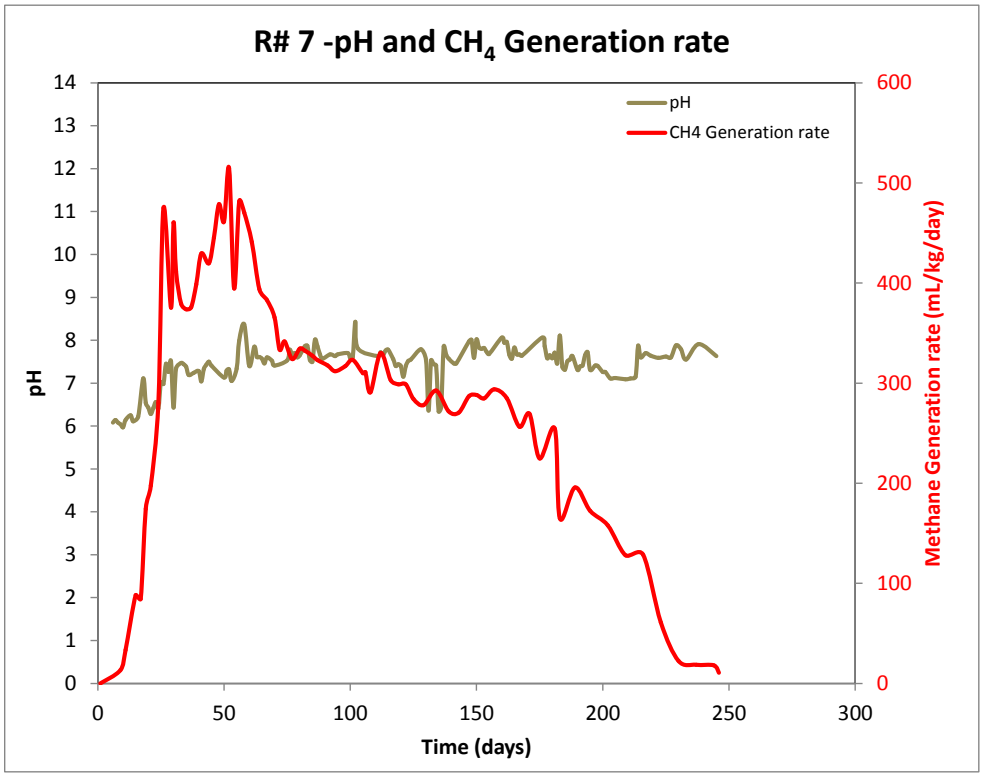

(b)

Figure B7: Gas generation rate and pH at 37°C from Reactor 7

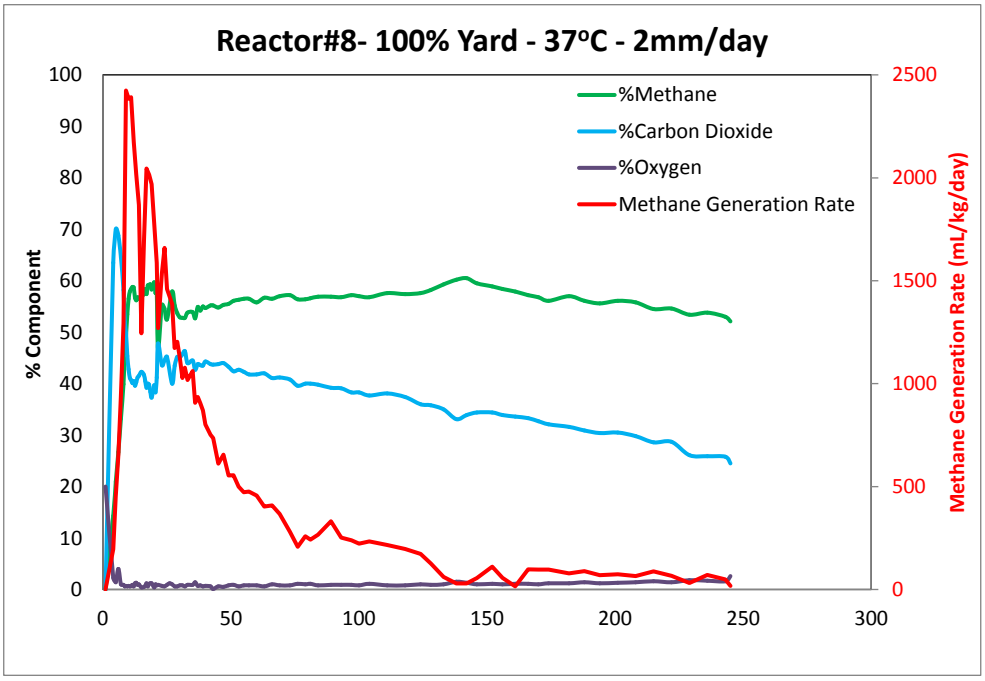

(a)

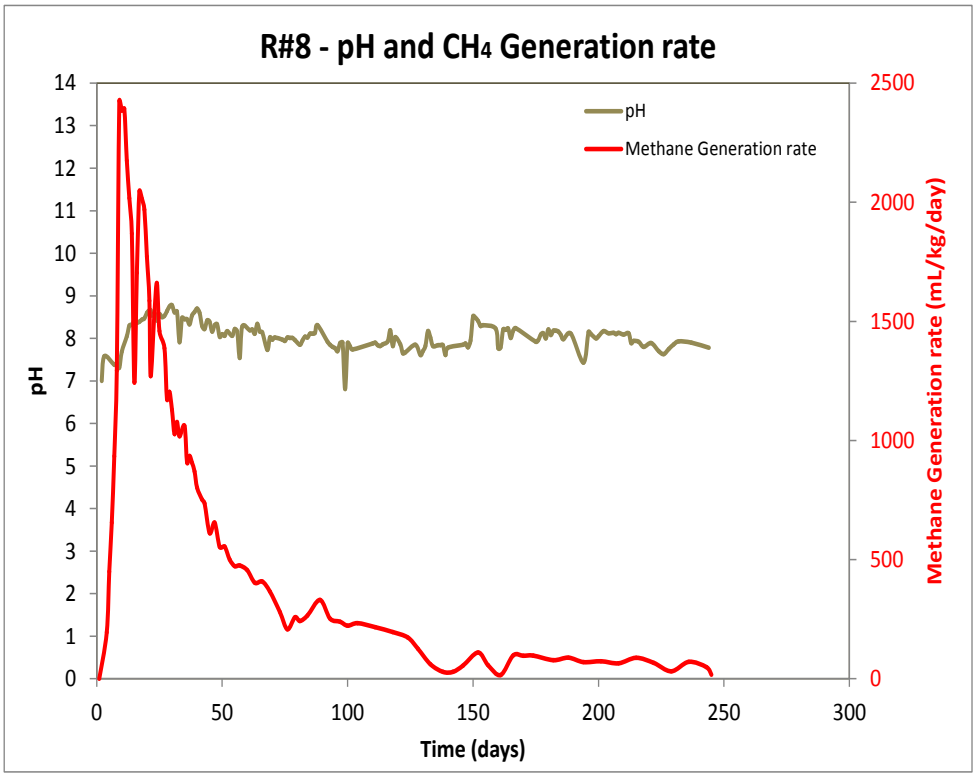

(b)

Figure B8: Gas generation rate and pH at 37°C from Reactor 8

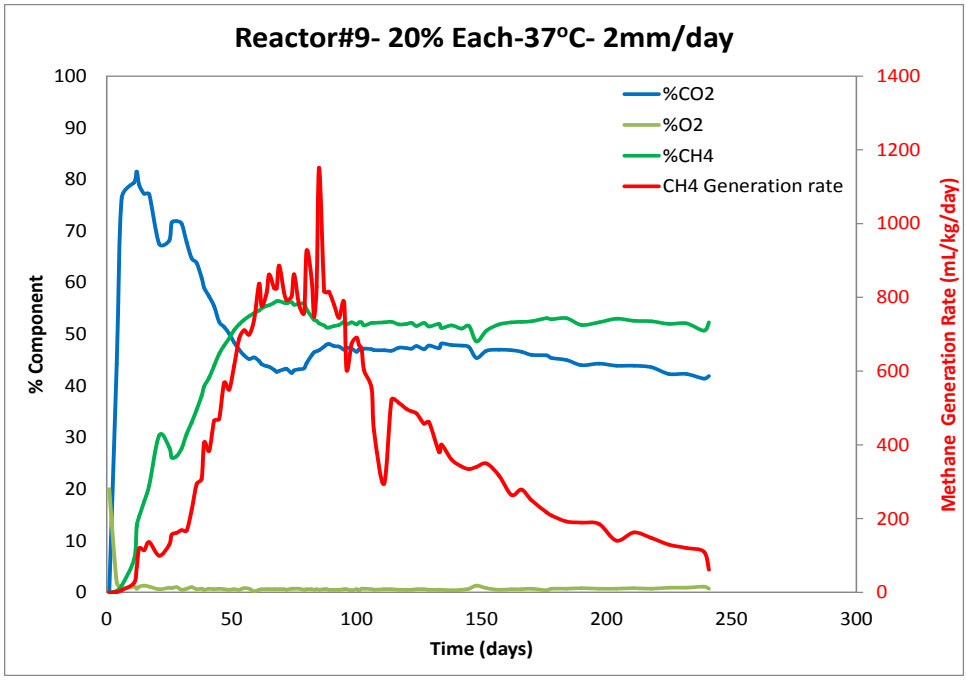

(a)

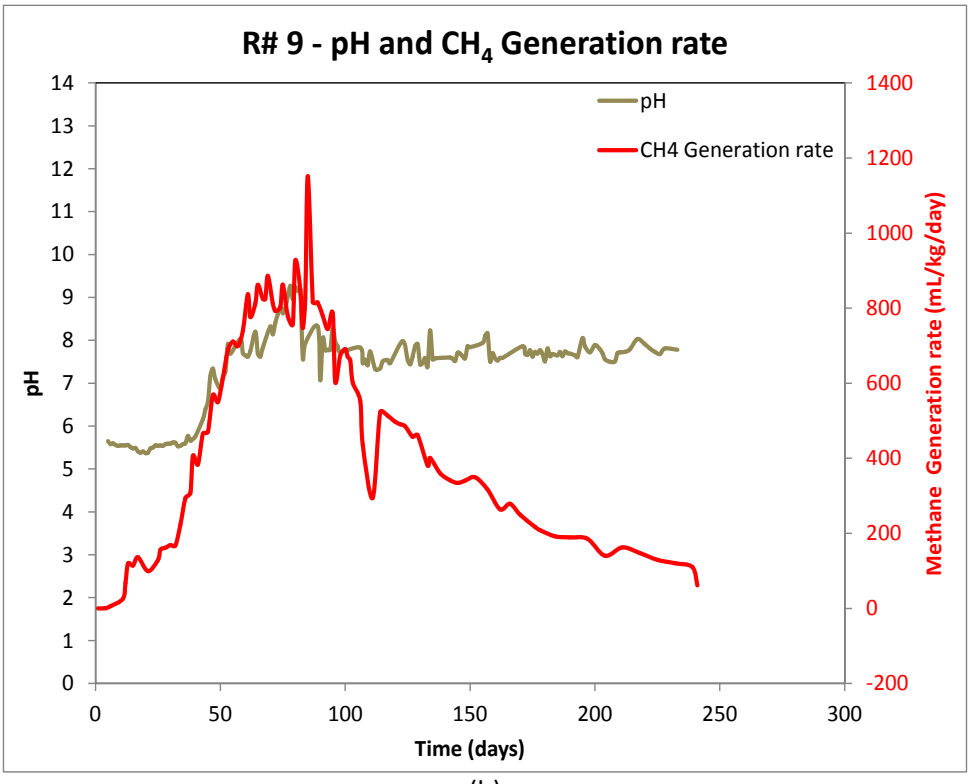

(b)

Figure B9: Gas generation rate and pH at 37°C from Reactor 9

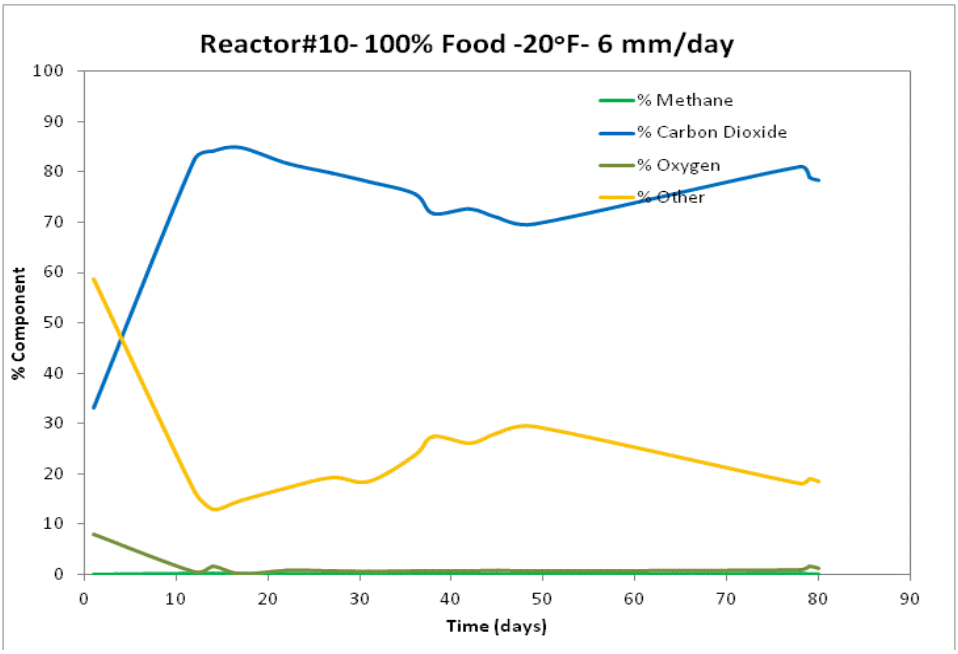

(a)

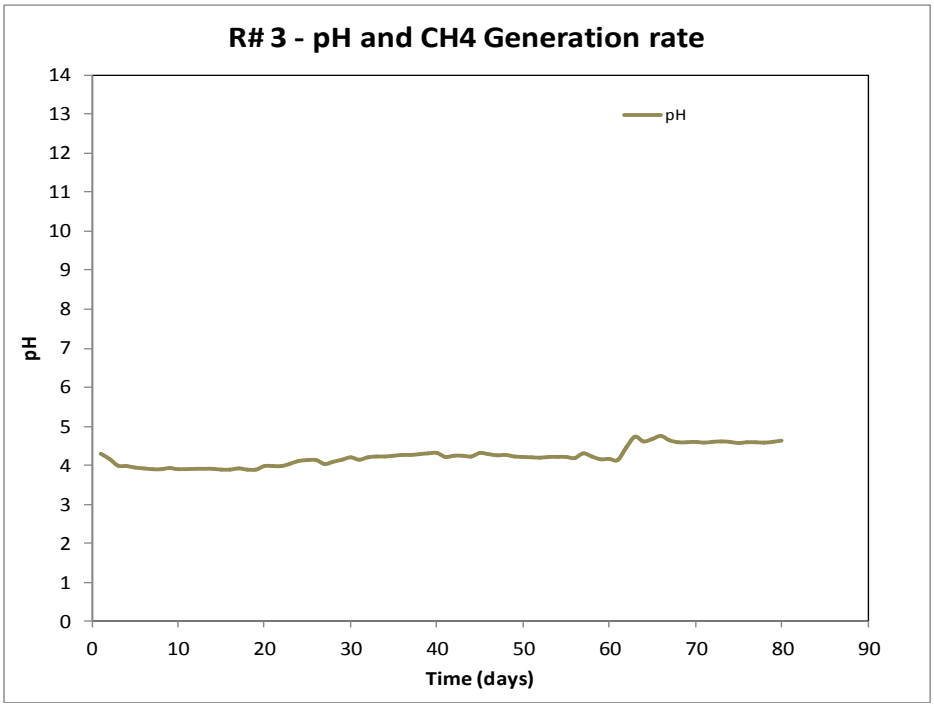

(b)

Figure B10: Gas generation rate and pH at 20°C from Reactor 10

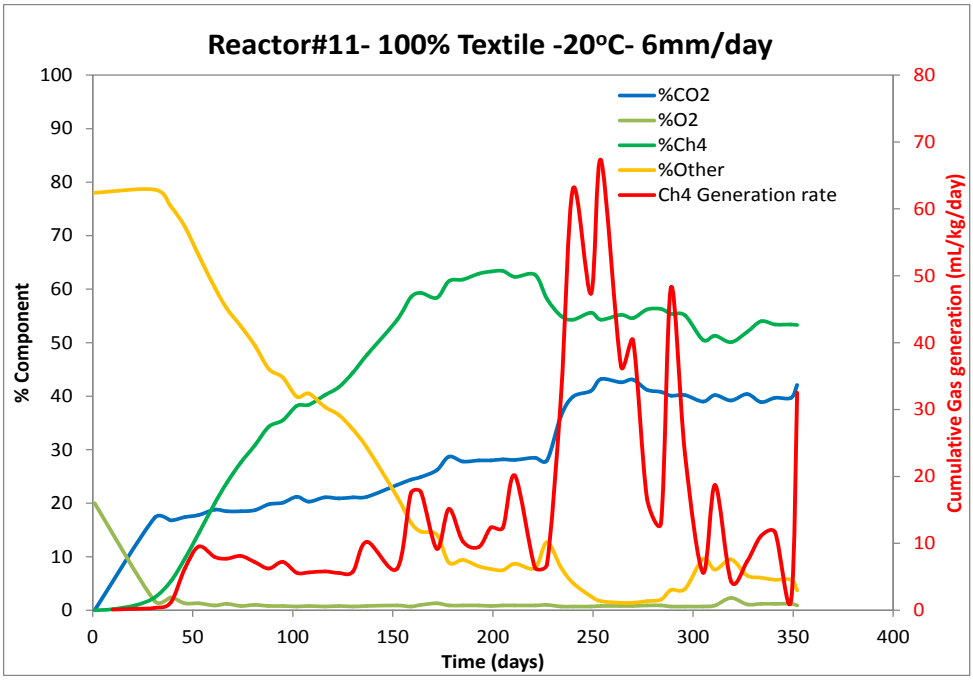

(a)

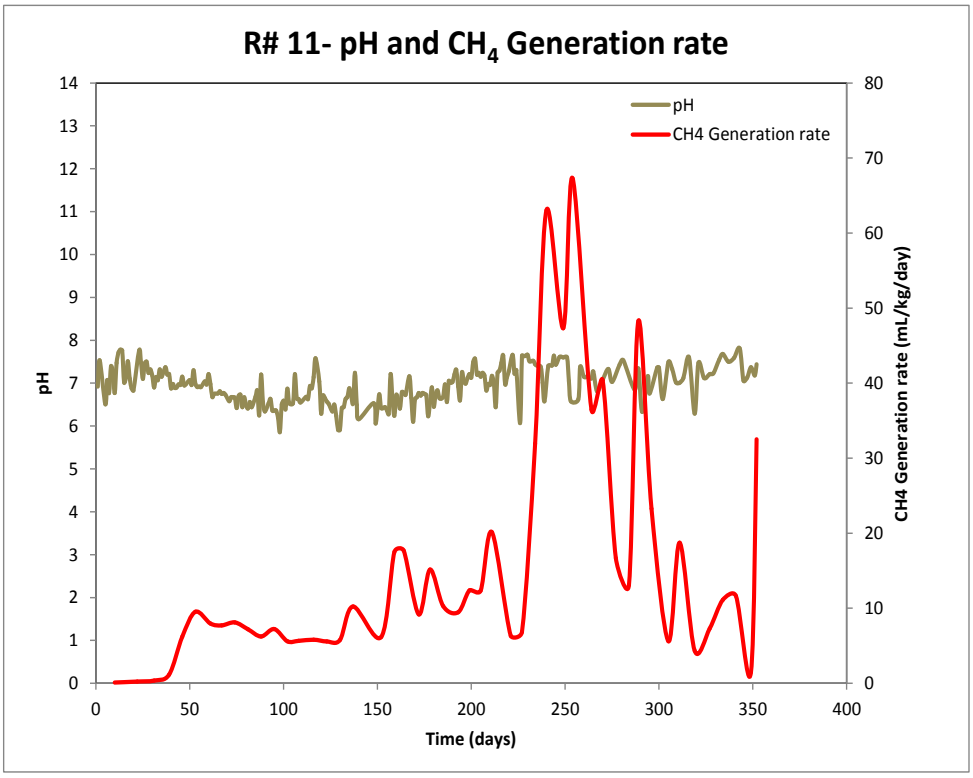

(b)

Figure B11: Gas generation rate and pH at 20°C from Reactor 11

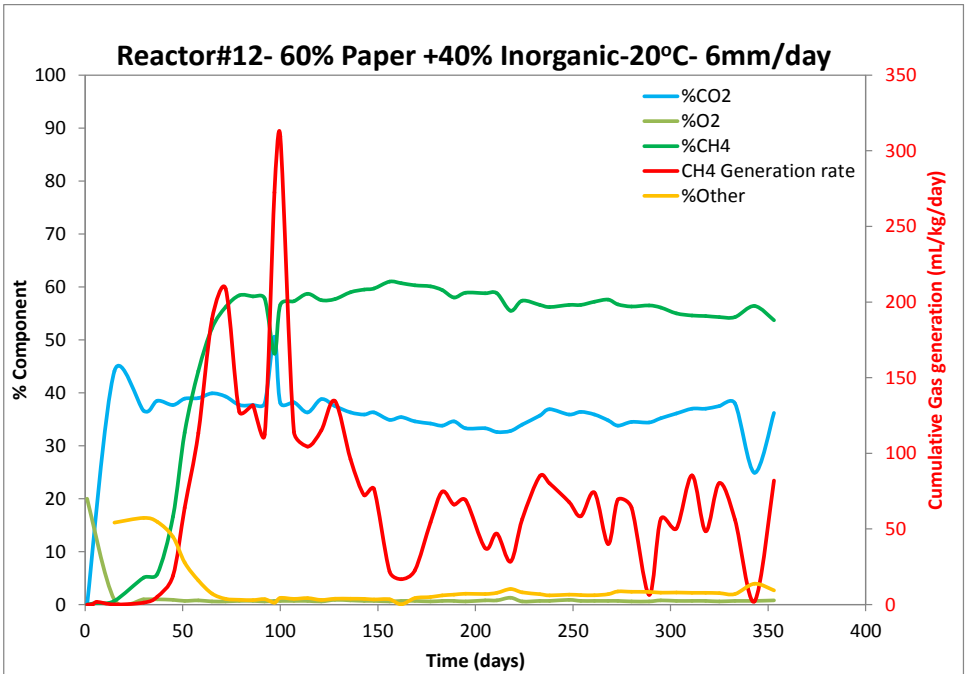

(a)

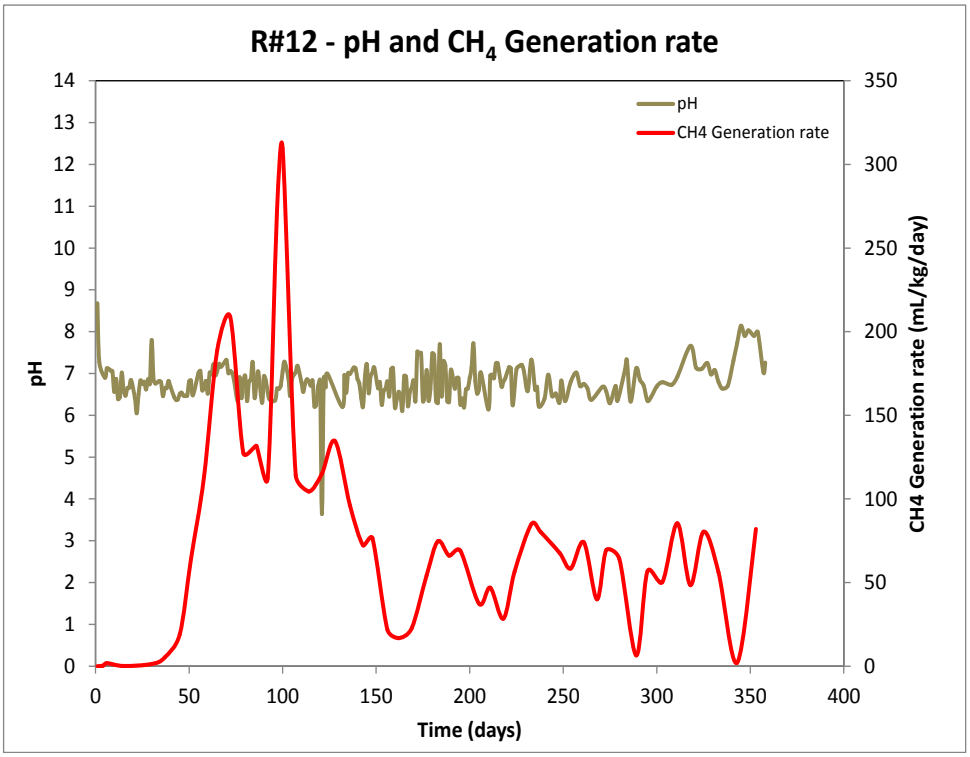

(b)

Figure B12: Gas generation rate and pH at 20°C from Reactor 12

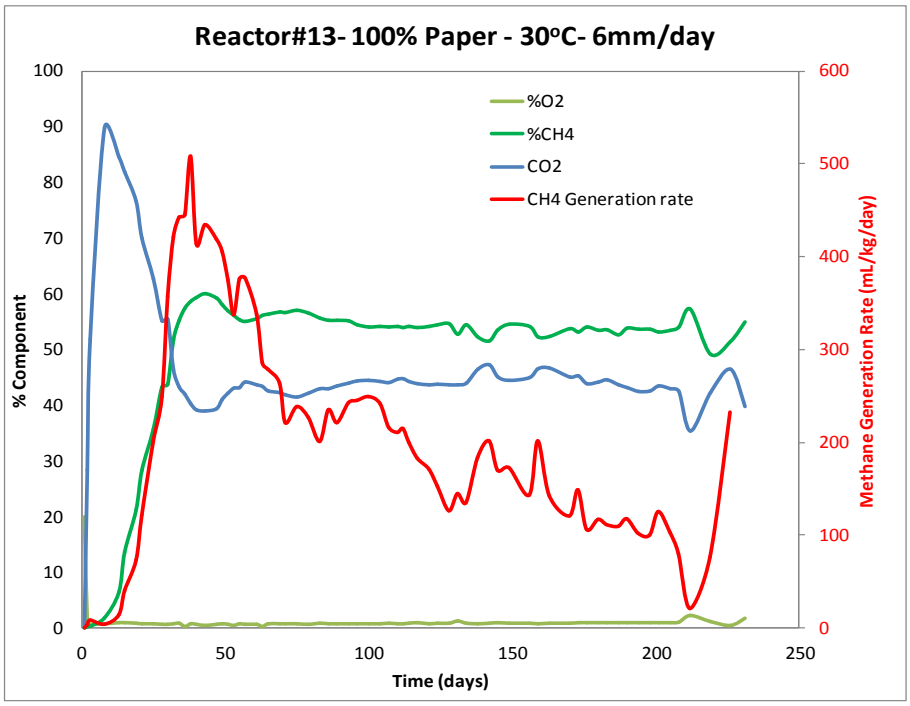

(a)

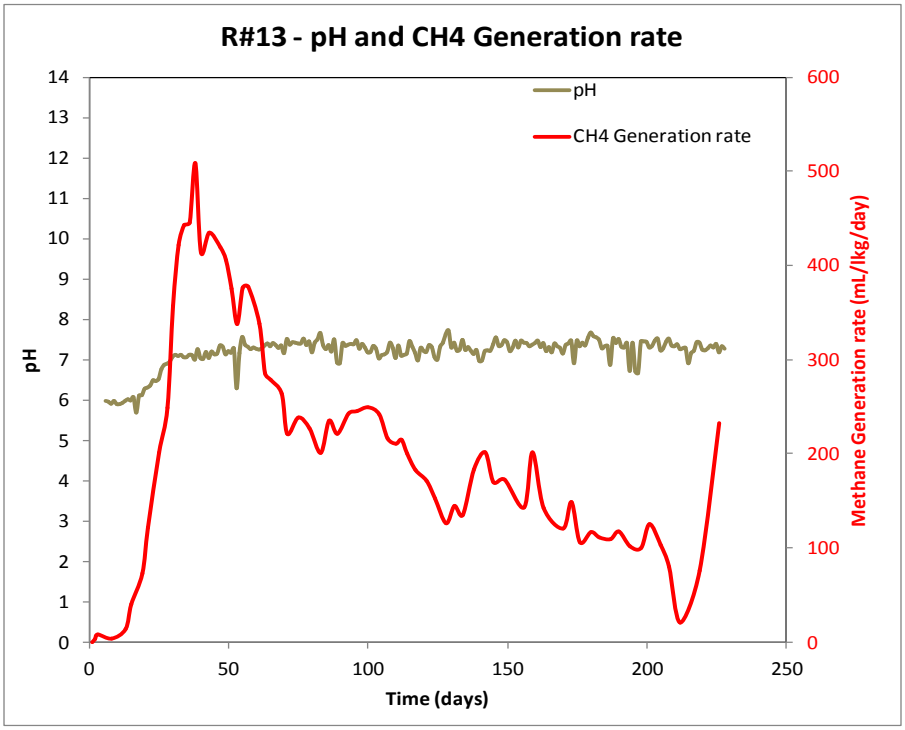

(b)

Figure B13: Gas generation rate and pH at 30°C from Reactor 13

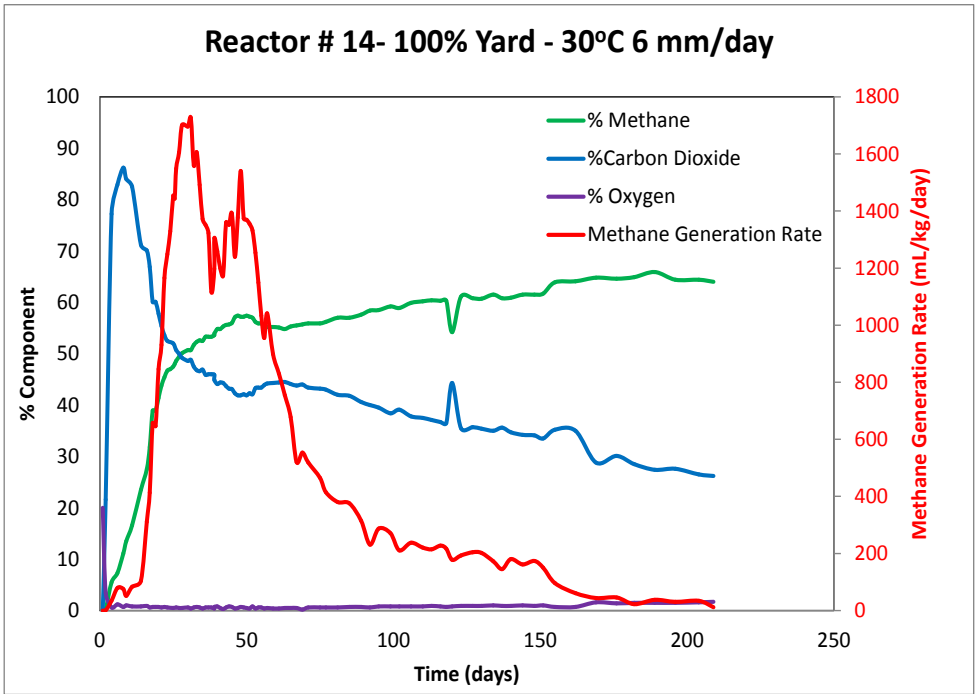

(a)

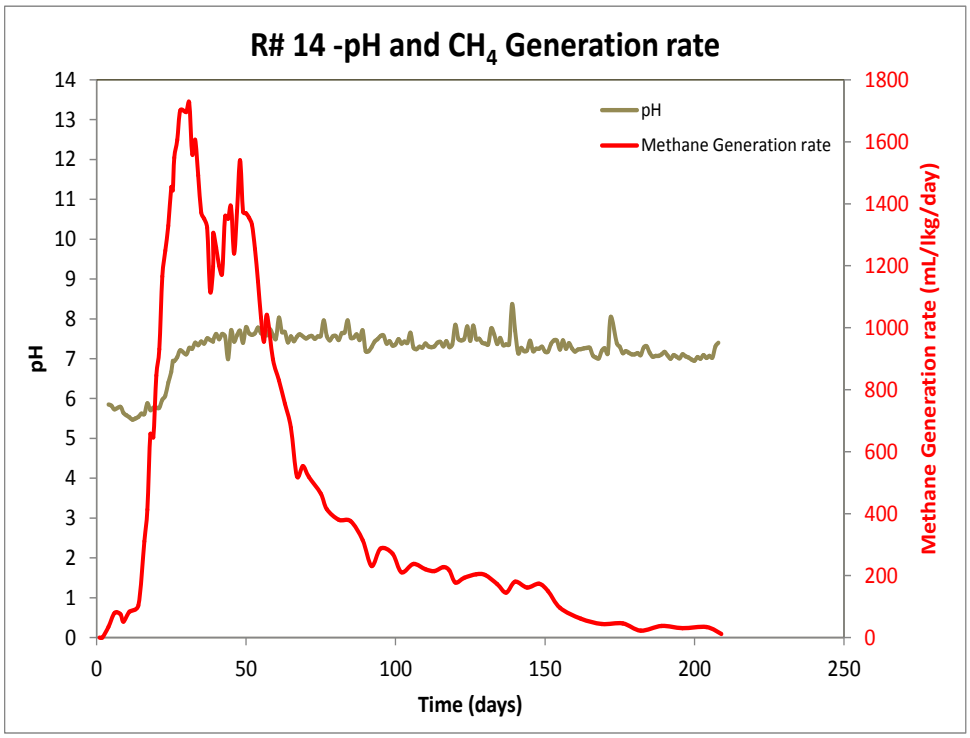

(b)

Figure B14: Gas generation rate and pH at 30°C from Reactor 14

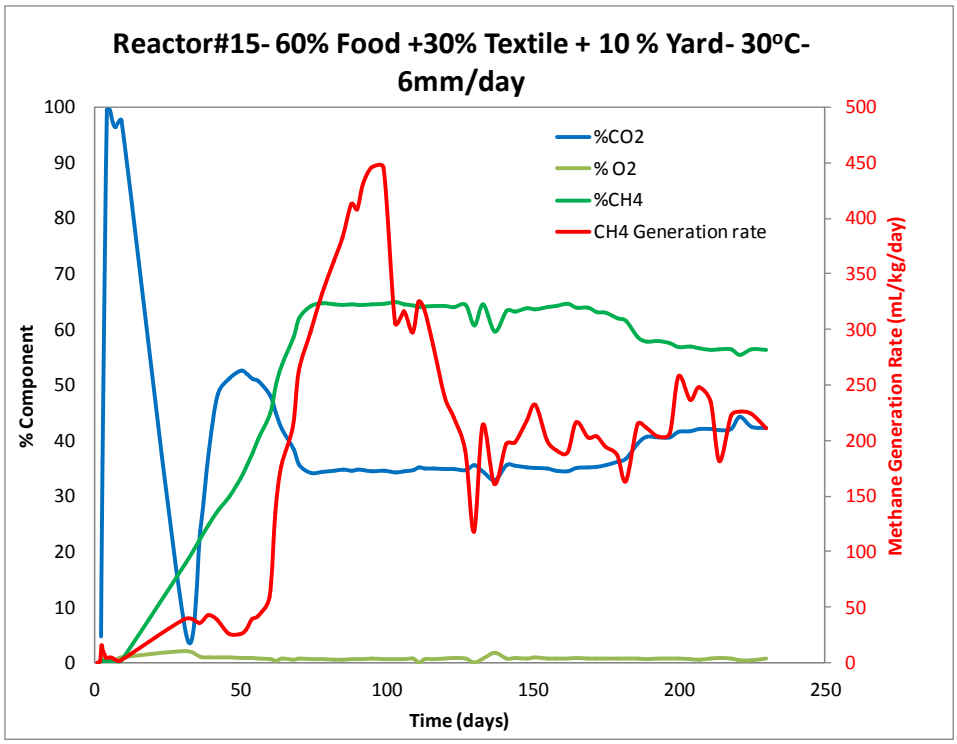

(a)

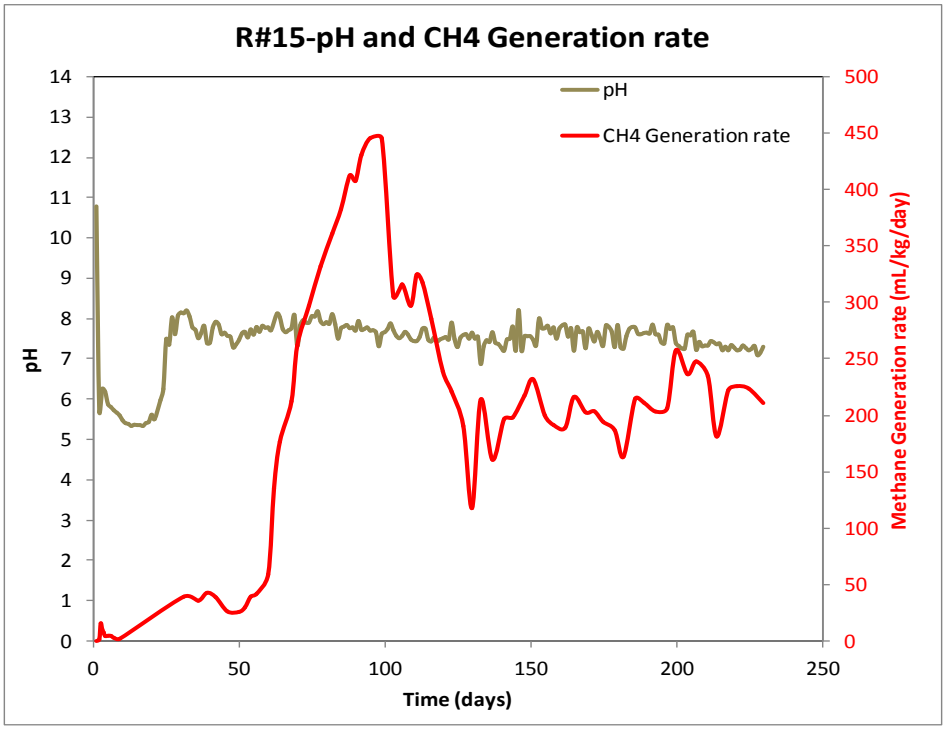

(b)

Figure B15: Gas generation rate and pH at 30°C from Reactor 15

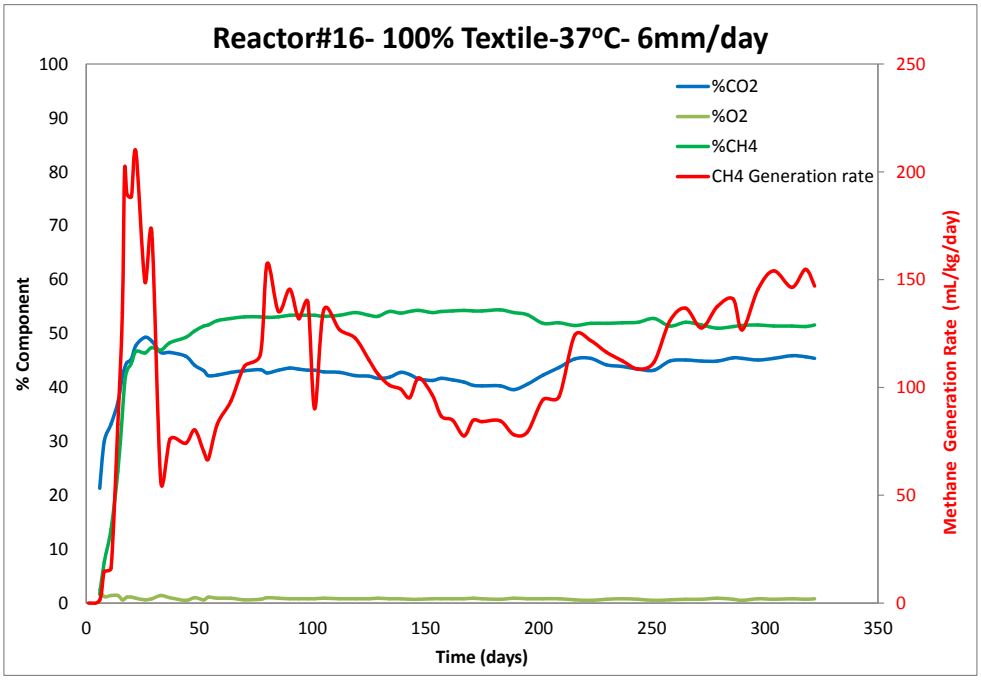

(a)

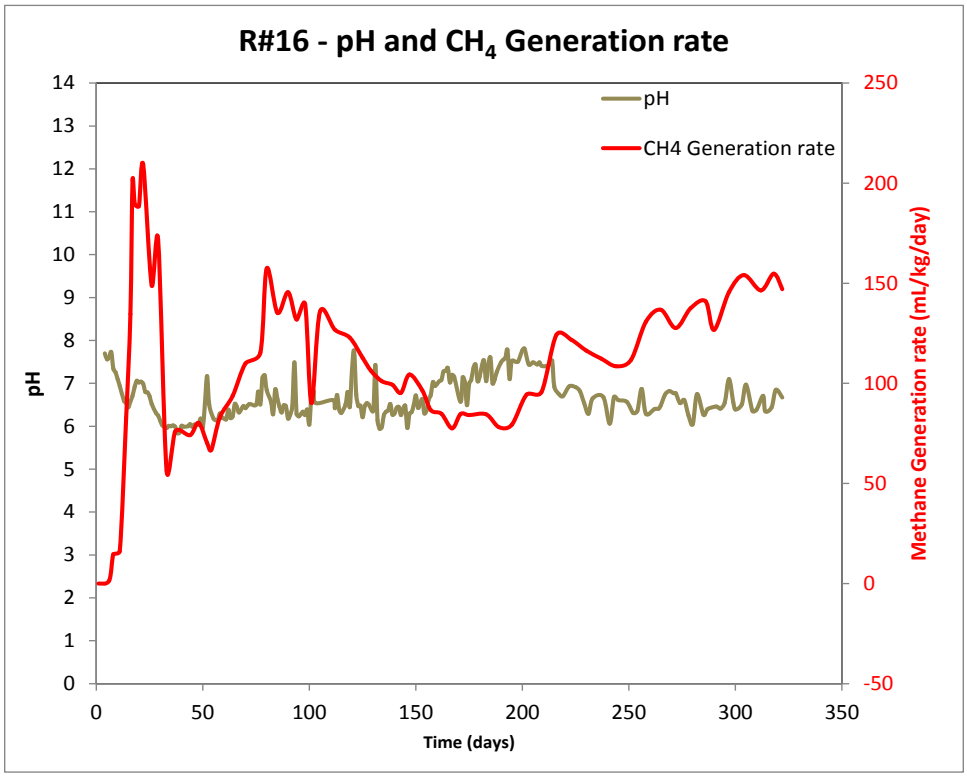

(b)

Figure B16: Gas generation rate and pH at 37°C from Reactor 16

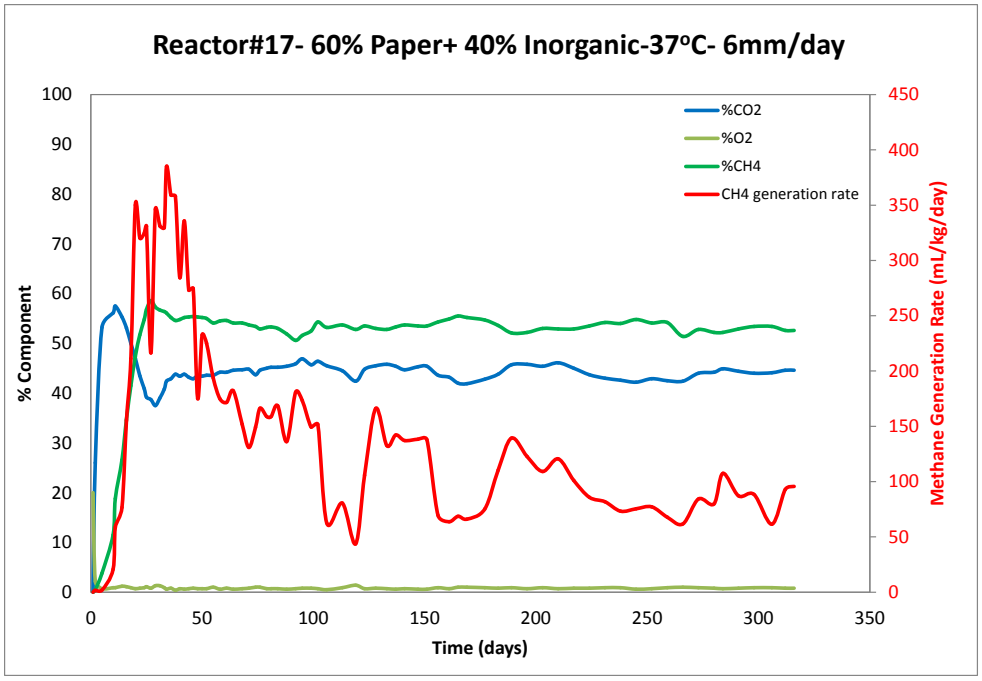

(a)

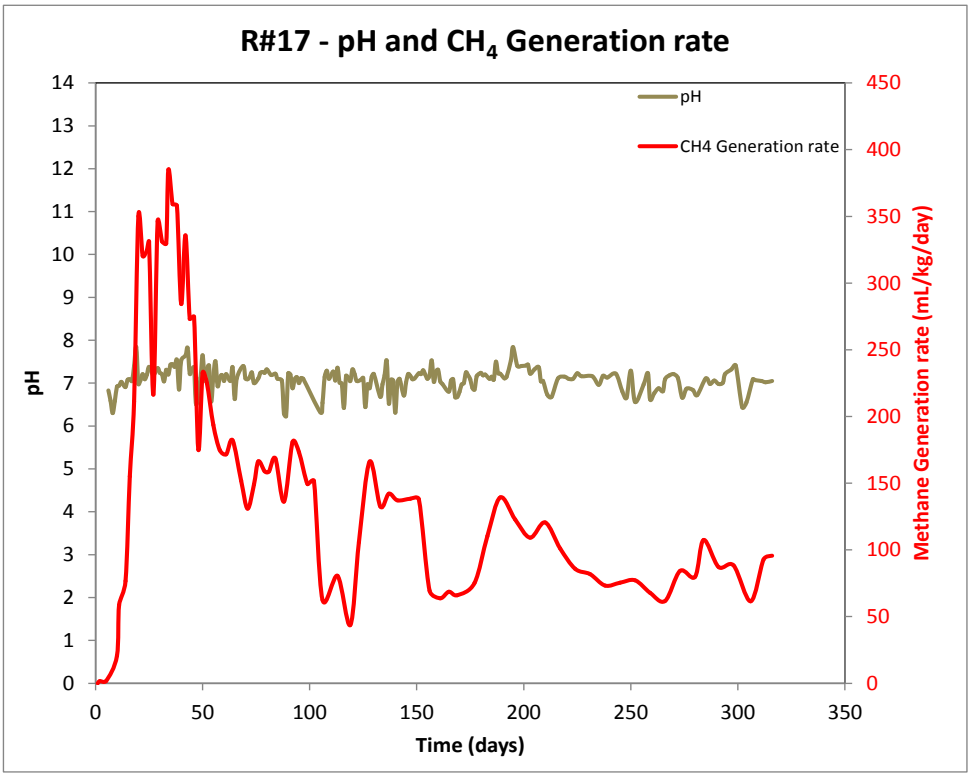

(b)

Figure B17: Gas generation rate and pH at 37°C from Reactor 17

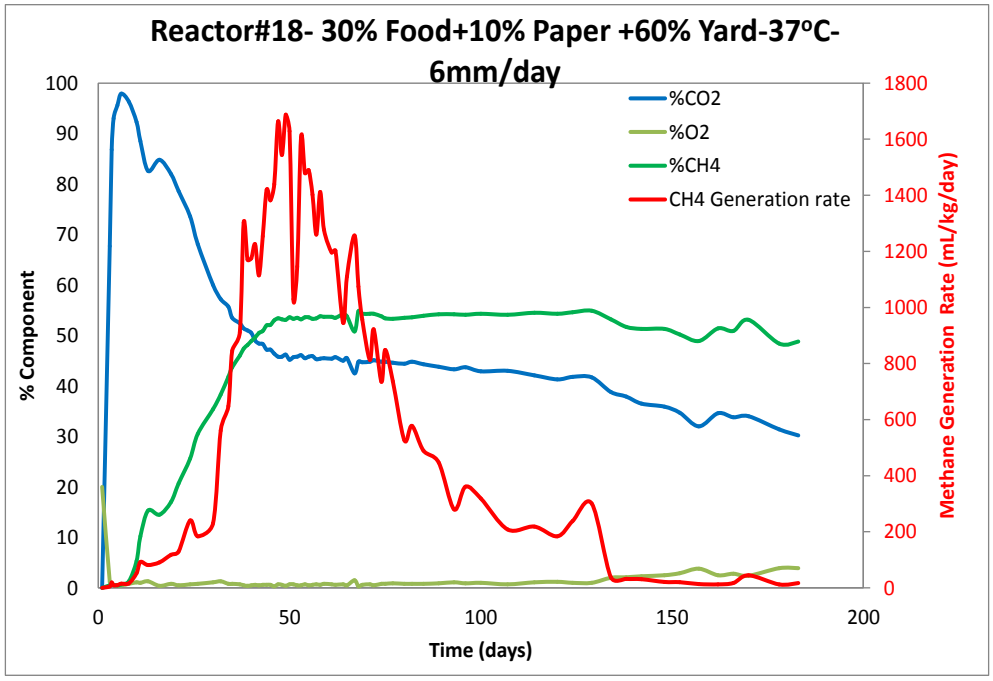

(a)

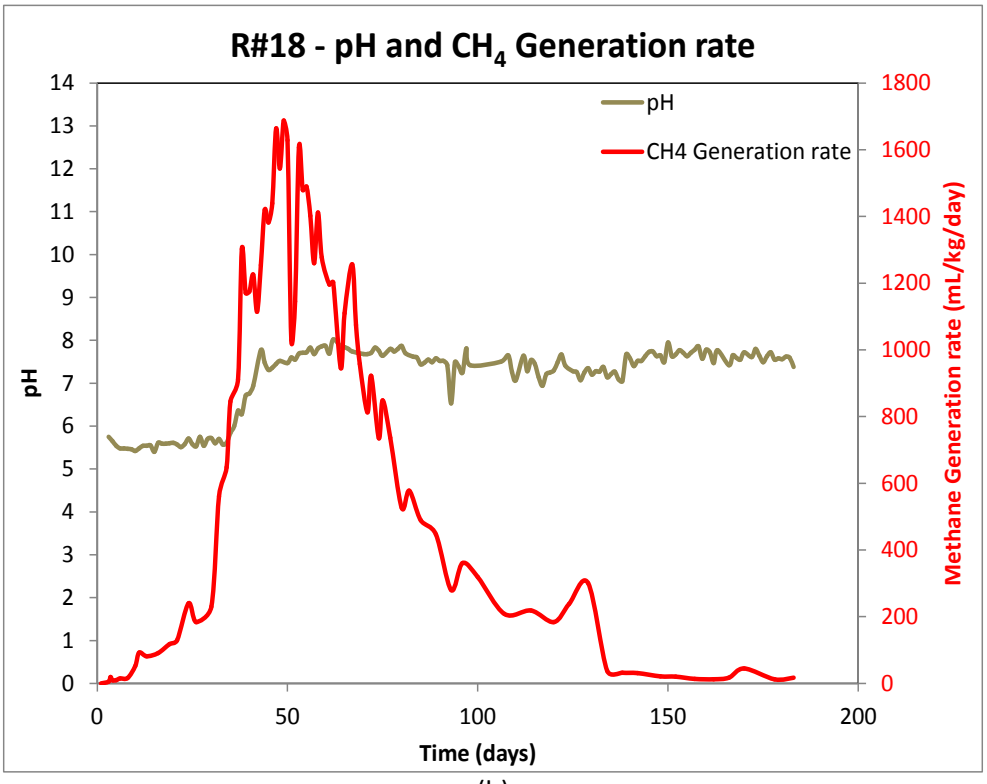

(b)

Figure B18: Gas generation rate and pH at 37°C from Reactor 18

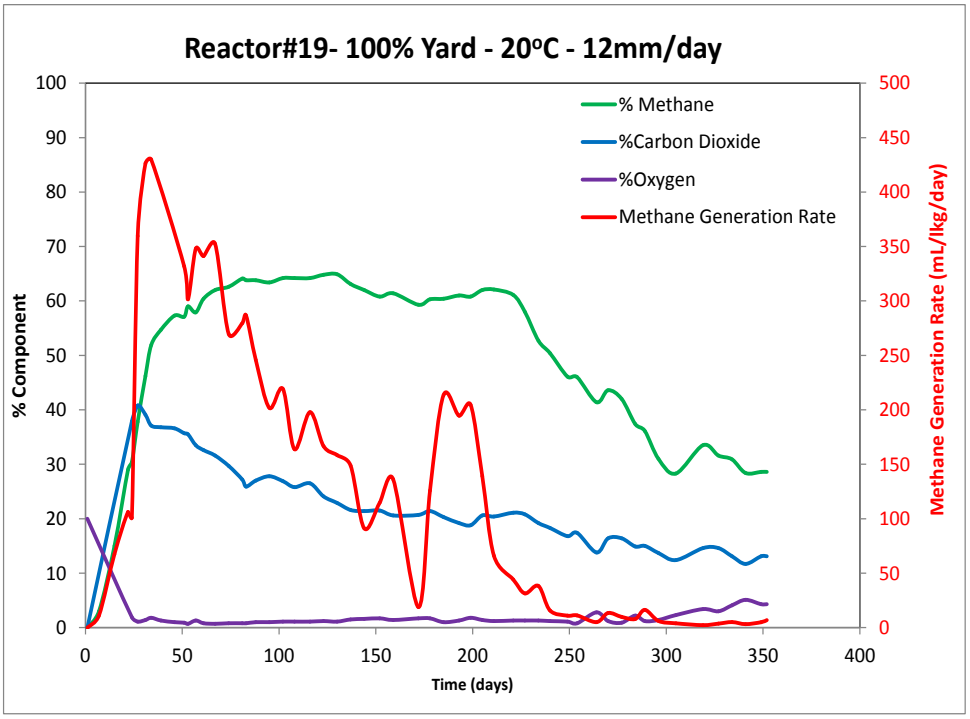

(a)

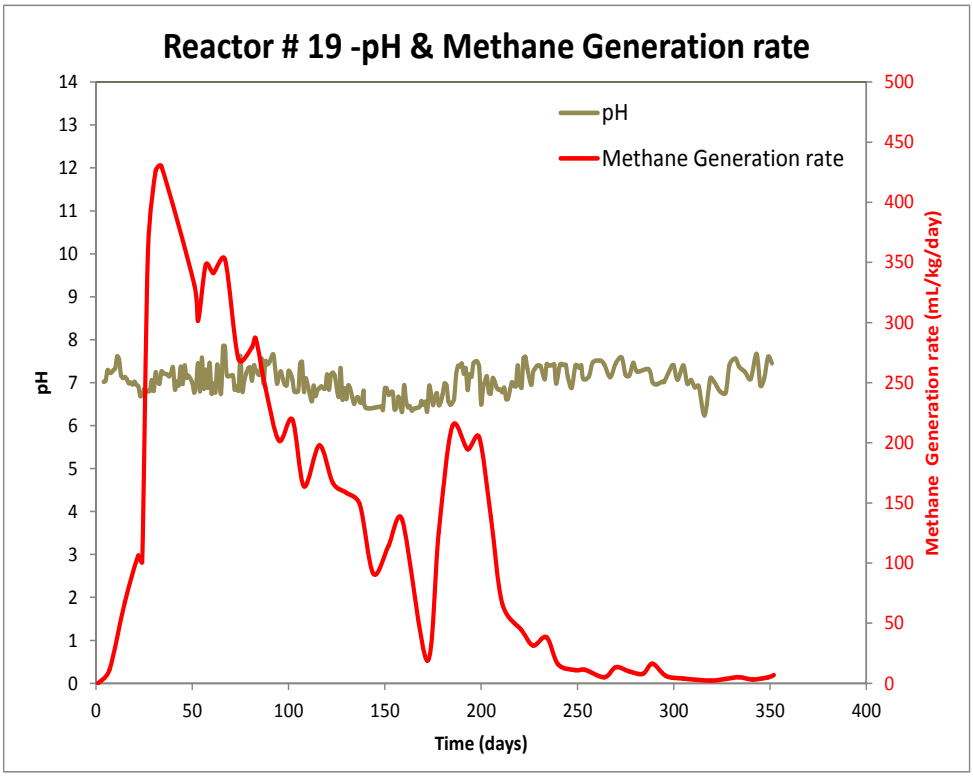

(b)

Figure B19: Gas generation rate and pH at 20°C from Reactor 19

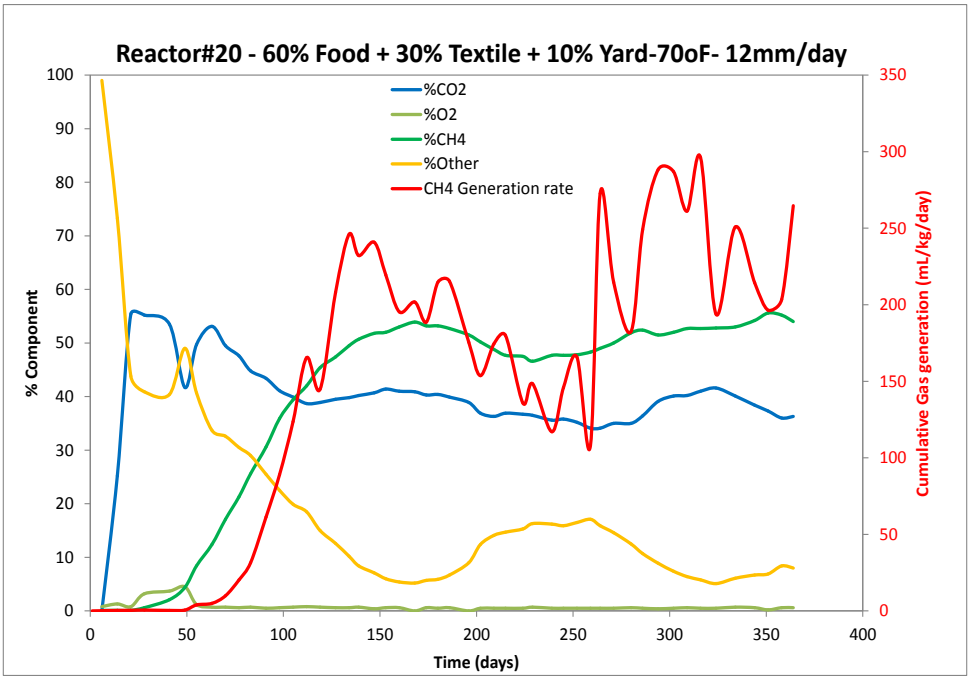

(a)

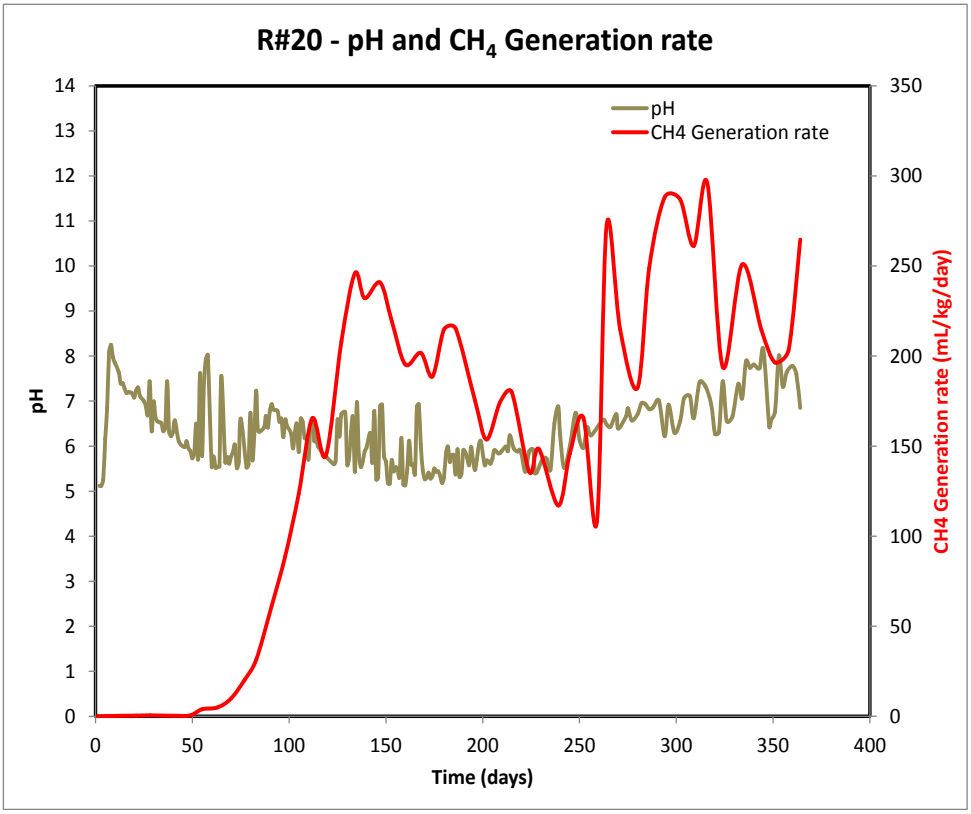

(b)

Figure B20: Gas generation rate and pH at 20°C from Reactor 20

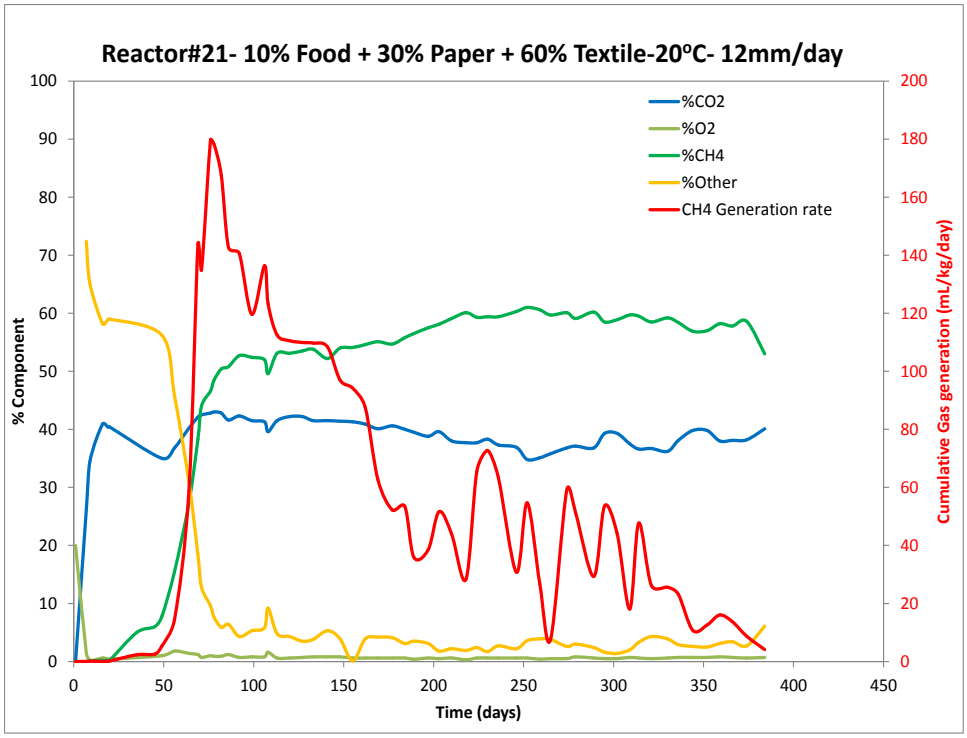

(a)

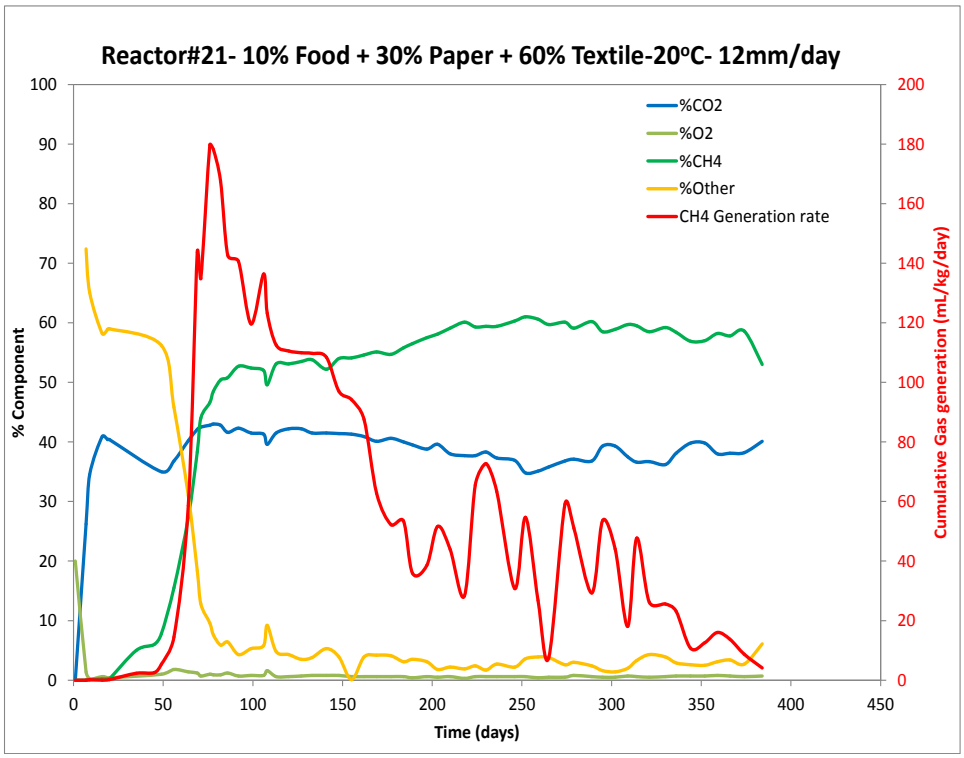

(b)

Figure B21: Gas generation rate and pH at 20°C from Reactor 21

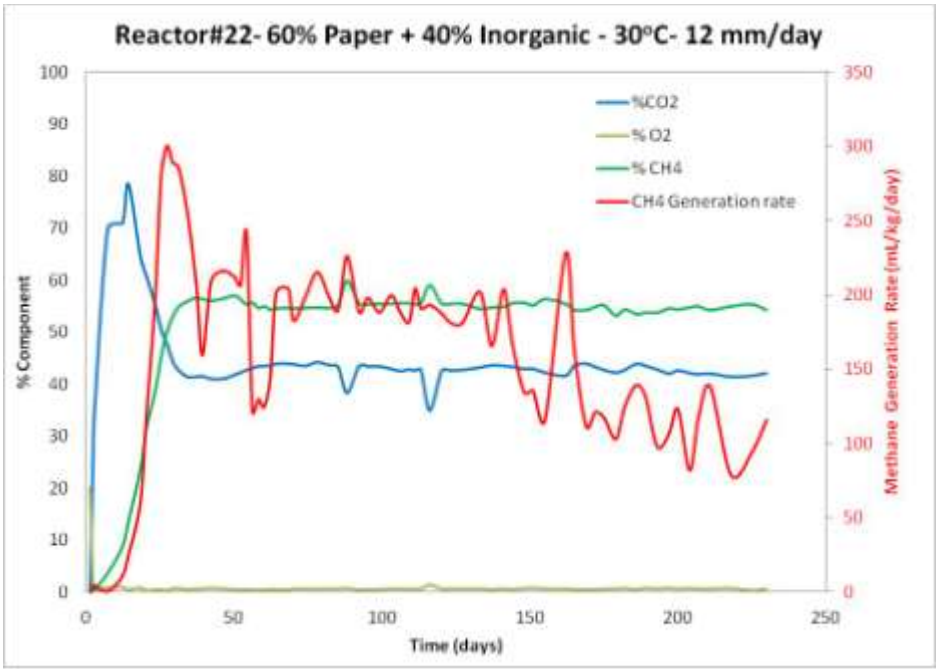

(a)

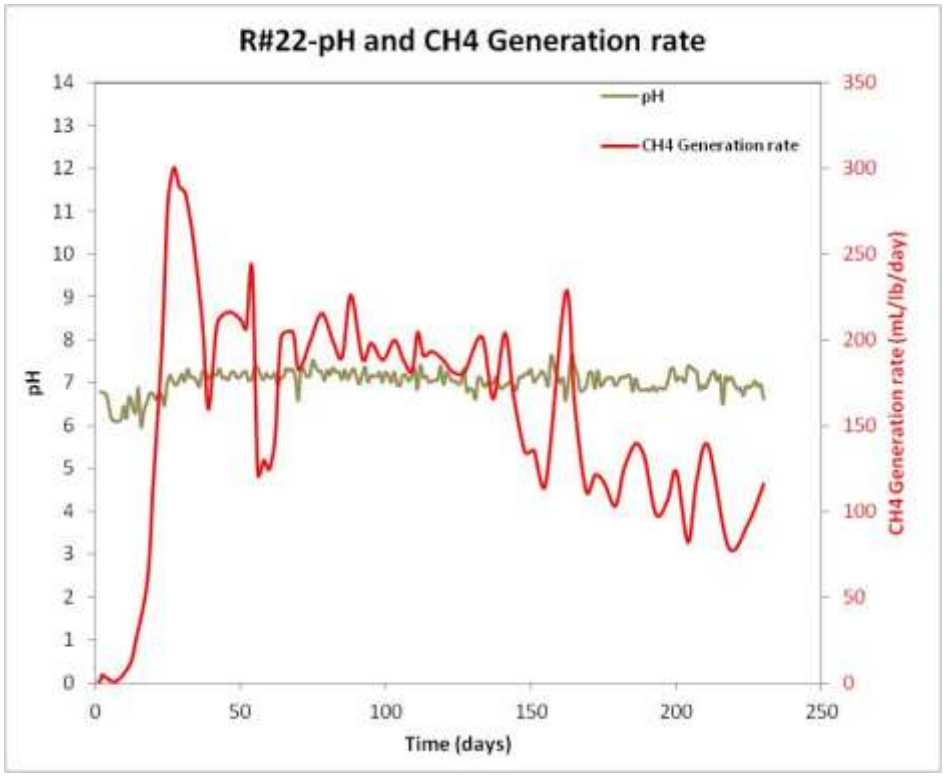

(b)

Figure B22: Gas generation rate and pH at 30°C from Reactor 22

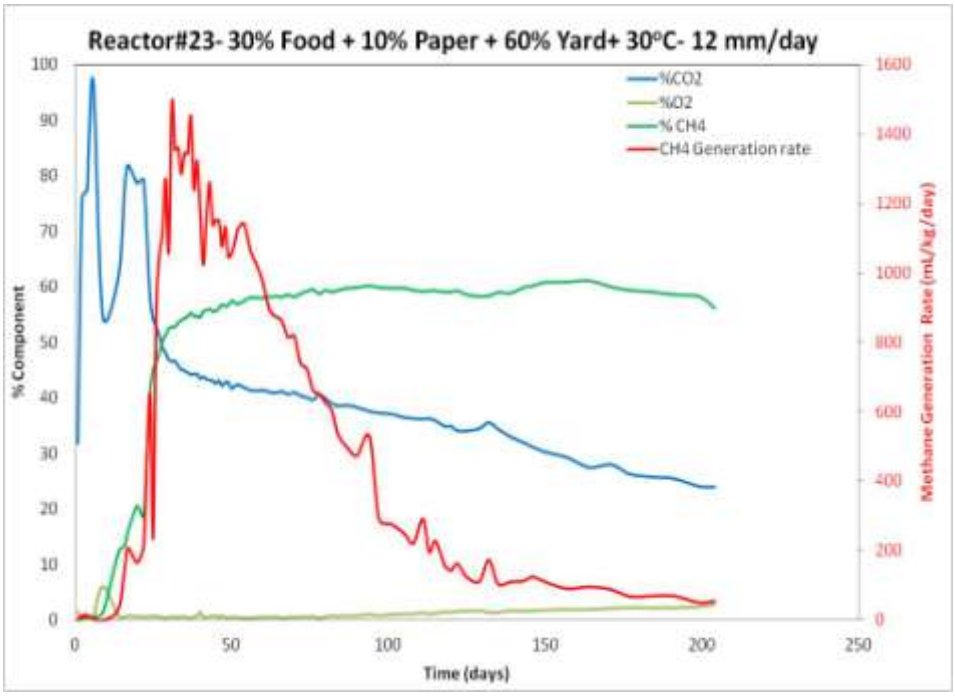

(a)

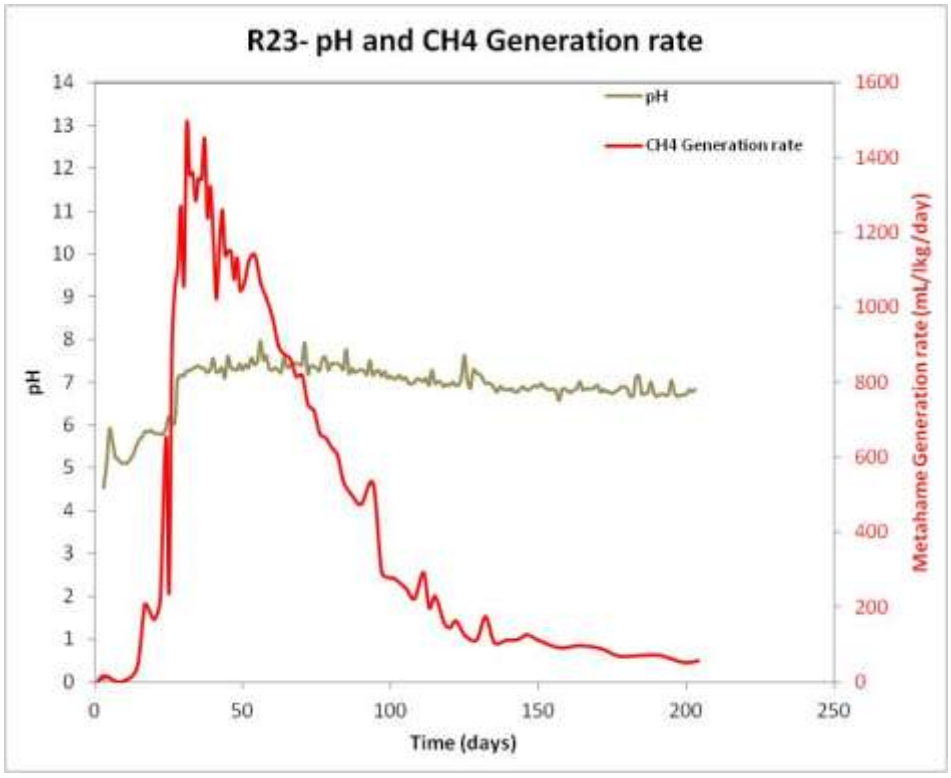

(b)

Figure B23: Gas generation rate and pH at 30°C from Reactor 23

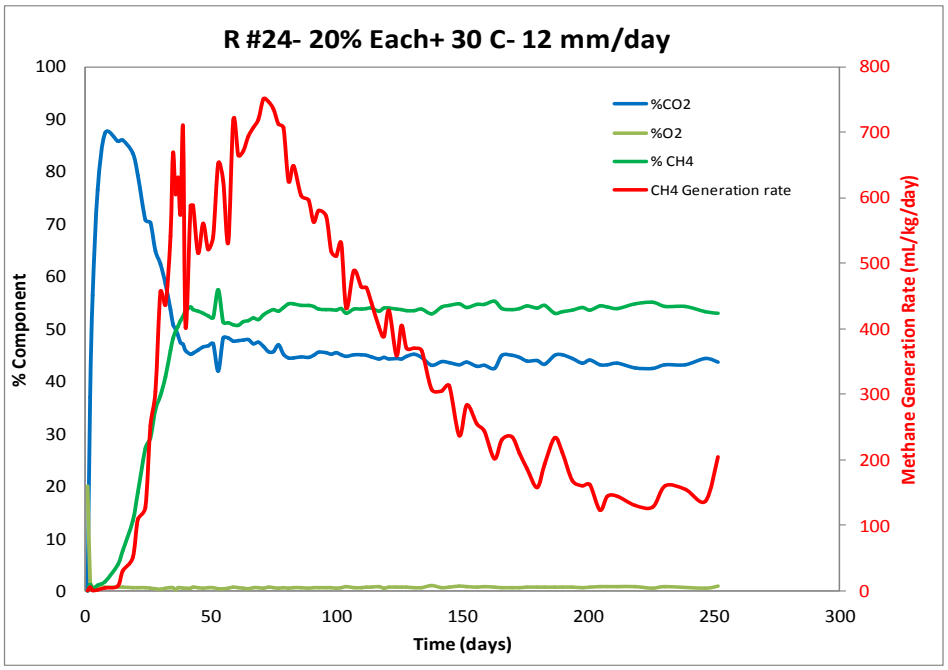

(a)

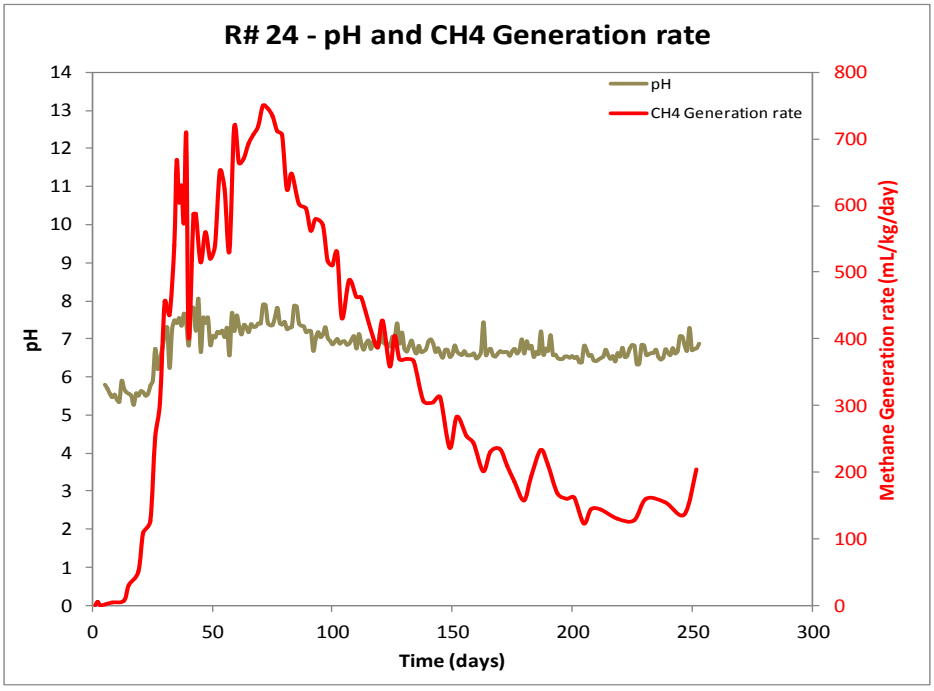

(b)

Figure B24: Gas generation rate and pH at 30°C from Reactor 24

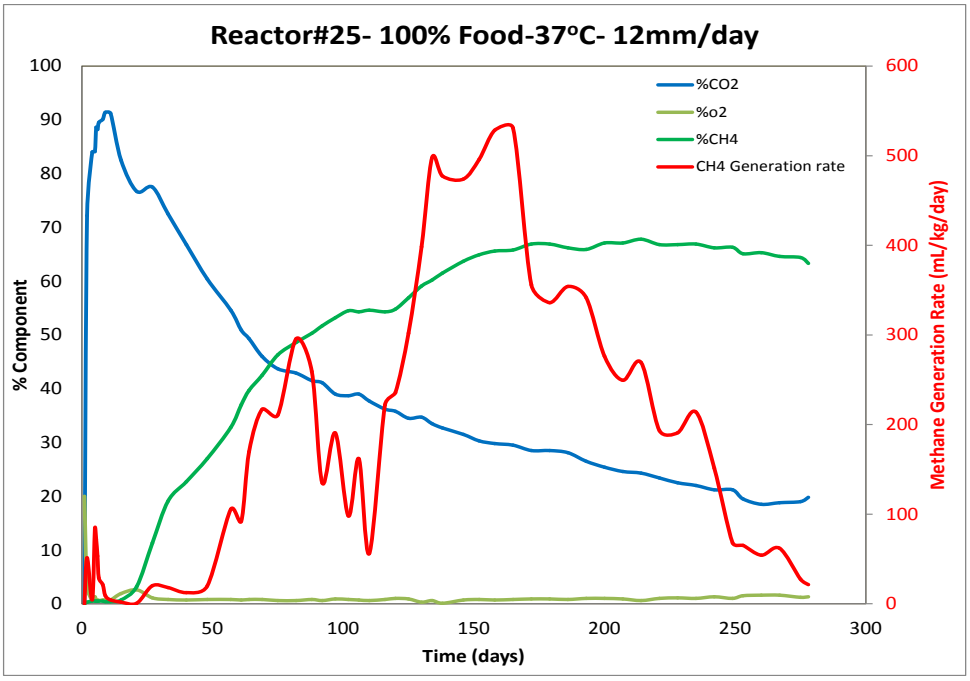

(a)

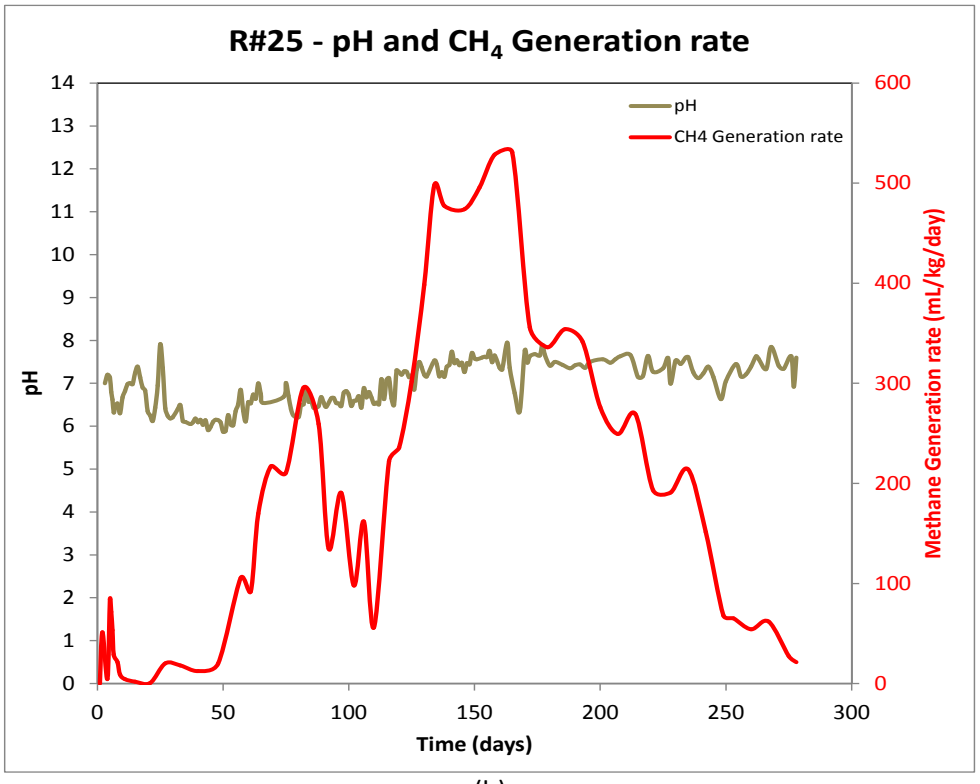

(b)

Figure B25: Gas generation rate and pH at 37°C from Reactor 25

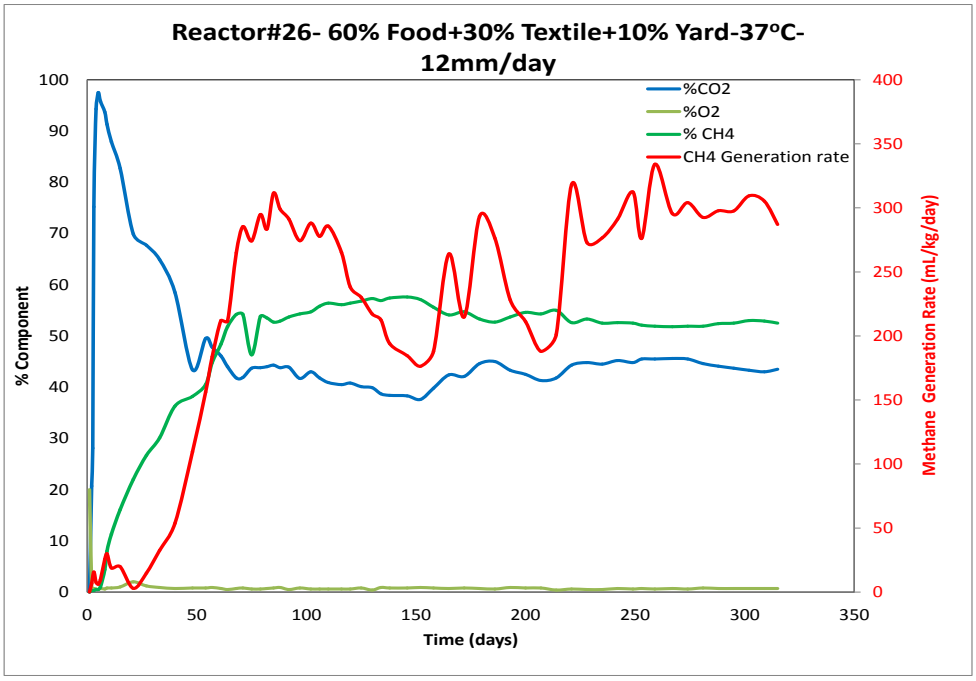

(a)

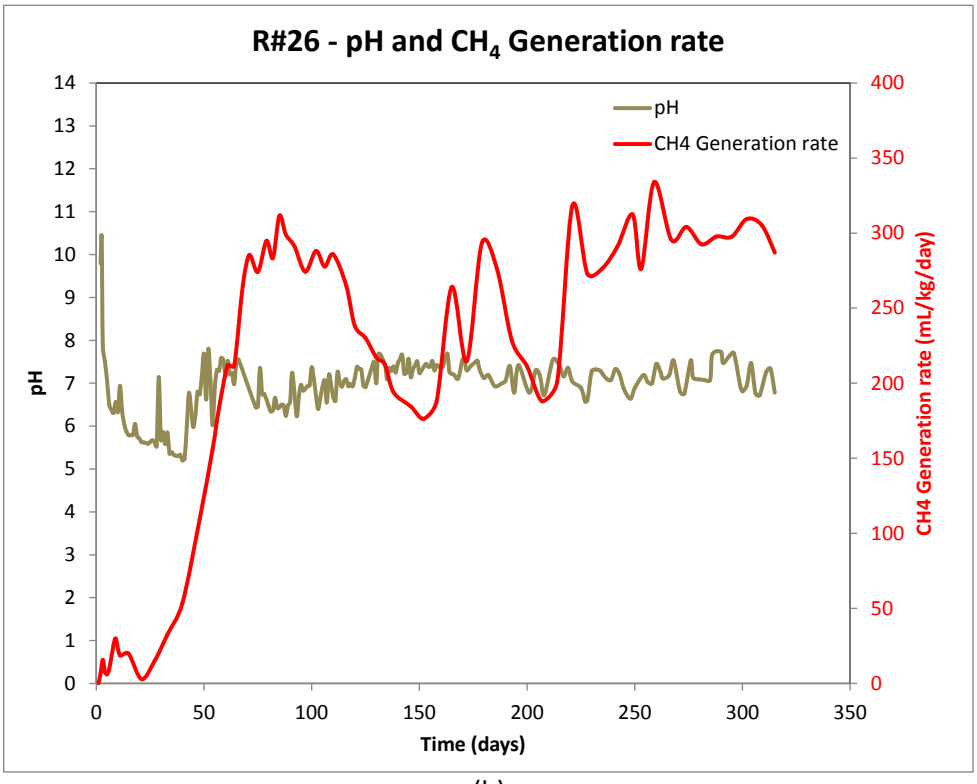

(b)

Figure B26: Gas generation rate and pH at 37°C from Reactor 26

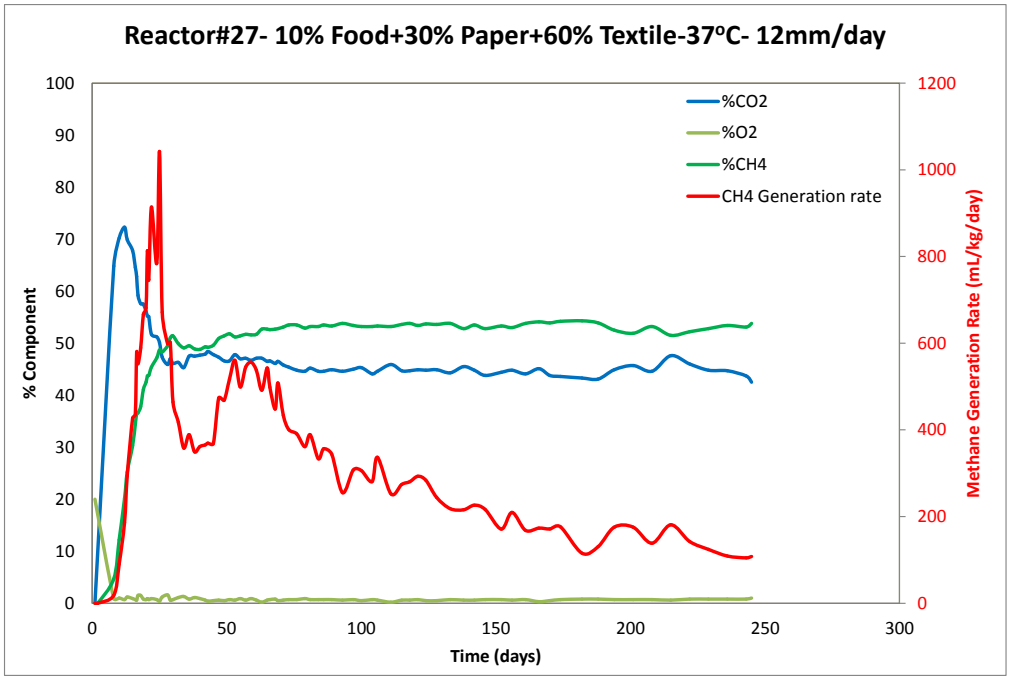

(a)

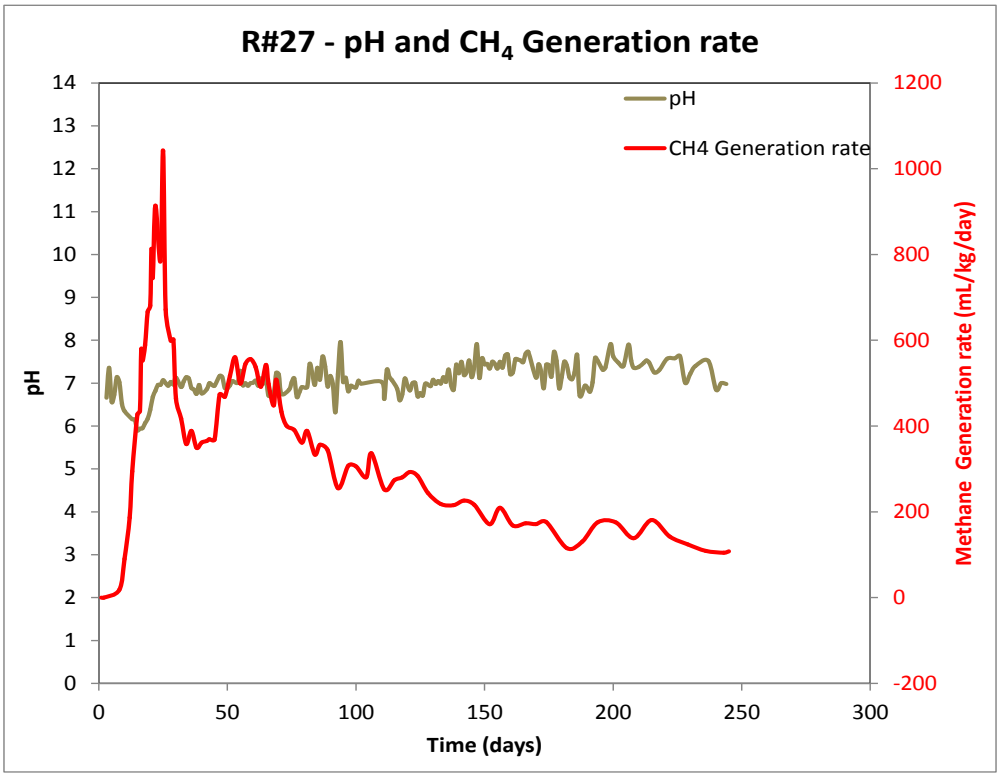

(b)

Figure B27: Gas generation rate and pH at 37°C from Reactor 27

APPENDIX C

CUMULATIVE METHANE GENERATION

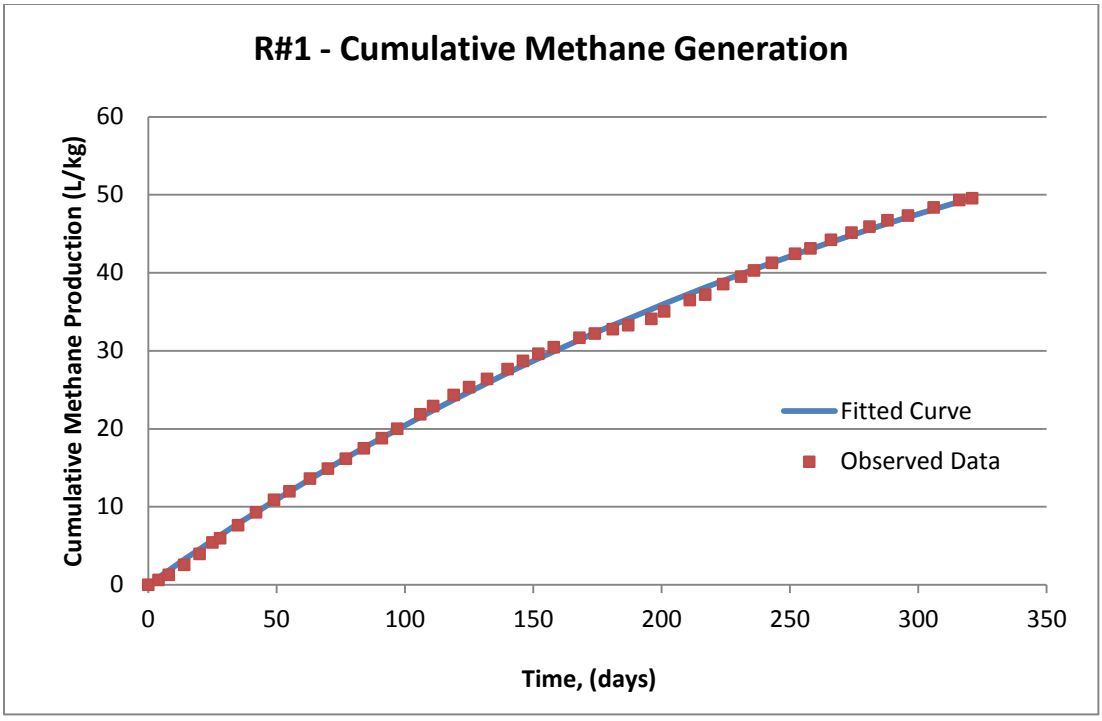

Figure C-1: Cumulative methane production rate for Reactor 1

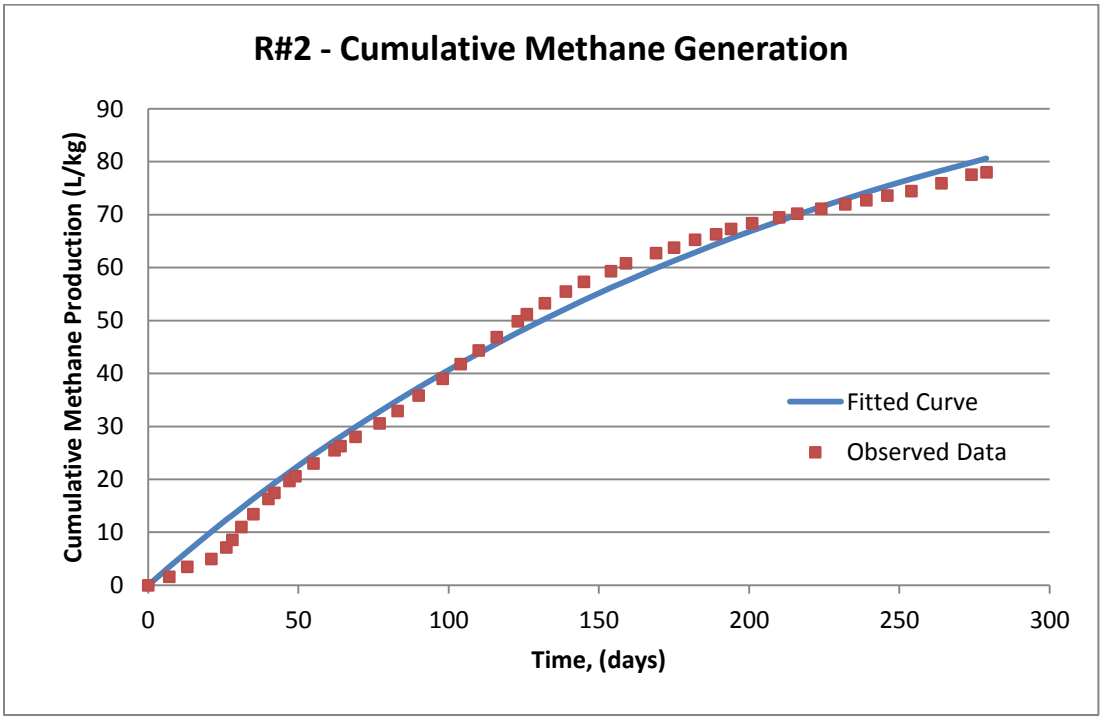

Figure C-2: Cumulative methane production rate for Reactor 2

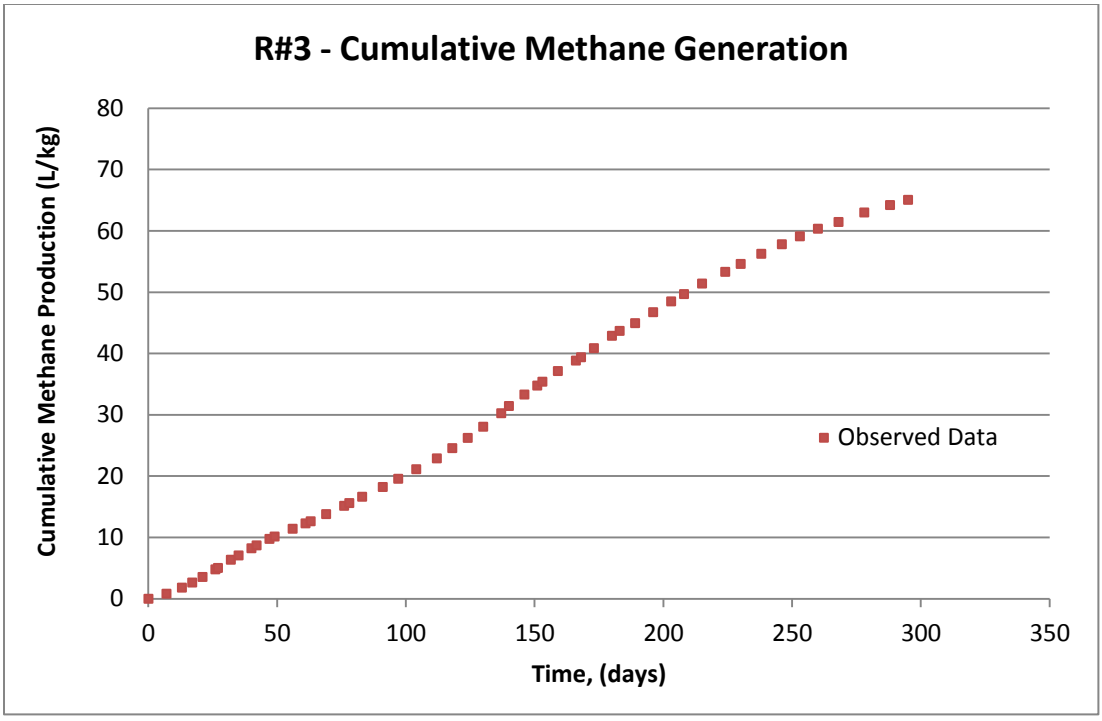

Figure C-3: Cumulative methane production rate for Reactor 3

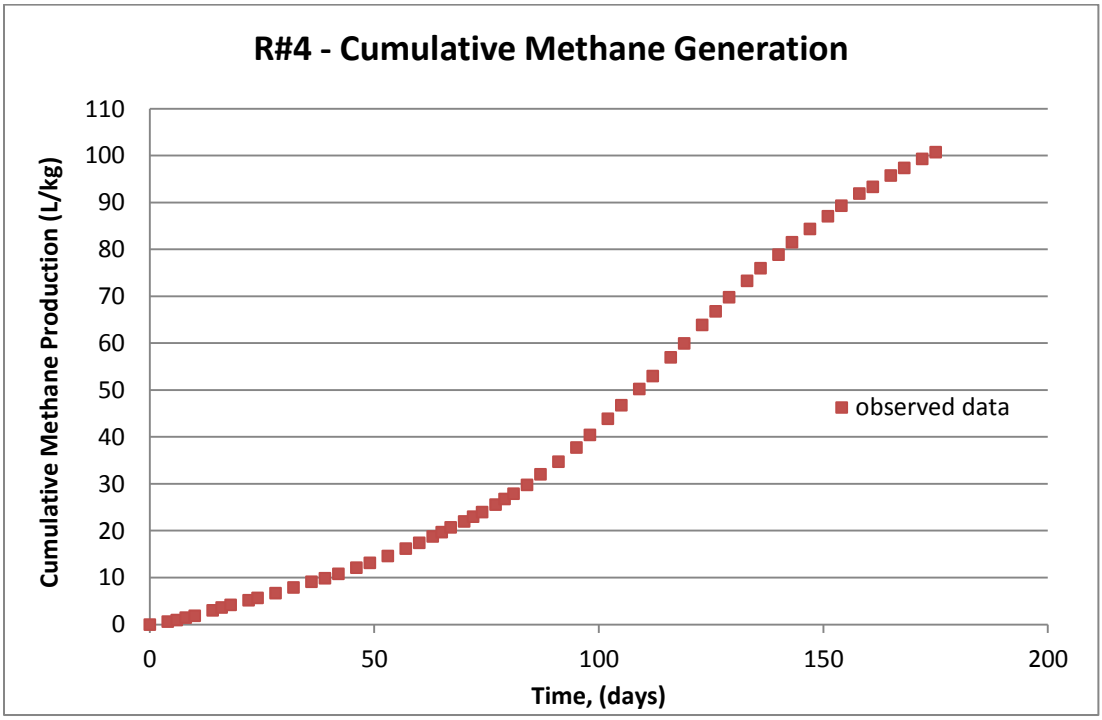

Figure C-4: Cumulative methane production rate for Reactor 4

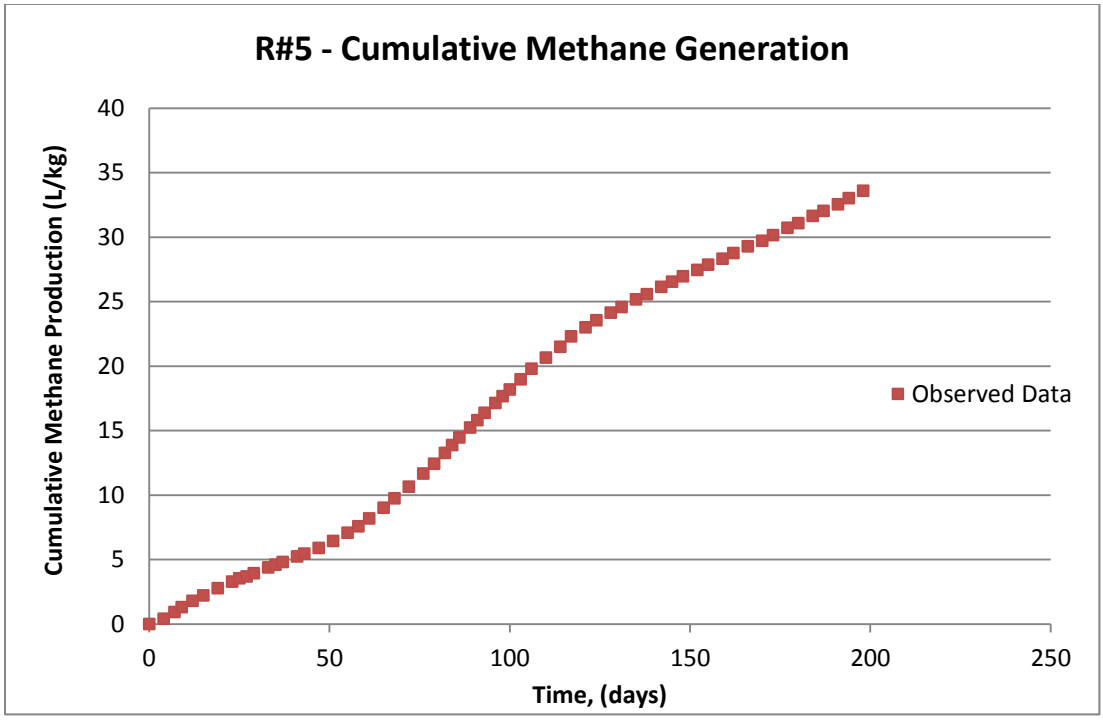

Figure C-5: Cumulative methane production rate for Reactor 5

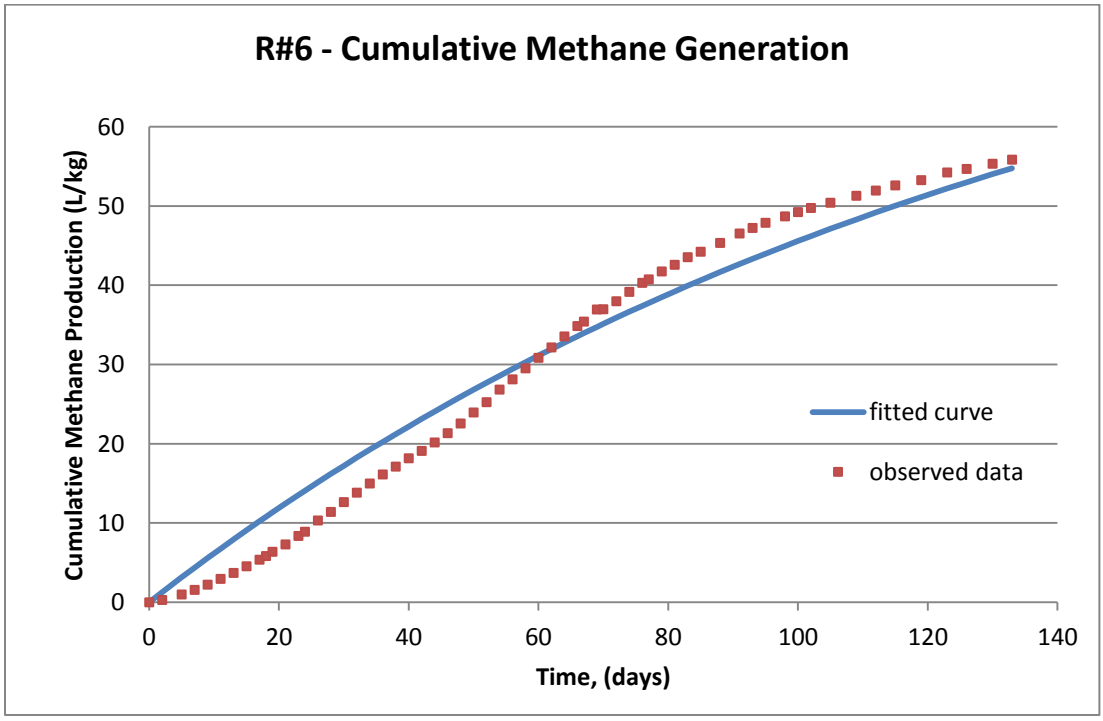

Figure C-6: Cumulative methane production rate for Reactor 6

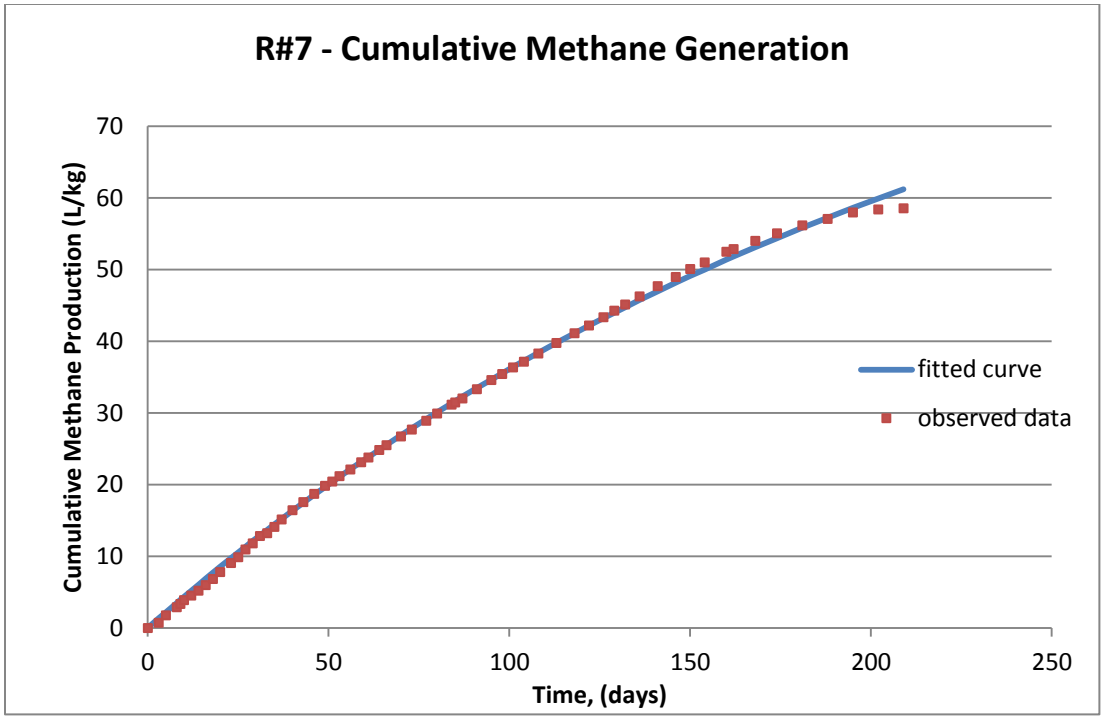

Figure C-7: Cumulative methane production rate for Reactor 7

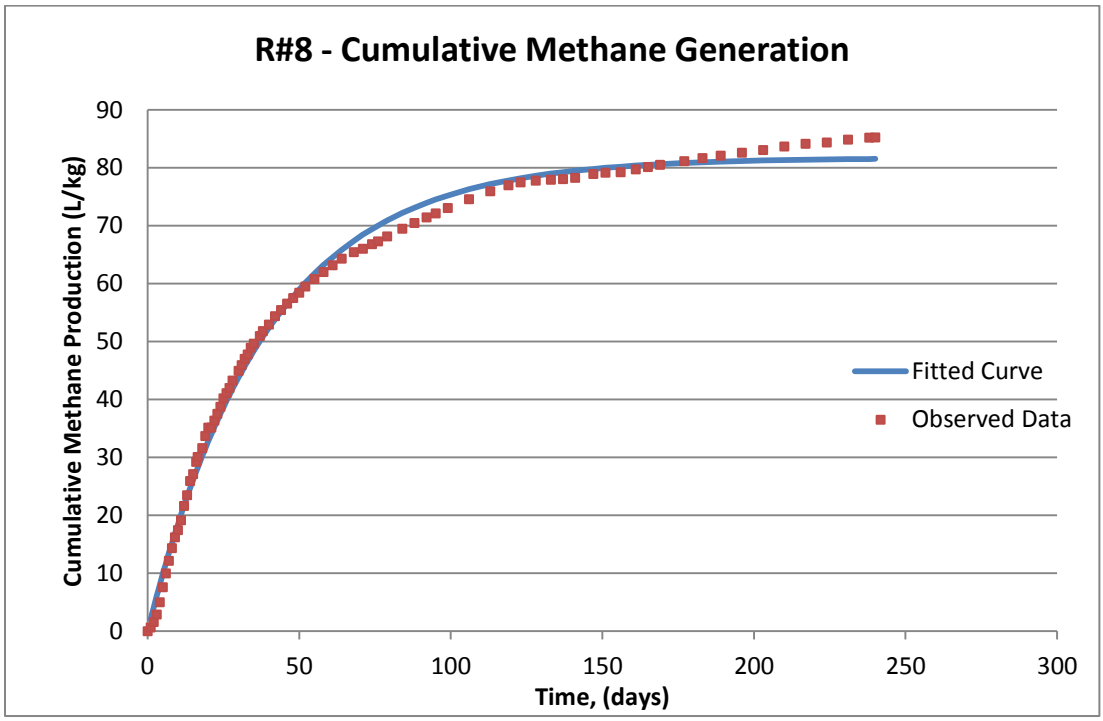

Figure C-8: Cumulative methane production rate for Reactor 8

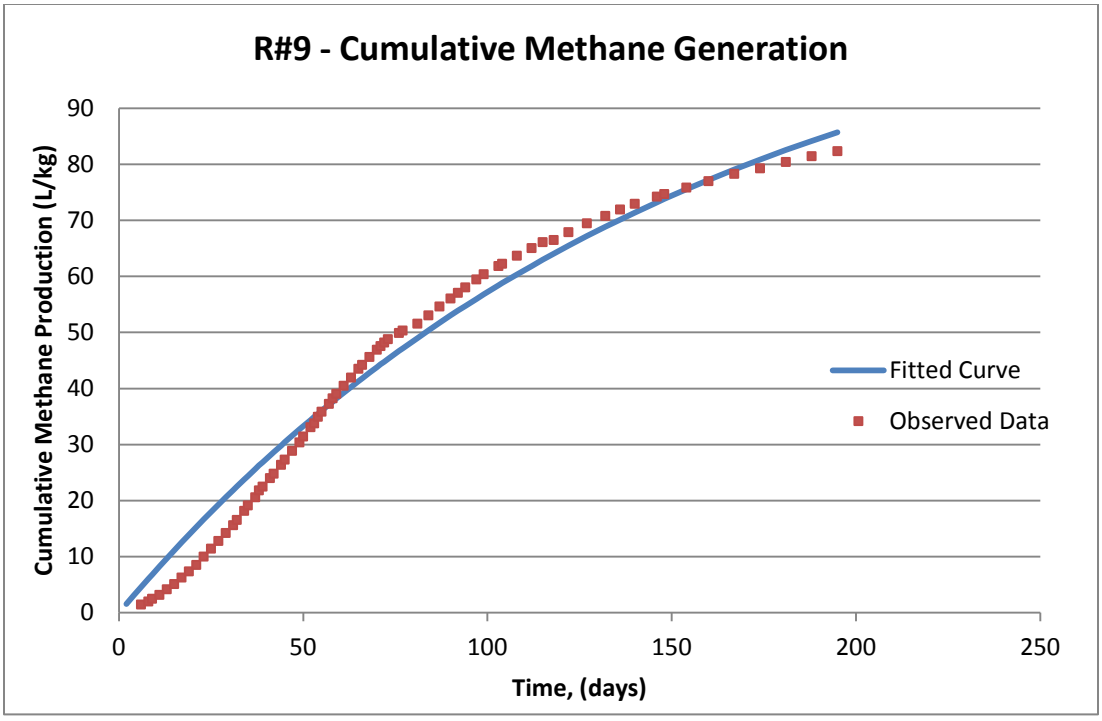

Figure C-9: Cumulative methane production rate for Reactor 9

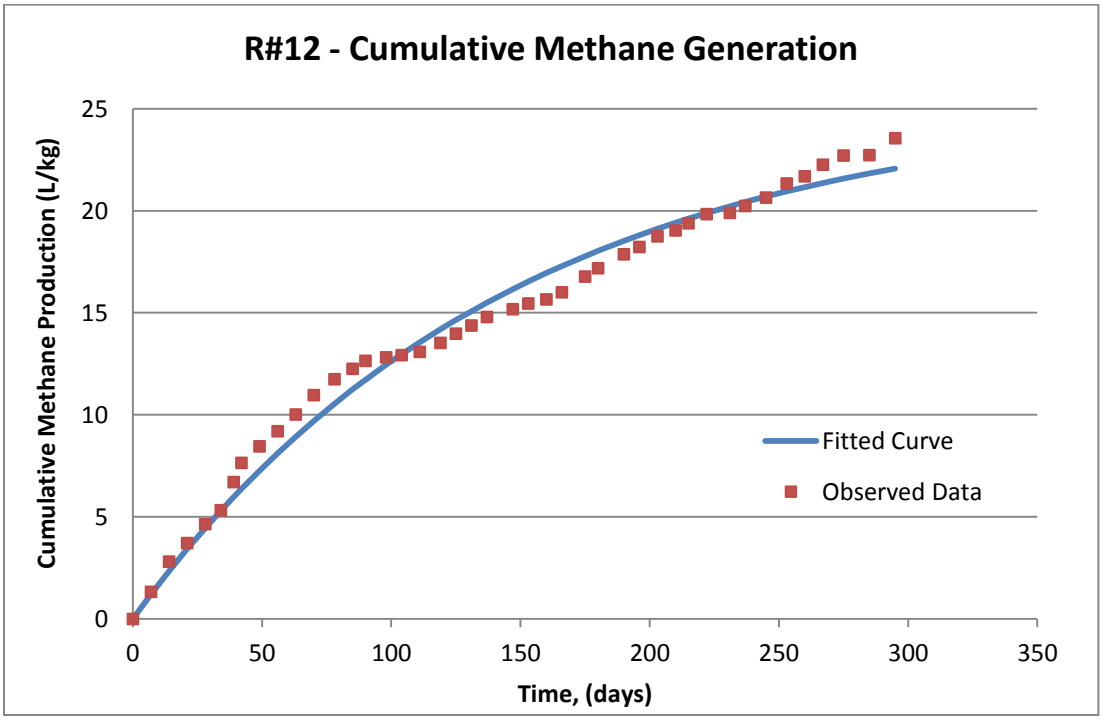

Figure C-10: Cumulative methane production rate for Reactor 12

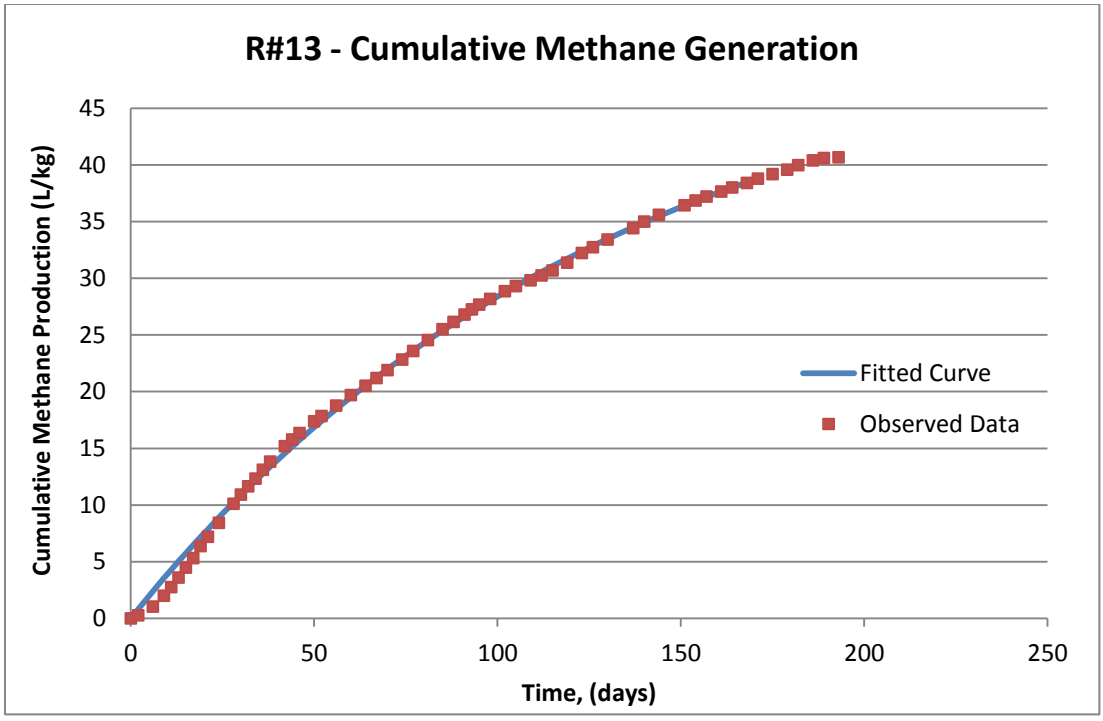

Figure C-11: Cumulative methane production rate for Reactor 13

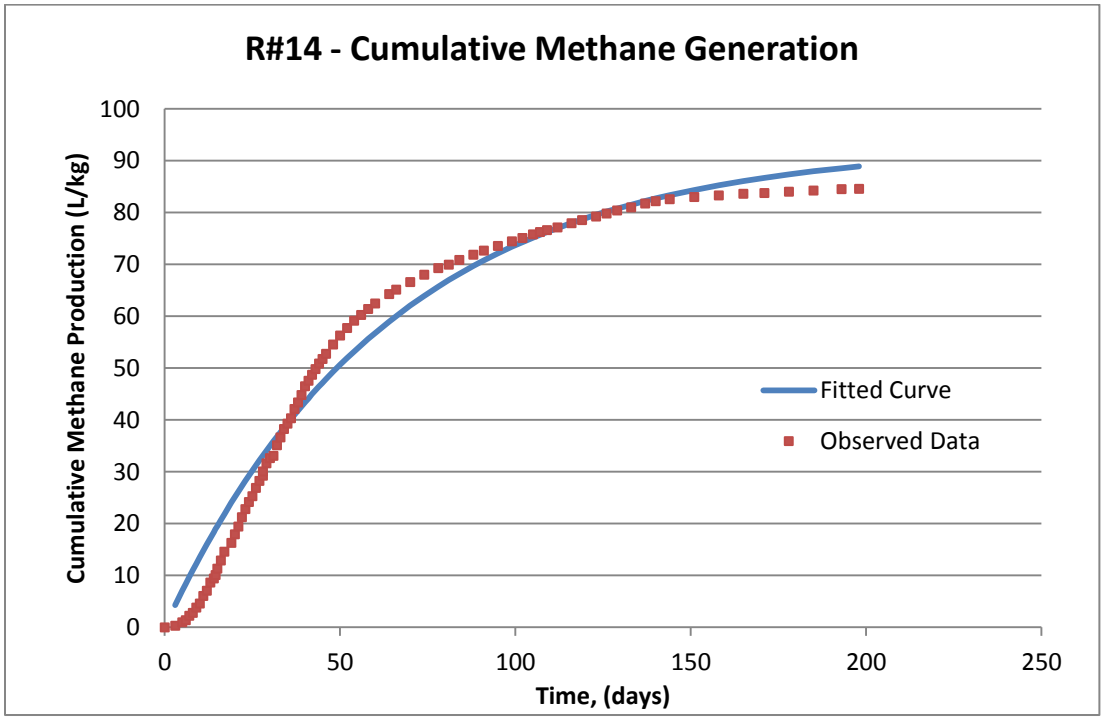

Figure C-12: Cumulative methane production rate for Reactor 14

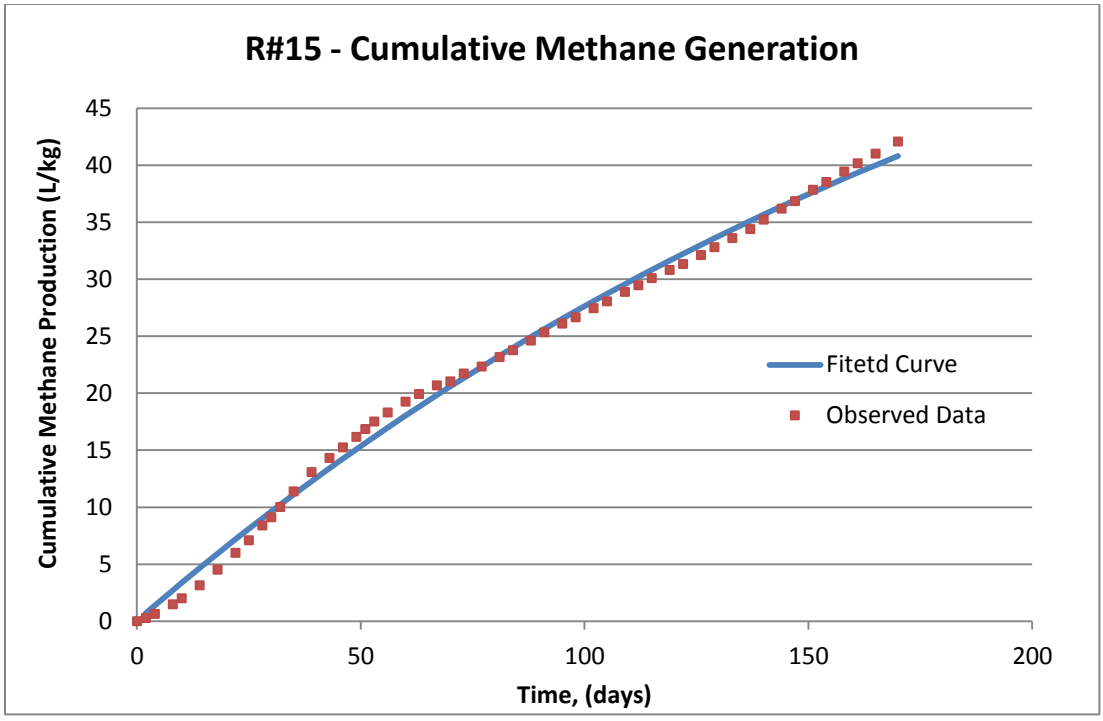

Figure C-13: Cumulative methane production rate for Reactor 15

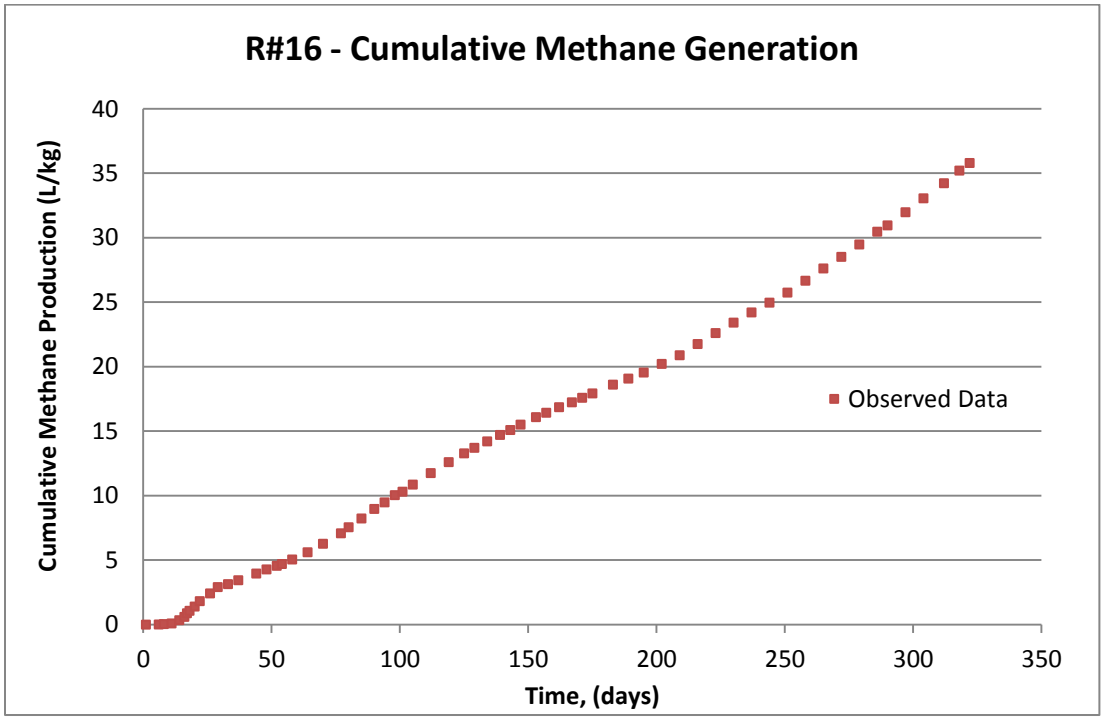

Figure C-14: Cumulative methane production rate for Reactor 16

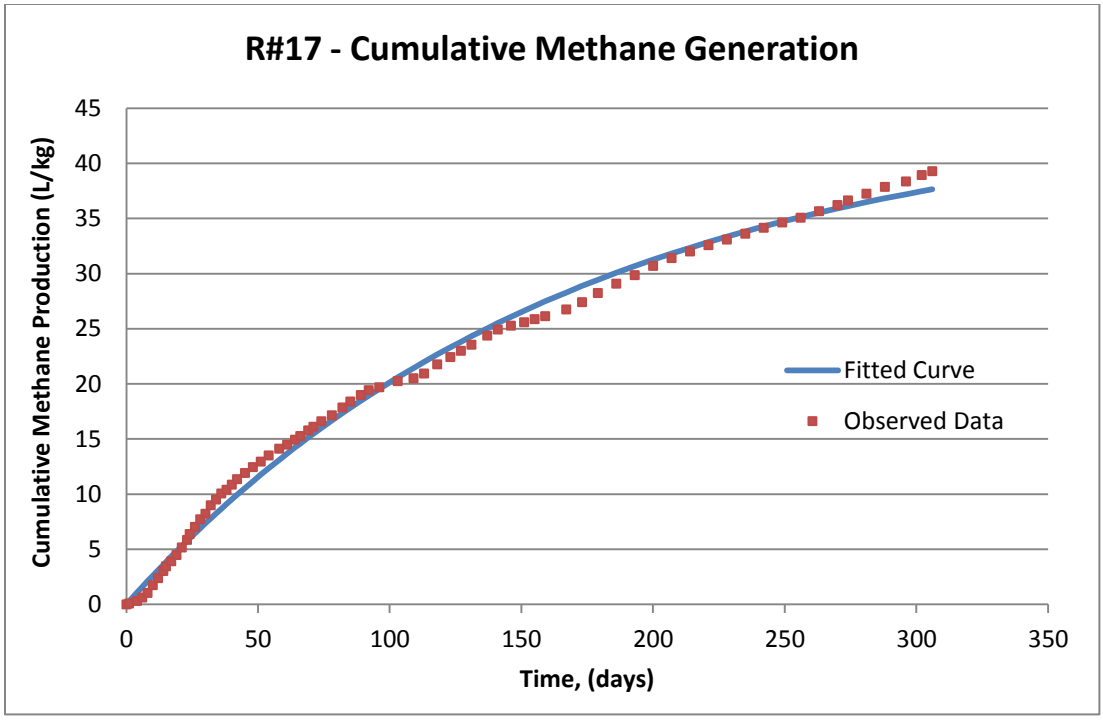

Figure C-15: Cumulative methane production rate for Reactor 17

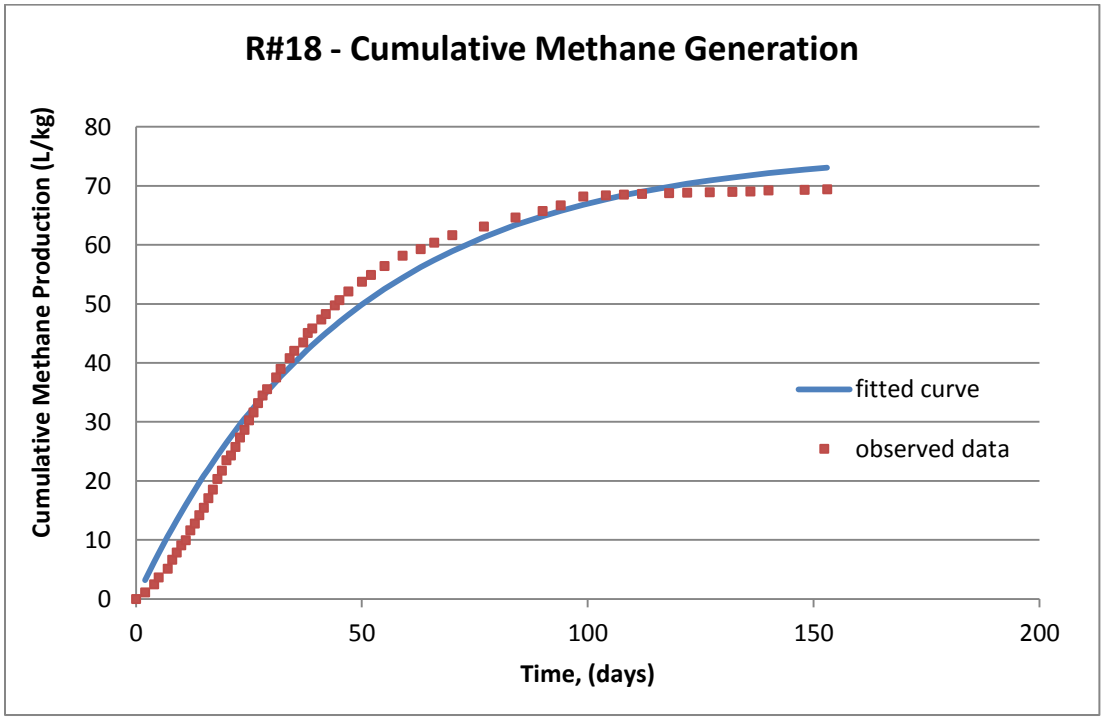

Figure C-16: Cumulative methane production rate for Reactor 18

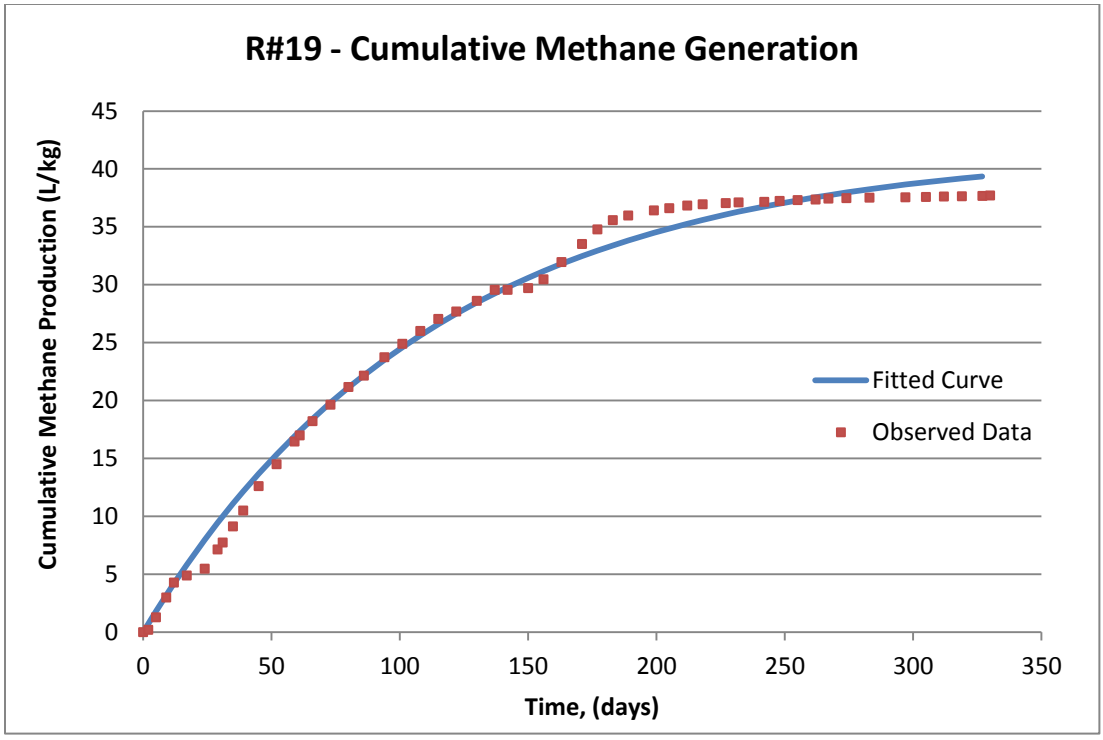

Figure C-17: Cumulative methane production rate for Reactor 19

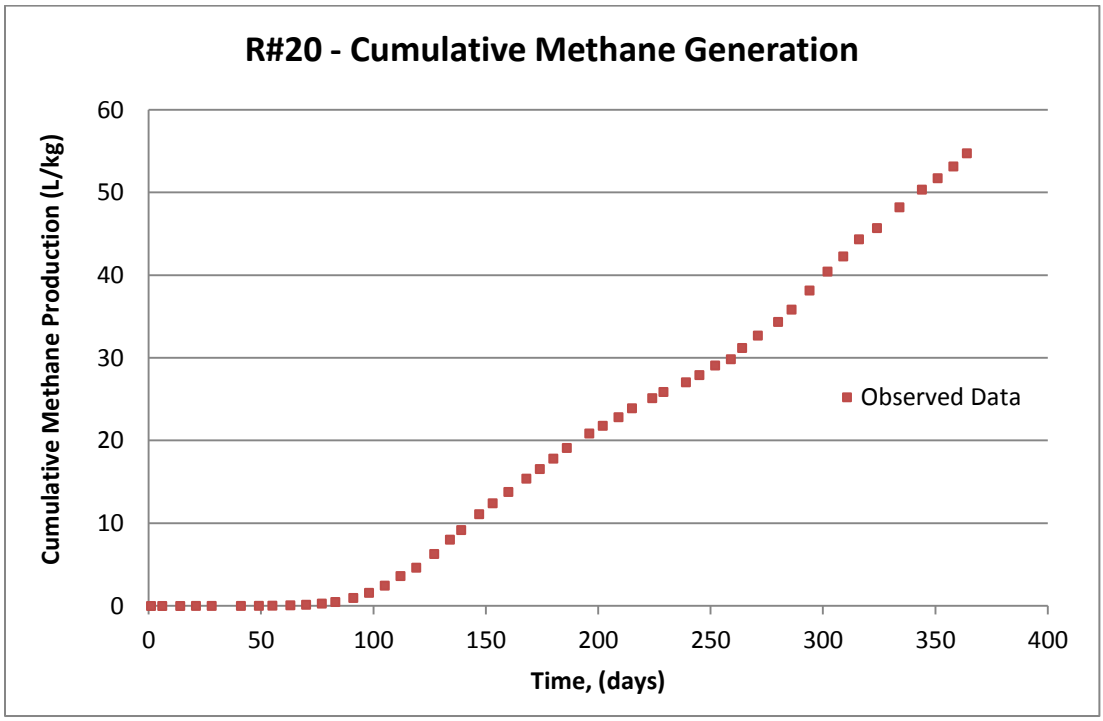

Figure C-18: Cumulative methane production rate for Reactor 20

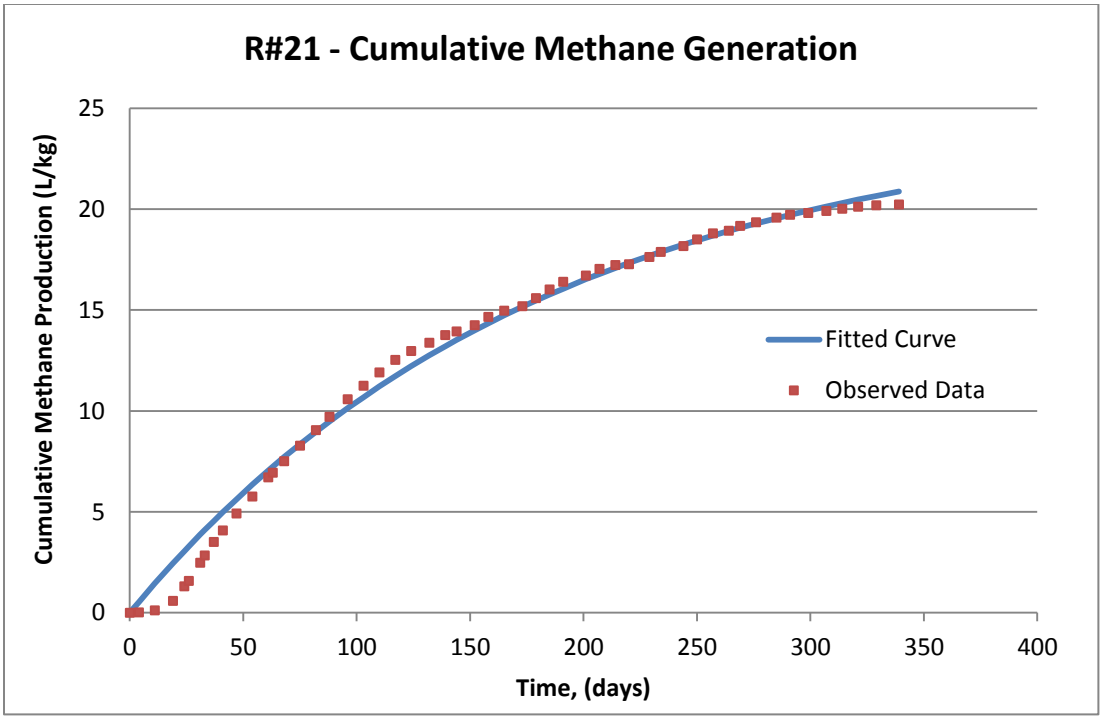

Figure C-19: Cumulative methane production rate for Reactor 21

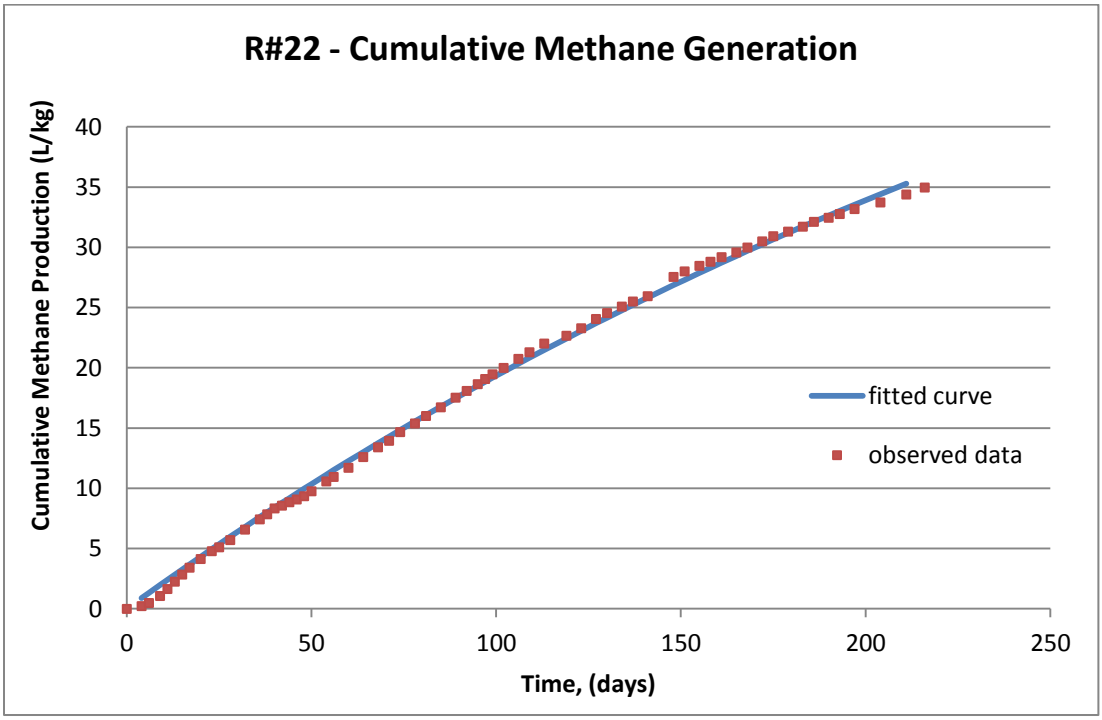

Figure C-20: Cumulative methane production rate for Reactor 22

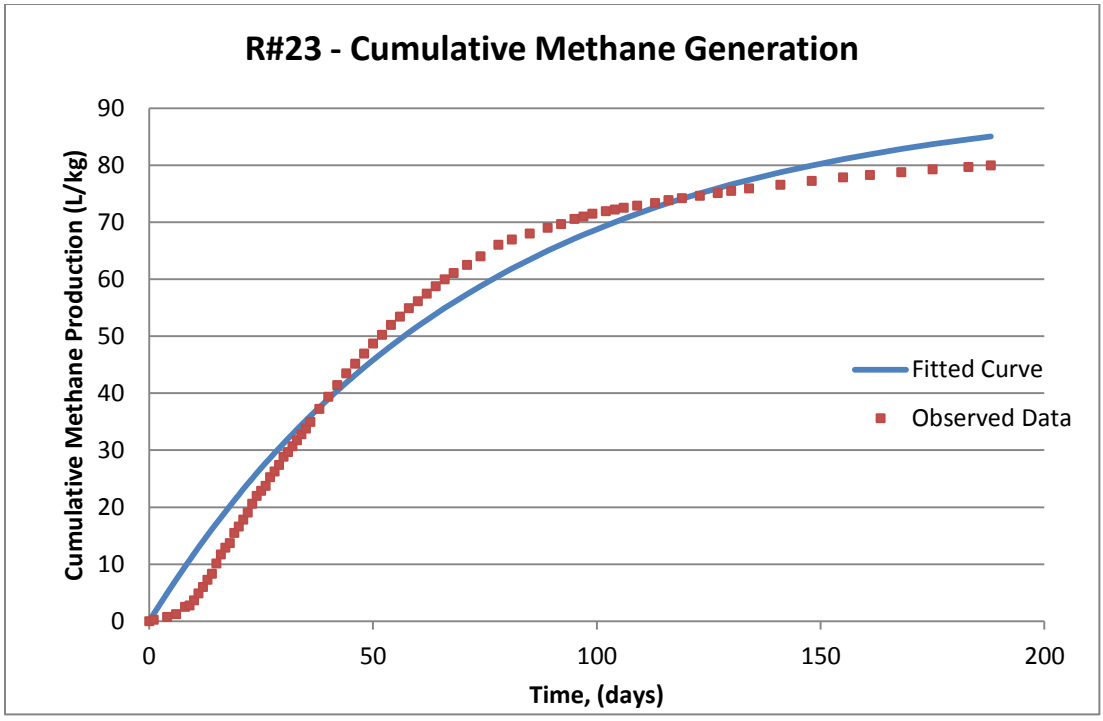

Figure C-21: Cumulative methane production rate for Reactor 23

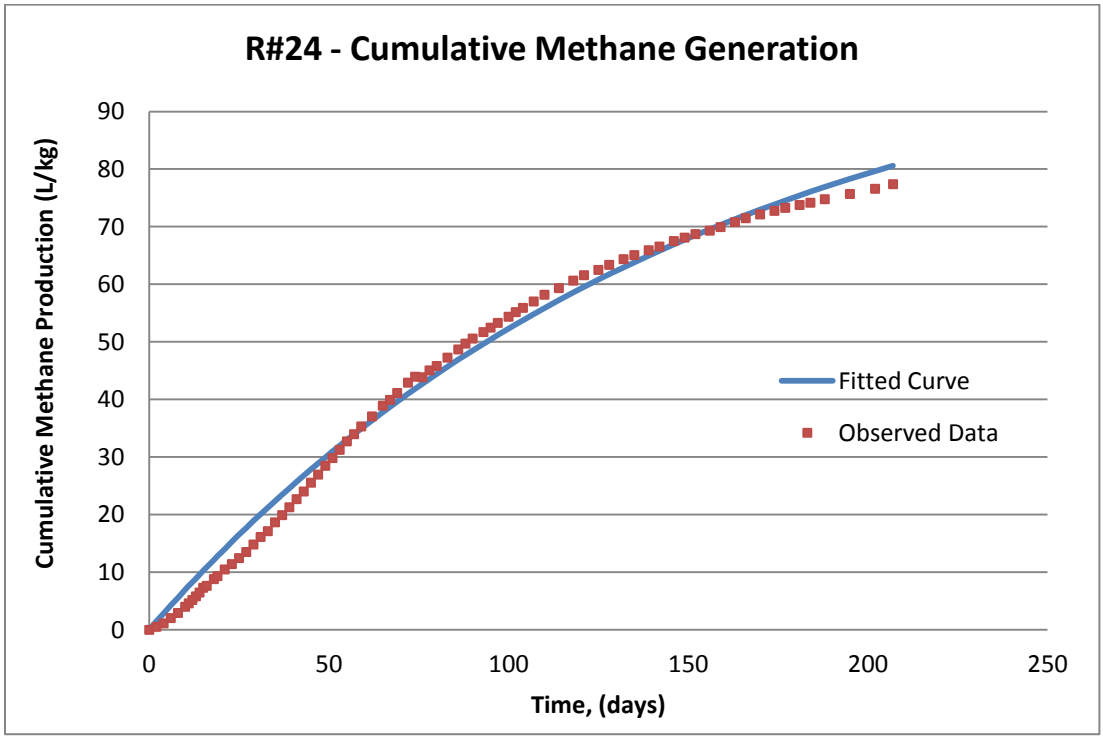

Figure C-22: Cumulative methane production rate for Reactor 24

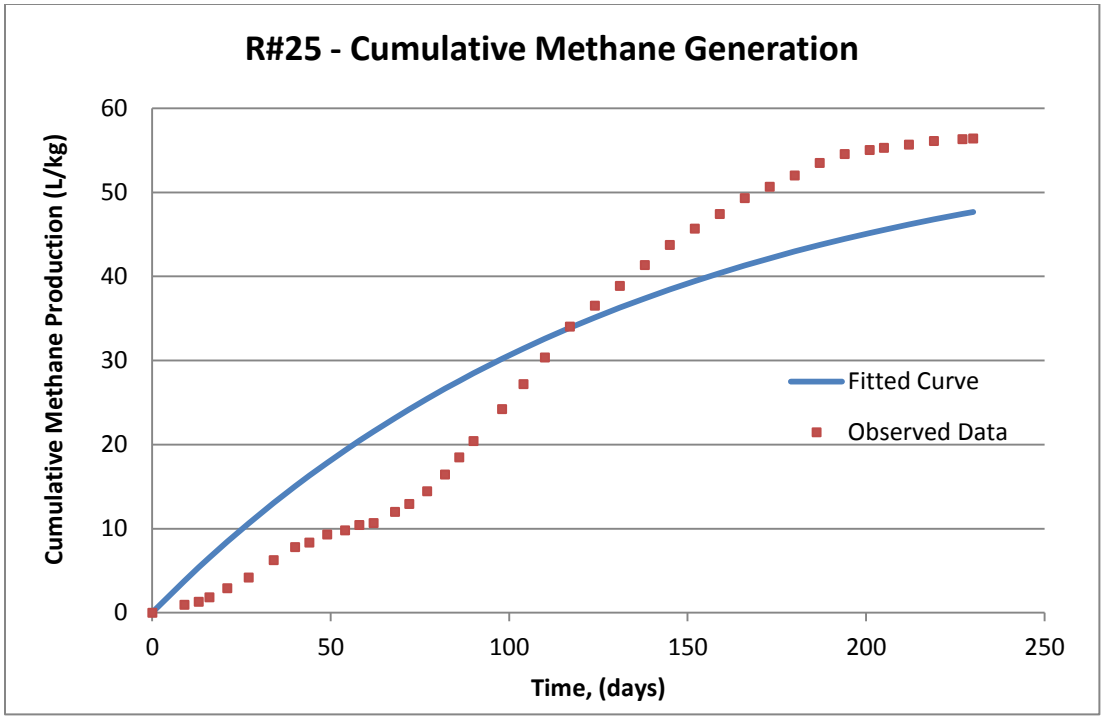

Figure C-23: Cumulative methane production rate for Reactor 25

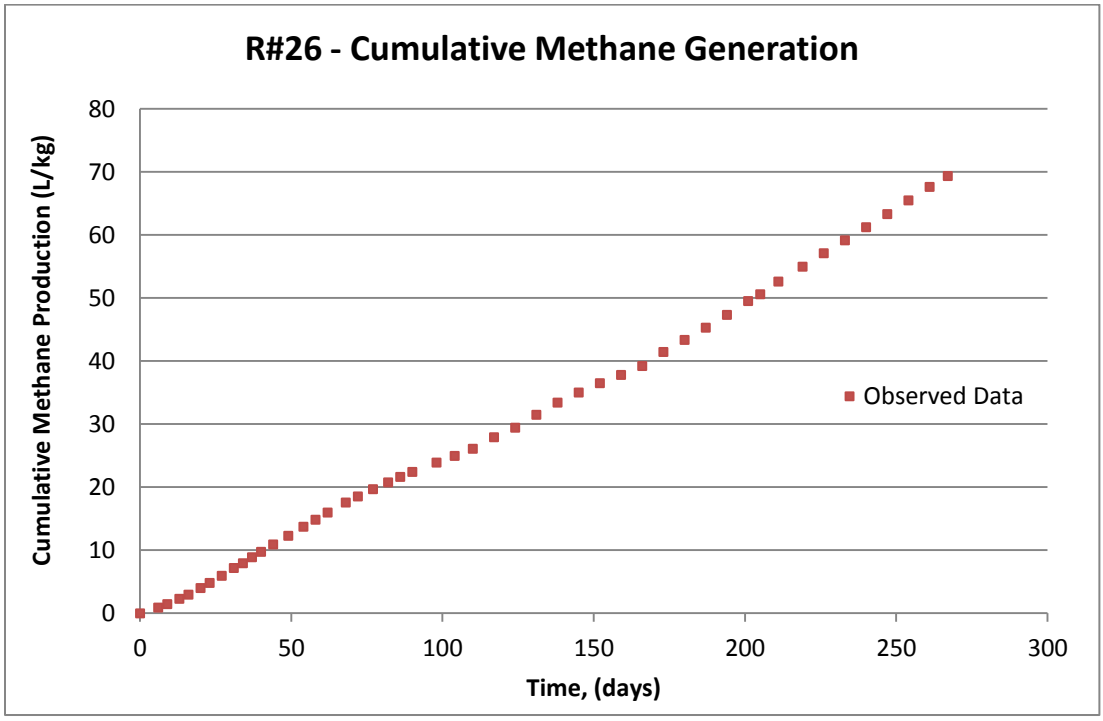

Figure C-24: Cumulative methane production rate for Reactor 26

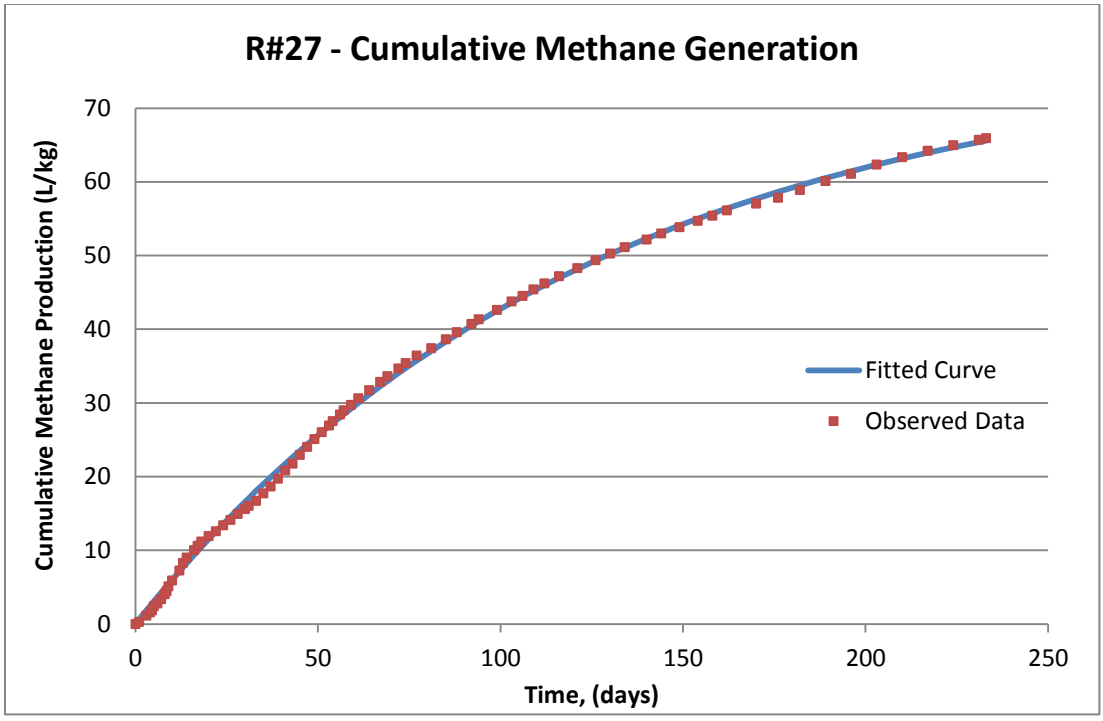

Figure C-25: Cumulative methane production rate for Reactor 27

APPENDIX D

MODEL DEVELOPMENT: SAS OUTPUTS

D-1: SAS Output for Square Root *k* Transformation

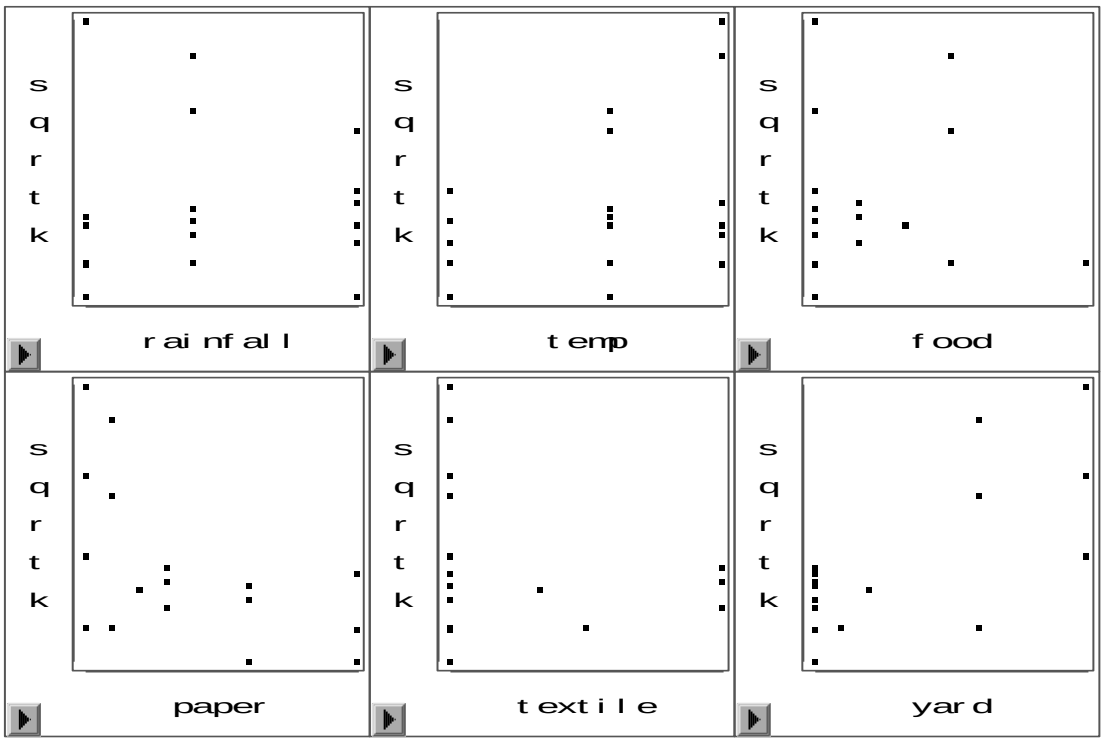

The REG Procedure
Model: MODEL1
Dependent Variable: sqrtk

Number of Observations Read	18
Number of Observations Used	18

Analysis of Variance

Source	DF	Sum of Squares	Mean Square	F Value	Pr > F
Model	6	3.91417	0.65236	4.46	0.0157
Error	11	1.60909	0.14628		
Corrected Total	17	5.52326			

Root MSE	0.38247	**R-Square**	0.7087
Dependent Mean	1.70497	**Adj R-Sq**	0.5498
Coeff Var	22.43254		

Parameter Estimates

Variable	DF	Parameter Estimate	Standard Error	t Value	Pr > |t|	Type I SS	Variance Inflation
Intercept	**1**	-9.27320	4.37758	-2.12	0.0577	52.32439	0
rainfall	**1**	0.00281	0.02427	0.12	0.9098	0.00372	1.22426
temp	**1**	0.03462	0.01394	2.48	0.0304	0.83976	1.05061
food	**1**	-0.00119	0.00876	-0.14	0.8941	0.00298	2.47363
paper	**1**	0.00163	0.00775	0.21	0.8376	2.18588	8.97250
textile	**1**	0.00457	0.00695	0.66	0.5247	0.32075	2.98122
yard	**1**	0.01280	0.00653	1.96	0.0760	0.56108	7.61798

The REG Procedure
Model: MODEL1
Dependent Variable: sqrtk

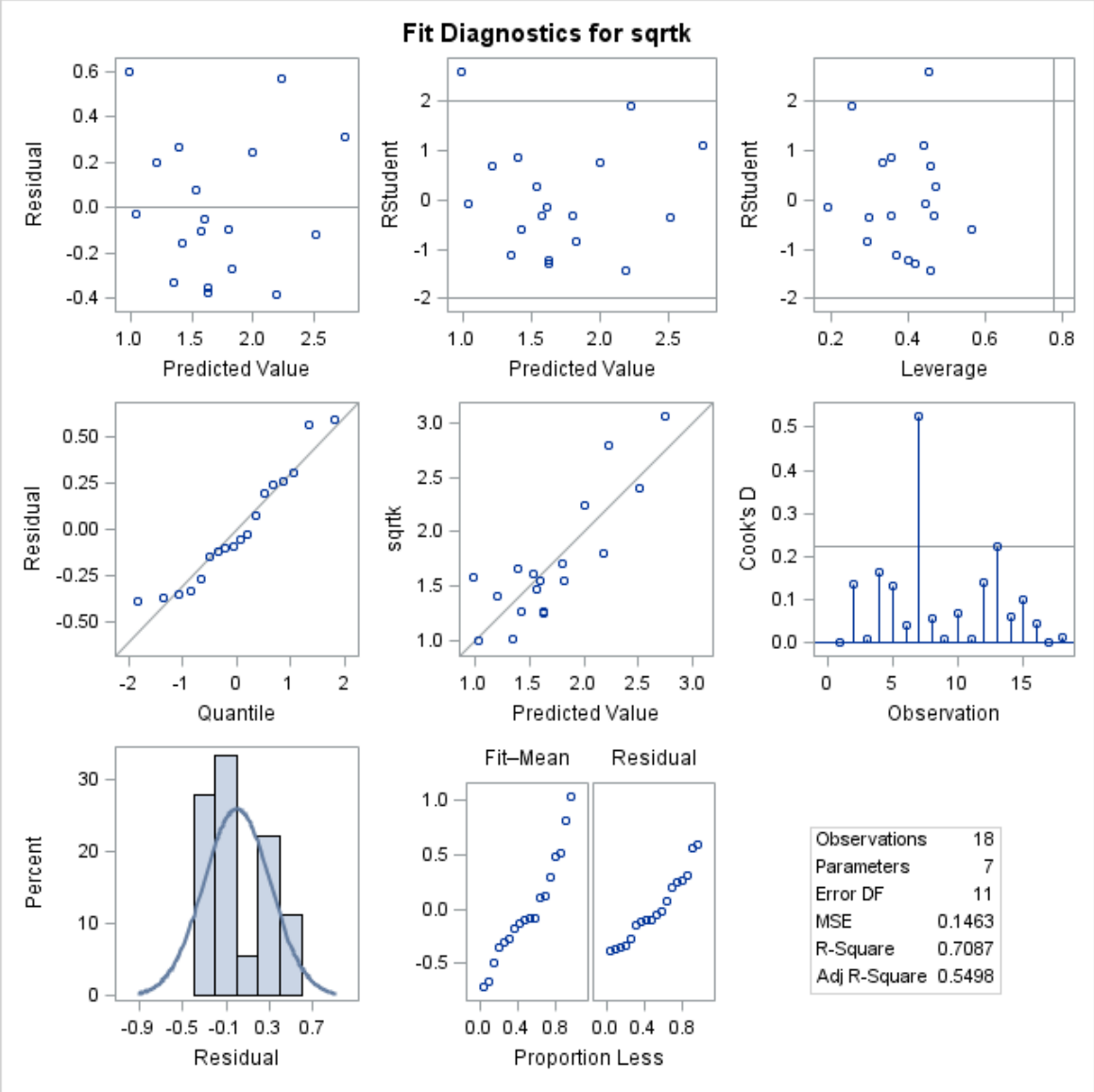

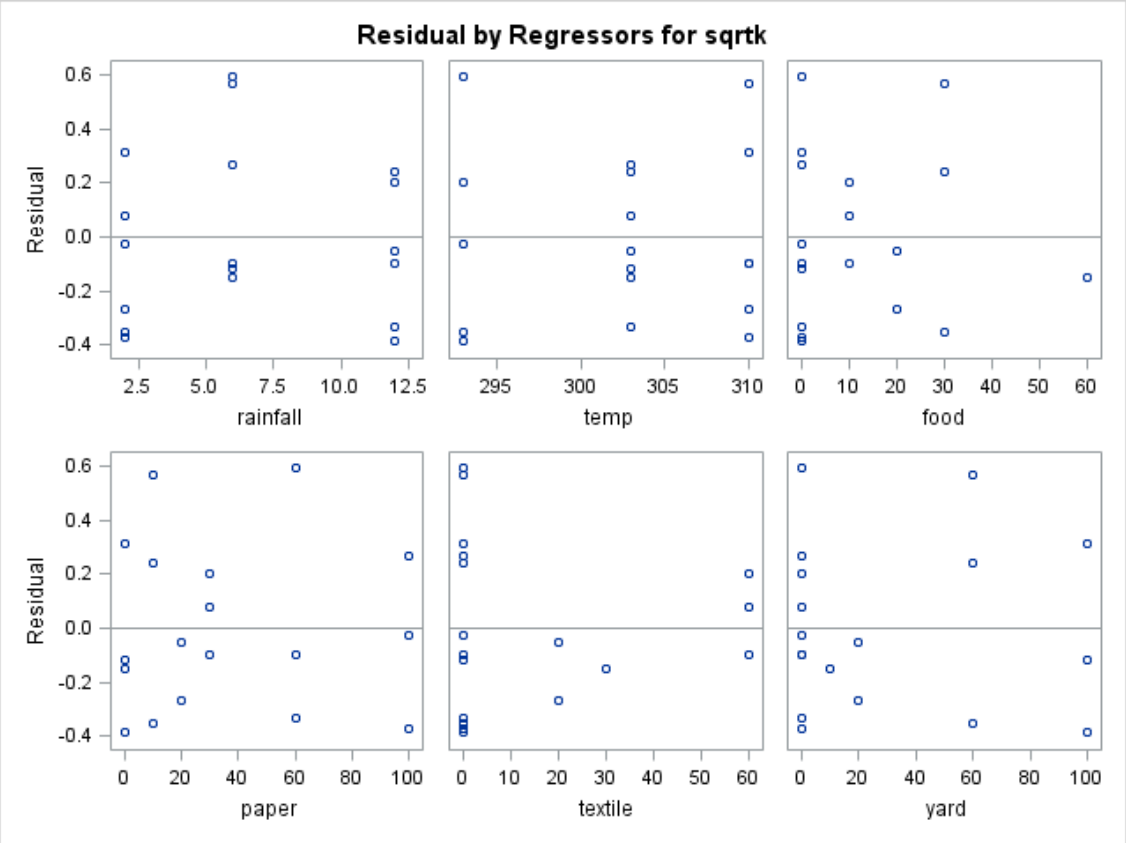
Residual by Regressors for sqrtk
Residual
0.6
0.4
0.2
0.0
-0.2
-0.4
2.5
5.0
7.5
10.0
12.5
rainfall
295
300
305
310
temp
0
10
20
30
40
50
60
food
paper
0
20
40
60
80
100
textile
yard

D-2: SAS Output for Log K Transformation

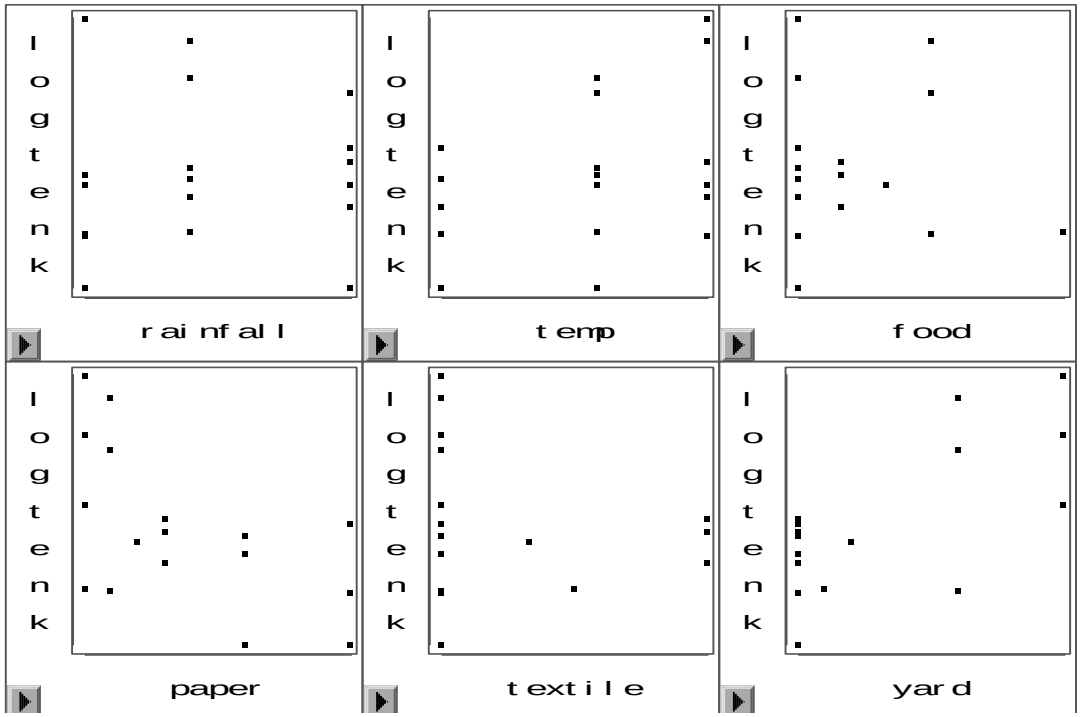

The SAS System

The REG Procedure
Model: MODEL1
Dependent Variable: logtenk

Number of Observations Read	18
Number of Observations Used	18

Analysis of Variance

Source	DF	Sum of Squares	Mean Square	F Value	Pr > F
Model	6	0.84213	0.14035	4.04	0.0219
Error	11	0.38213	0.03474		
Corrected Total	17	1.22425			

Root MSE	0.18638	**R-Square**	0.6879
Dependent Mean	0.42248	**Adj R-Sq**	0.5176
Coeff Var	44.11631		

Parameter Estimates							
Variable	**DF**	**Parameter Estimate**	**Standard Error**	**t Value**	**Pr > |t|**	**Type I SS**	**Variance Inflation**
Intercept	**1**	-4.65561	2.13328	-2.18	0.0517	3.21284	0
rainfall	**1**	0.00336	0.01183	0.28	0.7818	0.00068542	1.22426
temp	**1**	0.01600	0.00680	2.36	0.0381	0.18383	1.05061
food	**1**	-0.00082859	0.00427	-0.19	0.8497	0.00021338	2.47363
paper	**1**	0.00047127	0.00378	0.12	0.9030	0.49828	8.97250
textile	**1**	0.00260	0.00339	0.77	0.4589	0.04367	2.98122
yard	**1**	0.00581	0.00318	1.82	0.0956	0.11545	7.61798

The REG Procedure
Model: MODEL1
Dependent Variable: logtenk

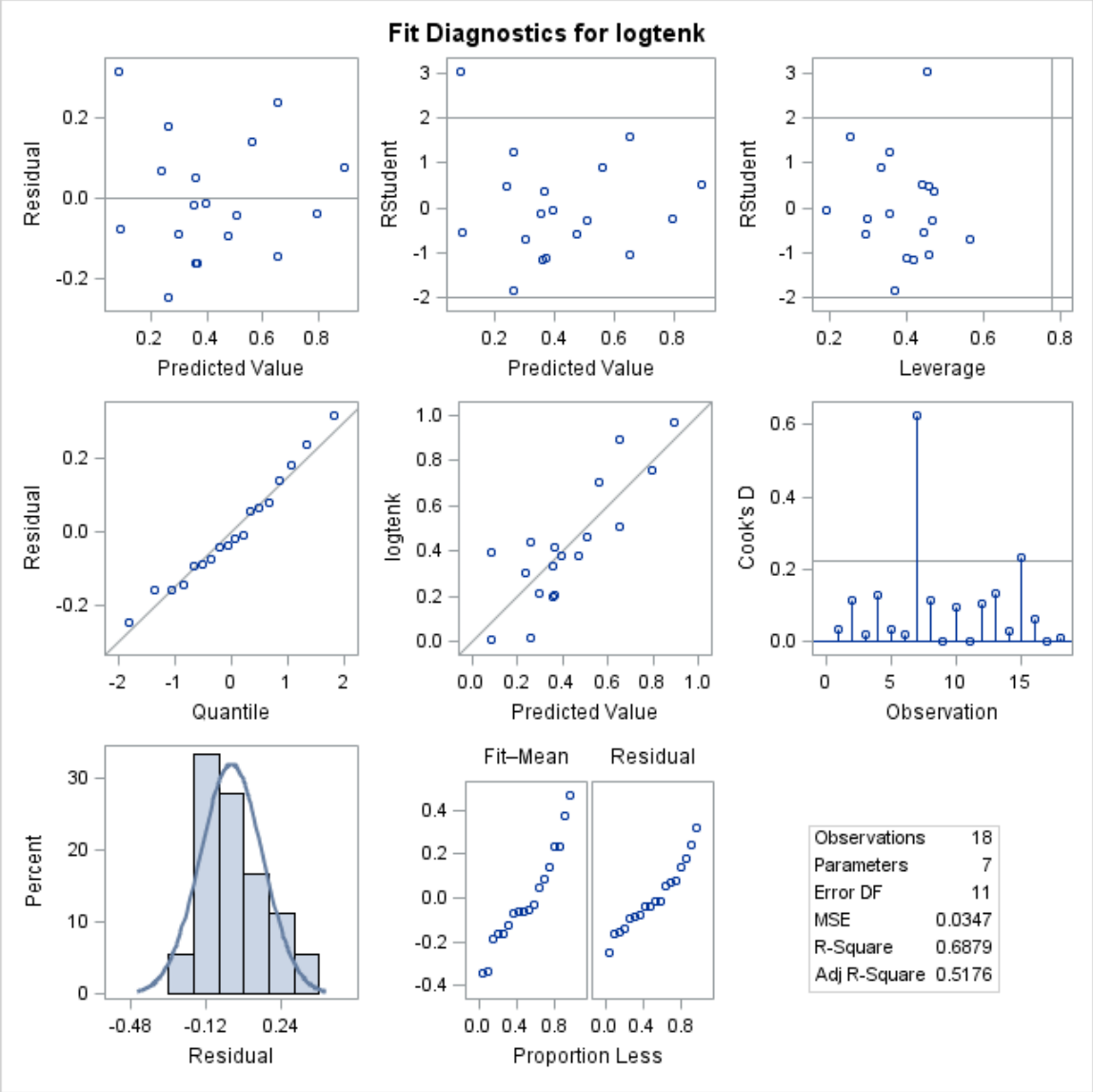

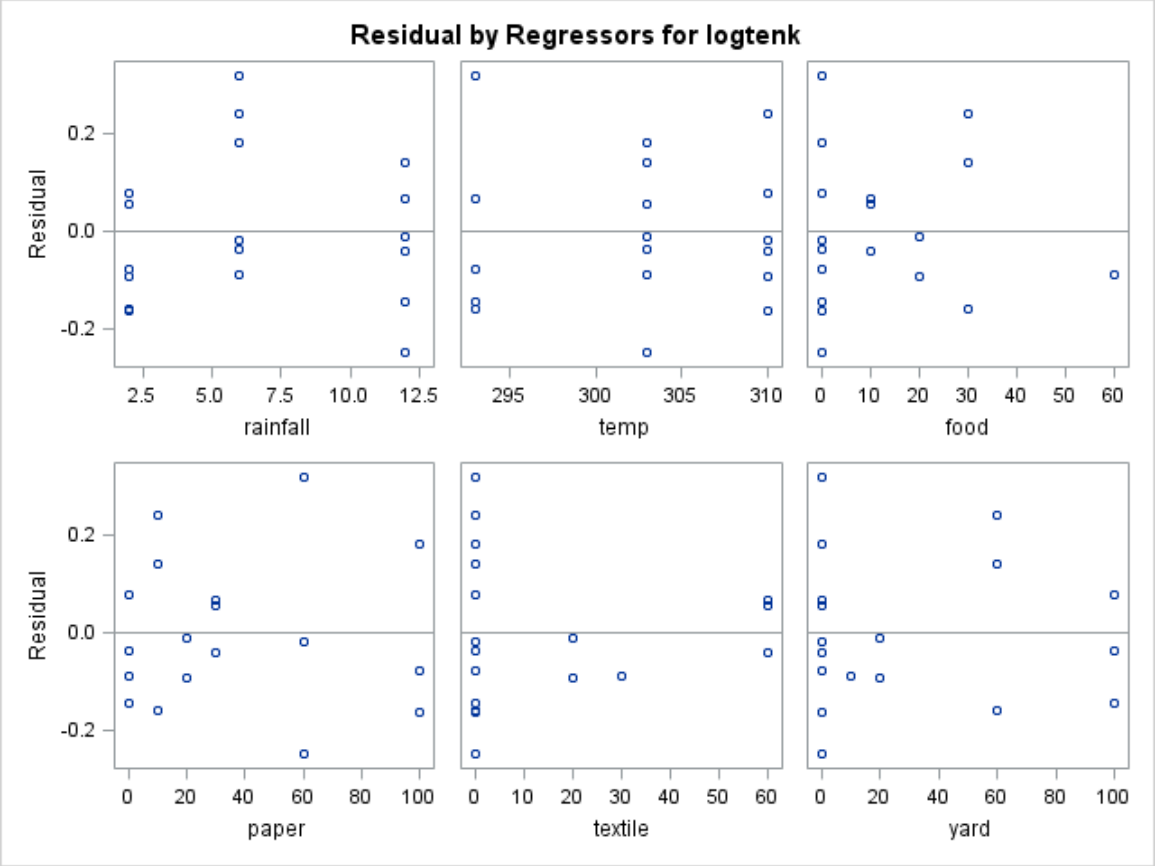
Residual by Regressors for logtenk
Residual
0.2
0.0
-0.2
2.5
5.0
7.5
10.0
12.5
rainfall
295
300
305
310
temp
0
10
20
30
40
50
60
food
0
20
40
60
80
100
paper
textile
yard

D-3: SAS Output for Inverse Square Root K Transformation

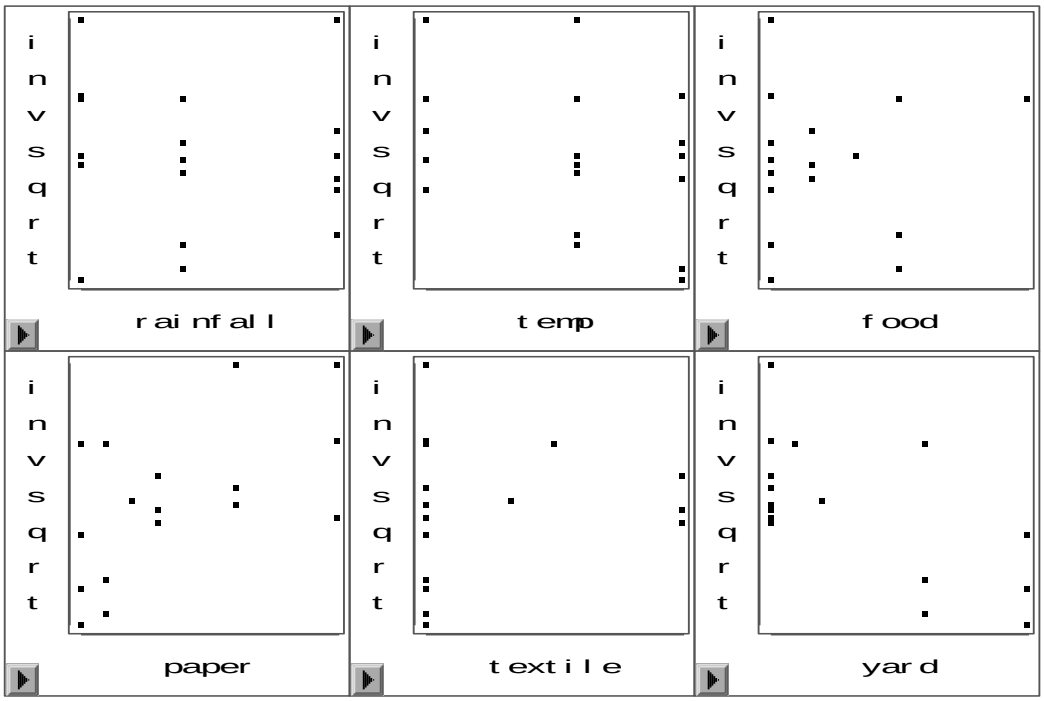

The REG Procedure
Model: MODEL1
Dependent Variable: invsqrtk

Number of Observations Read	18
Number of Observations Used	18

Analysis of Variance

Source	DF	Sum of Squares	Mean Square	F Value	Pr > F
Model	6	0.37327	0.06221	3.19	0.0458
Error	11	0.21464	0.01951		
Corrected Total	17	0.58791			

Root MSE	0.13969	**R-Square**	0.6349
Dependent Mean	0.64170	**Adj R-Sq**	0.4358
Coeff Var	21.76856		

Parameter Estimates

Variable	DF	Parameter Estimate	Standard Error	t Value	Pr > |t|	Type I SS	Variance Inflation
Intercept	**1**	3.99704	1.59883	2.50	0.0295	7.41204	0
rainfall	**1**	-0.00301	0.00886	-0.34	0.7402	0.00226	1.22426
temp	**1**	-0.01060	0.00509	-2.08	0.0615	0.08362	1.05061
food	**1**	0.00077871	0.00320	0.24	0.8123	0.00000791	2.47363
paper	**1**	-0.00000943	0.00283	-0.00	0.9974	0.23287	8.97250
textile	**1**	-0.00207	0.00254	-0.82	0.4316	0.00858	2.98122
yard	**1**	-0.00366	0.00239	-1.53	0.1532	0.04593	7.61798

The REG Procedure
Model: MODEL1
Dependent Variable: invsqrtk

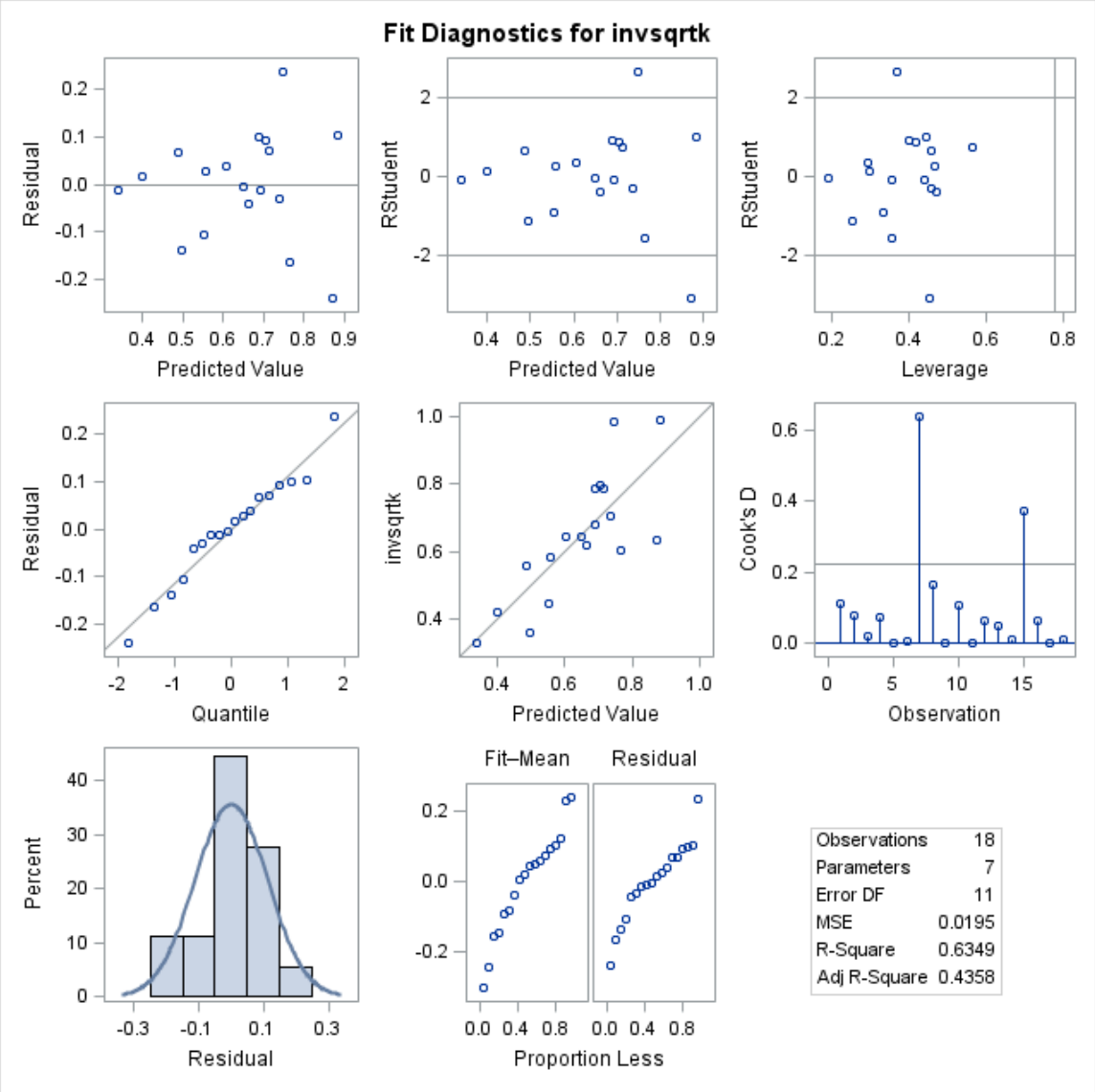

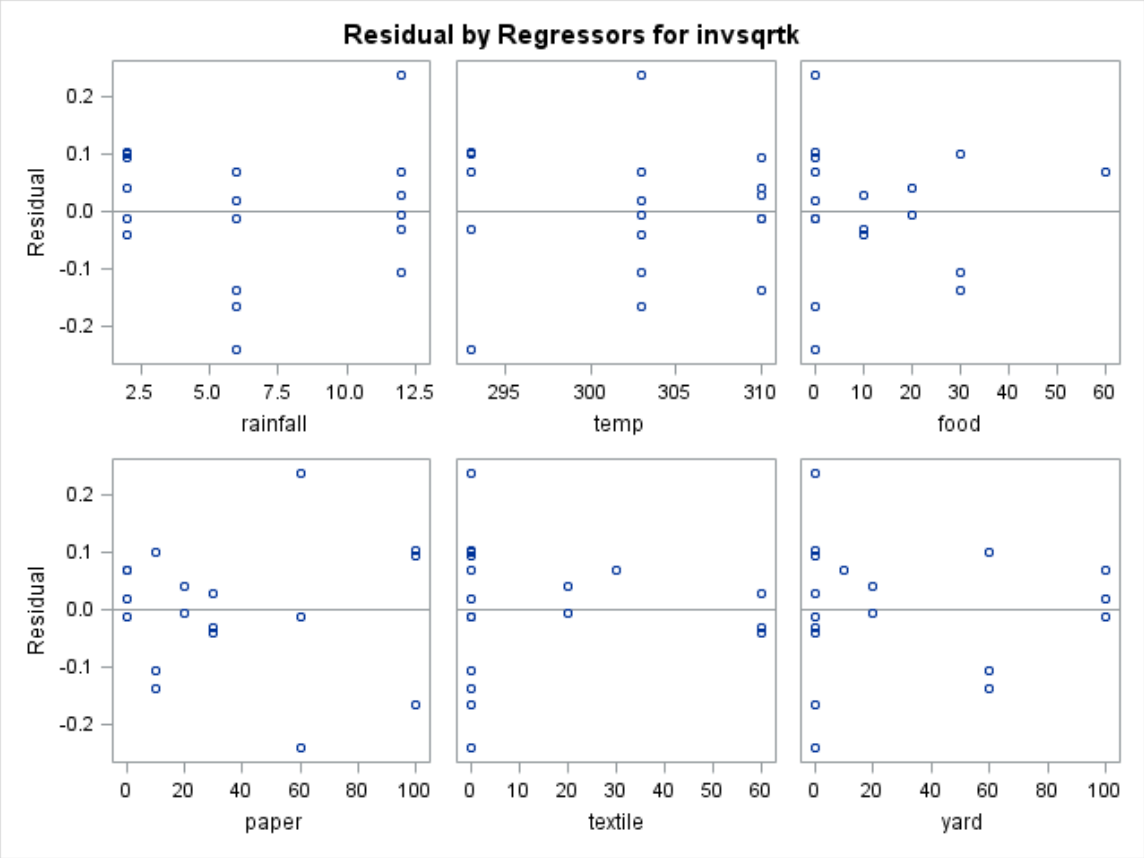
Residual by Regressors for invsqrtk
Residual
0.2
0.1
0.0
-0.1
-0.2
2.5
5.0
7.5
10.0
12.5
rainfall
295
300
305
310
temp
0
10
20
30
40
50
60
food
0
20
40
60
80
100
paper
textile
yard

D-4 SAS Output for Log K with Quadratic Transformation for Rainfall and Temperature

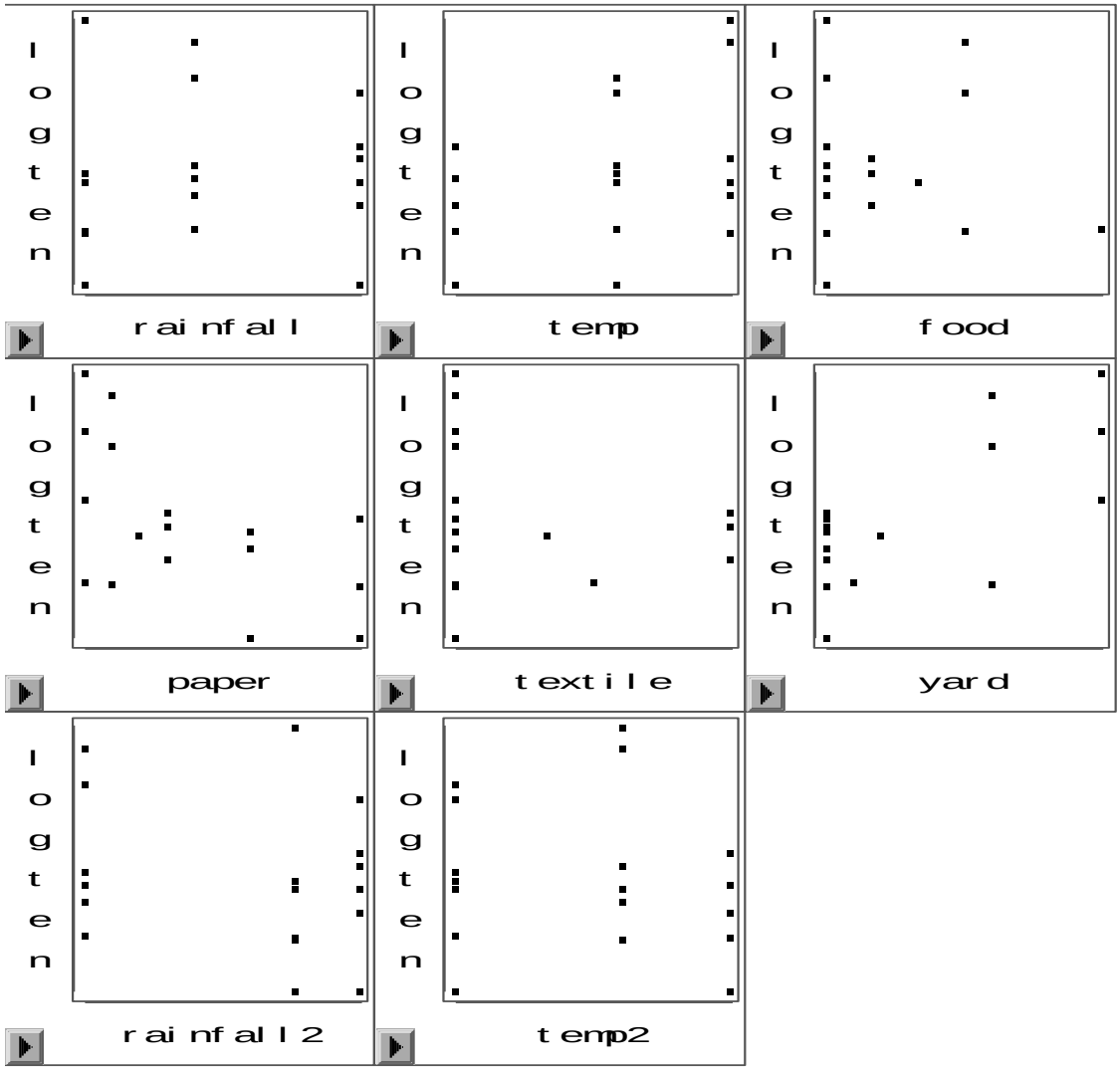

The REG Procedure
Model: MODEL1
Dependent Variable: logtenk

Number of Observations Read	18
Number of Observations Used	18

Analysis of Variance

Source	DF	Sum of Squares	Mean Square	F Value	Pr > F
Model	8	0.95226	0.11903	3.94	0.0283
Error	9	0.27200	0.03022		
Corrected Total	17	1.22425			

Root MSE	0.17384	**R-Square**	0.7778
Dependent Mean	0.42248	**Adj R-Sq**	0.5803
Coeff Var	41.14841		

Parameter Estimates

Variable	DF	Parameter Estimate	Standard Error	t Value	Pr > |t|	Type I SS	Variance Inflation
Intercept	**1**	-4.67309	2.28151	-2.05	0.0708	3.21284	0
rainfall	**1**	0.01096	0.01217	0.90	0.3913	0.00068542	1.49095
rainfall2	**1**	-0.13752	0.07205	-1.91	0.0886	0.06616	1.37895
temp	**1**	0.01593	0.00717	2.22	0.0535	0.16363	1.34455
temp2	**1**	0.02053	0.06107	0.34	0.7445	0.01163	1.44999
food	**1**	-0.00081868	0.00409	-0.20	0.8456	0.00029020	2.60160
paper	**1**	0.00149	0.00357	0.42	0.6869	0.53500	9.22357
textile	**1**	0.00476	0.00336	1.42	0.1897	0.01499	3.36389
yard	**1**	0.00698	0.00303	2.30	0.0470	0.15987	7.95142

The REG Procedure
Model: MODEL1
Dependent Variable: logtenk

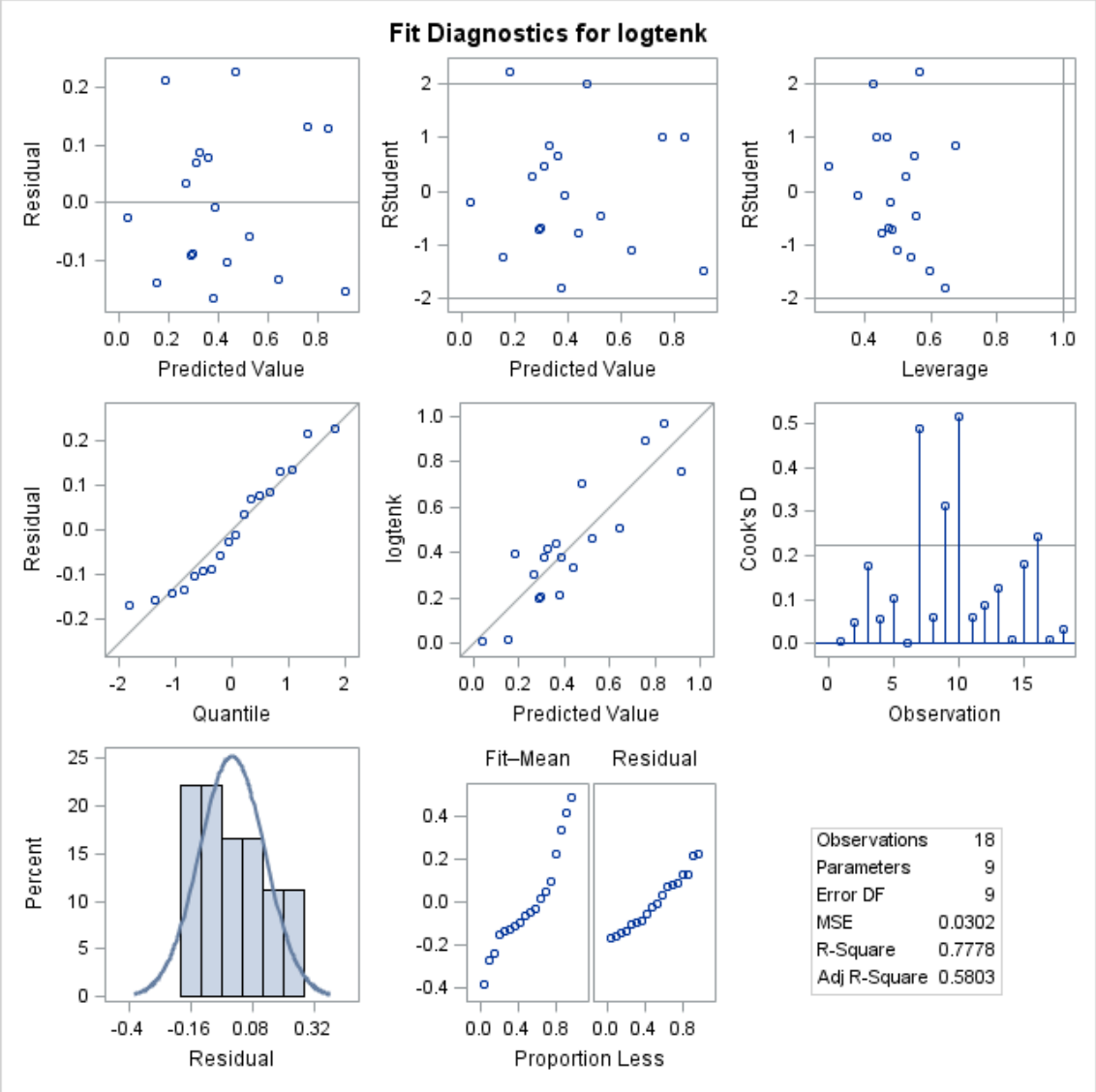

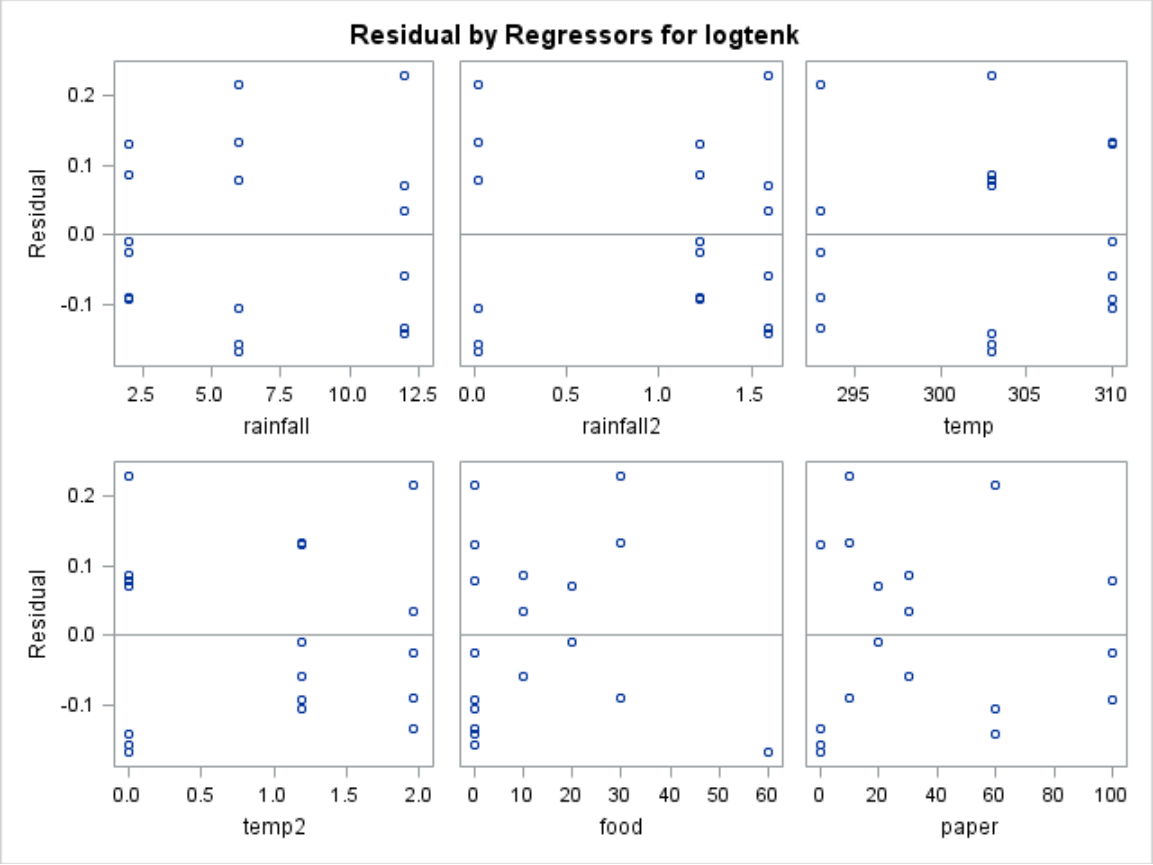
Residual by Regressors for logtenk
Residual
0.2
0.1
0.0
-0.1
2.5
5.0
7.5
10.0
12.5
rainfall
0.0
0.5
1.0
1.5
rainfall2
295
300
305
310
temp
0.0
0.5
1.0
1.5
2.0
temp2
0
10
20
30
40
50
60
food
0
20
40
60
80
100
paper

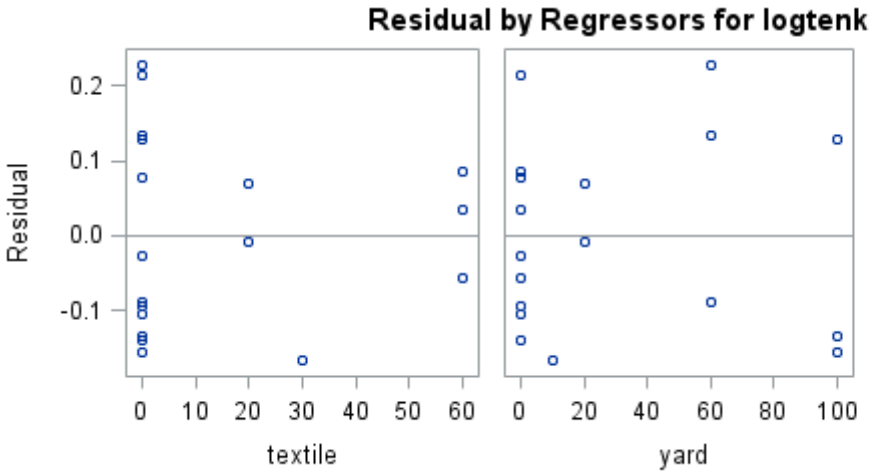
Residual by Regressors for logtenk
Residual
0.2
0.1
0.0
-0.1
0
10
20
30
40
50
60
textile
0
20
40
60
80
100
yard

D-5: SAS Output For Log K with Quadratic Transformation for Rainfall, Temperature and Textile

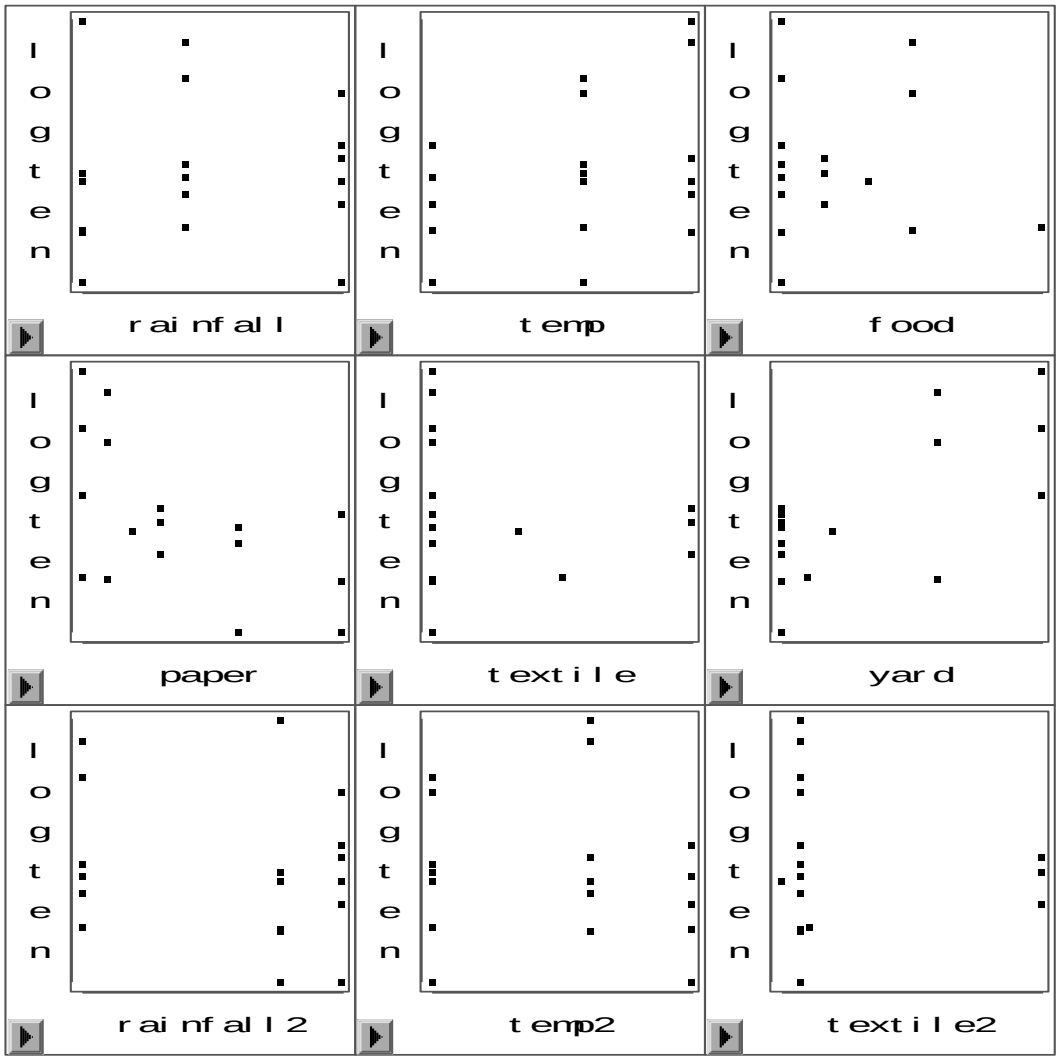

The REG Procedure
Model: MODEL1
Dependent Variable: logtenk

Number of Observations Read	18
Number of Observations Used	18

Analysis of Variance

Source	DF	Sum of Squares	Mean Square	F Value	Pr > F
Model	9	0.96483	0.10720	3.31	0.0533
Error	8	0.25942	0.03243		
Corrected Total	17	1.22425			

Root MSE	0.18008	**R-Square**	0.7881
Dependent Mean	0.42248	**Adj R-Sq**	0.5497
Coeff Var	42.62352		

Parameter Estimates

Variable	DF	Parameter Estimate	Standard Error	t Value	Pr > |t|	Type I SS	Variance Inflation
Intercept	**1**	-4.66735	2.36332	-1.97	0.0837	3.21284	0
rainfall	**1**	0.00919	0.01293	0.71	0.4976	0.00068542	1.56727
rainfall2	**1**	-0.12836	0.07607	-1.69	0.1300	0.06616	1.43253
temp	**1**	0.01614	0.00743	2.17	0.0618	0.16363	1.34733
temp2	**1**	0.01192	0.06475	0.18	0.8585	0.01163	1.51921
food	**1**	-0.00022138	0.00434	-0.05	0.9606	0.00029020	2.73524
paper	**1**	0.00051871	0.00401	0.13	0.9004	0.53500	10.85255
textile	**1**	0.00004697	0.00833	0.01	0.9956	0.01499	19.31128
textile2	**1**	0.06563	0.10538	0.62	0.5508	0.07464	11.59881
yard	**1**	0.00605	0.00348	1.74	0.1206	0.09781	9.75577

The REG Procedure
Model: MODEL1
Dependent Variable: logtenk

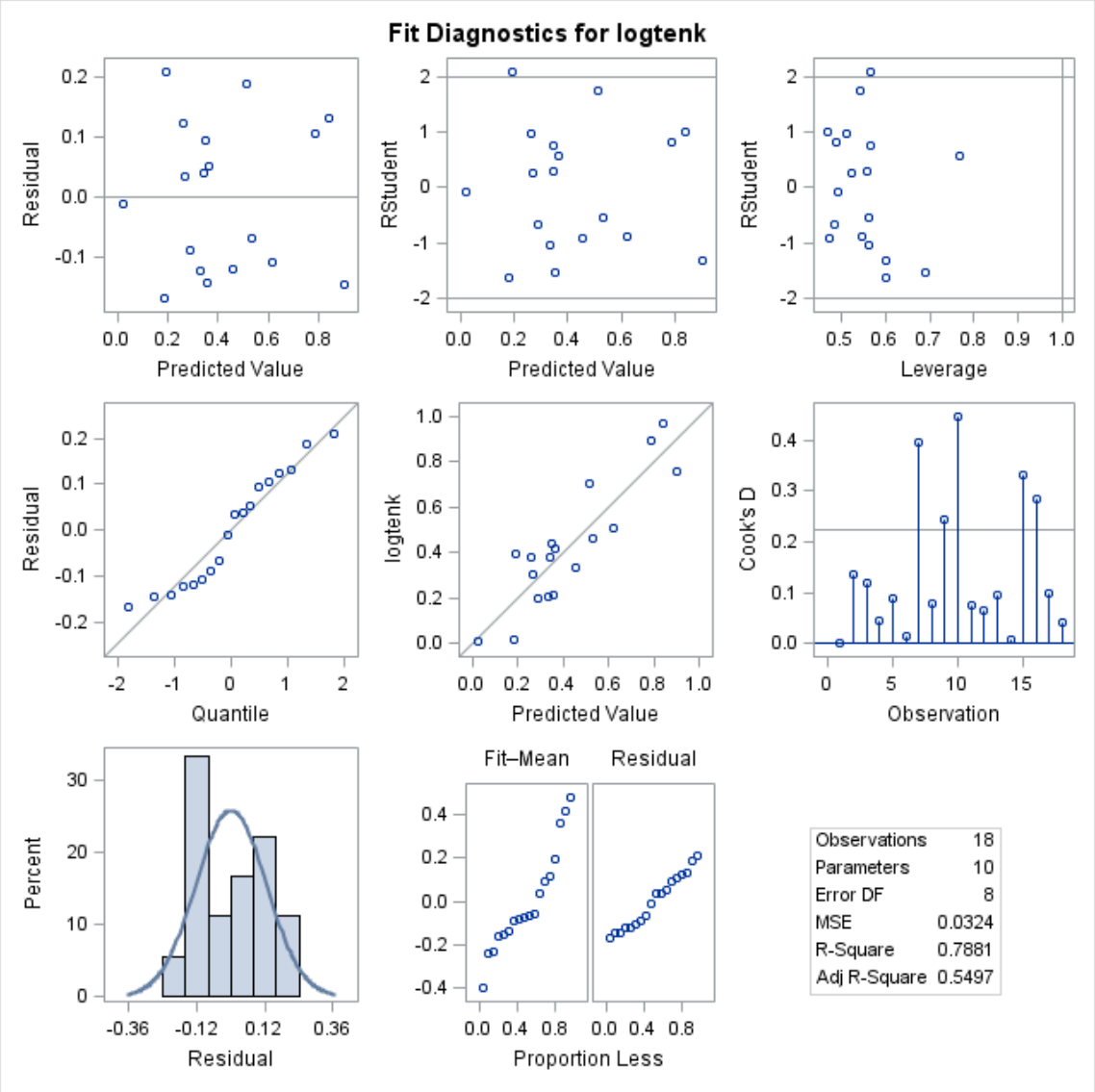

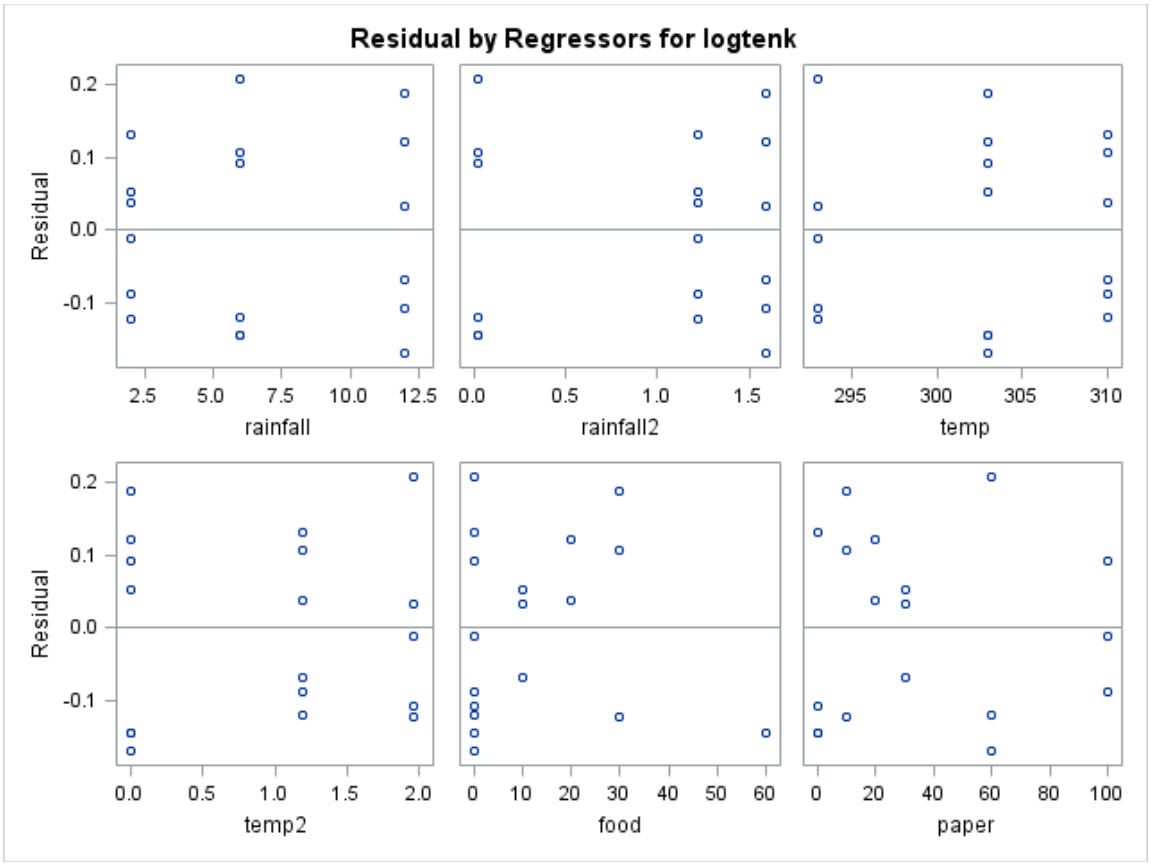
Residual by Regressors for logtenk
Residual
0.2
0.1
0.0
-0.1
2.5 5.0 7.5 10.0 12.5
rainfall
0.0 0.5 1.0 1.5
rainfall2
295 300 305 310
temp
0.0 0.5 1.0 1.5 2.0
temp2
0 10 20 30 40 50 60
food
0 20 40 60 80 100
paper


Residual by Regressors for logtenk
Residual
0.2
0.1
0.0
-0.1
0 10 20 30 40 50 60
textile
0 1 2 3 4
textile2
0 20 40 60 80 100
yard

D-6: SAS Output for Log K with Quadratic Transformation for Rainfall, Temperature, Textile, and Yard

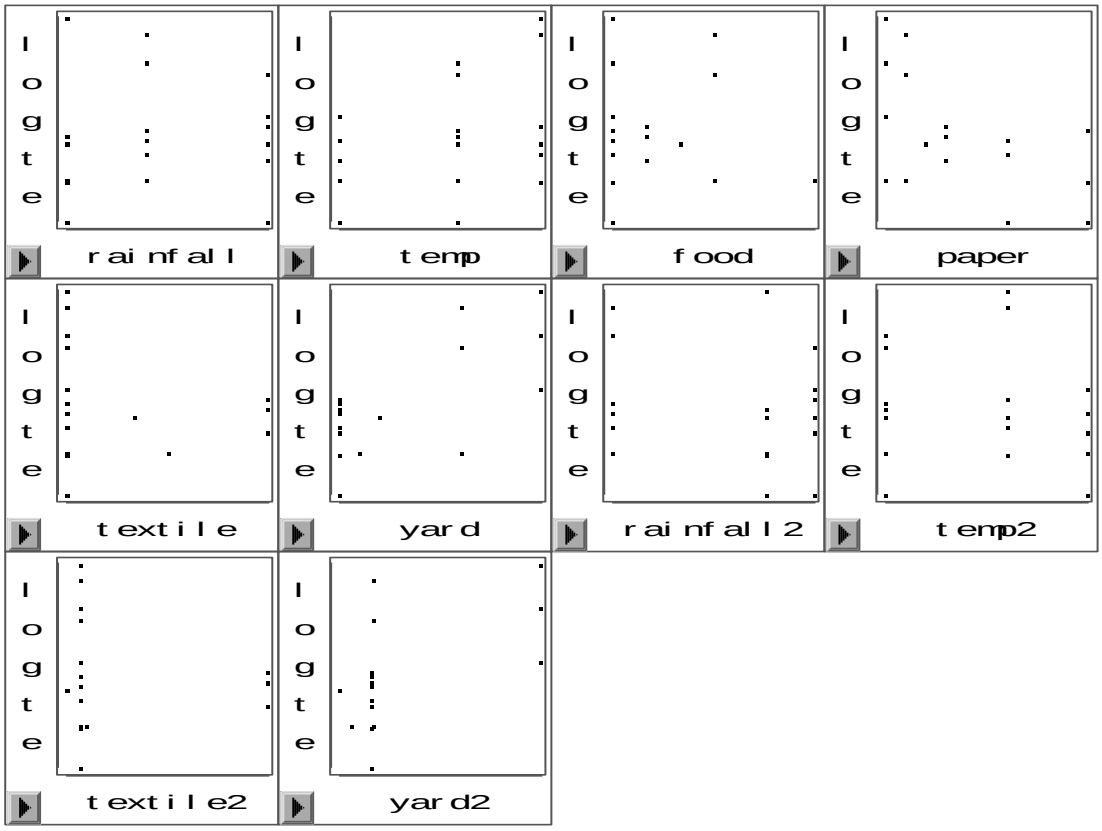

The REG Procedure
Model: MODEL1
Dependent Variable: logtenk

Number of Observations Read	18
Number of Observations Used	18

Analysis of Variance

Source	DF	Sum of Squares	Mean Square	F Value	Pr > F
Model	10	1.03040	0.10304	3.72	0.0472
Error	7	0.19385	0.02769		
Corrected Total	17	1.22425			

Root MSE	0.16641	**R-Square**	0.8417
Dependent Mean	0.42248	**Adj R-Sq**	0.6155
Coeff Var	39.38941		

Parameter Estimates

Variable	DF	Parameter Estimate	Standard Error	t Value	Pr > |t|	Type I SS	Variance Inflation
Intercept	**1**	-3.96527	2.23115	-1.78	0.1188	3.21284	0
rainfall	**1**	0.01045	0.01198	0.87	0.4118	0.00068542	1.57470
rainfall2	**1**	-0.18162	0.07836	-2.32	0.0536	0.06616	1.77983
temp	**1**	0.01398	0.00701	1.99	0.0863	0.16363	1.40320
temp2	**1**	0.00252	0.06015	0.04	0.9677	0.01163	1.53504
food	**1**	-0.00596	0.00547	-1.09	0.3126	0.00029020	5.09868
paper	**1**	0.00165	0.00378	0.44	0.6764	0.53500	11.27598
textile	**1**	0.00507	0.00836	0.61	0.5632	0.01499	22.78983
textile2	**1**	0.03005	0.10009	0.30	0.7727	0.07464	12.25247
yard	**1**	0.01178	0.00492	2.39	0.0480	0.09781	22.81809
yard2	**1**	-0.18523	0.12038	-1.54	0.1678	0.06557	10.22801

The REG Procedure
Model: MODEL1
Dependent Variable: logtenk

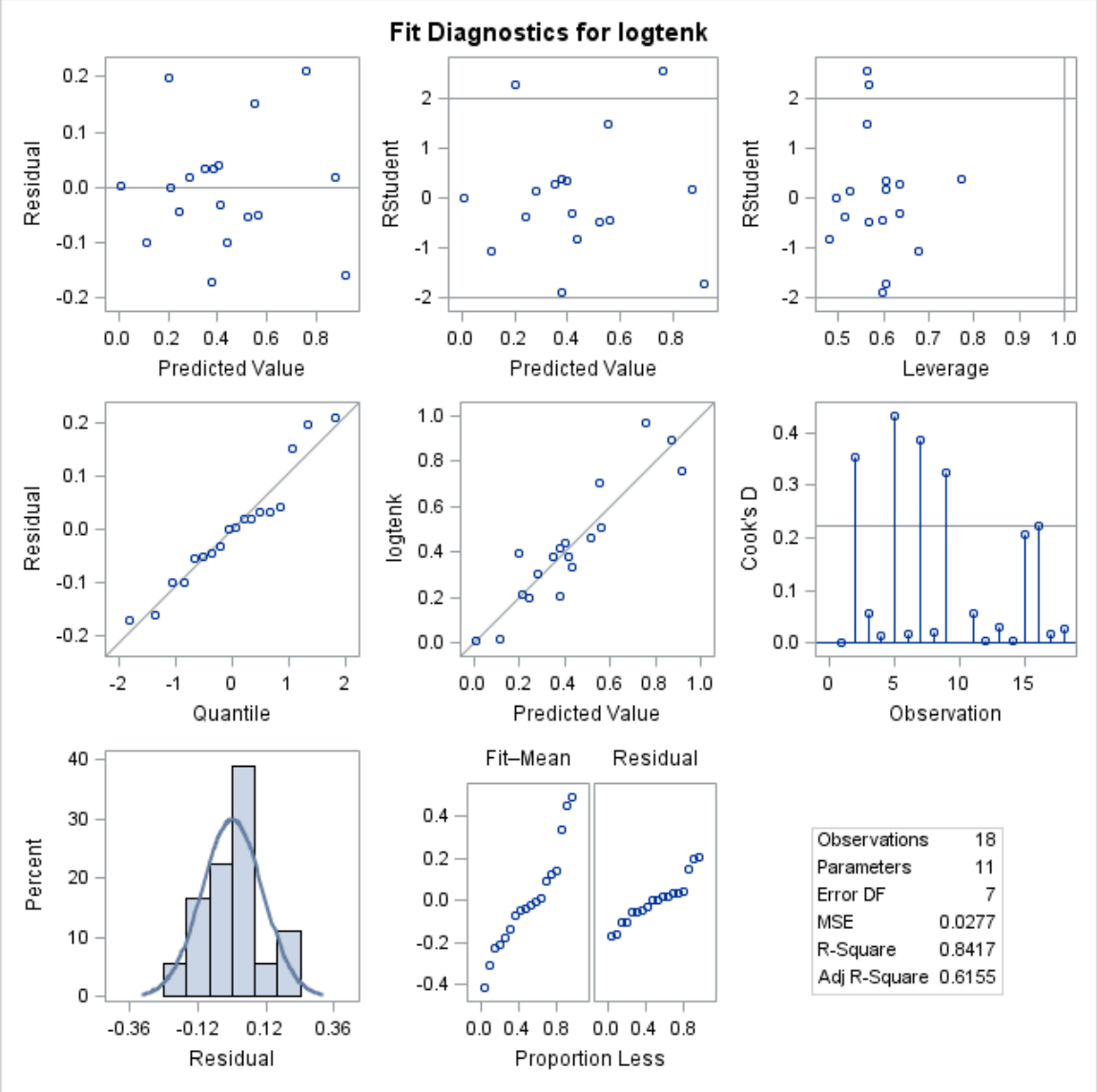

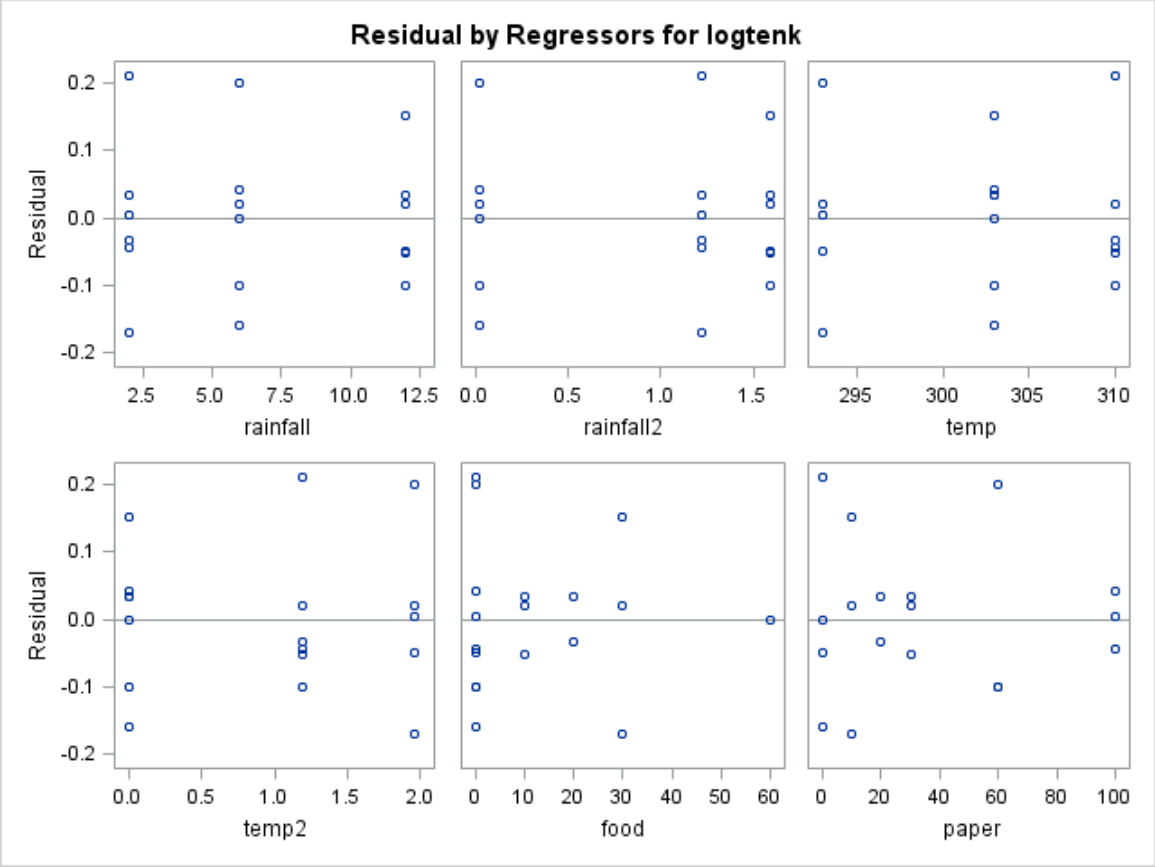
Residual by Regressors for logtenk
Residual
0.2
0.1
0.0
-0.1
-0.2
2.5
5.0
7.5
10.0
12.5
rainfall
0.0
0.5
1.0
1.5
rainfall2
295
300
305
310
temp
0.0
0.5
1.0
1.5
2.0
temp2
0
10
20
30
40
50
60
food
0
20
40
60
80
100
paper

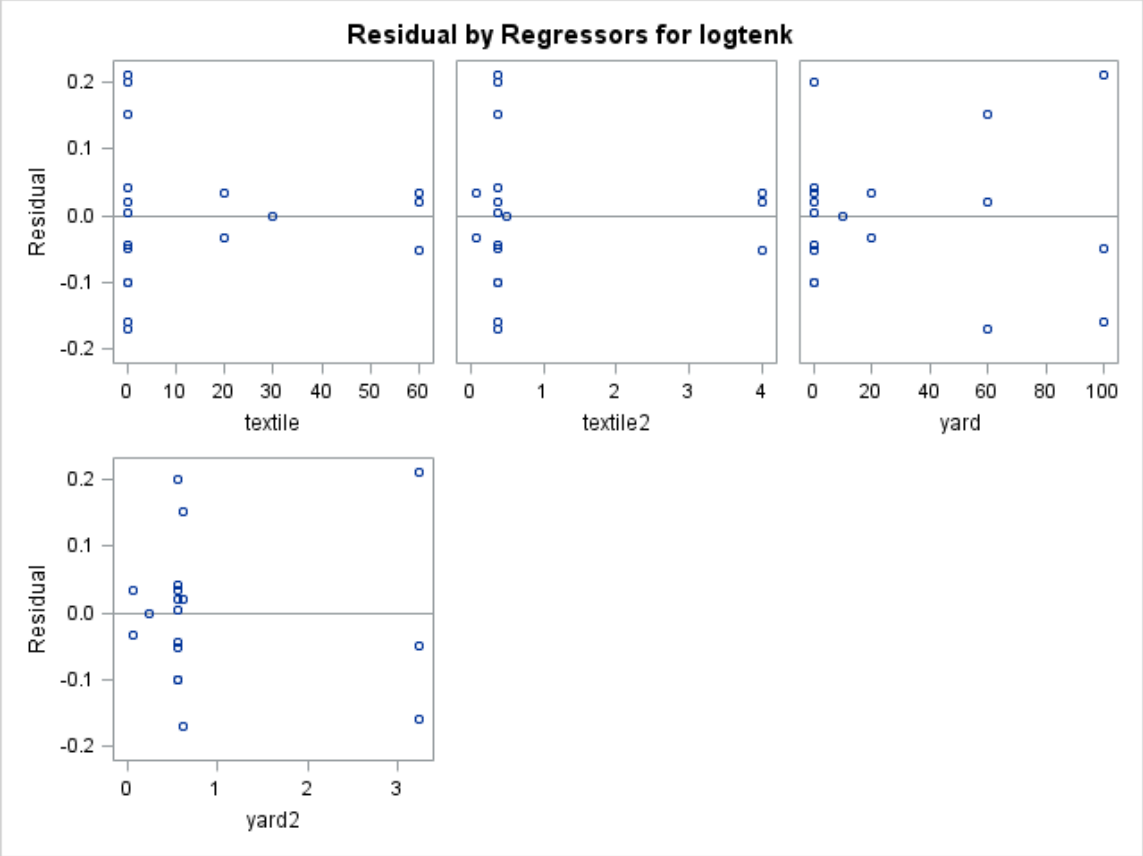
Residual by Regressors for logtenk
Residual
0.2
0.1
0.0
-0.1
-0.2
0 10 20 30 40 50 60
textile
0 1 2 3 4
textile2
0 20 40 60 80 100
yard
0 1 2 3
yard2

REFERENCES

1. Alexander, A., Burklin, C., Singleton, A., Eastern Research Group, I., and United States. Environmental Protection Agency. Office of Research and Development. (2005). *Landfill gas emissions model (LandGEM) version 3.02 user's guide.* Washington D.C.
2. Alvarez, J. M., and Martinez-Viturtia, A. (1986). "Laboratory simulation of municipal solid waste fermentation with leachate recycle." *Journal of Chemical Technology & Biotechnology,* 36(12), 547 - 556.
3. Amini, H. R., Reinhart, D. R., and Mackie, R. (2012). "Determination of first-order landfill gas modeling parameters and uncertainties." *Waste Management,* 32 305-316.
4. Angelidaki, I., Alves, M., Bolzonella, D., Borzacconi, L., Campos, J., Guwy, A., Kalyuzhnyi, S., Jenicek, P., and Lier, J. B. (2009). "Defining the biomethane potential (BMP) of solid organic wastes and energy crops: a proposed protocol for batch assays." *Water Science and Technology*, 59, 927-934.
5. Attal, A., Akunna, J., Camacho, P., Salmon, P., and Paris, I. (1992). "Anaerobic degradation of municipal wastes in landfill." *Water Science & Technology,* 25(7), 243-253.
6. Barlaz, M. A. (2006). "Forest products decomposition in municipal solid waste landfills." *Waste Manage.,* 26(4), 321-333.
7. Rhew R.D. and Barlaz, M. A. (1995). "Effect of lime-stabilized sludge as landfill cover on refuse decomposition." *J.Environ.Eng.,* 121 499.

8. Barlaz, M. A., Bareither, C. A., Hossain, A., Saquing, J., Mezzari, I., Benson, C. H., Tolaymat, T. M., and Yazdani, R. (2010). "Performance of North American bioreactor landfills. II: Chemical and biological characteristics." *J.Environ.Eng.,* 136 839.
9. Barlaz, M. A., Ham, R. K., Schaefer, D. M., and Isaacson, R. (1990). "Methane production from municipal refuse: a review of enhancement techniques and microbial dynamics." *Crit.Rev.Environ.Sci.Technol.,* 19(6), 557-584.
10. Barlaz, M., Eleazer, W., Odle Iii, W., Qian, X., and Wang, Y. (1997). "Biodegradative analysis of municipal solid waste in laboratory-scale landfills." *Environmental Protection Agency, Cincinnati, OH,* .
11. Barlaz, M. A., Ham, R. K., and Schaefer, D. M. (1990). "Methane production from municipal refuse: A review of enhancement techniques and microbial dynamics." *Critical Reviews in Environmental Science and Technology,* 19(6), 557-584.
12. Barlaz, M. A. (2006). "Forest products decomposition in municipal solid waste landfills." *Waste Manage.,* 26(4), 321-333.
13. Bilgili, M. S., Demir, A., and Varank, G. (2009). "Evaluation and modeling of biochemical methane potential (BMP) of landfilled solid waste: A pilot scale study." *Bioresour.Technol.,* 100(21), 4976-4980.
14. Bingemer, H., and Crutzen, P. J. (1987). "The production of methane from solid wastes." *Journal of Geophysical Research,* 92(D2), 2181-2187.
15. Bogner, J. E. (1990a). "Controlled study of landfill biodegradation rates using modified BMP assays." *Waste Manage.Res.,* 8(5), 329-352.
16. Bogner, J. E. (1990b). "Controlled Study of Landfill Biodegradation Rates Using Modified Bmp Assays." *Waste Management Research,* 8(1), 329-352.

17. Bookter, T. J., and Ham, R. K. (1982). "Stabilization of solid waste in landfills." *Journal of the Environmental Engineering Division,* 108(6), 1089-1100.
18. Brenda, B., Calvert, P. P., Pettigrew, C. A., and Barlaz, M. A. (1998). "Testing anaerobic biodegradability of polymers in a laboratory-scale simulated landfill." *Environ.Sci.Technol.,* 32(6), 821-827.
19. Brown, K. A., Smith, A., Burnley, S. J., Campbell, D. J. V., King, K., and Milton, M. J. T. (1999). "Methane Emissions from UK Landfills." *Rep. No. AEAT-5217,* AEA Technology Environment, Oxfordshire, UK.
20. Buivid, M., WiseM J, D., Remedios, E., and JenkinsW F, B. (1981). "Fuel gas enhancement by controlled landfilling of municipal solid waste." *Resources and Conservation,* 6(1), 3-20.
21. Chan, G., Chu, L., and Wong, M. (2002). "Effects of leachate recirculation on biogas production from landfill co-disposal of municipal solid waste, sewage sludge and marine sediment." *Environmental Pollution,* 118(3), 393-399.
22. Chanton, J. P., Powelson, D.K., Green R. B., (2009). "Methane Oxidation in Landfill Cover Soils: Is a 10% Default Value Resonable?" *Journal of Environmental Quality,* 38 (2), 654-663.
23. Chen, J., Wang, H., and Zhang, N. (2009). "Modified landfill gas generation model of first order kinetics and two stage reaction." *Emvironmental Science and Engineering (China),* 3(3), 313-319.
24. Chen, V. C. P., Tsui, K. L., Barton, R. R., and Meckesheimer, M. (2006). "A review on design, modeling and applications of computer experiments." *IIE Transactions,* 38(4), 273-291.
25. Chiampo, F., Conti, R., and Cometto, D. (1996). "Morphological characterisation of MSW landfills." *Resour.Conserv.Recycling,* 17(1), 37-45.

26. Chiemchaisri, C., Chiemchaisri, W., Kumar, S., and Hettiaratchi, J. P. A. (2007). "Solid waste characteristics and their relationship to gas production in tropical landfill." *Environ.Monit.Assess.,* 135(1), 41-48.
27. Cho, J. K., Park, S. C., and Chang, H. N. (1995). "Biochemical methane potential and solid state anaerobic digestion of Korean food wastes." *Bioresour.Technol.,* 52(3), 245-253.
28. Christensen, T. H., and Kjeldsen, P. (1989). "Basic Biochemical Processes in Landfills." *Sanitary Landfilling: Process, Technology, and Environmental Impact,* 29-49.
29. Chynoweth, D., Turick, C., Owens, J., Jerger, D., and Peck, M. (1993). "Biochemical methane potential of biomass and waste feedstocks." *Biomass Bioenergy,* 5(1), 95-111.
30. Cooper, C. D., Reinhart, D., Rash, F., Seligman, D., and Keely, D. (1992). "Landfill gas emissions." *Florida Center for Solid and Hazardous Wastes Management, Report,* 92-92.
31. Cruz, F. B. D., and Barlaz, M. A. (2010a). "Estimation of waste component-specific landfill decay rates using laboratory-scale decomposition data." *Environ.Sci.Technol.,* 44(12), 4722-4728.
32. Dean, A. M., and Voss, D. (1999). *Design and analysis of experiments.* Springer Verlag, .
33. Eggleston, H. S., Buendia, L., Miwa, L., and Ngara, T. (. (2006). "Intergovernmental Panel of Climate Change (IPCC) Guidelines for National Greenhouse Inventories." Tanabe, IGES, Japan.
34. Eleazer, W. E., Odle III, W. S., Wang, Y. S., and Barlaz, M. A. (1997). "Biodegradability of municipal solid waste components in laboratory-scale landfills." *Environ.Sci.Technol.,* 31(3), 911-917.
35. El-Fadel, M. (1999). "Simulating temperature variations in landfills." *J.Solid Waste Technol.Manage.,* 26(2), 78-86.

36. Faour, A. A., Reinhart, D. R., and You, H. (2007). "First-order kinetic gas generation model parameters for wet landfills." *Waste Manage.,* 27(7), 946-953.

37. Farquhar, G., and Rovers, F. (1973). "Gas production during refuse decomposition." *Water, Air, & Soil Pollution,* 2(4), 483-495.

38. Filipkowska, U., and Agopsowicz, M. (2004). "Solids waste gas recovery under different water conditions." *Polish Journal of Environmental Studies,* 13(6), 663-669.

39. Francois, V., Feuillade, G., Skhiri, N., Lagier, T., and Matejka, G. (2006). "Indicating the parameters of the state of degradation of municipal solid waste." *J.Hazard.Mater.,* 137(2), 1008-1015.

40. Godley, A., Lewin, K., Graham, A., and Smith, R. (2003). "Environment agency review of methods for determining organic waste biodegradability for landfill and municipal waste diversion." *Proceedings 8th European Biosolids and Organic Residuals Conference, Wakefield, UK,* 14.

41. Guermoud, N., Ouadjnia, F., Abdelmalek, F., and Taleb, F. (2009). "Municipal solid waste in Mostaganem city (Western Algeria)." *Waste Manage.,* 29(2), 896-902.

42. Gunaseelan, V. N. (2004). "Biochemical methane potential of fruits and vegetable solid waste feedstocks." *Biomass Bioenergy,* 26(4), 389-399.

43. Gurijala, K. R., and Suflita, J. M. (1993). "Environmental factors influencing methanogenesis from refuse in landfill samples." *Environ.Sci.Technol.,* 27(6), 1176-1181.

44. Gurijala, K., Sa, P., and Robinson, J. (1997). "Statistical Modeling of Methane Production from Landfill Samples." *Appl.Environ.Microbiol.,* 63(10), 3797-3803.

45. Ham, R. K., and Bookter, T. J. (1982). "Decomposition of solid waste in test lysimeters." *Journal of the Environmental Engineering Division,* 108(EE6), 1147-1170.

46. Hansen, T. L., Schmidt, J. E., Angelidaki, I., Marca, E., Jansen, J. C., Mosbæk, H., and Christensen, T. H. (2004). "Method for determination of methane potentials of solid organic waste." *Waste Manage.,* 24(4), 393-400.

47. Hanson, J. L., Yeşiller, N., and Oettle, N. K. (2010). "Spatial and Temporal Temperature Distributions in Municipal Solid Waste Landfills." *J.Environ.Eng.,* 136 804.

48. Hartz, K. E., Klink, R. E., and Ham, R. K. (1982). "Temperature Effects: Methane Generation from Landfill Samples." *Journal of the Environmental Engineering Division,* 108(4), 629-638.

49. Hernández-Berriel, M. C., Mañón-Salas, C., Sánchez-Yáñez, J., Lugo-de la Fuente, J., and Márquez-Benavides, L. (2010). "Influence of Recycling Different Leachate Volumes on Refuse Anaerobic Degradation." *The Open Waste Management Journal*, 155-166

50. Hernández-Berriel, M. C., Márquez-Benavides, L., González-Pérez, D., and Buenrostro-Delgado, O. (2008). "The effect of moisture regimes on the anaerobic degradation of municipal solid waste from Metepec (México)." *Waste Manage.,* 28 S14-S20.

51. I. Angelidaki, M. Alves, D. Bolzonella, L. Borzacconi, J. L. Campos, A. J. Guwy, S. Kalyuzhnyi, P. Jenicek and J. B. van Lier. (2009). "Defining the biomethane potential (BMP) of solid organic wastes and energy crops: a proposed protocol for batch assays." *Water Science and Technology,* 59(5).

52. Intergovernmental Panel on Climate Change (IPCC), 2007, "Changes in Atmospheric Constituents and in Radiative Forcing. *The Physical Science Basis. Contribution of Working Group I to the Fourth Assessment Report"* Cambridge University Press, Cambridge, United Kingdom and New York, NY, USA.

53. Intergovernmental Panel on Climate Change (IPCC), 2006, “IPCC Guidelines for National Greenhouse Gas Inventories”, Eggleston H.S., Buendia L., Miwa K., Ngara T. and Tanabe K. (eds), Institute for Global Environmental Strategies, Japan.

54. Isci, A., and Demirer, G. (2007). "Biogas production potential from cotton wastes." *Renewable Energy,* 32(5), 750-757.

55. Ivanova, L. K., Richards, D. J., and Smallman, D. J. (2008). "Assessment of the anaerobic biodegradation potential of MSW." *Proceedings of the Institution of Civil Engineers-Waste and Resource Management,* 167-180.

56. Jeon, E., Bae, S., Lee, D., Seo, D., Chun, S., Lee, N., and Kim, J. (2007). "Methane generation potential and biodegradability of MSW components." *Sardinia 2007 Eleventh International Waste Management and Landfill Symposium*.

57. Jones, H. A., and Nedwell, D. B. (1993). "Methane emission and methane oxidation in land-fill cover soil." *FEMS Microbiol.Lett.,* 102(3-4), 185-195.

58. Jones, K., Rees, J., and Grainger, J. (1983). "Methane generation and microbial activity in a domestic refuse landfill site." *Appl.Microbiol.Biotechnol.,* 18(4), 242-245.

59. Kamalan, H., Sabour, M., and Shariatmadari, N. (2011). "A review on available landfill gas models." *Journal of Environmental Science and Technology,* 4(2), 79-92.

60. Kelly, R. J., Shearer, B. D., Kim, J., Goldsmith, C. D., Hater, G. R., and Novak, J. T. (2006). "Relationships between analytical methods utilized as tools in the evaluation of landfill waste stability." *Waste Manage.,* 26(12), 1349-1356.

61. Komilis, D. P., and Ham, R. K. (2003). "The effect of lignin and sugars to the aerobic decomposition of solid wastes." *Waste Manage.,* 23(5), 419-423.

62. Lay, J. J., Li, Y. Y., and Noike, T. (1998). "Developments of bacterial population and methanogenic activity in a laboratory-scale landfill bioreactor." *Water Res.,* 32(12), 3673-3679.

63. Machado, S. L., Carvalho, M. F., Gourc, J. P., Vilar, O. M., and Do Nascimento, J. C. F. (2009). "Methane generation in tropical landfills: Simplified methods and field results." *Waste Manage.,* 29(1), 153-161.

64. Mason, R. L., Gunst, R. F., and Hess, J. L. (1989). "Statistical design and analysis of experiments." New York, Wiley.

65. Maurice, C., and Lagerkvist, A. (1997). "Seasonal variation of landfill gas emissions." *Proceedings of Sixth International Landfill Symposium in Sardinia,*Caliagri,Italy, 87-93.

66. Mehta, R., Yazdani, R., Augenstein, D., Bryars, M., and Sinderson, L. (2002). "Refuse decomposition in the presence and absence of leachate recirculation." *J.Environ.Eng.,* 128 - 228.

67. Meima, J., Naranjo, N. M., and Haarstrick, A. (2008). "Sensitivity analysis and literature review of parameters controlling local biodegradation processes in municipal solid waste landfills." *Waste Manage.,* 28(5), 904-918.

68. Mohammad Adil Haque. (2007). "Dynamic Characteristics and Stability Analysis of Municipal Solid Waste in Bioreactor Landfills." PhD thesis, University of Texas at Arlington, Texas.

69. Oonk, H. (2010). "Literature Review: Methane from Landfills: Methods to Quantify Generation, Oxidation and Emission." *Innovations in Environmental Technology,* .

70. Oonk, H., and Boom, T. (1995a). "Landfill Gas Formation, Recovery and Emissions." *Rep. No. TNO-report R 95-203,* Appledorm, Netherlands.

71. Oonk, H., and Boom, T. (1995b). "Validation of landfill gas formation models." *Studies in Environmental Science,* 65 597-602.

72. Owens, J., and Chynoweth, D. (1993). "Biochemical methane potential of municipal solid waste (MSW) components." *Water Science & Technology,* 27(2), 1-14.

73. Pidwirny, Michael. *Physical Geography.net: Fundamentals eBook*. "Global Distribution of Precipitation".http://www.physicalgeography.net/fundamentals/8g.html, accessed 7/11.

74. Qudais M., Qdais H.A. (2000). " Energy Content of Municipal Solid Waste in Jordan and its Potential Utilization". *Energy Conversion and Management,* 41, 983-991

75. Rao, M., Singh, S., Singh, A., and Sodha, M. (2000). "Bioenergy conversion studies of the organic fraction of MSW: assessment of ultimate bioenergy production potential of municipal garbage." *Appl.Energy,* 66(1), 75-87.

76. Rees, J. F. (1980). "Optimisation of methane production and refuse decomposition in landfills by temperature control." *Journal of Chemical Technology and Biotechnology,* 30(1), 458-465.

77. Reinhart, D. R., Faour, A. A., You, H., National Risk Management Research Laboratory (US). Air Pollution Prevention and Control Division, and University of Central Florida. (2005). *First-Order Kinetic Gas Generation Model Parameters for Wet Landfills.* US Environmental Protection Agency, Office of Research and Development, Washington D.C.

78. Ress, B. B., Calvert, P. P., Pettigrew, C. A., and Barlaz, M. A. (1998). "Testing Anaerobic Biodegradability of Polymers in a Laboratory-Scale Simulated Landfill." *Environmental Science & Technology,* 32(6), 821-827.

79. Sanphoti, N., Towprayoon, S., Chaiprasert, P., and Nopharatana, A. (2006). "The effects of leachate recirculation with supplemental water addition on methane production and waste decomposition in a simulated tropical landfill." *J.Environ.Manage.,* 81(1), 27-35.

80. Scharff, H., and Jacobs, J. (2006). "Applying guidance for methane emission estimation for landfills." *Waste Manage.,* 26(4), 417-429.

81. Shanmugam, P., and Horan, N. (2009). "Simple and rapid methods to evaluate methane potential and biomass yield for a range of mixed solid wastes." *Bioresour.Technol.,* 100(1), 471-474.

82. Shao, L., He, P. J., Hua, Z., Yu, X., Li-Guo J. (2005). " Methanogenesis acceleration of fresh landfilled waste by micraeration." *Journal of Environmental Sciences,*17(3),371-374

83. Shelton, D. R., and Tiedje, J. M. (1984). "General method for determining anaerobic biodegradation potential." *Appl.Environ.Microbiol.,* 47(4), 850.

84. Solid Waste Association of North America. (1997). "Comparison of Models for Predicting Landfill Methane Recovery." *Rep. No. GR-LG0075,* SWANA, Maryland.

85. Spokas, K., Bogner, J., Chanton, J., and Franco, G. (2009). "Developing a new field-validated methodology for landfill methane emissions in California." *Proc. Sardinia,* .

86. Staley, B. F., and Barlaz, M. A. (2009). "Composition of municipal solid waste in the united states and implications for carbon sequestration and methane yield." *J.Environ.Eng.,* 135 901.

87. Stege, G.A. (2010). "User's Model Columbia's Gas Model- Version 1.0.", US EPA's Landfill Methane Outreach Program, U.S. EPA, Washington D.C.

88. Stege, G.A. (2009). "User's Model Ukraine's Gas Model- Version 1.0.", US EPA's Landfill Methane Outreach Program, U.S. EPA, Washington D.C.

89. Stone, R., and Kahle, R. L. (1972). "Water and Sewage Sludge Absorption by Solid Waste." *Journal of the Sanitary Engineering Division,* 98(5), 731-743.

90. Taufiq, T. (2010). "Characteristics of Municipal Solid Waste." Master Thesis, University of Texas at Arlington, Texas.

91. Tchobanoglous, G., Theisen, H., and Vigil, S. A. (1993). *Integrated solid waste management: engineering principles and management issues.* McGraw-Hill New York, .

92. Thomas, H. A. (1937). "The" Slope" Method of Evaluating the Constants of the First-Stage Biochemical Oxygen-Demand Curve." *Sewage Works Journal,* 9(3), 425-430.

93. Thompson, S., Sawyer, J., Bonam, R., and Valdivia, J. (2009). "Building a better methane generation model: Validating models with methane recovery rates from 35 Canadian landfills." *Waste Manage.,* 29(7), 2085-2091.

94. Tolaymat, T. M., Green, R. B., Hater, G. R., Bariaz, M. A., Black, P., Branson, D., and Powell, J. (2010). "Evaluation of landfill gas decay constant for municipal solid waste landfills operated as bioreactors." *J.Air Waste Manage.Assoc.,* 60(1), 2187.

95. U.S. EPA. (1998). "Fate and Transport and Transformation Test Guidelines OPPTS 835.3400 Anaerobic Biodegradability of Organic Chemicals." *Rep. No. EPA 712-C-98-090,* .

96. United States Environmental Protection Agency (USEPA), 2005, "Landfill Gas Emissions Model (LandGEM) Version 3.02 User's Guide", Report no. EPA-600/R-05/047, U.S. Environmental Protection Agency, Office of Research and Development, Washington, DC

97. United States Environmental Protection Agency (USEPA), 2008. “Municipal Solid Waste in The United States: 2007 Facts and Figures”, Report no. EPA530-R-08-010, Office of Solid Waste, United States Environmental Protection Agency

98. United States Environmental Protection Agency (USEPA), 2011, “U.S. Greenhouse Gas Inventory Report: Inventory of U.S. Greenhouse Gas Emissions and Sinks: 1990-2009”, Report No. EPA 430-R-11-005, USEPA, Washington, DC

99. U.S. Environment Protection Agency (U.S. EPA) Landfill Methane Outreach Program: http://www.epa.gov/lmop/international/tools.html#a01 accessed 4/5/2012

100. Vavilin, V., Lokshina, L. Y., Jokela, J., and Rintala, J. (2004). "Modeling solid waste decomposition." *Bioresour.Technol.,* 94(1), 69-81.

101. Wang, Y. S., Byrd, C. S., and Barlaz, M. A. (1994). "Anaerobic biodegradability of cellulose and hemicellulose in excavated refuse samples using a biochemical methane potential assay." *J.Ind.Microbiol.Biotechnol.,* 13(3), 147-153.

102. Wang, Y. S., Odle, W. S., Eleazer, W. E., and Bariaz, M. A. (1997). "Methane potential of food waste and anaerobic toxicity of leachate produced during food waste decomposition." *Waste Manage.Res.,* 15(2), 149-167.

103. Wang-Yao, K., Towprayoon, S., Chiemchaisri, C., Gheewala, S. H., and Nopharatana, A. (2006). "Seasonal variation of landfill methane emissions from seven solid waste disposal sites in central Thailand." *Proc. of the 2nd Joint International Conference on ‘Sustainable Energy and Environment’(SEE 2006),* 21-23.

104. Weitz, K. A., Thorneloe, S. A., Nishtala, S. R., Yarkosy, S., and Zannes, M. (2002). "The Impact of Municipal Solid Waste Management on Greenhouse Gas Emissions in the United States." *Journal of Air and Waste Management Association,* 52 1000-1011.

105. Wreford, K., Atwater, J., and Lavkulich, L. (2000). "The effects of moisture inputs on landfill gas production and composition and leachate characteristics at the Vancouver Landfill Site at Burns Bog." *Waste Management and Research,* 18(4), 386-392.

106. Wu, B., Taylor, C. M., Knappe, D.R.U., Nanny, M.A., Barlaz, M. A. (2001). "Factors Controlling Alkylbenzene Sorption to Municipal Solid Waste." Environmental Science and Technology, 35, 4569-4576

107. Yeşiller, N., Hanson, J. L., and Liu, W. L. (2005). "Heat generation in municipal solid waste landfills." *J.Geotech.Geoenviron.Eng.,* 131 1330.

BIOGRAPHICAL INFORMATION

Richa received her bachelor's degree in Civil Engineering from the University of Pune, India. Subsequently, she obtained master's in Environmental Engineering from University of Mumbai, India. Her bachelor's and master's thesis focused on removal of heavy metals from industrial wastewater. After completing her master's degree, Richa worked as a proposal and design engineer for 3 years in a multinational company in India. In 2008, she joined The University of Texas at Arlington (UTA) as a doctoral student in Civil Engineering. She was awarded Environmental Research and Education Foundation's (EREF) student scholarship in 2011. She has also received SWANA's SCS/Stearns scholarship for two consecutive years in 2010 and 2011. In addition, Richa was awarded Air and Waste Management Association's (A&WMA) student scholarship and her poster won second place award at the A&WMA's national conference in 2011. Her research interests are in the areas of landfill gas modeling, renewable energy, and climate change.